Université du Québec
Institut National de la Recherche Scientifique
Institut Armand-Frappier

SIGNAL-DIRECTED ENDOPLASMIC RETICULUM AND GOLGI EXIT OF TURNIP MOSAIC VIRUS $6K_2$ PROTEIN FOR REPLICATION VESICLE CELLULAR BIOGENESIS

Par

Jun Jiang

Thèse présentée pour l'obtention
du grade de Philosophiae doctor (Ph.D.)
en Immunologie et Virologie

Jury d'évaluation

Président du jury et examinateur interne	Prof. Patrick Labonté INRS – Institut Armand-Frappier
Examinateur externe	Prof. Jacques Archambault Université de Montréal
Examinateur externe	Prof. Chen Liang Mcgill University
Co-directeur de recherche	Prof. Huanquan Zheng Mcgill University
Directeur de recherche	Prof. Jean-François Laliberté INRS – Institut Armand-Frappier

RÉSUMÉ

Les virus à ARN positif [ARN (+)] sont connus pour induire un remodelage des membranes intracellulaires de leurs cellules hôtes, ce qui conduit à la formation d'usines virales. Ces usines virales abritent les composantes nécessaires à la réplication du virus en soutenant la synthèse de l'ARN viral (ARNv). En général, au moins une protéine codée par l'ARNv est associée aux membranes et est responsable de ce remodelage membranaire. Cette protéine recrute d'autres protéines virales et de l'hôte pour l'assemblage du complexe de réplication dans les usines virales. Cependant, le processus de la biogenèse de ces usines virales est en grande partie inconnue.

Cette thèse se concentre sur l'étude de la biogenèse des vésicules de réplication (ou usines virales) du virus de la mosaïque du navet (TuMV). Le TuMV est un membre de la famille *Potyviridae*. Le génome viral code pour au moins 11 protéines matures. La protéine virale, associée à la membrane, $6K_2$ une masse molaire de 6 kDa et déclenche des modifications membranaires qui se traduisent par la formation de vésicules de réplication. Les objectifs de ce projet étaient les suivants: 1) caractériser les déterminants moléculaires de $6K_2$ pour la formation de vésicules de réplication; 2) identifier les facteurs de l'hôte qui sont impliqués dans la biogenèse cellulaire de vésicules de réplication induites par $6K_2$; et 3) d'évaluer le rôle des déterminants moléculaires ainsi que des facteurs de l'hôte qui interagissent avec $6K_2$ lors de l'infection par le TuMV.

Dans le premier objectif, j'ai montré qu'un motif combinatoire de $6K_2$ était capable d'adresser cette protéine vers la voie de sécrétion pour la biogenèse des vésicules de réplication. Grâce à l'utilisation de mutagenèse dirigée et d'imagerie de cellules vivantes, j'ai trouvé que l'extrémité N-terminale de $6K_2$ contenait un motif d'exportation du réticulum endoplasmique (RE). La suppression de ce motif a abouti à la rétention de la protéine $6K_2$ dans le RE. En outre, j'ai trouvé qu'un motif GXXXG dans le domaine

transmembranaire de $6K_2$ (TMD) était nécessaire pour la sortie des vésicules de réplication de l'appareil de Golgi. La mutation de ce motif a provoqué une rétention de ces vésicules dans l'appareil de Golgi et les a empêchées d'atteindre les chloroplastes.

Dans le second objectif, l'un des facteurs de l'hôte identifié est Sec24a, une composante des coatomers COPII. L'interaction $6K_2$-Sec24a a été validée par des expériences de double hybride dans la levure et de co-immunoprécipitation. La protéine Sec24a a été mutée (R693K) au niveau du site de liaison B permettant la reconnaissance de la protéine cargo. Cette dernière a perdu toute capacité d'interaction avec la protéine $6K_2$. En outre, l'extrémité N-terminale de $6K_2$ s'est avérée suffisante pour l'interaction avec Sec24a. Ces résultats indiquent que Sec24a interagit avec la protéine $6K_2$. D'autres protéines de l'hôte ont aussi été identifiées comme étant capables d'interagir avec $6K_2$. Ces dernières sont des protéines SNARE de l'appareil de Golgi: Bet11, Gos11 et Vamp714.

Dans le troisième objectif, le motif d'exportation du RE de $6K_2$ et le motif GXXXG d'exportation de l'appareil de Golgi se sont révélés être importants pour l'infection virale. Lorsque le tryptophane dans le motif d'exportation du RE a été remplacé par une alanine, le taux de réplication du virus muté ($TuMV^{W15A}$) a été réduit d'environ 60%. Plus important encore, le mouvement viral de cellule à cellule a été complètement aboli. Ces résultats indiquent que ce motif est nécessaire à la fois pour la réplication du virus et son mouvement. De même, pour le virus muté au niveau du motif GXXXG ($TuMV^{GV}$) la réplication a été affectée de façon importante.

L'importance de l'interaction $6K_2$-Sec24a a été évaluée en infectant la lignée G92 *d'Arabidopsis thaliana*. Cette lignée comporte une mutation dans la protéine Sec24a, le résidu Arginine en position 693 étant changé pour un résidu Lysine ($Sec24a^{R693K}$). Par rapport à la plante de type sauvage, un retard de l'infection par le virus a été observé. Dans le cas des protéines SNARE, des plantes knock-out pour certaines protéines SNARE du Golgi étudiées sont plus susceptibles à l'infection par le TuMV. Ce résultat a été confirmé en co-exprimant le virus avec les mutants dominants négatifs des SNARE

étudiées. Ces résultats suggèrent que l'interaction $6K_2$-Sec24a est nécessaire, tandis que l'interaction $6K_2$-Golgi SNARE joue un rôle négatif au cours de l'infection par le virus.

Pris ensemble, ces travaux ont fourni une meilleure compréhension de la biogenèse cellulaire des vésicules de réplication du TuMV.

---------- ----------

Jun Jiang **Jean-François Laliberté**

Étudiant Directeur de recherche

ABSTRACT

Positive-stranded RNA [(+) RNA] viruses are known to induce extensive intracellular membrane remodeling, which leads to the formation of viral factories. These viral factories house virus replication components, supporting the synthesis of viral RNA (vRNA). In general, at least one membrane-associated viral protein encoded by the vRNA is responsible for membrane remodeling and hijacks other viral and host proteins for the construction of viral factories. However, the cellular biogenesis of these viral factories is largely unknown.

This thesis investigates the cellular biogenesis of *Turnip mosaic virus* (TuMV) replication vesicles (or viral factories). TuMV is a member of the family *Potyviridae*. The viral genome encodes at least 11 mature proteins. The membrane-associated viral protein $6K_2$, which has a molecular weight of 6 kDa, is the viral protein that triggers membrane modification that results in the formation of replication vesicles. The aims of this project were to: 1) characterize the molecular determinants of $6K_2$ for the formation of replication vesicles; 2) identify host factors that are involved in the cellular biogenesis of $6K_2$-induced replication vesicles; and 3) evaluate the role of the molecular determinants and the interacting host factors for TuMV infection.

In the first aim, I showed that a combinatorial motif of $6K_2$ was able to direct this protein to follow the early secretory pathway for the biogenesis of replication vesicles. Using site-directed mutagenesis and live cell imaging, I found that the $6K_2$ N-terminal tail contains a tryptophan-based endoplasmic reticulum (ER) export motif. The deletion of this motif resulted in the ER retention of $6K_2$. Additionally, I found that the $6K_2$ trans-membrane domain (TMD) GXXXG motif was required for Golgi exit of $6K_2$-induced replication vesicles. The mutation of this motif caused Golgi retention of the replication vesicle, and was further prevented from reaching the chloroplasts.

In the second aim, one of the identified host factors is the coat protein complex II (COPII) coatomer Sec24a. The $6K_2$-Sec24a interaction was validated by yeast two-hybrid and co-immunoprecipitation experiments. The Sec24a^{R693K}, where the cargo protein recognition B-binding site is mutated, did not interact with the $6K_2$ protein. Furthermore, the $6K_2$ N-terminal tail was enough to mediate its interaction with Sec24a. These results indicate that Sec24a is an interactor of protein $6K_2$. Other host protein interactors of $6K_2$ are the Golgi SNARE (soluble N-ethylmaleimide-sensitive-factor attachment protein receptors) Bet11, Gos11 and Vamp714.

In the third aim, the characterized tryptophan-based ER export motif and the GXXXG Golgi exit motif were shown to be important for virus infection. When the tryptophan was replaced with alanine, the replication level of the mutated virus (TuMV^{W15A}) was decreased about 60%. More significantly, the virus cell-to-cell movement was completely abolished. These results indicate that the tryptophan-based motif is required for both the virus replication and movement. Similarly, TuMV replication was affected dramatically when the GXXXG motif was mutated.

The importance of the $6K_2$-Sec24a interaction was assessed by infecting G92 *Arabidopsis thaliana* plants, which contain a mutated Sec24a, the Arginine residue at position 693 being changed for a Lysine residue. Compared to the wild type plant, a delayed virus infection was observed. On the contrary, Golgi SNARE knockout plants showed an enhanced susceptibility to TuMV infection. This result was confirmed by co-expressing the virus with Golgi SNARE dominant negative proteins. These results suggest the $6K_2$-Sec24a interaction is necessary for virus infection, while the $6K_2$-Golgi SNARE interaction plays a negative role during virus infection.

Taken together, this work provides a better understanding of the cellular biogenesis of TuMV replication vesicles.

---------- ----------

Jun Jiang **Jean-François Laliberté**

Student Director of Research

SOMMAIRE RÉCAPITULATIF

Les virus à ARN positif [ARN(+)] sont connus pour induire un remodelage des membranes intracellulaires de la cellule hôte lors de l'infection en induisant la formation de compartiments viraux connus sous le nom d'usines virales. Ces usines virales sont riches en toutes sortes de facteurs permettant une réplication robuste de l'ARN viral. De même, ces usines virales offrent un microenvironnement de protection qui empêcherait la présence des RNAses cellulaires et des facteurs de l'hôte impliqués dans la réponse anti-virale.

Les virus à ARN (+) peuvent cibler tous les types de membranes cellulaires pour la construction d'usines virales. La source de la membrane détermine dans une certaine mesure la dynamique des usines virales. De nombreuses usines virales sont relativement statiques en raison des invaginations dans les membranes cellulaires dont elles dérivent. Ce genre d'usines virales est également nommé sphérules. Ces sphérules sont plus souvent issus des chloroplastes, des peroxysomes et des mitochondries. Par exemple, l'infection du *Turnip yellow mosaic virus* (TYMV) induit la formation de sphérules à partir de la membrane extérieure du chloroplaste. L'infection par le *Tomato bushy stunt virus* (TBSV) produit des corps multivésiculaires (MVBS) qui sont formés par des invaginations progressives de la membrane des peroxysomes. De manière comparable, les autres usines virales sont plutôt mobiles et prennent la forme de vésicules. Ces vésicules sont issues du réticulum endoplasmique (RE), et sont associées au cytosquelette. Par exemple, le *Tobacco mosaic virus* (TMV) et le *Potato virus X* (PVX) induisent la formation de vésicules à partir du RE pour la production virale.

En général, les virus à ARN (+) des plantes codent pour une protéine virale associée aux membranes, ce qui déterminera l'origine des usines virales. Par exemple, l'expression ectopique de la protéine 140K de TYMV cible les chloroplastes, la protéine p33 de TBSV réorganise les peroxysomes, et la protéine TGBp2 de PVX modifie le RE.

Deux domaines transmembranaires de la protéine TBSV p33 sont nécessaires pour son association aux peroxysomes, et un tronçon de 20 acides aminés est responsable de l'association de la protéine p27 *Red clover necrotic mosaic virus* (RCNMV) au RE. Toutefois, ces caractérisations se sont limitées à définir le domaine d'association aux membranes. Cette information est nécessaire mais insuffisante pour comprendre comment les protéines virales induisent la formation des usines virales. En outre, la protéine virale associée à la membrane peut passer d'un organite à un autre. Par exemple, la protéine p33 du TBSV se retrouve dans le RE en absence de peroxysomes. La protéine TGBp2 du *Potato mop-top virus* (PMTV) s'associe d'abord avec le RE, puis atteint les chloroplastes. Ainsi, la caractérisation du domaine de la protéine virale qui s'associe aux membranes ne semble pas suffire pour comprendre la façon dont les protéines virales induisent la formation des compartiments membranaires. Par exemple, la façon dont la protéine virale cible de manière séquentielle des membranes différentes n'est pas connue. Les facteurs de l'hôte qui interagissent avec la protéine associée à la courbure de la membrane doivent aussi être identifiés.

Une fois que les protéines virales se sont associées aux membranes, elles recrutent d'autres protéines virales et des facteurs de l'hôte pour l'assemblage du complexe de réplication. Les protéines virales comprennent l'ARN polymérase ARN-dépendante et l'hélicase pour satisfaire aux exigences de la synthèse de l'ARN viral (ARNv). Dans certains cas, une protéine de mouvement viral (MP) s'associe avec les usines virales pour le transport de l'ARNv. De plus en plus de facteurs de l'hôte sont trouvés comme étant présents dans le complexe de réplication. Ces facteurs de l'hôte identifiés sont nécessaires pour l'activité de synthèse d'ARNv. Par exemple, les protéines de choc thermique (HSP), les facteurs de traduction et des protéines kinases ont été trouvées pour faciliter la synthèse d'ARNv. Cet ensemble de facteurs de l'hôte a été trouvé dans diverses infections du virus (+) de la plante. D'autres facteurs de l'hôte joue un rôle critique dans le maintien de la morphologie des usines virales. Ces facteurs comprennent les reticulons, des facteurs du complexe de tri endosomal requis pour le transport (ESCRT), et des facteurs du métabolisme des lipides. Toutefois, l'identification

de ces facteurs est limitée seulement à une infection par le BMV et TBSV dans la levure, qui est leur hôte de substitution. Les facteurs de l'hôte qui contribuent à la biogenèse des usines virales pour les autres virus sont généralement inconnus. En outre, les facteurs de l'hôte peuvent fonctionner comme des facteurs de restriction. Par conséquent, l'identification des facteurs de l'hôte mènera à une meilleure compréhension de la biogenèse de l'usine virale et la réplication du virus.

Le virus de la mosaïque du navet (TuMV) est un virus à ARN(+) de la famille des Potyviridae. Le génome de 9,8 kb code pour une polyprotéine de 358 kDa. Le clivage de cette protéine résulte en au moins 11 protéines matures. La protéine virale $6K_2$ a un poids moléculaire de 6 kDa, et est la seule protéine virale nécessaire pour induire la formation des vésicules de réplication. L'utilisation d'une forme de $6K_2$ fusionnée à une protéine fluorescente dans le clone infectieux du TuMV (TuMV / $6K_2$: mCherry ou TuMV / $6K_2$: GFP), permet de suivre *in vivo* les vésicules de réplication virale par microscopie confocale. L'infection induite par le TuMV conduit à la formation de nombreuses vésicules de tailles hétérogènes (plage de diamètre de 0,6 à 4,3 µm). L'infection du TuMV est aussi accompagnée de la formation d'un ou deux amalgames de RE (plage de diamètre de 9 à 15 µm) le plus souvent situé dans la région périnucléaire. Les vésicules sont très mobiles, tandis que les amalgames de RE sont relativement statiques. Un lien fonctionnel a été observé entre les vésicules et les amalgames de RE, Les vésicules de réplication s'associent aux microfilaments pour leur mouvement intracellulaire. Les vésicules et le complexe de réplication peuvent se déplacer entre les cellules pour la transmission du virus. Des données récentes montrent enfin que les vésicules de réplication seraient les entités virales lors du mouvement à longue distance du TuMV.

Comment la protéine virale $6K_2$ induit la formation des vésicules de réplication demeure inconnu. Il a été montré que lors de la réplication, les potyvirus induisent la formation de vésicules de façon COPI et COPII dépendante. Cependant, ces études n'ont pas fourni une explication sur les mécanismes moléculaires impliqués entre $6K_2$ et la machinerie COPII, ainsi que sur l'identification de la composante COPII capable d'interagir

directement avec $6K_2$. On ne sait pas si d'autres facteurs de l'hôte contribuent à la formation des vésicules de réplication. Ainsi, mon projet est d'étudier la biogenèse des vésicules de réplication du TuMV.

Les objectifs de recherche ont été de:

1) Caractériser les déterminants moléculaires de la protéine $6K_2$ dans la biogenèse des vésicules de réplication;

2) D'identifier des facteurs de l'hôte impliqués dans la biogenèse des vésicules de réplication;

3) De comprendre l'importance des déterminants moléculaires de $6K_2$ ainsi que celle des facteurs de l'hôte au cours de l'infection virale.

Dans le premier objectif, j'ai obtenu et caractérisé divers mutants de $6K_2$. Dans un premier temps une expérience de cartographie par délétion du domaine N-terminal a été effectuée. La suppression progressive de l'extrémité N-terminale de $6K_2$ a conduit à la rétention de cette protéine dans le RE, en particulier quand une séquence de 12 d'acides aminés (du $7^{ème}$ acide aminé au $18^{ème}$) a été retirée. Cette région a été encore réduite à une séquence de 6 acides aminés (de l'acide aminé 13 au 18) en répétant la même expérience de cartographie du domaine N-terminal sur la base du mutant $6K_2^{GV}$ (voir ci-dessous). Des résidus d'acides aminés essentiels pour l'exportation de $6K_2$ à partir du RE ont été définies à l'intérieur de cette région en les remplaçant par un résidu alanine. Le résidu tryptophane en position 15 et les résidus de lysine à la position 14 et 17 ont tous été montrés comme étant importants pour l'exportation de la protéine du RE. Ainsi, un motif basé sur le tryptophane 15 a été défini pour l'exportation de $6K_2$ du RE.

J'ai aussi caractérisé le domaine transmembranaire de $6K_2$ (TMD). Par alignement de séquences, un motif GXXXG hautement conservée a été découvert. Lorsque les résidus de glycine ont été remplacés par des valines, la protéine $6K_2^{GV}$ mutée a été bloquée dans l'appareil de Golgi. Par conséquent, le motif GXXXG a été défini comme requis pour la sortie de $6K_2$ de l'appareil de Golgi.

Ces résultats suggèrent la présence d'un motif combinatoire dans $6K_2$ qui est composé du motif N-terminal d'exportation du RE et du motif TMD GXXXG pour la sortie du Golgi. Ces motifs adressent la protéine $6K_2$ dans la voie sécrétoire pour la biogenèse de la vésicule de réplication virale.

Des expériences de double hybride dans la levure et de co-immunoprécipitation nous ont permis de trouver que $6K_2$ est capable d'interagir avec Sec24a, une composante du complexe COPII. Ce coatomer reconnaît le cargo de protéines pour le diriger vers la sortie du RE. Cette interaction implique l'extrémité N-terminale de $6K_2$. En outre, cette interaction est perdue lorsque Sec24a est muté ($Sec24a^{R693K}$) au niveau du site de liaison B permettant la reconnaissance des protéines cargo.

Du fait que le mutant $6K_2^{GV}$ est retenu dans l'appareil de Golgi, j'ai enquêté sur des facteurs de l'hôte tels que des protéines SNARE résidentes du Golgi (récepteurs sensible au facteur d'activation N-éthylmaléimide soluble) potentiellement impliquées dans la biogenèse des vésicules de réplication. L'appareil de Golgi compte quelques SNAREs tel que Bet11, Gos11, Memb11 et Vamp714. Ces dernières localisent avec la protéine $6K_2$. Grâce à des expériences de co-immunoprécipitation, les Golgi SNARE Bet11, Gos11 Vamp714 se sont révélés capables d'interagir avec $6K_2$, mais pas Memb11. Ces résultats montrent que ces Golgi SNAREs sont d'autres interacteurs de $6K_2$. Ces résultats suggèrent que Sec24a et les Golgi SNAREs Bet11, Gos11 et Vamp714 sont des protéines de l'hôte capables d'interagir avec $6K_2$. L'interaction $6K_2$-Sec24a permet la sortie de la protéine virale du ER, tandis que le rôle des Golgi SNARE interagissant avec $6K_2$ demande encore de plus amples analyses.

Dans le troisième objectif, des plantes KO d'Arabidopsis thaliana et des mutants dominants négatifs ont été utilisés pour tester l'importance biologique des déterminants moléculaires de $6K_2$ (le motif d'exportation du RE et le motif GXXXG de sortie de l'appareil de Golgi) et les interactions entre $6K_2$ et des protéines de l'hôte ($6K_2$-Sec24a, $6K_2$-Golgi SNARE). J'ai utilisé un clone infectieux du TuMV doublement étiqueté avec des protéines fluorescentes (TuMV / $6K_2$: mCherry // GFP-HDEL) pour suivre le mouvement de cellule à cellule du virus. Lorsque le résidu tryptophane du motif d'export du RE a été remplacé par une alanine, le mouvement de cellule à cellule du virus a été complètement abolie. Par immunobuvardage, j'ai trouvé que le virus muté ($TuMV^{W15A}$) pouvait encore se répliquer, bien qu'à un niveau de réplication plus réduit (diminution d'environ 60%). De même, la réplication du virus a été affectée de façon importante lorsque le motif d'export du Golgi GXXXG a été muté. Dans les deux cas, le mouvement de virus a été aboli totalement.

L'importance de l'interaction $6K_2$-Sec24a a été validée en infectant la lignée G92 d'Arabidopsis thaliana, qui contient la mutation $Sec24a^{R693K}$. Le mouvement de cellule à cellule du virus et le mouvement systémique ont été retardés dans la lignée G92. De même, l'impact de l'interaction $6K_2$- Golgi SNARE a été testé en infectant de plantes knock-out pour les Golgi SNAREs correspondantes. Une infection accrue a été observée dans ces plantes KO. Ce résultat a été confirmé en co-exprimant le virus avec des mutants dominants négatifs des Golgi SNAREs. Ces résultats suggèrent que le motif d'export du RE, le motif GXXXG de sortie du Golgi ainsi que l'interaction de $6K_2$-Sec24a sont nécessaires pour avoir une réplication virale efficace et pour le mouvement viral, tandis que l'interaction $6K_2$-Golgi SNARE joue un rôle négatif dans l'infection virale.

Par conséquent mon travail a montré que:

1) Le motif N-terminal d'export du RE de la protéine virale $6K_2$ interagit avec Sec24a pour l'initiation du transport vésiculaire à partir du RE;

2) Le motif transmembranaire GXXXG de la protéine virale $6K_2$ est indispensable pour la sortie du Golgi des vésicules de réplication;

3) Certaines Golgi SNAREs sont des facteurs de restriction pour l'infection par le TuMV.

ACKNOWLEDGEMENTS

My deep gratitude goes first to my supervisor, professor Jean-François Laliberté, who expertly guided me through my PhD degree. Everything was new and challenging for me when I initiated my PhD study five years ago. My research field switched completely from the study of insect viruses to the study of plant viruses. It was very new for me and professor Laliberté was always standing by for me in case I needed any help. On a more personnel aspect, I also learned how to be a better husband and father from him. It will be forever in my memory when he happily accepted my wife to do her PhD study in this excellent team. These things changed my life!

I want to thank my co-director Dr. Huanquan Zheng (Mcgill University) for his professional advise on my research. He shared with me his deep knowledge of the field and provided me with all sorts of cellular markers, which made possible the discoveries that I made throughout my research project.

I want to thank my master supervisor Dr. Yi Li (Wuhan Bioengineering Institute). It is he who recommended me to professor Jean-François Laliberté, and thus provided me with this precious opportunity to do my PhD study at INRS-Institut Armand-Frappier.

I also want to thank Jessy Tremblay (INRS-Institut Armand-Frappier) for his expert assistance with the confocal microscopy imaging.

Many thanks to my current colleague Daniel Garcia Cabanillas, who did all the French translation for this thesis. Whenever we were together, we communicated and exchanged ideas on our research, and also what was happening throughout the world. We shared so many great moments in our life together! Thanks to my former colleague Romain Grangeon, who helped me to initiate this PhD project. Also, I much appreciated Maxime Agbeci and Fernanda Prieto Bruckner for their assistance in helping me in key experiments.

My appreciation also goes to Dr. Patrick Labonté (INRS-Institut Armand-Frappier), Dr. Chen Liang (Mcgill University) and Dr. Jacques Archambault (Université de Montréal), who agreed to evaluate this thesis.

Thanks the China Scholarship Council (CSC) provides me a four years financial support.

The last, I want to acknowledge my current colleague Juan Wan, who is also my wife, for her supports for almost ten years until now.

TABLE OF CONTENTS

LIST OF FIGURES

CHAPTER 1: INTRODUCTION

CHAPTER 2: $6K_2$ N-terminal tail and its ER export (Publication No. 1)

LIST OF TABLES

LIST OF ABBREVIATIONS

(+) RNA	positive-stranded RNA
3'-UTR	3'-untranslated region
5'-UTR	5'-untranslated region
Arf1	ADP ribosylation factor 1
AtpC	ATP-synthase γ-subunit
BaMV	Bamboo mosaic virus
BBSV	Beet black scorch virus
BFA	brefeldin A
BMV	Brome mosaic virus
bHLH	basic helix-loop-helix
bZIP	basic-domain leucine-zipper
CH25H	cholesterol 25-hydroxylas
CI	cylindrical inclusion
CIRV	Carnation Italian ringspot virus
CNV	Cucumber necrosis virus
CO-IP	co-immunoprecipitation
COOH	C-terminal end
COPI	coat protein complex I
COPII	coat protein complex II
CP	capsid protein
CPMV	Cowpea mosaic virus
CVB3	Coxsackievirus B3
DMVs	double-membrane vesicles
dsRNA	double-stranded RNA

dpi	days post infection
ECS	extra cellular space
ER	endoplasmic reticulum
EV71	Enterovirus 71
eEF1A	eukaryotic elongation factor 1A
eIF(iso)4E	eukaryotic translation initiation factor iso4E
eIF4E	eukaryotic translation initiation factor 4E
ERES	ER exit sites
ESCRT	endosomal sorting complexes required for transport
GFLV	Grapevine fanleaf virus
GFP	green fluorescent protein
HCMV	Human cytomegalovirus
HCV	Hepatitis C virus
HIV	Human immunodeficiency virus
HPV16	Human papillomavirus type 16
HSPs	heat shock proteins
HSP70	heat shock protein 70
IgG	Immunoglobulin G
LMV	Lettuce mosaic virus
MNSV	Melon necrotic spot virus
MOI	multiplicity of cellular infection
MP	movement protein
MT	microtubules
MVBs	multivesicular bodies
NH_2	N-terminal end
NPP1	N-glycosylated nucleotide pyrophosphatase/phosphodiesterase 1

ORFs	open reading frames
O-GlcNAc	O-linked N-acetylglucosamine
PABP	poly-A binding protein
PABP2	poly-A binding protein 2
PCC	Pearson’s Correlation Coefficient
PD	plasmodesmata
PIPO	Pretty Interesting *potyviridae* ORF
PI4KIIIβ	phosphatidylinositol-4-kinase IIIβ
PI4P	Phosphatidylinositol 4-phosphate
PIP	plasma membrane intrinsic protein
PDs	plasmodesmata
PE	phospholipid phosphatidylethanolamine
PKR	protein kinase
PM	plasma membrane
PMTV	Potato mop-top virus
pMVBs	peroxisomal multivesicular bodies
PPUs	pore plasmodesmal units
PPV	Plum pox virus
PVA	Potato virus A
PVX	Potato virus X
PVY	Potato virus Y
RCA	Rubisco activase
RCNMV	Red clover necrotic mosaic virus
RdRp	RNA-dependent RNA polymerase
RHPs	reticulon homology proteins
RHD3	root hair defective 3

RNP	ribonucleoprotein
RTN3	reticulon 3
RubisCO-LSU	ribulose-l,5-biphosphate carboxylase/oxygenase large subunit
SCAMP1	Secretory Carrier Membrane Protein 1
SMV	Soybean mosaic virus
SMVs	single-membrane vesicles
SNARE receptors	soluble N-ethylmaleimide-sensitive-factor attachment protein
ss +RNA	single-stranded positive-sense RNA
TBSV	Tomato bushy stunt virus
TEV	Tobacco etch virus
TGBp	triple gene block protein
TIC	translocon of the inner envelope membrane of chloroplasts
TMV	Tobacco mosaic virus
TMD	trans-membrane domain
TOC	translocon of the outer envelope membrane of chloroplasts
TOM1	Tobamovirus multiplication 1
ToMV	Tomato mosaic virus
TPR	tetratricopeptide repeats
t-SNARE	target membrane-associated SNARE
TuMV	Turnip mosaic virus
TYMV	Turnip yellow mosaic virus
UPR	unfolded protein response
VAP	vesicle-associated membrane protein-associated protein
VSV	Vesicular stomatitis virus

VPg	virus protein, genome linked
VRC	virus replication complex
vRdRp	viral RdRp
vRNA	viral RNA
vRNP	viral ribonucleoprotein
vSNARE	vesicle-associated SNARE
WT	wild type
WYMV	Wheat yellow mosaic virus
YFP	yellow fluorescent protein
YTH	yeast-two-hybrid

CHAPTER 1: INTRODUCTION

1. *Turnip mosaic virus*

Turnip mosaic virus (TuMV) represents one of the most economically important plant viruses. Among several proteins, the TuMV RNA genome encodes a small membrane-associated protein (viral protein $6K_2$, a 6 kDa protein composed of 53 amino acid residues) that manipulates the host cell endomembrane system for virus infection. This property makes TuMV one of the valuable models for studying virus-host interactions.

1.1 Taxonomy and generality

TuMV is a member of the largest genus *Potyvirus* in the family *Potyviridae*. The family *potyviridae* contains 8 genera, and as many as 190 virus species according to the recently released virus taxonomy report of the International Committee on Taxonomy of Viruses (2014). In general, the members of this family have a flexuous virus particle, of which the diameter ranges from 11 to 15 nm and the length between 650 and 950 nm.

This virus family is characterized by the production of inclusion bodies in the infected host cell. These are formed by the viral helicase, and are seen as pinwheels in the infected plant cells. The symptoms on plants infected by potyviruses may differ, but in general, plants show mosaic patterns on leaves, growth stunting, leaf curling and fruit distortion. Various transmission vectors, such as the aphid, fungi and white flies, disseminate the viruses of this family. Up to now, there is no effective chemical treatment for potyvirus infections. Instead, the most efficient way is to select for plants, or to produce transgenic plants, that are genetically resistant to the potyviruses.

1.2 Genome organization

The TuMV genome is a ~9.8 kb ss +RNA (Fig. 1). At the 5' end of the vRNA, the viral protein VPg (short for *virus protein, genome linked*) is covalently linked to the vRNA through a phosphodiester bond between the β-OH group of a serine or tyrosine residue and the 5' terminal uridine residue of the vRNA. The 3' end of the vRNA is polyadenylated. In the case of TuMV UK1 strain, the viral genome contains a 130 nt 5'-untranslated region (5'-UTR) and a 210 nt 3'-untranslated region (3'-UTR). The 5'-UTR promotes efficient, cap-independent translation of the vRNA in conjunction with the 3'-UTR (Kneller, Rakotondrafara et al. 2006). Excluding the UTRs, the remaining part of the viral genome is composed of two open reading frames (ORFs), with a short ORF embedded within the P3 cistron of the other (Chung, Miller et al. 2008). These two ORFs encode a 358 kDa polyprotein and a 7 kDa protein termed PIPO (Pretty Interesting *Potyviridae* ORF), respectively. The polyprotein is cleaved by three viral proteinases into ten mature proteins. These viral proteins are P1, HC-Pro, P3, $6K_1$, Helicase (or cylindrical inclusions), $6K_2$, VPg, Pro, RNA-dependent RNA polymerase (RdRp), and CP. PIPO is translated as a protein fusion with the N-terminal part of the viral protein P3, which is called P3N-PIPO due to the slippage at the transcriptional level (Olspert, Chung et al. 2015). These viral proteins are multifunctional, and support viral infection cooperatively (see below).

Like the other single-stranded positive-sense RNA (ss +RNA) plant viruses (Nagy and Pogany 2012), the viral RNA (vRNA) becomes naked after the penetration of the virus and the disassociation of the Capsid Protein (CP). The viral proteins are then synthesized immediately by using the invaded vRNA as the template. The resulting viral replication-related proteins initiate the progeny vRNA synthesis. After rounds of vRNA and protein synthesis, the virus movement is taking place. The plant viruses, either move as membrane-associated complexes or virions through the intercellular transport channel that is termed as plasmodesmata (PD) with the assistance of the viral movement-related proteins, and further across the plant vascular tissues for the systemic infection.

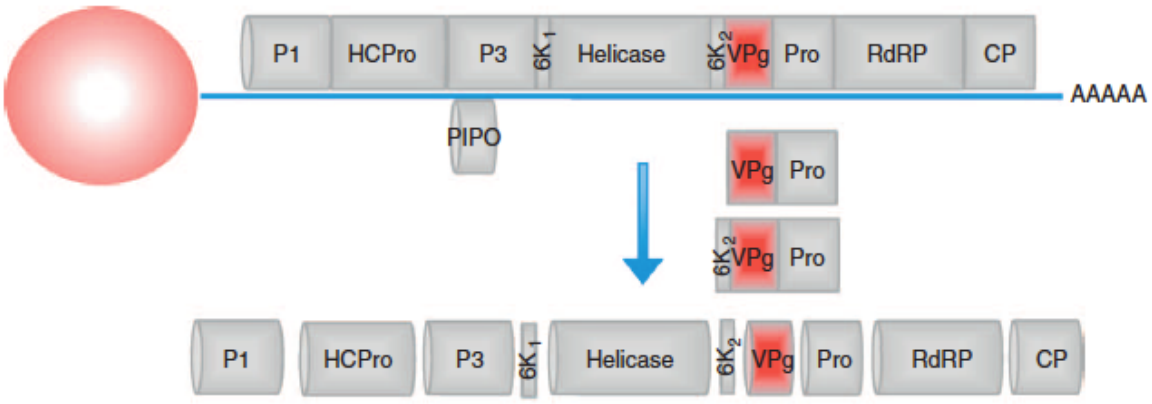

Figure 1. TuMV genome organization.

The vRNA is shown as a blue line, the covalently linked protein VPg at the 5' end of the vRNA is depicted as a red circle, and the AAAAA at the 3' end of the vRNA indicates the polyadenylated tail. The two ORFs are shown as gray rectangles, with the polyprotein shown above the vRNA and the PIPO protein shown below the vRNA. The blue arrow represents the processing event that converts the polyprotein into mature viral proteins, with the intermediates VPg-Pro and $6K_2$-VPg-Pro shown to the right. Adapted from (Jiang and Laliberte 2011).

1.3 Viral proteins

According to the relevance of the TuMV proteins related to this project, they are classified into four groups: replication vesicle inducing protein $6K_2$; replication related proteins (RdRp, VPg-Pro and helicase); movement related proteins (P3N-PIPO, HC-Pro and CP); other viral proteins (P1, P3 and $6K_1$). However, it is worth mentioning that several viral proteins are involved in both the virus replication and movement.

1.3.1 Replication vesicle inducing protein $6K_2$

Viral protein $6K_2$, which has a molecular weight of 6 kDa, is the only viral protein that induces the formation of TuMV replication vesicles (see below) (Schaad, Jensen et al. 1997). According to its predicted secondary structure, $6K_2$ is characterized as a membrane-associated protein composed of a 19-amino acid N-terminal tail, a 23-amino acid trans-membrane domain (TMD) and an 11-amino acid C-terminal tail (Fig. 2). It adopts a type II topology, where the N-terminal tail is located in the cytoplasm and the C-terminal tail is located in the lumen.

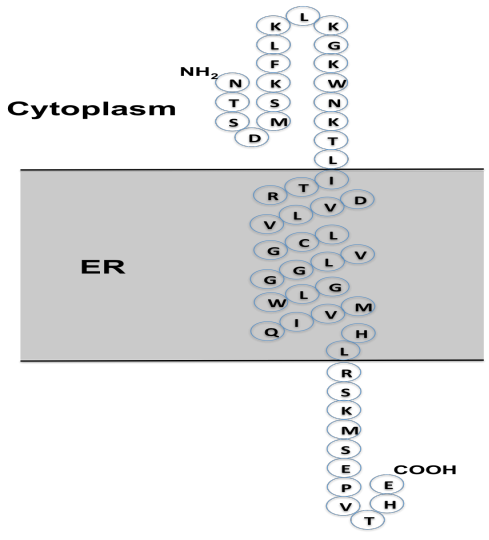

Figure 2. 6K_2 secondary structure prediction.

The amino acid residues of 6K_2 are shown in bold. The gray area that is delineated by the black lines represents the membrane lipid bilayers. NH_2, the N-terminal end; COOH, the C-terminal end; ER, endoplasmic reticulum.

1.3.2 Replication related proteins (RdRp, VPg-Pro and helicase)

Like any other RdRp, the RdRp of TuMV is responsible for vRNA synthesis. The RdRp contains two nuclear localization signals, and can shuttle between the cytoplasm and the nucleus. However, the underlying importance of this is not known. The presence of RdRp in the viral replication vesicle has been demonstrated, and may be mediated by the interaction of RdRp with both the VPg and Pro domain of $6K_2$-VPg-Pro (Li, Valdez et al. 1997, Fellers, Wan et al. 1998). The viral protein VPg can be uridylated by the RdRp, enabling VPg to act as a primer for complementary vRNA strand synthesis. Several host protein factors have been shown to interact with the RdRp. For instance, the RdRp interacts with the SUMO-Conjugating enzyme SCE1 in plant, with the lower level expression of SCE1 inhibits the TuMV infection (Xiong and Wang 2013). The RdRp also can interact with the host translation factor poly(A)-binding protein (PABP), but the function of this interaction is unknown (Wang, Ullah et al. 2000).

The helicase contains multiple RNA-binding domains (Fernandez and Garcia 1996). Its ATPase and RNA helicase activity is required for vRNA synthesis. The helicase interacts with the host photosystem I PSI-K protein, and this interaction plays a negative role in virus infection (Jiménez, López et al. 2006). Additionally, the helicase associates with the viral CP, and locates at the vicinity of plasmodesmata (PD), suggesting that it plays a role in virus movement (Rodriguez-Cerezo, Findlay et al. 1997). The helicase also functions as a pathogenic determinant (Jenner, Sanchez et al. 2000).

1.3.3 Movement related proteins (P3N-PIPO, HC-Pro and CP)

Generally, plant viruses encode proteins known as movement proteins (MPs) to facilitate the virus cell-to-cell and systemic spread. In the case of TuMV, there is no classically defined MP. However, some potyviral proteins have some properties that may classify them as MPs. The viral protein P3N-PIPO follows the secretory pathway, localizes to the PD, and move intercellularly by itself (Wei, Zhang et al. 2010, Vijayapalani, Maeshima et al. 2012). The expression level of P3N-PIPO can modulate

the deposition of TuMV helicase at the PD, which can further affect the formation of conical structure for virus movement. The PCap1 protein, a cation-binding protein that attaches to the plasma membrane (PM) via myristoylation, facilitates the PD location of P3N-PIPO (Vijayapalani, Maeshima et al. 2012). The host protein Synaptotagmin A that regulates the endomembrane protein trafficking, enhances the intercellular movement of P3N-PIPO (Uchiyama, Shimada-Beltran et al. 2014). Furthermore, P3N-PIPO is a virulence determinant in plants resistant to potyvirus (Choi, Hagiwara-Komoda et al. 2013).

The protein HC-Pro is a multifunctional protein. Three domains can be distinguished in the HC-Pro protein, with the N-terminal domain being required for aphid transmission, the central domain for suppression of host antiviral RNA silencing and the C-terminal domain for viral protease activity (Plisson, Drucker et al. 2003). The HC-Pro has been demonstrated to play a role in virus movement (Rojas, Zerbini et al. 1997). It has a diverse cellular distribution, with a pattern of uniform distribution throughout the cytoplasm, as large amorphous cytoplasmic inclusions, or as small dot-like inclusions in the cytoplasm that associate with the endoplasmic reticulum (ER) and microtubules (MT), or overlaps with MT (del Toro, Fernandez et al. 2014). HC-Pro interacts with several other viral proteins, such as the helicase, P1 and VPg-Pro. Meanwhile, many host protein interactors of HC-Pro have been identified. For example, HC-Pro interacts with the MT-associated protein HIP2 that is important for virus infection (Haikonen, Rajamaki et al. 2013); HC-Pro interacts with the chloroplast precursor of ferredoxin-5, which may lead to the perturbation of the chloroplast structure and function (Cheng, Liu et al. 2008). Recently, it has been shown that HC-Pro enhances the stability of viral CP and upregulates the yield of virions, resulting in the production of a virus progeny that is more infectious (Valli, Gallo et al. 2014).

The CP is necessary for virus particle assembly, and viral intercellular and long-distance movement. Up to 2000 copies of the CP form the protective shield of the virus particle. Structurally, the variable N- and C-terminal domains of the CP are exposed on the surface of the particle and enable inter-subunit interactions, thus facilitating assembly of

the virus particle (Anindya and Savithri 2003). Further characterization shows that the N- and C-terminal domains are required for the virus long-distance movement, while the central domain is essential for virus intercellular movement. Viral protein CP can also increase the size exclusion limit of the PD, prompting the transmission of virus infection. Posttranslational modifications, such as phosphorylation and O-GlcNAcylation, have been documented for the CP protein (Ivanov, Puustinen et al. 2003, Pérez, Udeshi et al. 2013).

1.3.4 Other viral proteins (P1, P3 and 6K1)

The viral protein P1, the N-terminal product of the polyprotein, is well known as one of the viral proteinases. It functions by an autoproteolytic mechanism at the junction of P1 and HC-Pro, and leads to the release of viral protein P1 from the polyprotein (Verchot, Koonin et al. 1991). The N-terminal portion of P1, which is the non-proteolytic domain, is dispensable for the virus infection. In contrast, the C-terminal part that contains the proteolytic domain and the protease cleavage recognition site is required for the virus viability. Further investigations showed that the protease recognition site, but not the proteolytic domain, is essential for virus infection (Verchot and Carrington 1995).

P1 is also a nucleic acid-binding protein (Soumounou and Laliberte 1994). By immunogold labeling, the P1 protein was found to associate with the inclusions induced by the helicase (Arbatova, Lehto et al. 1998). More recent data show that P1 displays a dynamic subcellular location, with the protein moving in and out of the nucleus at the early stage of virus infection (Martinez and Daros 2014). The deletion of P1 affects virus replication, and the virus cell-to-cell and systemic movement occurs at a reduced rate. When P1 was provided in trans, the virus replication level was enhanced several folds, suggesting a role for P1 in virus replication (Verchot and Carrington 1995). P1 was found to interact with the host 60S ribosomal subunits during infection, which stimulates the translation of the viral proteins (Martinez and Daros 2014).

P3 is characterized as a plant pathogenicity determinant. By exchanging the P3 genome fragments of two TuMV isolates, the UK1 and CDN1 strains showed switched infection symptoms. P3 was shown to determine the infection phenotype and the avirulence of TuMV (Jenner, Wang et al. 2003). Similar conclusions were obtained by comparing two other TuMV isolates (Suehiro, Natsuaki et al. 2004). Furthermore, the precursor protein P3-$6K_1$ also has been suggested to be a symptom determinant, while the cleavage of this precursor protein may play a regulatory role during virus infection (Riechmann, Cervera et al. 1995). On the other hand, P3 is also involved in virus replication. By immunogold labeling, P3 was found to associate with the viral replicase in infected cells (Rodriguez-Cerezo, Ammar et al. 1993). P3 localizes to the ER and forms punctate vesicles in association with the Golgi apparatus by following the early secretory pathway (Cui, Wei et al. 2010). These punctate structures also co-localize with the $6K_2$-induced replication vesicles. Additionally, viral protein P3 also interacts with host proteins, such as RuBisCo and actin-depolymerizing factor 2 (Lin, Luo et al. 2011, Lu, Wu et al. 2015).

No function of $6K_1$ has been reported, despite the fact that $6K_1$ is present as a mature protein during virus infection (Waltermann and Maiss 2006). The only information is that $6K_1$ is a soluble protein, although its predicted secondary structure suggests it is a membrane-associated protein (Jiang, Patarroyo et al. 2015)

2. Plant cell secretory pathway

Plant viruses have been shown to require the secretory pathway for infection of the host cell (see below). Consequently, an overview of this pathway is given here.

The plant cell secretory pathway is comprised of membrane compartments, such as the ER, the Golgi apparatus, the cytoplasm-limiting PM and furthermore the extra cellular space (ECS). These organelles contain specialized sets of components, thus enabling them to carry out their characteristic metabolic reactions efficiently, and further play important physiological roles during plant development. Active material exchange occurs among these organelles, making them functionally interlinked. Among these organelles, the ER and the Golgi apparatus are extremely important, as they are the gateway of the secretory pathway for the former and a sorting station for the later.

2.1 The ER and Golgi apparatus

The ER is the largest organelle of the endomembrane system. Morphologically, the ER of a plant cell is a polygonal network of sheets (also called cisternae) and tubules (Fig. 3A). It is connected with the nuclear envelope membrane, and is attached to the PM. Under certain situations, such as during cell division or in the presence of environmental stresses, the ER undergoes tubule-sheet shape transition (Gupton, Collings et al. 2006). Protein factors, such as the reticulons, DP1/Yop1 and Climp63, maintain and regulate the shape of the ER. The protein reticulons are enriched at the edges of the sheets and in highly bent tubules, while the Climp63 is only found in the sheets of the ER (Fig. 3B-C). The atlastin family of dynamin-like large GTPase, comprising the root hair defective 3 (RHD3), makes the ER an interconnected network (Chen, Stefano et al. 2011). Functionally, the ER is involved in protein synthesis, folding, modification, and trafficking. The ER is connected to many other organelles, thus giving rise to several different cellular trafficking pathways.

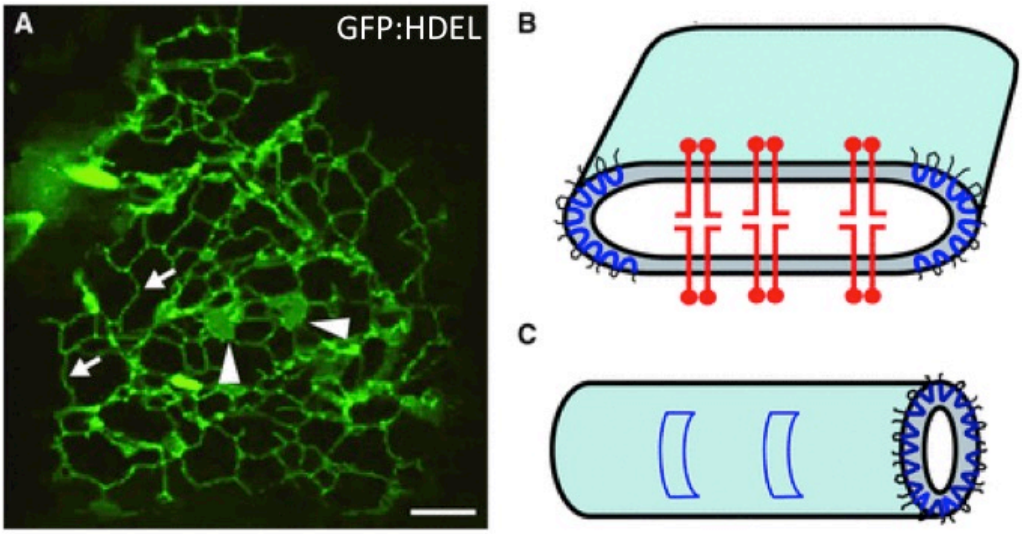

Figure 3. Morphology of the ER highlighted by GFP:HDEL.

(A) A spinning-disc image of mature *Arabidopsis thaliana* epidermal cell expressing GFP:HDEL. The ER tubules are indicated by the white arrows, and the ER sheets are indicated by the white arrowheads. Schematic diagrams showing the sheet (B) and the tubule (C) of the ER. The curvature - stabilizing protein reticulons (blue colored) and the sheet - inducing protein Climp63 (red colored) are shown. Images taken from (Chen, Doyle et al. 2012).

The Golgi apparatus consists of dispersed and functionally independent cisternae, with about 5-7 cisternae of each unit typically. These cisternae exhibit a polar organization both with respect to their architecture and their function, and are classified as the cis-, the medial- and the trans-Golgi cisternae. In contrast to most animal cells, the plant cell Golgi apparatus is widely distributed in the cytoplasm (Fig. 4A). The Golgi apparatus moves along actin tracks with periods of rapid movements alternating with slower and more wiggling motions. Although the Golgi apparatus was discovered more than one hundred years ago, there are several basic scientific questions that still need to be answered. For instance, how does the Golgi apparatus multiply?

To answer how the Golgi apparatus multiplies, three models have been proposed. The first one is the ‘disintegration and reassembly model’, suggesting that the components are derived from pre-existing Golgi. The second one is the ‘de novo construction model’, proposing that the Golgi apparatus is assembled from original building blocks. The third one is the ‘fission model’ that resembles the process of cell division. Electron tomography-generated three-dimensional reconstruction supports this model of Golgi division, with the assembling cis-and medial-Golgi cisternae being held together by a larger trans-Golgi cisterna (Fig. 4B). Furthermore, deeper characterization of the interplay between viral or host proteins with the Golgi apparatus is helpful to uncover how the Golgi apparatus functions.

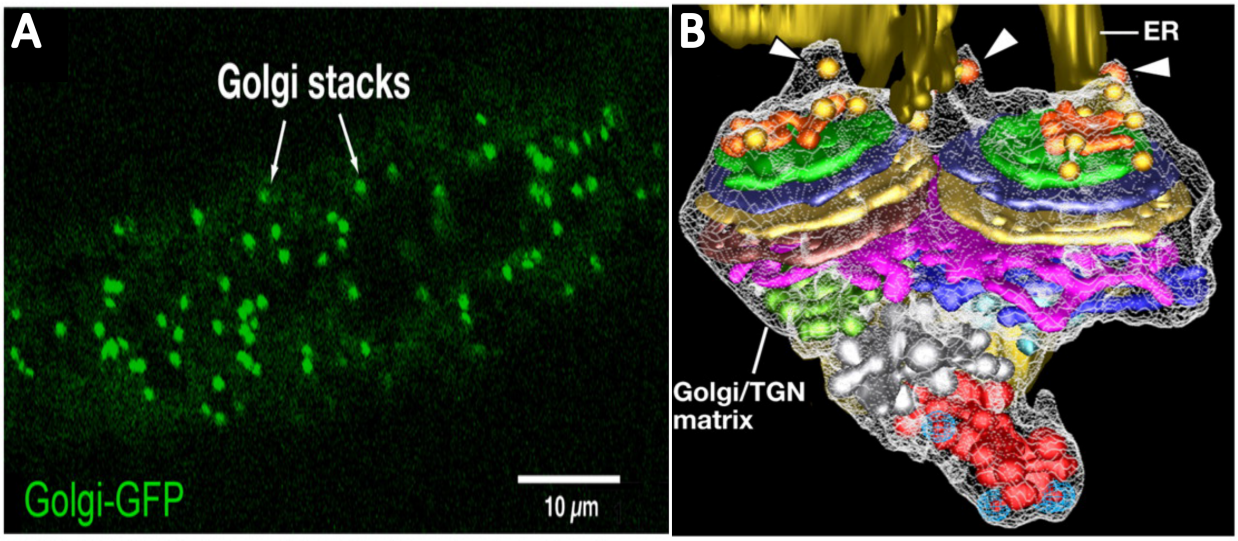

Figure 4. Plant cell Golgi apparatus.

(A) Fluorescent imaging of the Golgi apparatus in a Tobacco BY-2 cell expressing the Golgi marker α-1,2 mannosidase I:GFP fusion protein. (B) Three-dimensional tomography of a dividing Golgi apparatus in an Arabidopsis root meristem cell. The two most cis-cisternae of two Golgi apparatus are shown in orange and green, and the larger trans-cisternae shared by these two dividing Golgi apparatus is shown in pink. Images taken from (Staehelin and Kang 2008).

2.2 The secretory pathway

The secretory pathway is highly dynamic, and responds to environmental changes for the maintenance of the cell homeostasis. Accordingly, the secretory pathway can be subdivided into the early secretory pathway and the post-Golgi secretory pathway.

2.2.1 The early secretory pathway (ER-Golgi)

The early secretory pathway, which is composed of the ER and Golgi apparatus, functions in the proteins and lipids vesicular transport (Brandizzi and Barlowe 2013). Anterograde trafficking initiates as the cargo is being synthesized on the rough ER and incorporated into coat protein complex II (COPII) vesicles for Golgi targeting and proceeds until the cargo is sorted to its proper cellular destination. Retrograde trafficking, which goes in the reverse direction, occurs via coat protein complex I (COPI) vesicles and maintains the membrane integrity of ER. The guanine nucleotide exchange factor (GEF) Sec12 recruits the GTPase Sar1 to the ER exit sites (ERES), where the COPII coatomers Sec23-Sec24 and Sec13-Sec31 are gathered to initiate the ER-Golgi vesicular transport (Brandizzi and Barlowe 2013) (Fig. 5A). In parallel, the GTPase Arf1 facilitates the assembly of COPI coatomers on the Golgi membrane (Beck, Ravet et al. 2009) (Fig. 5B). Other proteins, such as the Rab GTPase and soluble N-ethylmaleimide-sensitive factor activating protein receptors (SNAREs), mediate the fusion of COPII- and COPI-vesicles with their target membranes.

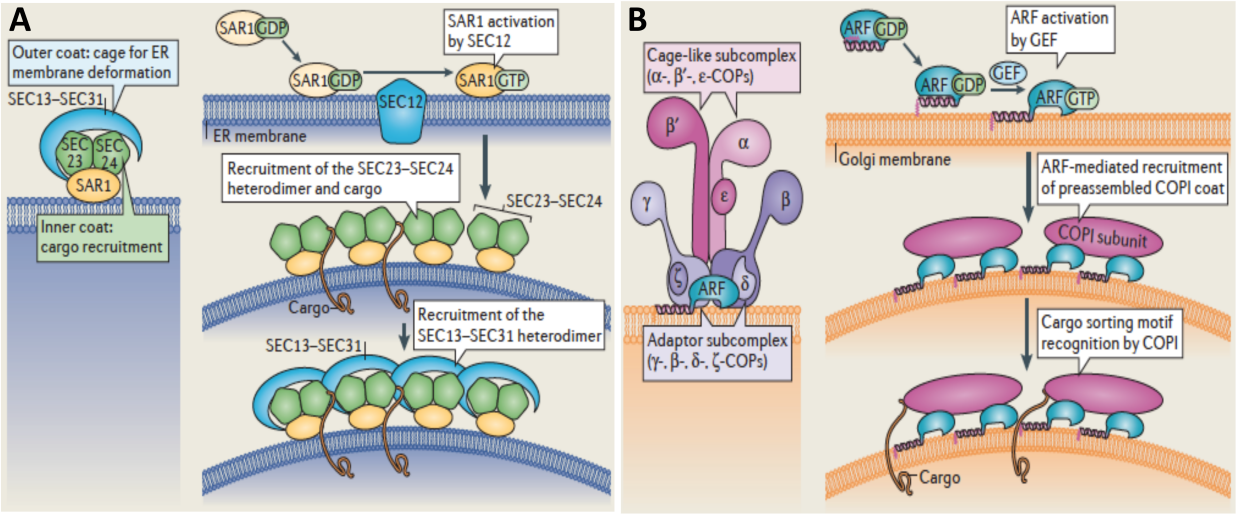

Figure 5. Diagram representation of COPII and COPI dependent ER-Golgi early secretory pathway.

(A) The ER membrane-anchored guanine nucleotide exchange factor (GEF) Sec12 activates the GTPase Sar1, and then the inner COPII coatomer Sec23-Sec24 and the outer coatomer Sec13-Sec31 are further recruited for the ER membrane deformation, resulting in the formation of COPII vesicle. (B) The ADP-ribosylation factor GEF activates the GTPase Arf, and the COPI coatomer subunits are then recruited. The assembled COPII and COPI coatomer complex is presented on the left side of each image. Images taken from (Brandizzi and Barlowe 2013).

The ‘dock, pluck and go’ model explains how the ER-derived COPII vesicle targets the cis-Golgi cisternae for cargo transport (Fig. 6). It suggests that the Golgi apparatus is induced by a ‘signal’, which maybe the ER exit signal located in the cargo, to stop at the ERES. The COPII vesicle then associates and fuses with the cis-Golgi cisternae in the vicinity. Finally, the Golgi apparatus resumes its original cellular movement that is performed at a higher speed.

To answer the question of the mechanism of cargo intra-Golgi transport, two models termed ‘vesicle shuttle’ and ‘cisternal progression/maturation’ have been proposed. The vesicle shuttle hypothesis proposes that the Golgi cisternae are quite stable, and the shuttling vesicles engulf the cargo for the cis- to medial-, and then to trans-Golgi trafficking. In contrast, the cisternae maturation model suggests that the cargo is stably associated with each individual cisternae, with the novel cisternae formed on the cis-side and the fragmentation of the old cisternae on the trans-side. At this stage, it is still unknown which model is more accurate.

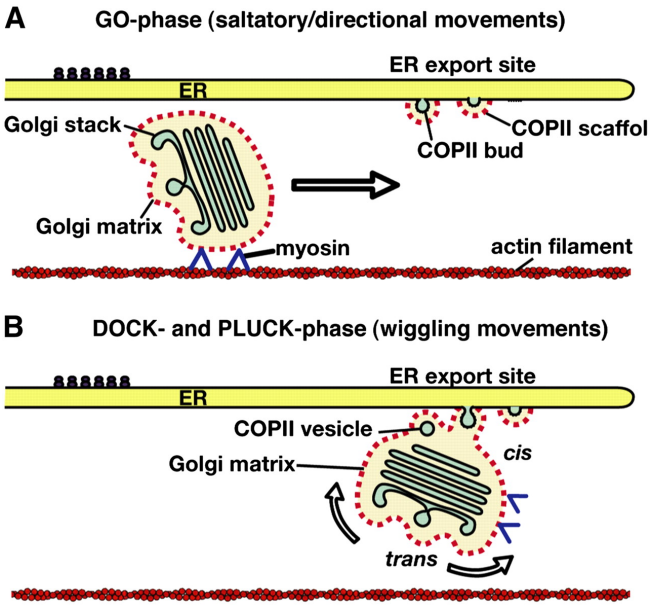

Figure 6. The 'dock, pluck and go' model of ER-Golgi vesicular transport.

(A) The Golgi apparatus traffics along an actin microfilament, being propelled by myosin motors. (B) The COPII vesicle attaches to the cis-Golgi cisternae and pulls the Golgi apparatus off the actin filament. Once the COPII vesicle has fused with the Golgi apparatus, the latter is then released by plucking. The Golgi apparatus then resumes its cellular movement. Image taken from (Staehelin and Kang 2008).

2.2.2 The post-Golgi secretory pathway (Golgi-PM-ECS)

The cargo, for instance metabolic enzymes, may reside in the Golgi apparatus. The other cargo, such as the ER-resident proteins that escaped from the ER, can be retrieved back to the ER. However, many other cargos are further selectively transported to the PM or the ECS. Generally, these cargos play critical roles in responding to exogenous environmental cues. By comparison, the trafficking route Golgi-PM-ECS is not well defined. For instance, the machinery involved is not extensively characterized; the mechanism for cargo protein targeting, especially in the case of soluble proteins, is unknown. However, it has been found that the targeting of several PM-located proteins, such as the protein family aquaporins, is signal dependent (Hachez, Besserer et al. 2013).

2.3 The component Sec24 and SNAREs

Many different components work together to maintain the proper function of the secretory pathway. In many cases, the COPII coatomer Sec24 selectively incorporate the cargo into the transport vesicle at ER. The accurate vesicle targeting is then mediated by the Rab GTPases and the SNAREs, with the Rab GTPases recognize the tethering factors that are located on the target membranes and the SNAREs bring the vesicle membrane and target membrane close enough for membrane fusion to take place. Here, the Sec24 and SNAREs are introduced.

2.3.1 Selective cargo incorporation by Sec24

The COPII coatomers Sec23 and Sec24 have similar structures. These two proteins are both composed of five structural domains, including the 'truck' domain, the zinc-finger domain, the α-helical domain, the β-barrel domain and the gelsolin domain (Fig. 7) (Lee and Miller 2007). However, Sec24 is the only coatomer thought to recognize cargos that are incorporated into COPII vesicles (Miller, Antonny et al. 2002). The multiple cargo binding sites of Sec24 are functionally independent and can recognize the export signal located in the cargo (Fig. 7) (Mossessova, Bickford et al. 2003). The Arabidopsis genome encodes three types of Sec24 homologs (AtSec24a, AtSec24b and AtSec24c). All these Sec24s have a similar expression level and cellular distribution pattern. AtSec24a has been shown to be involved in protein COPII-dependent ER-Golgi apparatus transport (Faso, Chen et al. 2009), while AtSec24b and AtSec24c may have a similar cellular function that is essential in male and female gametogenesis (Tanaka, Nishimura et al. 2013).

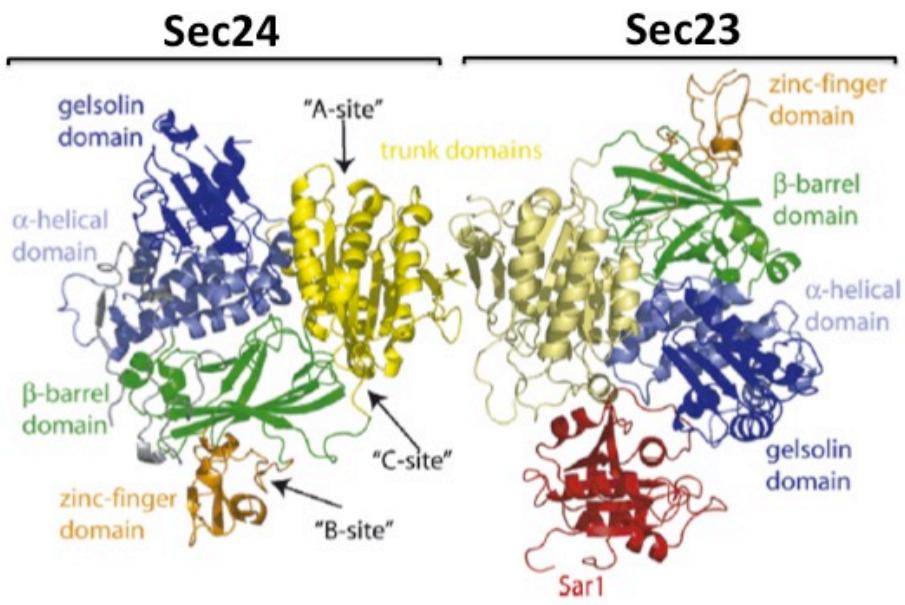

Figure 7. Domain arrangement of COPII coatomer Sec24 and Sec23.

The interacting COPII GTPase Sar1 is colored in red and Sec23 and Sec24 are colored according to their domain structures as indicated. The three cargo binding sites (A-site, B-site and C-site) of Sec24 are indicated. Image adapted from (Lee and Miller 2007).

2.3.2 Vesicle fusion fidelity conferred by SNAREs

In general, SNAREs are trans-membrane proteins characterized by a specific domain termed the SNARE motif that is located in their cytoplasmic tail. The fact that only certain combinations of SNARE motifs can recognize each other and interact, ensures proper vesicle fusion events to take place. Simply, these SNAREs can be classified as vesicle-associated SNARE (v-SNARE) or target membrane-associated SNARE (t-SNARE). Once the cargo has been incorporated into the vesicle, the other factors such as the Rab GTP tethers the vesicle to target membranes. The associated v-SNARE then recognizes three t-SNAREs, forming a hetero-tetrameric complex that brings two lipid bilayers together for the vesicle fusion to occur (Fig.8).

Plant viruses can actively modify these membrane compartments during virus infection. By hijacking host cell secretory pathway components, viruses can utilize this secretory pathway for the formation of replication vesicles (see below).

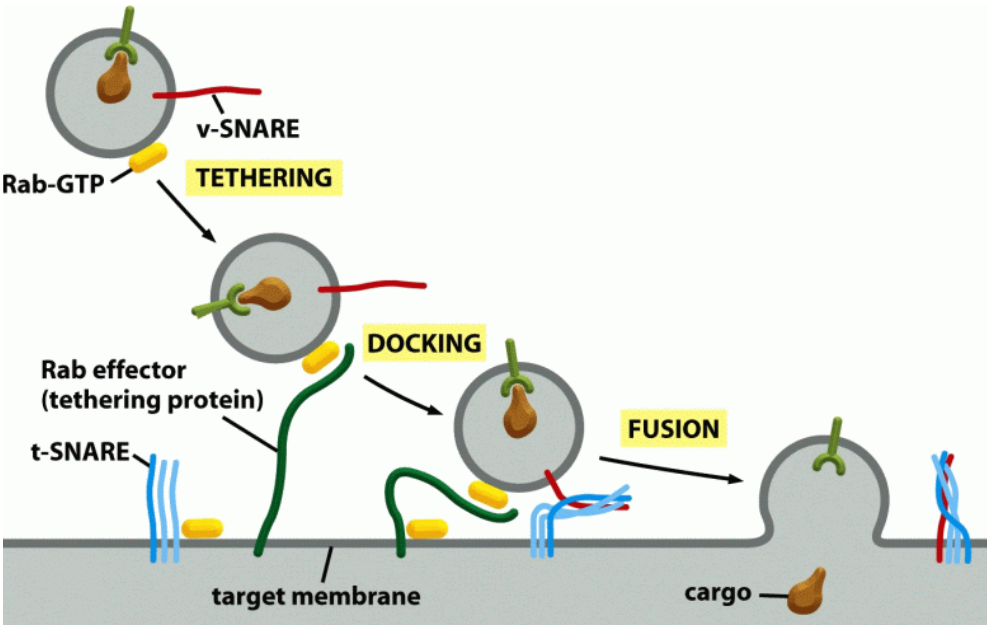

Figure 8. The SNAREs mediated vesicle fusion.

The transport vesicle associated Rab-GTP (colored in yellow) recognizes the Rab effector (also called tethering protein, colored in dark green) that is located in the target membrane. The v-SNARE (colored in red) then interacts with the t-SNAREs (colored in blue), and brings the membrane together for fusion and leads to the release of the cargo to the proper cellular locations. Image adapted from (Bruce Alberts 2007).

3. TuMV-induced cellular remodeling

TuMV infection actively modifies the host cell endomembrane system, leading to the formation of replication vesicles. Those replication vesicles, induced by the $6K_2$ protein, originate from the ER membrane (Schaad, Jensen et al. 1997, Beauchemin and Laliberté 2007). By inserting the coding sequence of $6K_2$:GFP (or $6K_2$:mCherry) into the TuMV infectious clone (Fig. 9A), the virus-induced replication vesicles can be visualized using confocal laser scanning microscopy. TuMV infection induces the formation of numerous heterogeneously sized vesicles (diameter range from 0.6 - 4.3 µm) as well as the production of one or two ER amalgamates (diameter range from 9 - 15 µm) that more often is located in the perinuclear region (Fig. 9B) (Cotton, Grangeon et al. 2009, Grangeon, Agbeci et al. 2012). At the ultrastructural level, ER dilation is observed early in infection, which is followed by the formation of single membrane vesicles (SMVs) and double membrane vesicles (DMVs) (Grangeon, Agbeci et al. 2012, Wan, Basu et al. 2015) (Fig. 9C). The ER amalgamate is made of convoluted membranes, as observed under electron microscopy (Wan, Basu et al. 2015). Those vesicles can fuse with the ER amalgamates, or exit from the ER amalgamates (Grangeon, Agbeci et al. 2012).

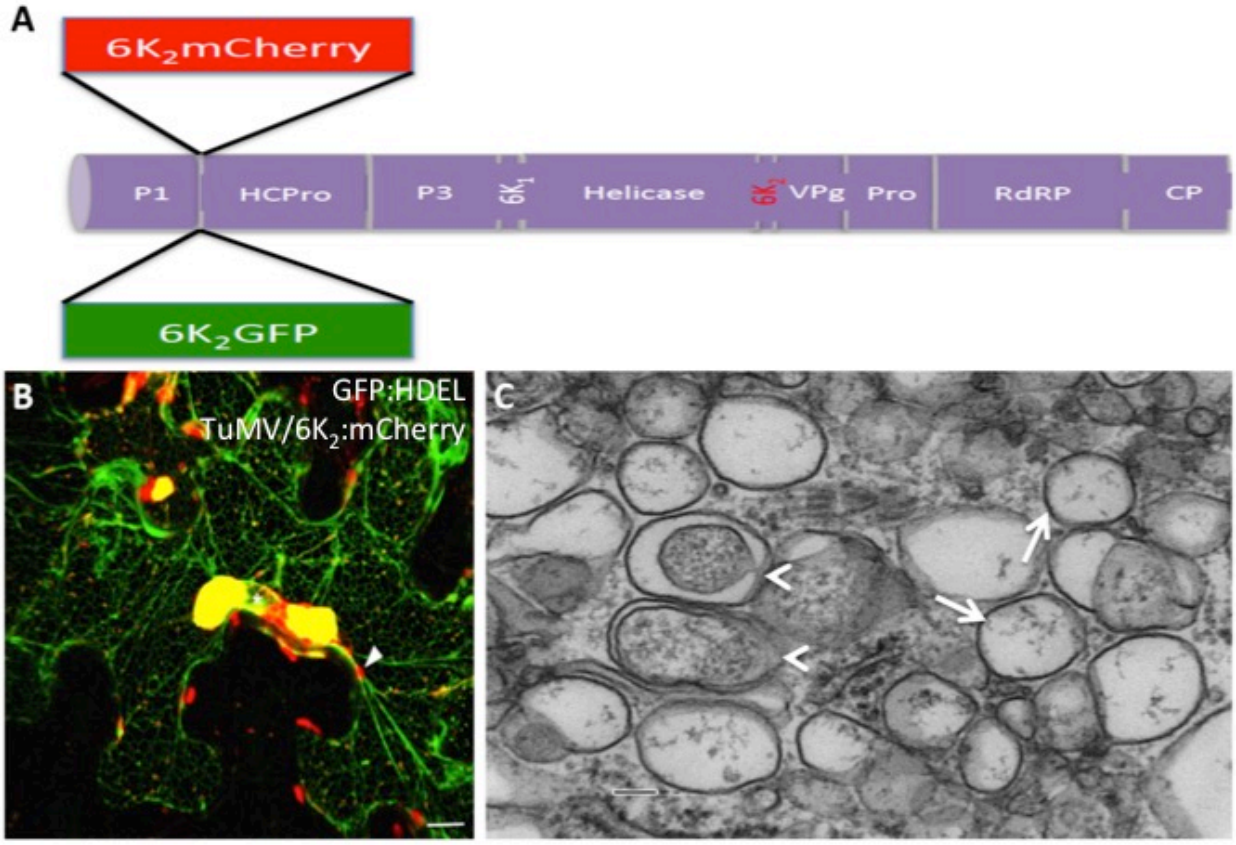

Figure 9. Fluorescent tagging of TuMV infectious clone.

(A) Coding sequence of $6K_2$:mCherry (shown in red) or $6K_2$:GFP (shown in green) was inserted into the TuMV infectious clone (shown in purple) between the viral protein P1 and HC-Pro, and the resulting construct is TuMV/$6K_2$:mCherry or TuMV/$6K_2$:GFP. An epidermal cell co-expressing TuMV/$6K_2$:mCherry with ER marker GFP:HDEL is shown in (B). (C) The single membrane vesicles (indicated by arrows) and double membrane vesicles (indicated by arrowheads) induced by TuMV in a *N. benthamiana* cell. Image (B) is taken from (Grangeon, Agbeci et al. 2012), (C) is taken from (Wan, Basu et al. 2015).

Those replication vesicles contain components that are required for vRNA synthesis. Those identified host factors include eukaryotic translation initiation factor (iso) 4E [eIF(iso)4E], eukaryotic translation initiation factor 1A (eIF1A) and poly(A) binding protein 2 (PABP2), as well as the viral proteins VPg-Pro, viral RNA-dependent RNA polymerase (vRdRp) and helicase (Cotton, Grangeon et al. 2009). The polyprotein cleavage intermediate $6K_2$-VPg-Pro can recruit more host and viral factors (Fig. 10), resulting in the assembly of a much larger virus replication complex (VRC).

Besides its role in vRNA synthesis, the replication vesicle also supports the virus intracellular and intercellular movement. The intracellular trafficking of the vesicle requires microfilaments, and the presence of a microfilament depolymerizing reagent thus impairs virus movement (Cotton, Grangeon et al. 2009). The vesicle is highly dynamic, with an average velocities of 0.45 ± 0.27 μm/s (Cotton, Grangeon et al. 2009). The vesicle, together with its infectious content, reaches the PD (Grangeon, Jiang et al. 2013). Ultimately, the vesicle crosses the PD and initiates a new round of virus infection in the adjacent non-infected cells (Grangeon, Jiang et al. 2013).

However, it is still unknown how the viral protein $6K_2$ induces the formation of replication vesicles. In particular, what are the molecular determinants of $6K_2$ needed for the production of replication vesicles? Which host factors are involved in the cellular biogenesis of replication vesicles?

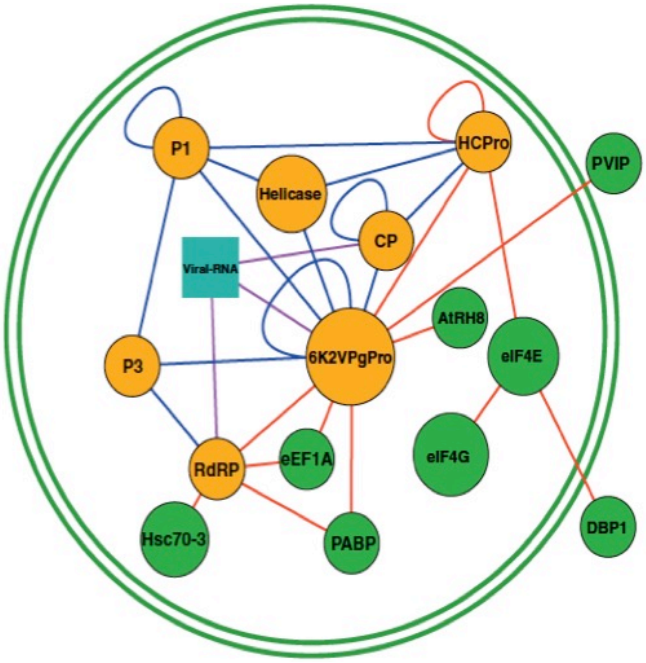

Figure 10. The protein interaction network between the viral and host factors within the TuMV replication vesicle.

The TuMV replication vesicle is indicated by the double solid green line. The viral proteins are shown in orange, the host proteins are shown in green and the vRNA is shown in light blue. Taken from (Jiang and Laliberte 2011).

Note: The following sections 4-8 are adapted from a book chapter: Jiang, J. and Laliberté, J.F. Current Topics in Plant Virology: Membrane association for plant virus replication and movement, Springer. (expected October 2015)

4. Cellular remodeling by other plant viruses

Similar to TuMV, the replication of the other (+) RNA plant viruses highly depends on the plant cell endomembrane system. In the presence of a virus infection, extensive endomembrane reorganization is taking place. This leads to the formation of viral factories that house the VRCs. The architecture of these viral factories differs among different viruses, although similarities exist.

4.1 Spherule-shape viral factories

Some (+) RNA plant virus infections lead to the formation of spherules, which are 50-400 nm sized membranous invaginations of the limiting membrane of organelles, such as the peroxisome, the mitochondrion and the chloroplast (Prod'homme, Jakubiec et al. 2003, McCartney, Greenwood et al. 2005, Hwang, McCartney et al. 2008). One common characteristic of these different spherules is that they are static, in opposition to the motile, ER-derived, vesicular-shape viral factories (see below).

Infection by *Tomato bushy stunt virus* (TBSV) or *Cucumber necrosis virus* (CNV) causes the formation of multivesicular bodies (MVBs) (Fig. 11A) (Russo and Martelli 1972, Rochon, Singh et al. 2014). These MVBs contain spherical to ovoid compartments of 80-150 nm in diameter that are progressively formed by inward invagination of the boundary membrane of the peroxisome (Russo, Di Franco et al. 1983). The interior of the spherules is connected to the cytoplasm through pores (Fig. 11A) that allow the import of replication proteins and vRNA templates and the export of progeny vRNAs. Other viruses, such as the *Carnation Italian ringspot virus* (CIRV) and the *Melon necrotic spot virus* (MNSV), also induce the production of MVBs, but from the

mitochondrial membrane (Hwang, McCartney et al. 2008, Gomez-Aix, Garcia-Garcia et al. 2015).

In few cases, (+) RNA plant virus-induced spherules are derived from the ER membrane. *Brome mosaic virus* (BMV) induces the invagination of the perinuclear ER membrane, leading to the formation of 50-70 nm spherules in its surrogate host yeast cell (Fig. 11B) (Schwartz, Chen et al.). Under certain situations, the large, karmellae-like, multilayer stacks of appressed double membrane structures are formed instead of the spherical compartments (Fig. 11C) (Schwartz, Chen et al. 2004). Replication of *Beet black scorch virus* (BBSV) is also confined within the ER-derived spherules (Fig. 11D) (Cao, Jin et al. 2015). A three-dimensional electron tomographic reconstruction shows the presence of multiple ER-derived vesicle packets (Fig. 11E). Each vesicle packet contains few to hundreds of independent spherules that result from the invaginations of the ER membrane. Each packet is connected to other packets through the formation of tubules, a rare rearrangement event among virus-induced membrane reorganizations. The interior of the spherules contains condensed or fibrillar materials that are presumably nucleic acids.

The morphology of these spherules is well characterized, and it is acknowledged that vRNA replication is taking place within these structures. However, not much is known about how viral proteins and vRNA templates are targeted to these sites, and how progeny vRNAs leave these compartments. Furthermore, how other virus replication processes, such as vRNA translation, encapsidation and intracellular movement are linked to the spherules remains elusive.

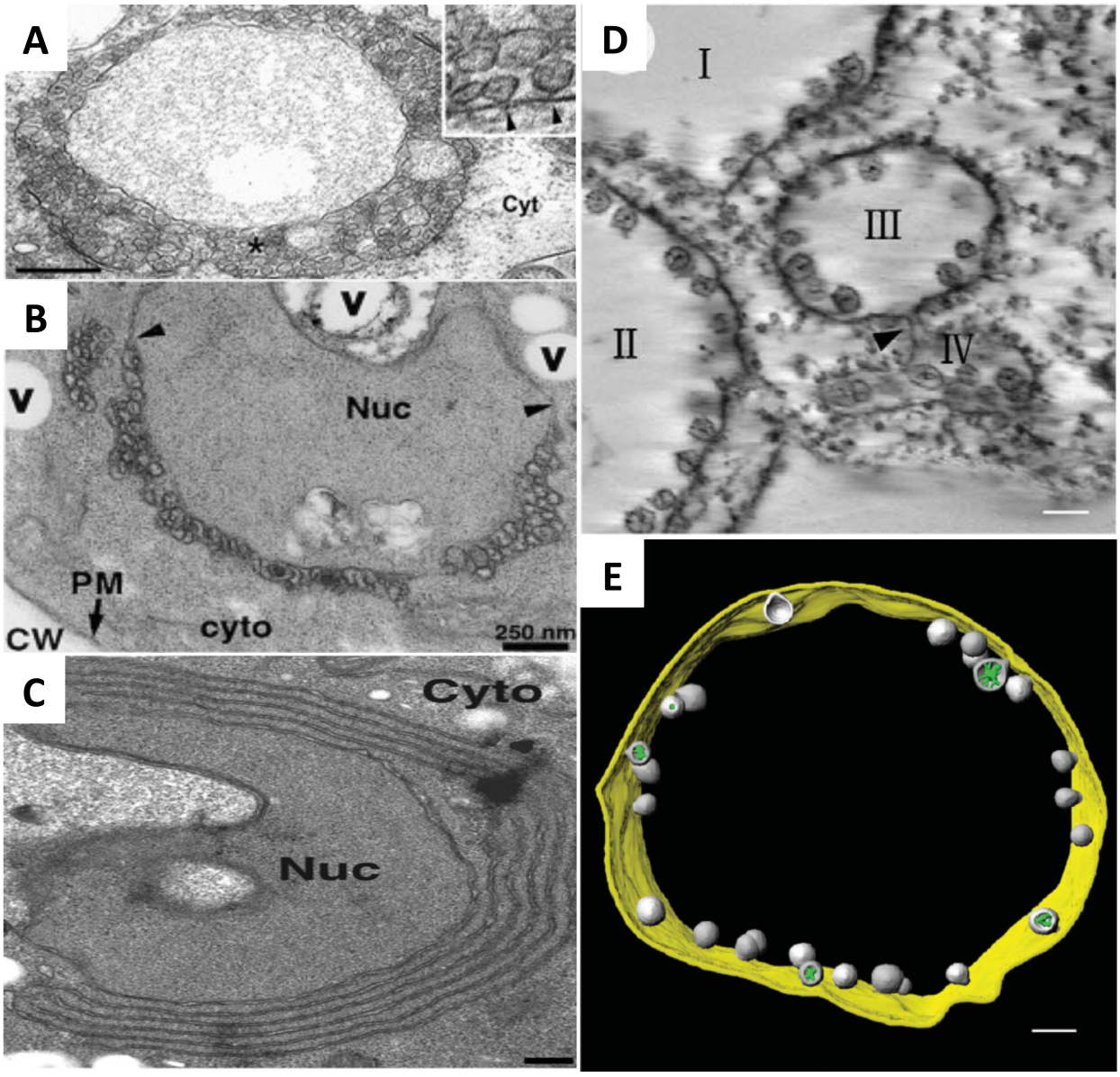

Figure 11. Plant virus-induced membrane remodeling.

(A) Electron micrograph of TBSV-induced MVBs (indicated by star) in a *N. benthamiana* mesophyll cell. The arrowheads in the inset denote the pores that connect the interior of the spherules with the cytoplasm. (B) The perinuclear ER-derived spherules induced by the membrane-associated viral 1a protein of BMV, in its surrogate host yeast cell. Similar spherules are seen in the cells expressing the 1a protein plus low level of $2a^{pol}$ protein. The arrowheads indicate the perinuclear ER, and the arrow indicates the

plasma membrane. (C) In the presence of 1a and high level of $2a^{pol}$ protein, the double membrane multilayer structures are formed. (D) The ER-derived vesicle packets (indicated by I, II, III, IV) induced by BBSV in a *N. benthamiana* cell. The arrowhead points to the tubule that connects the vesicle packets. (E) The three dimensional view of a single vesicle packet is shown. Gold color denotes the ER membrane, gray the BBSV-induced spherules, and green the fibrillar materials within the spherules. Bar in (A) = 500 nm, Bars in (C-E) = 100 nm. Cyt or Cyto, cytoplasm ; Nuc, nucleus; PM, plasma membrane ; V, vacuole ; CW, cell wall. Image (A) is reproduced from (McCartney, Greenwood et al. 2005); (B) is adapted from (Schwartz, Chen et al. 2002); (C) is adapted from (Schwartz, Chen et al. 2004); (D) and (E) are taken from (Cao, Jin et al. 2015).

4.2 Vesicle-shape viral factories

More frequently, (+) RNA plant virus infection leads to the reorganization of the ER for the production of motile vesicles, which range from 30 to 300 nm in diameter. These ER-derived vesicles have been observed during infection by *Grapevine fanleaf virus* (GFLV), *Cowpea mosaic virus* (CPMV), *Tomato mosaic virus* (ToMV), *Bamboo mosaic virus* (BaMV), *Potato virus X* (PVX) and *Tobacco mosaic virus* (TMV) (Carette, Stuiver et al. 2000, Ritzenthaler, Laporte et al. 2002, Mitra, Krishnamurthy et al. 2003, Kawakami, Watanabe et al. 2004, Cotton, Grangeon et al. 2009, Wu, Lee et al. 2011).

These ER-derived vesicles contain several viral and host proteins. However, limited characterization has been carried out to identify the components of these replication vesicles. Host factors, such as the heat shock proteins (HSPs) and the eukaryotic translation factors, are commonly hijacked and relocated into the replication vesicles (Nishikiori, Dohi et al. 2006, Cotton, Grangeon et al. 2009). In the case of ToMV infection, the replication vesicles also contain the host factors *Tobamovirus multiplication* 1 (TOM1) and TOM2A that are required for efficient virus replication (Nishikiori, Dohi et al. 2006). The chloroplast proteins, such as the ATP-synthase γ-subunit (AtpC) and Rubisco activase (RCA), are also recruited to the TMV-induced replication vesicles and involved in defense response (Bhat, Folimonova et al. 2013).

These vesicles are motile and are involved in the intracellular movement of the vRNA. The trafficking of ER-derived vesicles requires the ER/actin network (Heinlein, Padgett et al. 1998, Cotton, Grangeon et al. 2009, Genoves, Navarro et al. 2009, Cui, Wei et al. 2010). In particular, the motility of these vesicles highly depends on myosin XI-K (Kawakami, Watanabe et al. 2004, Amari, Lerich et al. 2011, Peremyslov, Klocko et al. 2012, Agbeci, Grangeon et al. 2013). Different steps of virus infection need distinct myosins. For instance, class XI myosins contribute mainly to TMV intracellular propagation and trafficking, whereas class VIII myosins are specifically required for MP targeting and moving the virus infectious unit across the PD (Amari, Di Donato et al.

2014). In contrast, the intracellular vRNA movement is more often microtubule-based for animal viruses (Dohner and Sodeik 2005).

5. Lipids for virus infection

Plant virus infections actively rearrange the pre-existing host cell endomembrane system. Very often, the infection by a plant virus induces the de novo synthesis of lipids. Being fundamental building blocks of cellular membranes, lipids play an important role in plant virus infection.

5.1. Lipids for virus replication

The deprivation of lipid synthesis dramatically impairs virus production (Carette, Stuiver et al. 2000, Ritzenthaler, Laporte et al. 2002, Sharma, Sasvari et al. 2011). Accordingly, virus infection enhances lipid biosynthesis (Lee and Ahlquist 2003, Barajas, Xu et al. 2014). Furthermore, virus infection changes the host cell lipid composition (Fernández-Calvino, Osorio et al. 2014). For instance, the amount of unsaturated fatty acid determines the fluidity and plasticity of membranes, thereby governing the number and the morphology of the viral factories (Lee, Ishikawa et al. 2001, Lee and Ahlquist 2003). To ensure efficient replication, viruses preferentially hijack certain kinds of lipids. For example, the phospholipid phosphatidylethanolamine (PE) is relocalized to vRNA replication sites in order to build a PE-enriched microenvironment for the replication of TBSV (Xu and Nagy 2015). The presence of PE would promote vRNA binding to the vRdRp, thus facilitating vRNA replication (Pogany and Nagy 2015).

The question is how are lipids redirected to viral factories. For animal viruses, such as *Coxsackievirus B3* (CVB3), the lipid kinase phosphatidylinositol-4-kinase IIIβ (PI4KIIIβ) is recruited to membranes during infection, which leads to the formation of Phosphatidylinositol 4-phosphate (PI4P) lipid-enriched viral factories (Hsu, Ilnytska et al. 2010). Although it is not known whether plant viruses can modify the microenvironment in a similar way, a direct lipid transfer from the cellular membrane to the viral factories has been proposed. For instance, TBSV co-opts the host VAP proteins (vesicle-associated membrane protein-associated proteins) to facilitate the formation of membrane contact sites between the sterol biosynthetic ER membrane and viral

factories (Barajas, Xu et al. 2014). TBSV further recruits the oxysterol-binding protein-related proteins that are host lipid transfer proteins, likely channeling the sterols to the viral factories.

5.2. Lipids and systemic virus movement

Virus intercellular movement within different types of cells results in the systemic infection of the plant. Initially, the virus replicates in the epidermal cells that are the outmost cell layer of the plant leaf tissue. The infectious unit, which is internalized, enters the mesophyll cells that are specialized for photosynthesis, crosses sequentially the bundle sheath and the vascular parenchyma cells to reach the transport conducting tubes (phloem and xylem) of the plant. At this point, viruses spread rapidly throughout the plant.

Most plant viruses utilize the phloem for their systemic movement (Cruz, Roberts et al. 1998, Silva, Wellink et al. 2002). The sieve element, which is the conducting tube of the phloem, is enucleated when it becomes mature and depends on the associated companion cell for the maintenance of its function. The viral infectious unit moves through the specialized PD termed pore plasmodesmal unit (PPU) for the phloem loading. The xylem, despite being overlooked, can also support the virus systemic movement (Verchot, Driskel et al. 2001, Moreno, Thompson et al. 2004). The vessel element is the conducting unit of the xylem. The perforation plate, which is formed during the programmed cell death of the vessel element, is the opening for the viral infectious unit systemic movement through the xylem. The pit, which is located on the side wall of the mature vessel element, is the presumed place for the viral infectious unit to load into the xylem (Opalka, Brugidou et al. 1998).

In the case of TuMV, Wan et al. have found that replicating vesicles are present both in the phloem and xylem (Wan, Cabanillas et al. 2015). Interestingly, these $6K_2$-induced vesicle aggregates contain large amount of lipids, revealing their importance for plant virus systemic infection. The membrane-containing aggregates in the phloem are

suspected to be the site for virion assembly, and the assembled virions are then released for phloem transport (Fig. 12A). Individual $6K_2$-induced vesicle movement for phloem transport is also possible. On the other hand, $6K_2$-induced vesicles are thought to enter the xylem vessel through pit membranes, and to replicate in the xylem vessel. Once the xylem vessel becomes a hollow vessel, the vesicles then move upward along the flow of water (Fig. 12B).

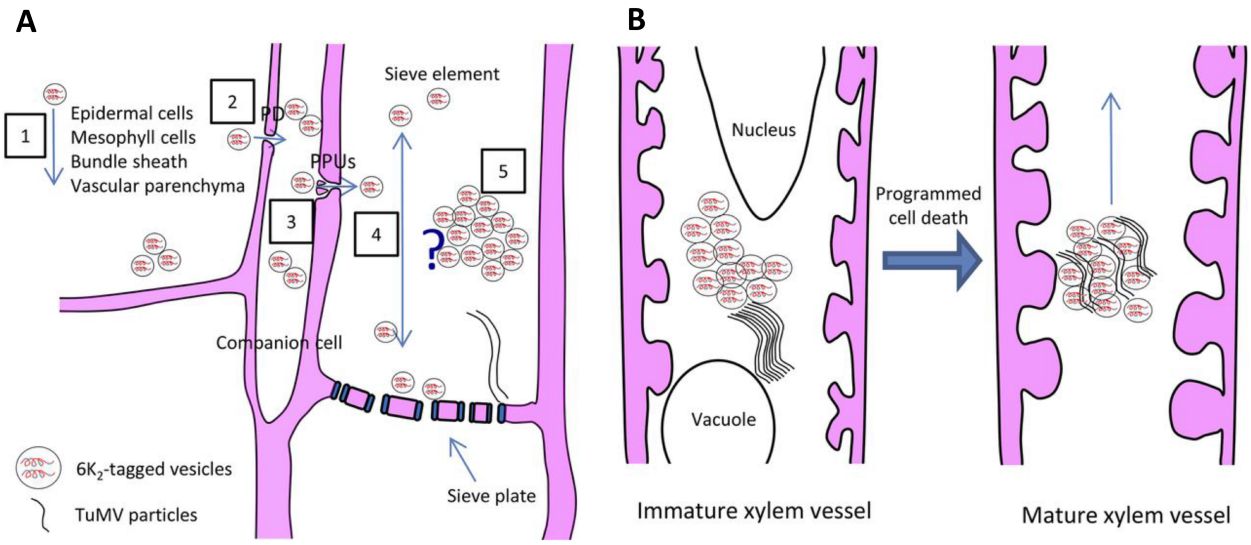

Figure 12. TuMV systemic movement.

(A) Schematic model for TuMV moving through the phloem. The viral membrane-associated $6K_2$ protein-induced replication vesicles move from the infected epidermal cells to mesophyll cells, and then to bundle sheath and to vascular parenchyma (step 1), and further reach the companion cells through the PDs (step 2). The virus replicates in all of these cells, and the newly synthesized replication vesicles move across the PPUs for phloem loading (step 3). Once in the sieve element, the individual replication vesicles move through the sieve elements (step 4), or form aggregates for the assembly of the virions involved in systemic movement (step 5). (B) Schematic model for the TuMV moving through the xylem. The replication vesicles reach the immature xylem vessel through the pits, and replicate in the cell. After programmed cell death, the immature xylem vessels become hollow vessels, in which the infectious units then move upward along the flow of water. Reproduced from (Wan, Cabanillas et al. 2015).

6. The motile vesicle - mediator of vRNA replication and movement

It was traditionally believed that vRNA replication and vRNA movement were separate events. It is now becoming clear that vesicles are not only used for vRNA synthesis, but also for vRNA movement. In other words, by inducing membranous vesicles, virus replication and movement are coupled. This tight coupling may explain why certain viruses quickly establish the systemic infection of the plant.

The PVX genome encodes three viral proteins (TGBp1, TGBp2 and TGBp3) from overlapping ORFs, termed the triple gene block. The membrane-associated TGBp2 reorganizes the ER membrane for the formation of motile vesicles, to which the membrane-associated TGBp3 is also recruited (Schepetilnikov, Manske et al. 2005, Samuels, Ju et al. 2007). TGBp1 is recruited to modify PDs and to facilitate the deposition of CP for binding and moving progeny vRNAs across into non-infected cells (Howard, Heppler et al. 2004). All three proteins have been defined as MPs before it was found out that TGBp2/3-tagged vesicles support vRNA synthesis also. These replicating vesicles are located at the cytoplasmic orifices of PDs. This arrangement suggests a coreplicational model for intercellular movement of vRNA (Tilsner, Linnik et al. 2013).

A long-standing question is what is the viral infectious unit that goes through PDs into the neighboring healthy cells? In the case of icosahedral viruses, the infectious unit is the virion itself (Halk and McGuire 1973, Ritzenthaler, Schmit et al. 1995). Very often, the genome of these viruses encodes MPs that oligomerize to form tubules that go through PDs. Within these tubules are the virions that are moving into healthy cells. The situation is different for filamentous viruses, where it is presumed that a vRNP complex is the infectious unit. The full nature of this complex still needs to be defined for most viruses, but observations suggest that for TMV the intercellular movement of vRNP complexes is carried out in the form of vesicles containing VRCs (Kawakami, Watanabe et al. 2004). Movement of such vesicles has been captured by live cell imaging in a single TuMV-infected cell (Grangeon, Jiang et al. 2013). The whole process, which

includes the production and the movement of the VRCs from the infected cell into non-infected cells, takes 2-4 h (Kawakami, Watanabe et al. 2004, Agbeci, Grangeon et al. 2013). Intercellular movement of membrane-bound VRCs might be a very efficient way of rapidly spreading the infection throughout the whole plant. The number of viral genomes entering and replicating within a cell has been called the multiplicity of cellular infection (MOI) (Gutiérrez, Michalakis et al. 2012). In the case of TuMV, the MOI has been estimated to be close to one (Gutiérrez, Michalakis et al. 2012).

7. Membrane-associated viral proteins

Plant viral genomes encode at least one membrane-associated protein that triggers membrane rearrangement (Table 1). These viral proteins, which are part of VRCs, associate with the membrane either through TMDs and/or amphipathic helices (Zhang, Zhang et al. 2005, Liu, Westler et al. 2009). Host membrane proteins may further mediate the association of VRCs with cellular membranes. For instance, the membrane association of the ToMV 180K replication protein is strengthened by interaction with two host membrane proteins, TOM1 and ARL8 (Nishikiori, Mori et al. 2011).

Ectopic expression of these membrane-associated proteins very often induces membranous structure assemblies similar to virus-induced viral factories (Schwartz, Chen et al. 2002, Wei and Wang 2008). In some instances, viral proteins by themselves may alter cellular membranes, inducing membrane proliferation and dilation, but they are not able to produce spherule-shape or vesicle-shape viral factories, suggesting that other viral proteins and possibly vRNA are involved in viral factory biogenesis (McCartney, Greenwood et al. 2005, Cao, Jin et al. 2015). These membrane-associated viral proteins contain functional domains that interact with host membrane-shaping factors for the formation of viral factories (see below).

A frequent observation is that these membrane-associated viral proteins, such as the p33 protein of TBSV, the 1a protein of BMV and the $6K_2$ protein of *Plum pox virus* (PPV), form oligomers (Rajendran and Nagy 2004, Zilian and Maiss 2011, Diaz, Gallei et al. 2012). Protein self-interaction is one way to induce membrane curvature (McMahon and Gallop 2005, Miller and Krijnse-Locker 2008). It has been suggested that the 1a protein of BMV induces replication vesicles by forming a capsid-like interior shell within the spherules (Diaz, Gallei et al. 2012).

Table 1: The functions of membrane-associated viral proteins of plant virus TBSV, BMV, TuMV and BaMV/PVX.

Virus	Membrane-associated viral protein	Membrane targeted	Functions	References
TBSV	p33	Peroxisome (switch to ER in the absence of peroxisome)	Upregulates phospholipid biosynthesis; recruits ESCRT factors for VRCs assembly; selectively vRNA recruitment; interacts with the $p92^{pol}$; binds eEF1A to promote VRCs assembly and (-) vRNA synthesis.	(Rajendran and Nagy 2004, Pogany, White et al. 2005, Jonczyk, Pathak et al. 2007, Li, Pogany et al. 2009, Barajas, Martin et al. 2014, Barajas, Xu et al. 2014)
	$p92^{pol}$	Peroxisome	vRdRp; interacts with p33; recruits GAPDH to the VRCs.	(Rajendran and Nagy 2004, Huang and Nagy 2011)
BMV	1a	ER	Induces the formation of viral factories; recruits the vRNA to the viral factories; hijacks reticulons for membrane curvature.	(Schwartz, Chen et al. , Wang, Lee et al. 2005, Liu, Westler et al. 2009, Diaz, Wang et al. 2010)
	$2a^{pol}$	ER	vRdRp; interacts with the capsid protein maybe for genome packaging.	(Chaturvedi and Rao 2014)
TuMV	$6K_2$	ER	VRCs assembly; virus intracellular, intercellular and long distance movement.	(Agbeci, Grangeon et al. 2013, Grangeon, Jiang et al. 2013, Wan, Cabanillas et al. 2015)
	P3	ER	Virus pathogenesis; symptom and avirulence determinant; genome amplification.	(Jenner, Wang et al. 2003, Cui, Wei et al. 2010)
BaMV/ PVX	TGBp1		RNA binding; suppresses host gene silencing; virus movement; regulates the size exclusion limit of the PD; induces the formation of X-body.	(Wung, Hsu et al. 1999, Howard, Heppler et al. 2004, Tilsner, Linnik et al. 2012)
	TGBp2	ER	Induces VRCs formation; interacts with TGBp3.	(Ju, Brown et al. 2007, Samuels, Ju et al. 2007)
	TGBp3	ER	Associates with the virions for virus delivery; interacts with TGBp2.	(Samuels, Ju et al. 2007, Chou, Hung et al. 2013)

8. Host proteins in viral factory formation

Although membrane-associated viral proteins directly target cellular membranes, this targeting further involves the participation of host proteins that have key roles in membrane dynamics. These host factors are the host reticulon homology proteins (RHPs), the endosomal sorting complexes required for transport (ESCRT) factors, and the early secretory pathway components.

8.1 RHPs and ESCRT factors

The RHPs are members of a family of membrane-associated proteins that principally localize to the ER (Yang and Strittmatter 2007). These proteins contain two hydrophobic segments that associate with the outer leaflet of membranes, thus facilitating membrane curvature (Voeltz, Prinz et al. 2006). In yeast cell, the depletion of RHPs (Rtn1p, Rtn2p and Yop1p) does not affect the BMV viral proteins 1a and $2a^{pol}$ localizing to the perinuclear ER membrane, but the viral proteins fail to induce the formation of spherules, indicating the importance of the RHPs in viral factory biogenesis (Diaz, Wang et al. 2010). The RHPs were shown to interact with the viral protein 1a within the spherules. The abundance and the morphology of the virus-induced spherules are regulated by the RHPs. In particular, the diameter of spherules induced by BMV decreases from 50-70 nm to an average of 27 nm when the Rtn2p and Yop1p are deleted. Meanwhile, the virus produces two-fold more spherules in this double-knockout yeast cell (Diaz, Wang et al. 2010). The RHPs are also co-opted by several animal viruses to their replication site. The viral protein 2C encoded by Enterovirus 71 and Poliovirus interacts with the host reticulon 3 (RTN3). The RTN3 is important for virus replication, as the reduced expression of RTN3 impairs vRNA synthesis and viral protein translation (Tang, Yang et al. 2007).

ESCRT factors are involved in various cellular membrane bending and separation processes, including cytokinesis and formation of MVBs. These processes require the sequential assembly of ESCRT complexes (ESCRT-0, -I, -II, -III) on the membrane, and an accessory protein complex to disassemble the ESCRT complexes from the membrane for recycling (Schmidt and Teis 2012). The membrane-associated viral proteins can interact with ESCRT components (Barajas and Nagy 2010, Diaz, Zhang et al. 2015). For example, the p33 protein of TBSV interacts with the ESCRT-I Vps23p factor and the accessory factor Bro1p in its surrogate host yeast cell. This interaction leads to the recruitment of Vps23p to the replication site (peroxisome-derived), and the disruption of this interaction results in an increased sensitivity of the vRNA to nuclease activity (Barajas, Jiang et al. 2009). Interestingly, CIRV, which modifies the mitochondrion for the formation of MVBs, hijacks the same ESCRT Vps23p factor for its replication (Richardson, Clendening et al. 2014). In the case of BMV, the viral protein 1a associates with the ESCRT-III Snf7p factor, but the factor Vps23p is not required (Diaz, Zhang et al. 2015). Potentially, these ESCRT factors may be involved in viral factory formation for other viruses. The model shown in Fig. 13 highlights the contribution of the RHPs and the ESCRT factors for BMV-induced spherule formation.

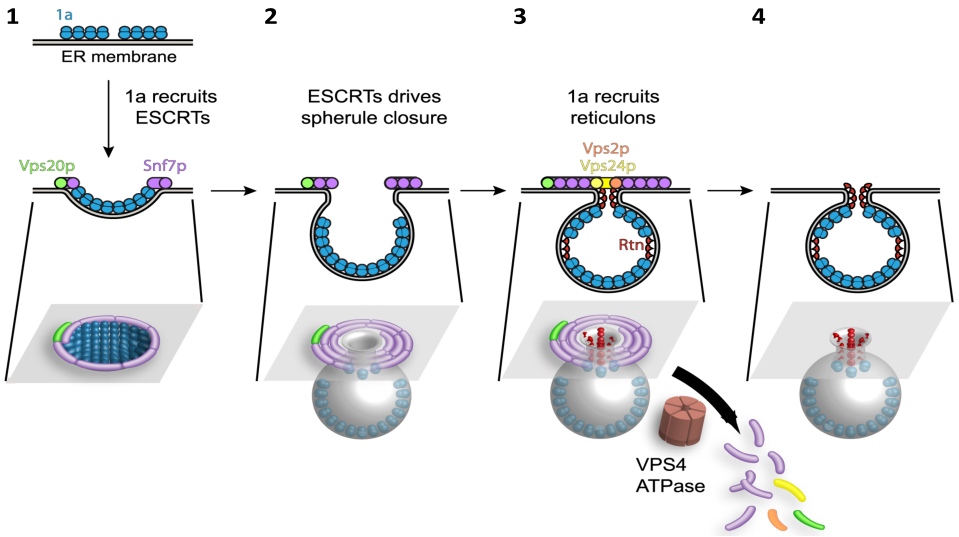

Figure 13. Model for the contribution of RHPs and ESCRT factors for BMV spherule formation.

The membrane-associated 1a protein associates with the ER membrane through its amphipathic helix, and the oligomerization of 1a protein initiates the membrane curvature. The ESCRT factors, Vps20p and Snf7p, are recruited to the deformed ER membrane site (step 1). The membrane rim is constricted by the ESCRT factors, to drive spherule closure with progressive formation of a pore (step 2). The other ESCRT factors (e.g. Vps2p, Vps24p) and the RHPs localize to and maintain the stability of the spherule (step 3). The ESCRT ATPase Vps4p disassembles the ESCRT machinery for further recycling, resulting in the formation of the BMV spherule with the pore to its final size (step 4). Reproduced from (Diaz, Zhang et al. 2015).

8.2 Early secretory pathway components

The secretory pathway has been shown to be important in the biogenesis of vesicle-shape viral factories (Ribeiro, Foresti et al. 2008, Wei and Wang 2008, Hyodo, Mine et al. 2013, Sun, Andika et al. 2014). The selective uptake of viral proteins into COPII vesicles is mediated by an ER export signal, and several of them have been characterized. However, no clearly defined ER export motif has been identified for plant viral proteins (Wu, Lee et al. 2011).

Several secretory pathway components have been shown to directly interact with viral proteins. A GTPase, such as Arf1, preferentially binds to the C-terminal region of the viral protein p27 of *Red clover necrotic mosaic virus* (RCNMV) (Hyodo, Mine et al. 2013). The COPII GTPase, Sar1 interacts with the P2 protein of *Wheat yellow mosaic virus* (WYMV) (Sun, Andika et al. 2014). Furthermore, as the regulators of the secretory pathway, the SNAREs can be hijacked by the viruses for the formation of vesicles. For example, the ER localized SNARE-like protein VAP27 can interact with the 60K helicase of CPMV (Carette, Verver et al. 2002). The TuMV $6K_2$ protein also can interact with VAP27 protein, and by binding VAP27, $6K_2$ associates also with Syp71, which is involved in vesicle fusion (Wei, Zhang et al. 2013). The model shown in Fig. 14 illustrates the early secretory pathway involvement in viral factory formation.

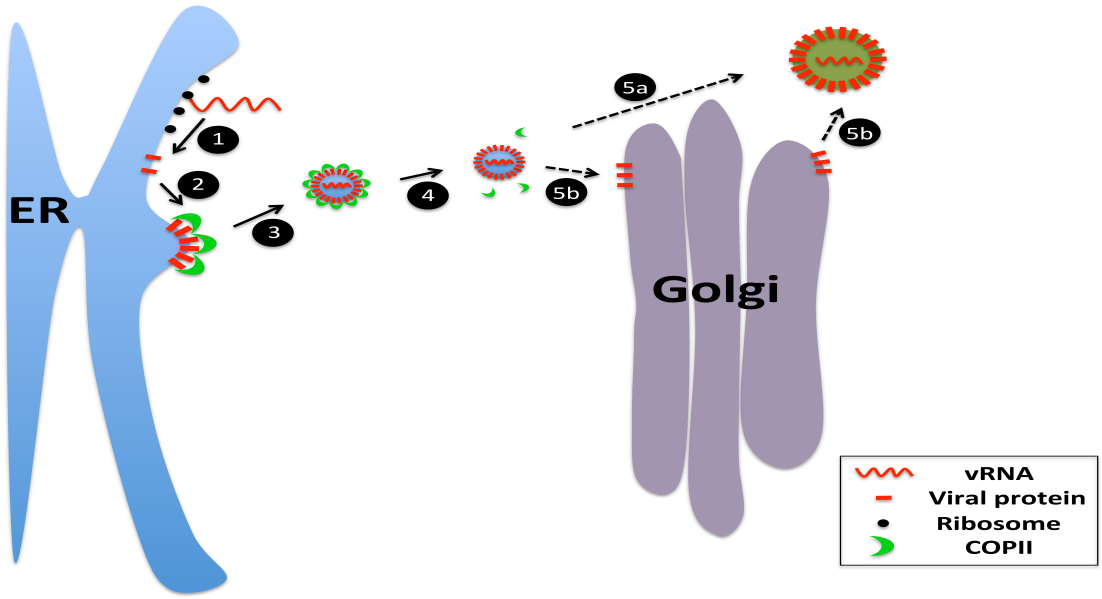

Figure 14. Model for the early secretory pathway dependent vesicle-shape viral factory formation.

vRNAs are translated on ER-associated ribosomes, and the synthesized viral membrane-associated proteins integrate to, or associate with, membranes (step 1). The COPII components are then recruited to initiate vesicle formation (step 2). The pre-formed vesicles bud from the ER membrane (step 3), and are shielded by COPII components (step 4). These vesicles may bypass the Golgi bodies and mature into vesicle-shape viral factories (step 5a), or may fuse with the Golgi membrane, which then exit from Golgi bodies to form the vesicle-shape viral factories (step 5b).

9. Problematic and research objectives

The accumulated data concerning the cellular biogenesis of the $6K_2$-induced replication vesicle are that the replication vesicle is derived from the ER (Schaad, Jensen et al. 1997) and that the early secretory pathway is required for its formation (Wei and Wang 2008). More information is however needed to uncover the molecular mechanism that leads to their biogenesis. For instance, what are the molecular determinants of $6K_2$ required for the production of replication vesicle and what are the components of the secretory pathway responsible for the vesicular transport of $6K_2$?

Based on the accumulated information on the involvement of the secretory pathway in virus infection, the hypothesis that is proposed is that $6K_2$ possibly interacts with certain protein components of the early secretory pathway, such as the COPII coatomer Sec24a and the vesicle trafficking regulators SNARE proteins.

The research objectives are to: 1) Characterize the critical amino acid residues of $6K_2$ needed for vesicle formation. Specifically, what are the amino acid residues responsible for $6K_2$ ER and Golgi exit? 2) Identify the host protein factors involved in $6K_2$-induced replication vesicle formation. 3) Evaluate the contribution of critical amino acid residues and specific host factors for TuMV infection.

Thus, my project is to formulate a molecular model for the formation of $6K_2$-induced replication vesicles. In this project, site-directed mutagenesis was used to obtain a series of $6K_2$ mutant proteins. The ability of these mutant proieins to induce replication vesicle formation was evaluated by live cell imaging using confocal laser scanning microscopy and by co-expressing them with different cellular fluorescent markers. These mutations were further introduced into the virus infectious clone to assess their impact on virus infection. Protein interaction assays, such as the yeast two-hybrid system and co-immunoprecipitation experiments, were used to test the interaction of $6K_2$ with selected host protein factors. Corresponding knockout plants and co-

expression of dominant negative mutant proteins were finally used to confirm the role of these host factors in virus infection.

CHAPTER 2: 6K_2 N-terminal tail and its ER export (Publication No. 1)

The vesicle-forming $6K_2$ protein of turnip mosaic virus interacts with the COPII coatomer Sec24a for viral systemic infection

Journal of Virology

July 2015, Vol. 89, No. 13, p.6695-6710.

Jun Jiang[1], Camilo Patarroyo[2], Daniel Garcia Cabanillas[1], Huanquan Zheng[2], and Jean-François Laliberté[1#]

*

1. INRS-Institut Armand-Frappier, 531 Boulevard des Prairies, Laval, Québec, H7V 1B7, Canada
2. Department of Biology, McGill University, 1205 Dr. Penfield Avenue, Montréal, Québec, H3A 1B1, Canada

Author for correspondence: Prof. Jean-François Laliberté

INRS-Institut Armand-Frappier

531 boulevard des Prairies, Laval, Québec,Canada H7V 1B7

Tel: 1.450.687.5010

Fax: 1.450.686.5501

Email: jean-francois.laliberte@iaf.inrs.ca

Contribution of student

This manuscript has been published in *Journal of Virology*. I designed and performed almost all of the experimental work (Fig. 1-7, 8B-C, 9B-D and Table. 1-2) and analysed data with advice from my supervisor Professor Jean-François Laliberté. I prepared the first draft of this manuscript, and Jean-Francois Laliberté and Huanquan Zheng helped me improve the writing. My colleague Camilo Patarroyo contributed to Fig. 8A, 9A and 9E-F. Daniel Garcia Cabanillas contributed to the yeast two-hybrid assay.

Résumé

Les virus à ARN positif réorganisent le système endomembranaire de leurs cellules hôtes pour produire des quasi-organites appelés usines virales afin de coordonner divers processus viraux tels que la traduction et la réplication de leur génome. Il est également de plus en plus clair que renfermer des complexes d'ARN viral au sein de telles structures membranaires est important pour la propagation du virus de cellule à cellule à travers l'hôte. Dans les cellules végétales infectées par le virus de la mosaïque du navet (TuMV), un membre de la famille *Potyviridae*, des vésicules mobiles dérivant du réticulum endoplasmique (RE) sont produites et portent l'ARN viral jusqu'aux plasmodesmes pour le livrer dans des cellules voisines non infectées. La protéine virale $6K_2$ est responsable de la formation de ces vésicules, mais l'implication précise de $6K_2$ dans leurs biogenèses reste inconnue. Nous montrons ici que $6K_2$ est associée à des membranes cellulaires. Des délétions successives et des expériences de mutagenèse dirigée nous ont permis de définir une séquence de 12 acides aminés dans le domaine N-terminal de $6K_2$ pour l'export de la protéine hors du RE. En particulier, nous avons mis en évidence un résidu tryptophane hautement conservé chez les potyvirus et deux résidus lysine qui sont importants pour la formation des vésicules. Lorsque le résidu tryptophane a été changé en alanine dans la polyprotéine virale, la réplication du virus avait encore lieu mais à un niveau réduit. En revanche, le mouvement de cellule à cellule fut complètement aboli. Des expériences de double hybride chez la levure et de co-immunoprécipitations ont montré que $6K_2$ pouvait interagir avec Sec24a, un membre des coatomers COPII. Le mouvement systémique du TuMV a été retardée dans une plante mutante d'Arabidopsis thaliana comportant une forme de Sec24a défectueuse. Ainsi, le mouvement intracellulaire des vésicules de réplication du TuMV nécessite l'exportation de $6K_2$ depuis le RE, qui a lieu grâce à l'interaction du domaine N-terminal de la protéine virale avec Sec24a.

Importance

De nombreux virus de plantes réorganisent le réticulum endoplasmique (RE) pour produire des vésicules qui sont associées avec le complexe de réplication du virus. La protéine virale $6K_2$ du virus de la mosaïque du navet (TuMV) est connue pour induire la formation de vésicules, à partir du RE, qui contiennent l'ARN viral ainsi que les protéines virales et de l'hôte nécessaires à la synthèse de l'ARN viral. Ces vésicules non seulement supportent la synthèse d'ARN viral mais sont également impliquées dans le trafic intracellulaire des ARN viraux. Dans cette étude, nous avons trouvé que le domaine N-terminal soluble de $6K_2$ est requis pour l'exportation de la protéine et pour la formation de vésicules. L'exportation de $6K_2$ n'est pas absolument nécessaire à la réplication de l'ARN viral, mais est nécessaire pour le mouvement de cellule à cellule du virus. En outre, nous avons constaté que $6K_2$ interagissait physiquement avec le coatomer COPII Sec24a et qu'un mutant d'Arabidopsis thaliana comportant une forme de Sec24a défectueuse induisait un retard dans l'infection systémique du TuMV.

Abstract

Positive sense RNA viruses remodel host cell endomembranes to generate quasi-organelles known as viral factories to coordinate diverse viral processes such as genome translation and replication. It is also becoming clear that enclosing viral RNA complexes within membranous structures is important for virus cell-to-cell spread throughout the host. In plant cells infected by turnip mosaic virus (TuMV), a member of the family *Potyviridae*, peripheral motile endoplasmic reticulum (ER)-derived viral vesicles are produced that carry the viral RNA to plasmodesmata for delivery into adjacent non-infected cells. The viral protein $6K_2$ is responsible for the formation of these vesicles but how $6K_2$ is involved in their biogenesis is unknown. We show here that $6K_2$ is associated with cellular membranes. Deletion mapping and site-directed mutagenesis experiments defined a soluble N-terminal 12 amino acid stretch, in particular a potyviral highly conserved tryptophan residue and two lysine residues that were important for vesicle formation. When the tryptophan residue was changed to an alanine in the viral polyprotein, virus replication still took place, albeit at a reduced level, but cell-to-cell movement of the virus was abolished. Yeast two-hybrid and co-immunoprecipitation experiments showed that $6K_2$ interacted with Sec24a, a COPII coatomer component. Appropriately, TuMV systemic movement was delayed in an *Arabidopsis thaliana* mutant line defective in Sec24a. Intercellular movement of TuMV replication vesicles thus requires ER export of $6K_2$, which is mediated by the interaction of the N-terminal domain of the viral protein with Sec24a.

Importance

Many plant viruses remodel the endoplasmic reticulum (ER) for generating vesicles that are associated with the virus replication complex. The viral protein $6K_2$ of Turnip mosaic virus (TuMV) is known to induce ER-derived vesicles that contain vRNA as well as viral and host proteins required for vRNA synthesis. These vesicles not only sustain vRNA synthesis, they are also involved in the intercellular trafficking of vRNA. In this investigation, we found that the N-terminal soluble domain of $6K_2$ is required for ER export of the protein and for the formation of vesicles. ER export is not absolutely required for vRNA replication, but is necessary for virus cell-to-cell movement. Furthermore, we found that $6K_2$ physically interacts with the COPII coatomer Sec24a and that an *Arabidopsis thaliana* mutant line with a defective Sec24a shows a delay in the systemic infection by TuMV.

Introduction

Positive strand RNA viruses replicate on cellular membranes in order to achieve efficient virus production. These membranous structures have been termed viral factories and are associated with virus replication complexes (VRCs) (den Boon and Ahlquist 2010, Laliberté and Sanfaçon 2010). Electron microscopy coupled to tomography has recently been used to get an elaborate 3-dimensional view of animal virus-induced membranous structures. For instance, picorna-, corona- and arteriviruses induce the formation of endoplasmic reticulum (ER) - derived interconnected single- and double-membrane vesicles, cumulating into the formation of a complex meshwork of membranes (Knoops, Kikkert et al. 2008, Belov, Nair et al. 2012, Knoops, Bárcena et al. 2012). In the case of plant viruses, VRCs are associated with membranous structures that are derived from various organelles, such as the ER, mitochondria, chloroplasts, or peroxisomes (Carette, Stuiver et al. 2000, Prod'homme, Jakubiec et al. 2003, McCartney, Greenwood et al. 2005, Hwang, McCartney et al. 2008). Host factors such as RNA-binding proteins, cellular chaperones, and membrane-shaping proteins are recruited to these sites in support of viral RNA (vRNA) replication (Diaz and Ahlquist 2012, Nagy and Pogany 2012, Verchot 2012).

One or two viral proteins are responsible for membrane alteration, which concomitantly recruit viral and host factors to form functional VRCs. For example, brome mosaic virus (BMV) RNA replication protein 1a localizes to the ER and induces inward spherule formation into the ER lumen in its yeast surrogate host (Schwartz, Chen et al. 2002). These spherules sequester vRNA template and the viral RNA polymerase 2a. Potato virus X (PVX) triple gene block protein 2 (TGBp2) induces ER-derived granule formation, and cooperates with TGBp1/3 to accomplish virus replication and plasmodesmata (PD) targeting (Tilsner, Linnik et al. 2013). The molecular determinants for membrane alteration of several viral proteins have been investigated. In general, these viral proteins contain functional domains for membrane anchorage, protein-protein interactions and organelle targeting. For red clover necrotic mosaic virus (RCNMV), a stretch of 20 amino acids was identified in the N-terminal region of the

auxiliary replicase protein p27 that is sufficient for its membrane association. This domain also contains amino acids that are required for VRC formation and negative-strand vRNA synthesis (Kusumanegara, Mine et al. 2012). The melon necrotic spot virus (MNSV) p7B is a type II integral membrane protein and the short extra-membrane N- and C-terminal tails were shown to be essential the protein to be exported out of the ER and transported to the Golgi apparatus and finally to PDs (Genovés, Pallás et al. 2011). Similarly, the C-terminal tail of the bamboo mosaic virus (BaMV) TGBp3 contains a sorting signal that target infectious viral components to cortical ER for cell-to-cell transmission (Wu, Lee et al. 2011).

Few host factors involved in virus-induced membrane alteration have been identified. For instance, the turnip mosaic virus (TuMV) $6K_2$ protein interacts with the SNARE (soluble N-ethylmaleimide-sensitive-factor attachment protein receptor) Vap27 protein, and by binding Vap27, $6K_2$ associates also with Syp71, which are proteins involved in vesicle fusion (Wei, Zhang et al. 2013). The p27 auxiliary replication protein of RCNMV, which is needed for the association of the replication complex with ER membranes (Kusumanegara, Mine et al. 2012), interacts with the ADP ribosylation factor 1 (Arf1) (Hyodo, Mine et al. 2013), a small GTPase that is implicated in the formation of the COPI vesicles (Brandizzi and Barlowe 2013). The p33 replication protein of tomato bushy stunt virus (TBSV) coopts the proteins of the endosomal sorting complexes (ESCRT) that are required for transport of properly assembled VRC on the peroxisome membrane (Barajas, Jiang et al. 2009, Barajas and Nagy 2010). Finally, in yeast, BMV 1a protein interacts with, and incorporates reticulons for spherule formation and maintenance of an open channel to the cytoplasm to facilitate import of vRNA templates and export of progeny vRNA (Diaz, Wang et al. 2010).

TuMV is a positive sense RNA virus that belongs to the genus *Potyvirus* in the family *Potyviridae* (Mayo 1995). The viral genome, about 9.8kb in length, is linked covalently to a viral protein known as VPg (virus protein, genome linked) at the 5’ terminus and is polyadenylated at the 3’ terminus. The single open reading frame (ORF) encodes a 358 kDa polyprotein that is processed by three viral proteinases into at least 11 mature

proteins. TuMV infection reorganizes the host cell endomembrane system and blocks protein secretion at the ER-Golgi interface (Grangeon, Agbeci et al. 2012). This reorganization leads to the formation of at least two types of structures: a large perinuclear globular structure and peripheral motile ER-derived vesicles. The perinuclear globular structure is an amalgamation of ER, Golgi bodies, COPII coatomers and chloroplasts (Grangeon, Agbeci et al. 2012), and contain vRNA as well as viral proteins such as $6K_2$, VPg-Proteinase, the RNA-dependent RNA polymerase (RdRp), the cytoplasmic inclusion (CI) helicase protein, and host proteins such as the eukaryotic translation initiation factor (iso)4E [eIF(iso)4E], poly(A)-binding protein (PABP), eukaryotic translation elongation factor 1A (eEF1A) (Cotton, Grangeon et al. 2009). The perinuclear structure is a collection of numerous 100 nm-sized vesicles, and is functionally linked to the peripheral motile ER-derived vesicles (Grangeon, Agbeci et al. 2012). These vesicles traffic on transvacuolar strands and actin filaments toward PDs and move through these channels to the neighboring cells (Cotton, Grangeon et al. 2009, Grangeon, Jiang et al. 2013).

The 6 kDa viral protein $6K_2$ is responsible for the formation of vesicles (Beauchemin, Boutet et al. 2007). It has been shown that vesicle formation was COPII dependent (Wei and Wang 2008, Grangeon, Agbeci et al. 2012). These studies, however, did not indicate what COPII component is directly interacting with $6K_2$, and how mechanistically this involvement takes place. It is also not known if involvement of COPII components is required for vRNA replication per se, or for intracellular/intercellular movement of the vRNA. In this study, we identified a tryptophan-based motif within the N-terminal cytoplasmic tail of $6K_2$ that is necessary for ER export of $6K_2$, leading to the formation of viral vesicles and cell-to-cell movement of TuMV. We further showed that $6K_2$ interacts with the COPII coatomer Sec24a, and that viral systemic spread is reduced in a Sec24a defective *Arabidopsis thaliana* mutant line. We hypothesize that $6K_2$ exits from the ER by interacting with the COPII machinery and this ER export is necessary for virus intercellular movement to take place.

Materials and Methods

Secondary structure prediction of $6K_2$

Prediction was done using algorithms available online: TMHMM (Krogh, Larsson et al. 2001) (http://www.cbs.dtu.dk/services/TMHMM-2.0/), SOSUI (Hirokawa, Boon-Chieng et al. 1998) (http://harrier.nagahama-i-bio.ac.jp/sosui/sosui_submit.html), TopPRED (Claros and von Heijne 1994) (http://mobyle.pasteur.fr/cgi-bin/portal.py?#forms::toppred), ΔG Prediction Server (Hessa, Kim et al. 2005) (http://dgpred.cbr.su.se/), MEMSAT (Jones, Taylor et al. 1994) (http://www.sacs.ucsf.edu/cgi-bin/memsat.py), DAS (Cserzo, Wallin et al. 1997) (http://www.sbc.su.se/~miklos/DAS/), PredictProtein (Rost, Yachdav et al. 2004) (https://www.predictprotein.org/), SPLIT (Juretic, Zoranic et al. 2002) (http://split4.pmfst.hr/split/4/). The hydrophobicity index was calculated using MPTOPO (Jayasinghe, Hristova et al. 2001).

Molecular clones and site-directed mutagenesis

Coding sequence of TuMV $6K_1$ and $6K_2$ were amplified by PCR using TuMV infectious clone pCambiaTuMV (Cotton, Grangeon et al. 2009) as template. For construction of pCambia/$6K_1$:mCherry, PCR product of $6K_1$ was digested with BamHI, followed by ligation with pCambia/mCherry (Thivierge, Cotton et al. 2008), also digested with BamHI. Similar to the steps above, PCR product of $6K_2$ was digested with XbaI and BamHI, and then inserted into vector pCambia/mCherry to generate pCambia/$6K_2$:mCherry. Mutagenesis was performed using QuikChange II XL site-directed mutagenesis kit (Agilent), following the manufacturer's instructions. For mutants pCambia/$6K_2$:mCherry Δ1-6, Δ1-12, Δ1-18, $W_{15}A$, K_7A, $K_{10}A$, $K_{12}A$, $K_{14}A$, $K_{17}A$ and $K_{14\text{-}17}A$, pCambia/$6K_2$:mCherry was used as the template. For mutant pCambiaTuMV^{W15A}, template pCambiaTuMV was used. For mutant pNX32-Sec24a^{R693K}, template pNX32-Sec24a was used. A fragment flanked by KpnI and ApaI from plasmid pCambiaTuMV^{W15A} was used to replace the KpnI/ApaI fragment of vector

pCambiaTuMV/6K_2:mCherry (Cotton, Grangeon et al. 2009) and pCambiaTuMV/6K_2:mCherry//GFP-HDEL (Grangeon, Agbeci et al. 2012), and the resulting constructs were pCambiaTuMV^{W15A}/6K_2:mCherry and pCambiaTuMV^{W15A}/6K_2:mCherry//GFP-HDEL respectively. DNA fragment harboring the coding sequence of 6K_2^{W15A}:mCherry flanked by SacII was obtained by PCR using pCambia/6K_2^{W15A}:mCherry as template. A similar procedure described by Beauchemin et al. (Beauchemin, Bougie et al. 2005) was followed to generate pCambiaTuMV^{W15A}/6K_2^{W15A}:mCherry. For construction of pCambia/N_2-TMD_1-C_1:mCherry, two complementary oligonucleotides were annealed. Equal amount of both oligos were mixed and heated to 95°C for 2 min, and then ramped cool to 25°C over a period of 45 min. Prepared DNA fragment was digested with SalI, and then inserted into pCambia/6K_1:mCherry/SalI that the predicted N-terminal part was replaced with SalI endonuclease restriction site. All constructs were verified by sequencing.

Protein expression in plants

Transient expression was performed by agroinfiltration on 4-week-old *N. benthamiana* plants as described previously (Sparkes, Runions et al. 2006). *Agrobacterium tumefaciens* AGL1 containing recombinant expression plasmid were selected on LB ampicillin-kanamycin plates, and then were cultured overnight. Bacterial cultures were centrifuged and suspended with water solution containing 10mM $MgCl_2$ and 150μM acetosyringone. The bacterial optical density at 600 nm (OD_{600}) was adjusted to 0.03 for GFP-HDEL (Chen, Stefano et al. 2011), to 0.1 for YFP-Sec24a (Grangeon, Agbeci et al. 2012), and to 0.3 for 6K_2 and its mutants expression. For coexpression, equal volumes of the bacterial suspension were mixed thoroughly. Agroinfiltrated plants were kept in growth chamber for 3-5 days until analysis. For brefeldin A (BFA) treatment, 10 μg/ml BFA solution was applied 24h before observation.

Protoplast isolation and transfection

Protoplast isolation and transfection were performed essentially described by Yoo et al. (Yoo, Cho et al. 2007). Four-week old leaves were cut into 1mm strips and incubated with enzyme solution [1.5% cellulase R10, 0.2% macerozyme R10, 0.4M mannitol, 20mM KCl, 20mM MES (pH 5.7), 10mM $CaCl_2$, 0.1% BSA]. Vacuum infiltration was applied and leaves were kept in the dark for 4h. The enzyme solution was diluted with equal volume of W5 solution [2mM MES (pH 5.7), 154mM NaCl, 125mM $CaCl_2$, 5mM KCl], and was filtered with a 41-µm nylon mesh. The flow-through was centrifuged at 100×*g* for 3min. The pellet was resuspended in W5 solution and kept on ice for 30min. After centrifugation at 100×*g* for 3min, the W5 solution was removed and the MMg solution [4mM MES (pH 5.7), 0.4M mannitol, 15mM $MgCl_2$] was added to adjust the protoplast density to 2×10^6 ml^{-1}. 100µl protoplast and 10µg of expression plasmid were mixed with equal volume of 40% PEG solution, and incubated at room temperature for 20min. Equal volume of W5 solution was added to stop the transfection. Finally, the protoplasts were resuspended and incubated with WI solution [4mM MES (pH 5.7), 0.5M mannitol, 20mM KCl] at room temperature for 40h until analysis.

Cellular fractionation, membrane partitioning and immunoblotting

Cellular fractionation experiment was performed as described in (Thivierge, Cotton et al. 2008). For membrane partitioning, approximately 4g leaf tissues expressing $6K_2$:mCherry or N_2-TMD_1-C_1:mCherry were homogenized in lysis buffer (20mM HEPES, pH 6.8, 250mM mannitol, 150mM potassium acetate and 1M $MgCl_2$). Membrane pellets were obtained as for cellular fractionation experiment. The pellets were suspended in 10 volumes of 1% Triton X-100, 100mM Na_2CO_3, 4M urea, or 1M KCl and incubated on ice for 30min. These samples were centrifuged at 30,000×*g* for 30min to separate the soluble fraction (S30) and the membrane fraction (P30). These fractions were then diluted 5 times for immunoblotting. For immunoblotting, protein samples were analyzed by 12% SDS-PAGE, and then transferred to nitrocellulose membrane. Rabbit antisera were used at the following dilutions: anti-CP at 1:2500 (Cotton, Grangeon et al. 2009),

anti-RFP (Sigma) 1:10000, anti-GFP (Sigma) 1:10000. The secondary antibody was horseradish peroxidase-coupled goat anti-rabbit immunoglobulin G (IgG).

Confocal Microscopy

Agroinfiltrated leaf sections were imaged using Zeiss LSM780 inverted confocal microscopy with a 20X objective, 40X, and/or 63X oil immersion objective. Argon and HeNe lasers were used to excite fluorescent proteins and signals from both green and red channels were collected simultaneously. GFP and YFP were excited at 488nm, and the emission light was captured at 500nm to 535nm; mCherry was excited at 561nm, and the emission light was captured at 580nm to 640nm. Image processing was performed with ZEN 2011 software and Image J.

Yeast two-hybrid assay

Experiments were carried out following Grefen et al. (Grefen, Lalonde et al. 2001). THY-AP4 (MATa ura3 leu2 lexA::lacZ::trp1 lexA::HIS3 lexA::ADE2) and THY-AP5 (MATα URA3 leu2 trp1 his3 loxP::ade2) yeast strains were used. Bait vector pNC-WT-WRC1 allowing a LV-Cub-6K_2 fusion and prey vector pNX32-DEST allowing a NubG-prey (proteins of interest) fusion were utilized to perform pairwise interaction assays of membrane proteins. Yeast transformations were performed using the lithium acetate-based protocol, followed by the mating procedure. The mated colonies carrying both constructs were selected in a SD-LW medium. To test bait and prey interactions, independent positive-mated colonies were plated for selection both on SD-LW and SD-LWH+3-AT+X-Gal media.

CO-IP purification

After agrobacterium-mediated transient expression for 3 days, *N. benthamiana* leaves (approximately 0.3g) were harvested, and ground to powder in liquid nitrogen. Ground

tissues were transferred into a tissue homogenizer and mixed with 3.0 ml of IP buffer [50 mM Tris (pH 7.5), 150 mM NaCl, 10% glycerol, 0.1% Nonidet P-40, 5 mM dithiothreitol, and 1×cOmplete Protease Inhibitor Cocktail (Roche)]. The crude lysates were then centrifuged at 20,000×g for 15 min at 4°C. After centrifugation, 1ml of the supernatant was incubated with GFP-Trap resin (Chromotek). Elution of the bound proteins was done according to the manufacturer's instructions.

Results

$6K_2$ is associated with cellular membranes

It has been shown that the TuMV protein $6K_2$ is responsible for the production of vesicles that are associated with virus replication and intracellular as well as intercellular movement (Cotton, Grangeon et al. 2009, Grangeon, Jiang et al. 2013). These vesicles originate from the ER (Beauchemin and Laliberté 2007, Grangeon, Agbeci et al. 2012). To identify the molecular determinants of TuMV $6K_2$ in vesicle biogenesis, secondary structure predictions based on TMHMM, SOSUI and TopPRED and other algorithms were performed (von Heijne 1992, Hirokawa, Boon-Chieng et al. 1998, Krogh, Larsson et al. 2001). These algorithms predict that $6K_2$ is a single-pass integral membrane protein (Table 1). These predictions indicate the presence of a 19-amino acid N-terminal and an 11-amino acid C-terminal tails and a trans-membrane domain (TMD) composed of 23 amino acids (Fig. 1A). These predictions also indicate that $6K_2$ has a type II topology. This is exemplified by the TMHMM algorithm, which predicts that the N-terminal tail of $6K_2$ is likely located in the cytosol and the C-terminal tail outside (i.e. in the lumen of the ER or inside of the vesicle) (Fig. 1B). This prediction is based on the positive-inside rule (von Heijne and Gavel 1988) due to the presence of a lysine-rich region in the predicted N-terminal tail of $6K_2$. Beauchemin and Laliberté (Beauchemin and Laliberté 2007) demonstrated that the VPg-Pro domain of the precursor form $6K_2$-VPg-Pro is located in the lumen of $6K_2$-induced vesicles, providing experimental support to this prediction.

To confirm experimentally that $6K_2$ is a membrane-associated protein, its coding sequence was fused at the 5' end of the coding sequence of the fluorescent protein mCherry in the binary vector pCambia 1380. *N. benthamiana* leaf tissue expressing $6K_2$:mCherry was homogenized three days after agroinfiltration, and the cellular extract was subjected to low-speed centrifugation to obtain the total protein fraction (S3), which was then separated by high-speed centrifugation into a soluble protein fraction (S30) and a membrane-associated protein fraction (P30). Western blot using a rabbit serum

against mCherry showed the presence of $6K_2$:mCherry in the P30 fraction but not in the S30 fraction, indicating that $6K_2$ was membrane associated (Fig. 1C). Presence of soluble mCherry in the S30 fraction, and of the Golgi-resident trans-membrane protein ST-YFP (Brandizzi, Snapp et al. 2002) in the P30 fraction (Fig. 1C) confirmed that the extraction procedure clearly separated soluble from membrane-associated proteins. The $6K_2$:mCherry P30 fraction was divided into several aliquots, which were treated with either 1% Triton X-100 to release integral membrane proteins, 100mM Na_2CO_3 (pH 11) to dislodge proteins residing in membrane lumens, and 4M urea to release peripheral membrane proteins (Fig. 1D). Western blot showed that Triton X-100 treatment released $6K_2$ to the supernatant, while Na_2CO_3 had no effect on membrane association of $6K_2$. Urea released some $6K_2$ in the S30 fraction, but the viral protein essentially remained associated with the membrane fraction.

TABLE 1 Computer analysis of the TuMV $6K_2$ amino acid sequence

Algorithm	Integral membrane protein present	No. of TM segments (starting/ending aa)[a]
TMHMM	Yes	1 (20/39)
SOSUI	Yes	1 (20/42)
TopPRED	Yes	1 (22/42)
ΔG Prediction Server	Yes	1 (18/39)
MEMSAT	Yes	1 (24/40)
DAS	Yes	1 (21/39)
PredictProtein	Yes	1 (22/39)
SPLIT	Yes	1 (22/39)

[a] aa, amino acid.

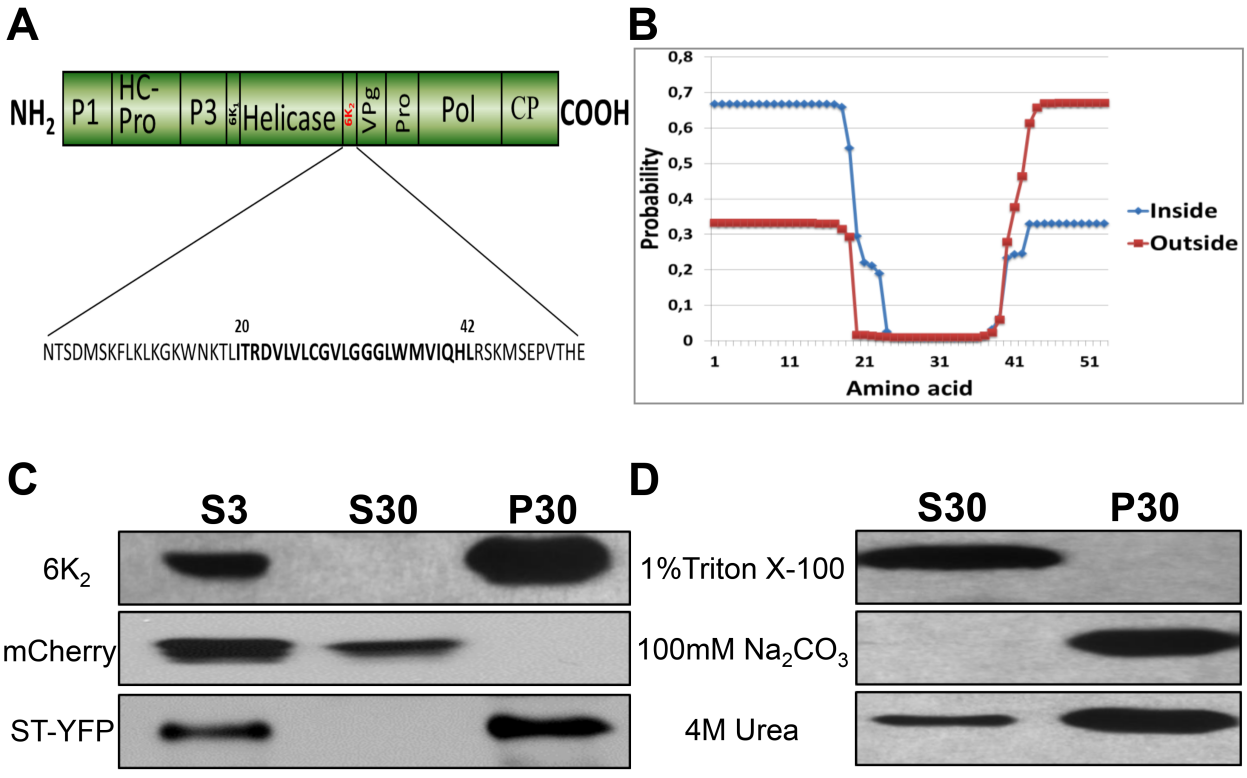

Figure 1. $6K_2$ is membrane-associated.

(A) Schematic representation of the TuMV open reading frames, with $6K_2$ highlighted in red. $6K_2$ amino acid sequence is shown below, with the predicted trans-membrane domain shown in bold. (B) $6K_2$ topology prediction using TMHMM server. The probability values of each amino acid residue located inside (shown in blue) and outside (shown in red) are plotted against the corresponding amino acid position. (C) Immunoblot analysis of total, soluble and membrane-associated proteins of $6K_2$:mCherry, mCherry and ST-YFP. *N. benthamiana* plants were agroinfiltrated with $6K_2$:mCherry, mCherry or ST-YFP and kept in growth chamber for 3 days. Total proteins (S3) were extracted and soluble proteins (S30) were separated from membrane-associated proteins (P30) by centrifugation at 30,000×g. (D) Membrane-enriched fractions of $6K_2$:mCherry were treated with 1% Triton X-100, or 100mM Na_2CO_3, or 4M urea for 30min at 4°C. After centrifugation, S30 and P30 fractions were applied for immunoblot analysis. Proteins were separated by SDS-PAGE and analyzed by Western blotting using a rabbit serum against RFP or GFP.

The N-terminal tail of $6K_2$ renders cytosolic $6K_1$ membrane-associated

One object of this investigation was to characterize the molecular determinants of $6K_2$ for vesicle production. One approach that is often taken is to compare two seemingly similar proteins and look at what is common or different between them that may explain their biological properties. The TuMV genome codes for another viral protein known as $6K_1$, which has the same molecular weight as $6K_2$. Secondary structure predictions suggest that $6K_1$ is an integral membrane protein, with an N-terminal tail, TMD and C-terminal tail composed of three, twenty and twenty-nine amino acids, respectively (Fig. 2A). $6K_1$:mCherry, however, was distributed in the cytosol and nucleus (Fig. 2B), and had the same subcellular distribution as soluble mCherry (Fig. 2C). A cellular fractionation experiment was performed and Western blot analysis showed the presence of $6K_1$:mCherry in the S30 fraction but not in the P30 fraction (Fig. 2D), confirming that $6K_1$ is a soluble protein when expressed ectopically. The soluble subcellular distribution may be explained by the ΔG_{app} of the TMD of $6K_1$ being higher than the one for $6K_2$ (ΔG_{app} $6K_1$= 0.749 *vs* ΔG_{app} $6K_2$= -0.116). ΔG_{app} is defined as the free energy required for the insertion of peptide from water to a lipid environment (Jayasinghe, Hristova et al. 2001). A negative value for ΔG_{app} indicates that the peptide has a high probability of being recognized as a TMD and integrated into a membrane.

A major difference between the two viral proteins is the predicted length of the N-terminal cytoplasmic tail, which is 3 and 19 residues for $6K_1$ and $6K_2$, respectively (Fig. 2A *vs* 1A). The cytoplasmic tail of membrane proteins that enter the early secretory pathway (ER-Golgi protein transport) often interact with membrane-associated factors, for instance, with the COPII coatomer Sec24a (Barlowe 2003). In order to see if the N-terminal cytoplasmic tail of $6K_2$ could induce membrane association of $6K_1$ through interaction with a membrane-associated host factor(s), the predicted N-terminal tail of $6K_1$ was replaced with the N-terminal tail of $6K_2$ and the resulting construct was named N_2-TMD_1-C_1 (the lower script indicating the $6K_1$ or $6K_2$ origin of the domain) (Fig. 2E). The expression pattern of N_2-TMD_1-C_1:mCherry in *N. benthamiana* cells looked similar to cells expressing $6K_1$:mCherry or mCherry (Fig. 2F). However, cellular membrane

fractionation experiments showed the presence of N_2-TMD_1-C_1:mCherry in the S30 fraction but also in the P30 fraction (Fig. 2G). The P30 fraction was subjected to different chemical treatments and Western blot analysis showed that treatments with 1M KCl, 100mM Na_2CO_3 (pH 11) and 4M urea released the protein to the supernatant (Fig. 2H). These results indicate that N_2-TMD_1-C_1 is peripherally associated with membranes. It suggests that the $6K_2$ N-terminal tail may interact with a host protein that resides in, or is peripherally associated with, membranes. Interaction with certain lipids is also possible. Alternatively, the addition of the N-terminal tail of $6K_2$ to $6K_1$ may have induced structural changes within the latter that favored its membrane association.

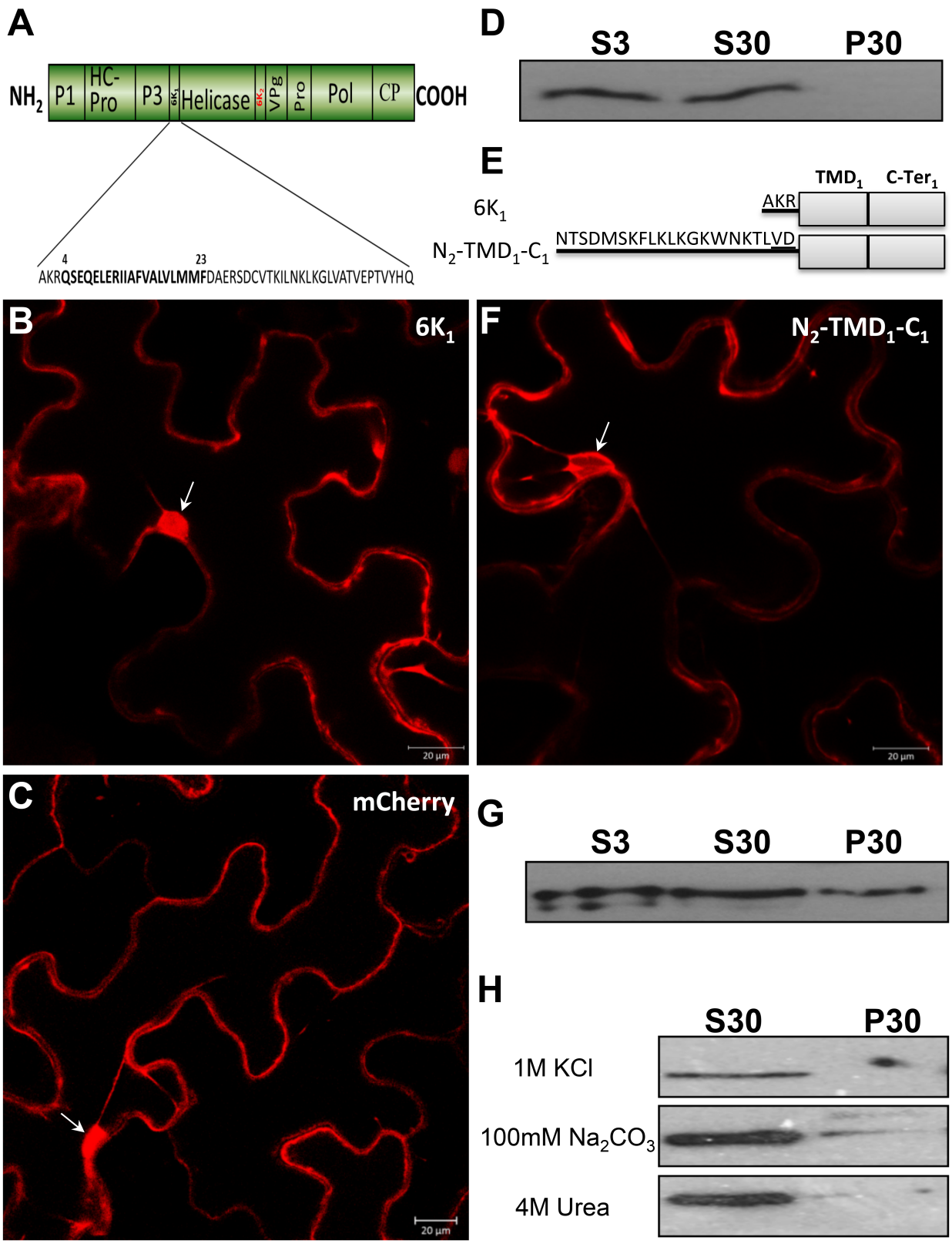
A
NH2
P1
HC-Pro
P3
6K1
Helicase
6K2
VPg
Pro
Pol
CP
COOH
4
23
AKRQSEQELERIIAFVALVLMMFDAERSDCVTKILNKLKGLVATVEPTVYHQ
D
S3
S30
P30
E
TMD1
C-Ter1
6K1
AKR
N2-TMD1-C1
NTSDMSKFLKLKGKWNKTLVD
B
6K1
20 µm
F
N2-TMD1-C1
20 µm
C
mCherry
20 µm
G
S3
S30
P30
H
S30
P30
1M KCl
100mM Na2CO3
4M Urea

Figure 2. The N-terminal tail of $6K_2$ renders cytosolic $6K_1$ membrane-associated.

(A) Protein $6K_1$ secondary structure prediction. $6K_1$ amino acid sequence is shown below and the predicted TMD is shown in bold. (B-C) Confocal microscopy imaging of leaf epidermal cell of *N. benthamiana* expressing $6K_1$:mCherry (B) or mCherry (C) 3 days after agroinfiltration. (D) Fractionation of $6K_1$:mCherry total proteins (S3) into soluble (S30) and membrane (P30) fractions, and detected by Western blot. (E) Schematic representation of chimeric protein N_2-TMD_1-C_1 with protein $6K_1$ is presented above. Black lines represent the N-terminal of each protein and amino acid residues are shown. $6K_1$ TMD and C-terminal tail are indicated by gray rectangles. Underlined amino acid residues VD are encoded by the incorporated SalI endonuclease restriction site. (F) Confocal microscopy imaging of leaf epidermal cell of *N. benthamiana* expressing N_2-TMD_1-C_1:mCherry 3 days after agroinfiltration. (G-H) *N. benthamiana* leaves expressing N_2-TMD_1-C_1:mCherry, and the resulting S3, S30 and P30 were analyzed (G). P30 fractions were incubated with 1M KCl, 100mM Na_2CO_3, or 4M urea, and then followed by ultracentrifugation and immunoblotting (H). All Western blots were performed with antibodies against RFP. All confocal images are optical images (1-µm thick). The nucleus is indicated by the white arrow.

The N-terminal tail of $6K_2$ is required for ER export

Mapping experiments with the purpose of identifying the region in the N-terminal tail that is critical for $6K_2$ vesicle formation were thus undertaken. Site-directed mutagenesis was conducted to progressively delete six amino acids of the $6K_2$ N-terminal tail, generating $6K_2^{\Delta 1\text{-}6}$:mCherry, $6K_2^{\Delta 1\text{-}12}$:mCherry and $6K_2^{\Delta 1\text{-}18}$:mCherry (Fig. 3A). Agroinfiltrated *N. benthamiana* epidermal cells expressing the entire $6K_2$ fused to mCherry or the truncated $6K_2$ fluorescent protein fusions were observed three days later. Ectopic expression of $6K_2$:mCherry and $6K_2^{\Delta 1\text{-}6}$:mCherry induced the formation of punctate structures that did not significantly co-localize with the ER marker GFP-HDEL (Fig. 3B-C). However, the expression pattern of $6K_2^{\Delta 1\text{-}12}$:mCherry (Fig. 3D) and of $6K_2^{\Delta 1\text{-}18}$:mCherry (Fig. 3E) was mostly reticulate, and overlapped with the ER marker. The Pearson's Correlation Coefficient (PCC) Rr values, which provide a quantitative estimate of co-localization (Dunn, Kamocka et al. 2011), was calculated. The PCC Rr value for GFP-HDEL with $6K_2$:mCherry was 0.04 ± 0.03, which was not significantly different from the 0.08 ± 0.06 value for GFP-HDEL with $6K_2^{\Delta 1\text{-}6}$:mCherry (Fig. 3F). The PCC Rr values, however, were significantly higher for GFP-HDEL with $6K_2^{\Delta 1\text{-}12}$:mCherry (0.24 ± 0.05), or with $6K_2^{\Delta 1\text{-}18}$:mCherry (0.42 ± 0.11), thereby confirming the increased retention of the latter two deletion mutants in the ER. The reticulate pattern of $6K_2^{\Delta 1\text{-}12}$:mCherry and of $6K_2^{\Delta 1\text{-}18}$:mCherry was not the result of higher expression than $6K_2$:mCherry and $6K_2^{\Delta 1\text{-}6}$:mCherry since Western blot analysis showed that the expression level of the truncated $6K_2$ proteins was similar to that of wt $6K_2$ (Fig. 3G). Cellular fractionation experiments followed by Western blot analysis showed that $6K_2^{\Delta 1\text{-}18}$:mCherry was found in the P30 fraction, indicating that this deletion mutant was still membrane-associated (Fig. 3H). In conclusion, progressively deleting the N-terminal tail led to $6K_2$ retention in the ER. These results indicate that the N-terminal tail contains amino acids that are important for $6K_2$ vesicle formation from the ER. These amino acids are likely located between residue 7 and 18 in the N-terminal tail of $6K_2$.

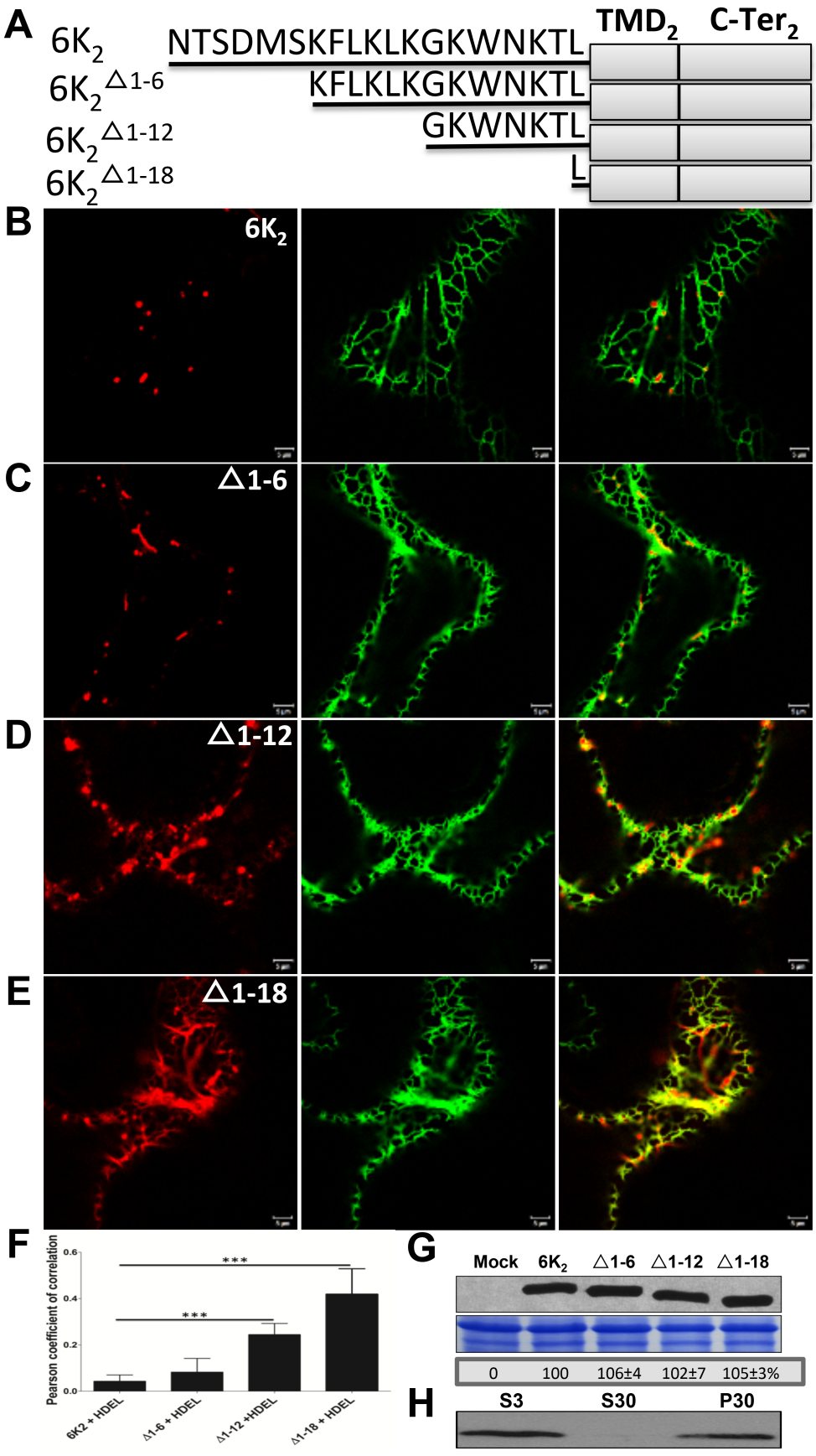
A
6K2
NTSDMSKFLKLKGKWNKTL
6K2 Δ1-6
KFLKLKGKWNKTL
6K2 Δ1-12
GKWNKTL
6K2 Δ1-18
L
TMD2
C-Ter2
B
6K2
C
Δ1-6
D
Δ1-12
E
Δ1-18
F
Pearson coefficient of correlation
***
***
6K2 + HDEL
Δ1-6 + HDEL
Δ1-12 +HDEL
Δ1-18 + HDEL
G
Mock
6K2
Δ1-6
Δ1-12
Δ1-18
0
100
106±4
102±7
105±3%
H
S3
S30
P30

Figure 3. The N-terminal tail is required for ER export of $6K_2$.

(A) Schematic representation of $6K_2$ and truncated $6K_2^{\Delta 1\text{-}6}$, $6K_2^{\Delta 1\text{-}12}$ and $6K_2^{\Delta 1\text{-}18}$. Black lines represent the N-terminal of each protein and amino acid residues are shown. $6K_2$ TMD and C-terminal tail are indicated by gray rectangles. (B to E) Representative *N. benthamiana* epidermal cells co-expressing $6K_2$:mCherry (B), $6K_2^{\Delta 1\text{-}6}$:mCherry (C), $6K_2^{\Delta 1\text{-}12}$:mCherry (D) or $6K_2^{\Delta 1\text{-}18}$:mCherry (E) with ER marker GFP-HDEL were imaged using confocal microscopy. These images are optical images (1-µm thick). (F) Co-localization statistical analysis between GFP-HDEL and the wt or the truncated $6K_2$ vesicles by calculation of the Pearson's correlation coefficient Rr values. Significant differences (Student's t tests; $P < 0.001$) are indicated by asterisks. Mean values +/- S.D. of three independent experiments are shown. (G) Wt $6K_2$:mCherry and its N-terminal truncations detected by Western blot. Bottom panels show equal loading verified by Coomassie-staining. (H) Immunoblot analysis of S3, S30 and P30 fractions of $6K_2^{\Delta 1\text{-}18}$:mCherry. All Western blots were performed with antibodies raised against RFP.

A conserved tryptophan residue and two lysine residues in the N-terminal tail of $6K_2$ are important for ER export

In order to pinpoint amino acids important for ER export, we compared different potyvirus $6K_2$ N-terminal tail amino acid sequences. Sequence alignment revealed several highly conserved lysine and tryptophan residues between residues 7 and 18 (Fig. 4A). Di-basic motifs have been shown to be involved in protein ER export (Giraudo and Maccioni 2003, Schoberer, Vavra et al. 2009) and the $6K_2$ N-terminal tail contains many lysine residues. The resulting single point mutants $6K_2^{K7A}$, $6K_2^{K10A}$, $6K_2^{K12A}$, $6K_2^{K14A}$, and $6K_2^{K17A}$ were produced and expressed as mCherry fusions in *N. benthamiana*. Expression of these mutants all induced punctate structures (data not shown), similar to those observed with wt $6K_2$:mCherry (Fig. 4B). However, when K14 and K17 were simultaneously replaced with alanine, the resulting double mutant ($6K_2^{K14A-K17A}$) still produced punctate structures but was also partially retained in the ER (Fig. 4C). The highly conserved tryptophan residue was also substituted for alanine and the mutant ($6K_2^{W15A}$) protein expressed in *N. benthamiana*. Even though expression of $6K_2^{W15A}$:mCherry induced the formation of punctate structures, ER retention was observed (Fig. 4D). Thus, the $6K_2^{K14A-K17A}$ and $6K_2^{W15A}$ mutations did not lead to complete ER retention, but rather slowed down ER export of the viral protein. The PCC Rr value for GFP-HDEL with $6K_2^{K14A-K17A}$:mCherry was 0.22 ± 0.03, and with $6K_2^{W15A}$:mCherry was 0.32 ± 0.04, values that were significantly higher than with $6K_2$:mCherry (0.04 ± 0.03) (Fig. 4E). We verified that the modified expression pattern was not a result of differential $6K_2$ protein expression levels. Western blot analysis showed that $6K_2^{K14A-K17A}$ and $6K_2^{W15A}$ were expressed at similar level as $6K_2$ (Fig. 4F). In conclusion, the tryptophan residue at position 15 and the lysine residues at position 14 and 17 are involved in $6K_2$ export from the ER.

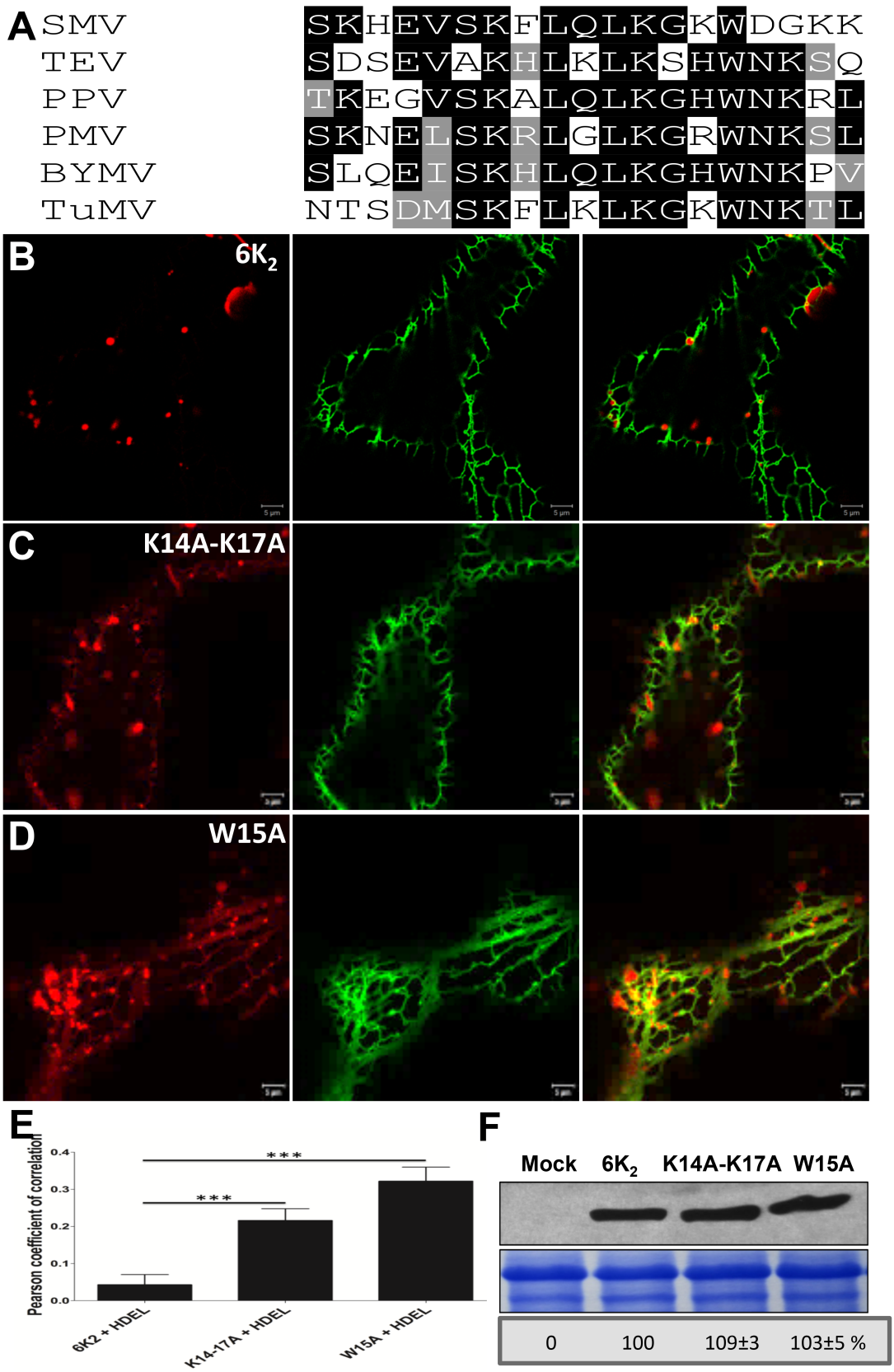
A
SMV SKHEVSKFLQLKGKWDGKK
TEV SDSEVAKHLKLKSHWNKSQ
PPV TKEGVSKALQLKGHWNKRL
PMV SKNELSKRLGLKGRWNKSL
BYMV SLQEISKHLQLKGHWNKPV
TuMV NTSDMSKFLKLKGKWNKTL
B 6K2
C K14A-K17A
D W15A
E
Pearson coefficient of correlation
0.4
0.3
0.2
0.1
0.0
***
***
6K2 + HDEL
K14-17A + HDEL
W15A + HDEL
F
Mock
6K2
K14A-K17A
W15A
0
100
109±3
103±5 %

Figure 4. A conserved tryptophan residue and two lysine residues are important for $6K_2$ ER export.

(A) Blast alignment of predicted potyviral $6K_2$ N-terminal tail amino acid sequences. SMV, soybean mosaic virus; TEV, tobacco etch virus; PPV, plum pox virus; PMV, peanut mottle virus; BYMV, bean yellow mosaic virus; TuMV, turnip mosaic virus. Identical amino acid residues that are highly conserved are highlighted by black box, and similar amino acid residues are indicated by gray box. (B to D) Confocal images of *N. benthamiana* epidermal cells co-expressing wt $6K_2$ (B), $6K_2^{K14A\text{-}K17A}$ (C) or $6K_2^{W15A}$ (D) with the ER marker GFP-HDEL. These images are optical images (1-µm thick). (E) Co-localization statistical analysis between GFP-HDEL and the wt or the mutated $6K_2$ vesicles by calculation of the Pearson's correlation coefficient Rr values. Significant difference (Student's t tests; $P < 0.001$) is indicated by asterisk. Mean values +/- S.D. of three independent experiments are shown. (F) Wt $6K_2$:mCherry, $6K_2^{K14A\text{-}K17A}$:mCherry and $6K_2^{W15A}$:mCherry detected by Western blot with antibodies raised against RFP. Bottom panels show equal loading verified by Coomassie-staining.

Tryptophan residue is required for TuMV systemic movement

The above experiments indicated that the tryptophan residue located at position 15 in the N-terminal tail of $6K_2$ is important for ER export of the viral protein. We consequently introduced this mutation into an infectious viral clone ($TuMV^{W15A}$) to test its impact on virus infection. As a negative control, the core GDD motif of the viral RdRp was mutated to VNN ($TuMV^{VNN}$) to produce a replication defective virus (Li and Carrington 1995). Mock, TuMV, $TuMV^{W15A}$ and $TuMV^{VNN}$ were agro-inoculated in *N. benthamiana* plant leaf tissues. At 5 dpi, plants infected with TuMV showed significant growth stunting while plants infected with $TuMV^{W15A}$ were similar to mock infected plants (data not shown). Virus production was analyzed by immunoblotting using a rabbit serum against CP (Cotton, Grangeon et al. 2009). Fig. 5A shows a high level of CP production for TuMV and a faint accumulation for $TuMV^{VNN}$ in agroinfiltrated leaves. Agroinfiltration with $TuMV^{W15A}$ showed a ~60% reduction in CP production, indicating it was replication competent even though it did not reach as high a level as wt TuMV. CP production was also assessed 40h later following transfection of *N. benthamiana* protoplasts with mock, $p35STuMV^{VNN}$, $p35STuMV^{W15A}$ and p35STuMV by Western blotting. Fig. 5B shows that $p35STuMV^{W15A}$ produced less CP than wt TuMV, suggesting that viral RNA replication was affected by the mutation. Systemic virus movement in upper non-agroinfiltrated leaves was also evaluated by Western blotting. A strong CP signal was detected in TuMV-infected plants, while no CP was observed for $TuMV^{W15A}$ and $TuMV^{VNN}$ at 5 dpi (Fig. 5C). Furthermore, no CP was detected when Western analysis was performed two weeks later (data not shown), even though $TuMV^{W15A}$ replicated at half the level of wt TuMV according to the protoplast experiment. In conclusion, the replacement of tryptophan 15 of $6K_2$ with an alanine residue affected cellular virus replication, and virus systemic movement.

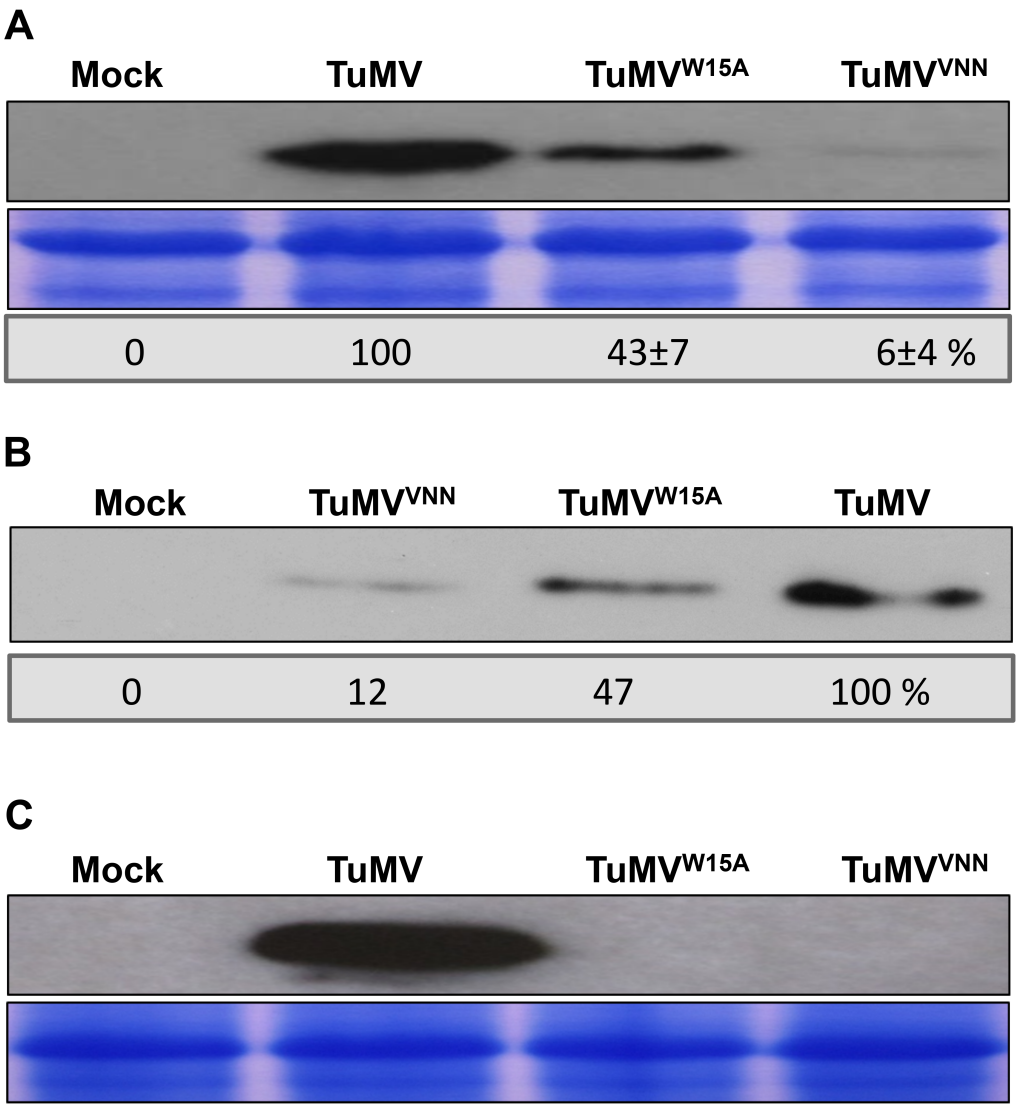

Figure 5. Tryptophan residue is required for TuMV systemic movement.

(A) Agroinfiltrated leaves of Mock-, TuMV-, TuMV^{W15A}- and TuMV^{VNN}-infected *N. benthamiana* were evaluated by Western blot analysis 5 days later. (B) *N. benthamiana* protoplasts were transfected with mock, p35STuMV^{VNN}, p35STuMV^{W15A} and p35STuMV, and CP was detected by Western blot 40h after transfection. (C) Upper non-agroinfiltrated leaves from (A) were analyzed by Western blot. Bottom panels of (A) and (C) show equal protein loading verified by Coomassie-staining. All immunoblotting were performed with anti-TuMV CP rabbit serum.

TuMV^{W15A} replication but not virus intercellular movement is partially complemented by cis expression of 6K$_2$

The W15A mutation reduced virus production in protoplasts and inoculated leaves, and prevented plant systemic infection. We then designed an experiment to explore whether TuMV^{W15A} replication and/or movement could be cis-complemented by expression of wt 6K$_2$. We constructed modified infectious clones TuMV^{W15A}/6K$_2$^{W15A}:mCherry and TuMV^{W15A}/6K$_2$:mCherry, in which 6K$_2$^{W15A}:mCherry and 6K$_2$:mCherry coding sequence were inserted between the P1 and HC-Pro coding sequence in the TuMV^{W15A} backbone, respectively (Fig. 6A). *N. benthamiana* epidermal cells were then agroinfiltrated with the above constructs and Western blot analysis was performed with the anti-CP serum. Higher amount of CP accumulation was detected for TuMV^{W15A}/6K$_2$:mCherry than for TuMV^{W15A}/6K$_2$^{W15A}:mCherry, but less than for TuMV/6K$_2$:mCherry (Fig. 6B). This experiment indicates that TuMV^{W15A} replication could be partially complemented by wt 6K$_2$ when expressed in cis.

We next tested if wt 6K$_2$ could complement the W15A mutation for cell-to-cell movement. We used a plasmid that contained an expression cassette for TuMV tagged with 6K$_2$:mCherry and another expression cassette for GFP-HDEL, both under the control of CaMV 35S promoter and within the left and right border sequences of the T-DNA (designated as TuMV/6K$_2$:mCherry//GFP-HDEL, Fig. 6A). With this dual cassette construct, we showed that we can distinguish primary infection foci when cells express both mCherry and GFP, from secondary infection foci when cells express mCherry alone (Agbeci, Grangeon et al. 2013). We replaced the tryptophan with alanine of the endogenous 6K$_2$, and the resulting construct was assigned as TuMV^{W15A}/6K$_2$:mCherry//GFP-HDEL (Fig. 6A). Agroinfiltrated leaves were examined five days later by confocal microscopy with a 20X objective. As expected, TuMV expressing 6K$_2$:mCherry could move beyond the primary infected cells (Fig. 6C), while TuMV^{W15A} was restricted exclusively to the primary infection foci (Fig. 6D). Almost every TuMV-infected cell samples analyzed (n=45) showed several cell layers of virus movement, while no movement was observed for TuMV^{W15A}-infected cell samples (n=40) (Fig. 6E).

These results indicate that virus cell-to-cell movement cannot be complemented by wt $6K_2$ expressed in cis. Possibly, $6K_2^{W15A}$ acts as a dominant negative mutant that affects wt $6K_2$ function.

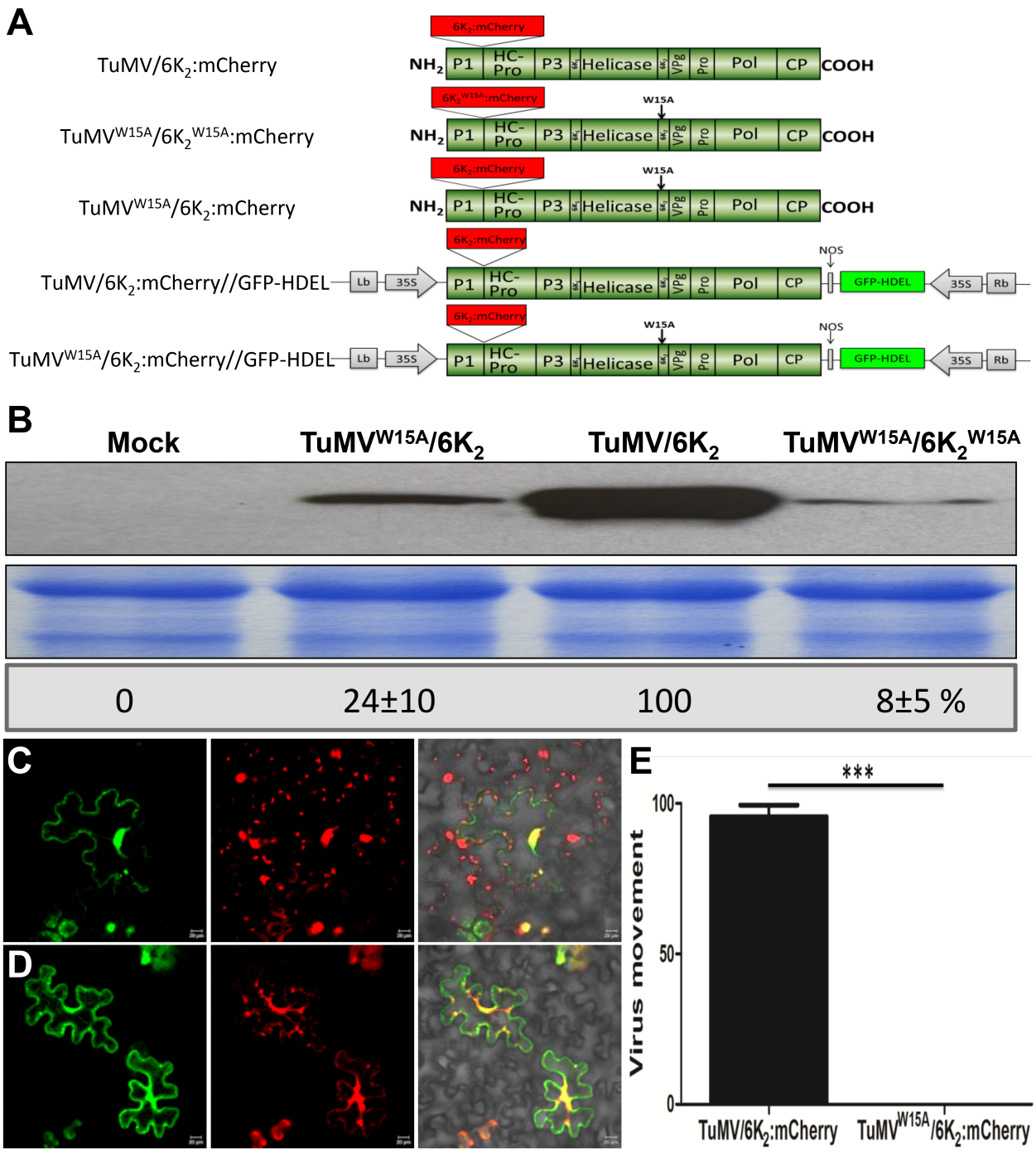

Figure 6. TuMV^{W15A} replication but not virus movement is complemented by cis expression of wild type 6K$_2$.

(A) Schematic representation of TuMV/$6K_2$:mCherry, TuMV^{W15A}/$6K_2^{W15A}$:mCherry, TuMV^{W15A}/$6K_2$:mCherry, TuMV/$6K_2$:mCherry//GFP-HDEL and TuMV^{W15A}/$6K_2$:mCherry//GFP-HDEL. One copy of $6K_2$ (wild type or mutated) between P1 and HC-Pro is shown as red box. Endogenous $6K_2$ is located between Helicase and VPg, and W15A mutation is indicated by arrow. Gray rectangles represent the left and right borders of T-DNA and gray arrows represent the CaMV 35S promoter. (B) Detection of CP accumulation in leaves infected with Mock, TuMV^{W15A}/$6K_2$:mCherry, TuMV/$6K_2$:mCherry and TuMV^{W15A}/$6K_2^{W15A}$:mCherry with anti-TuMV CP serum. Coomassie blue staining (bottom panel) shows equal protein loading. (C-D) Confocal images of TuMV/$6K_2$:mCherry//GFP-HDEL (C) and TuMV^{W15A}/$6K_2$:mCherry//GFP-HDEL (D) infected *N. benthamiana* epidermal cells. Optical images (2-μm thick) of green, red and merge colors are shown. (E) Statistical analysis of virus cell-to-cell movement of TuMV/$6K_2$:mCherry//GFP-HDEL and TuMV^{W15A}/$6K_2$:mCherry//GFP-HDEL infection foci in percentage. Significant difference (Student's t tests; $P < 0.001$) is indicated by asterisk. Mean values +/- S.D. of three independent experiments are shown.

$6K_2$ co-localizes and interacts with the COPII coatomer Sec24a

$6K_2$ vesicles use the secretory pathway through the Golgi apparatus to reach PDs from the ER (Agbeci, Grangeon et al. 2013, Grangeon, Jiang et al. 2013), and COPII vesicular trafficking has been shown to be involved in $6K_2$ intracellular movement (Wei and Wang 2008, Grangeon, Agbeci et al. 2012). COPII vesicle formation involves the guanine nucleotide exchange factor Sec12 that recruits GTPase Sar1 to ER export sites (ERES), which then interacts with Sec23-Sec24 and Sec13-Sec31 complexes to initiate vesicular transport involved in protein ER export (Brandizzi and Barlowe 2013). Sec24 is the factor that interacts with cargo proteins for their ER-to-Golgi vesicular transport. The Arabidopsis genome encodes three Sec24 homologs (Sec24a, Sec24b, and Sec24c). AtSec24a has been shown to be involved in protein COPII-dependent ER-Golgi transport (Brandizzi and Barlowe 2013), while AtSec24b and AtSec24c may have a similar cellular function that is essential in male and female gametogenesis (Tanaka, Nishimura et al. 2013).

To verify if $6K_2$ ER export may involve interaction with Sec24a, we first checked for co-localization between the two proteins. We expressed the COPII marker YFP-Sec24a (Grangeon, Agbeci et al. 2012) in leaves infected with TuMV/$6K_2$:mCherry. Partial co-localization was found with YFP-Sec24a and $6K_2$:mCherry (Fig. 7A). This partial co-localization likely reflects the dynamic nature of $6K_2$, which is expected to leave COPII vesicles upon entry in the Golgi apparatus (Agbeci, Grangeon et al. 2013). Blocking ER-to-Golgi trafficking should consequently increase the co-localization between the two proteins. We consequently treated cells infected with TuMV/$6K_2$:mCherry and expressing YFP-Sec24a with BFA, an antibiotic that inhibits protein retrieval from Golgi to ER (Nebenfuhr, Ritzenthaler et al. 2002). Fig. 7B shows that there was near complete co-localization of $6K_2$ vesicles with Sec24a in the presence of BFA. The PCC Rr value for the perfectly co-localized cis-Golgi markers ERD2:GFP with Man49:mCherry (Grangeon, Agbeci et al. 2012) was 0.69 ± 0.05 (Fig. 7C). The PCC Rr value of Sec24a with $6K_2$ in the absence of BFA was 0.10 ± 0.02, but was significantly higher in the presence of BFA (0.32 ± 0.03). This outcome is similar to what has been observed

previously (Grangeon, Agbeci et al. 2012). This indicates that when ER-to-Golgi trafficking is perturbed, $6K_2$ vesicles localize more frequently with Sec24a.

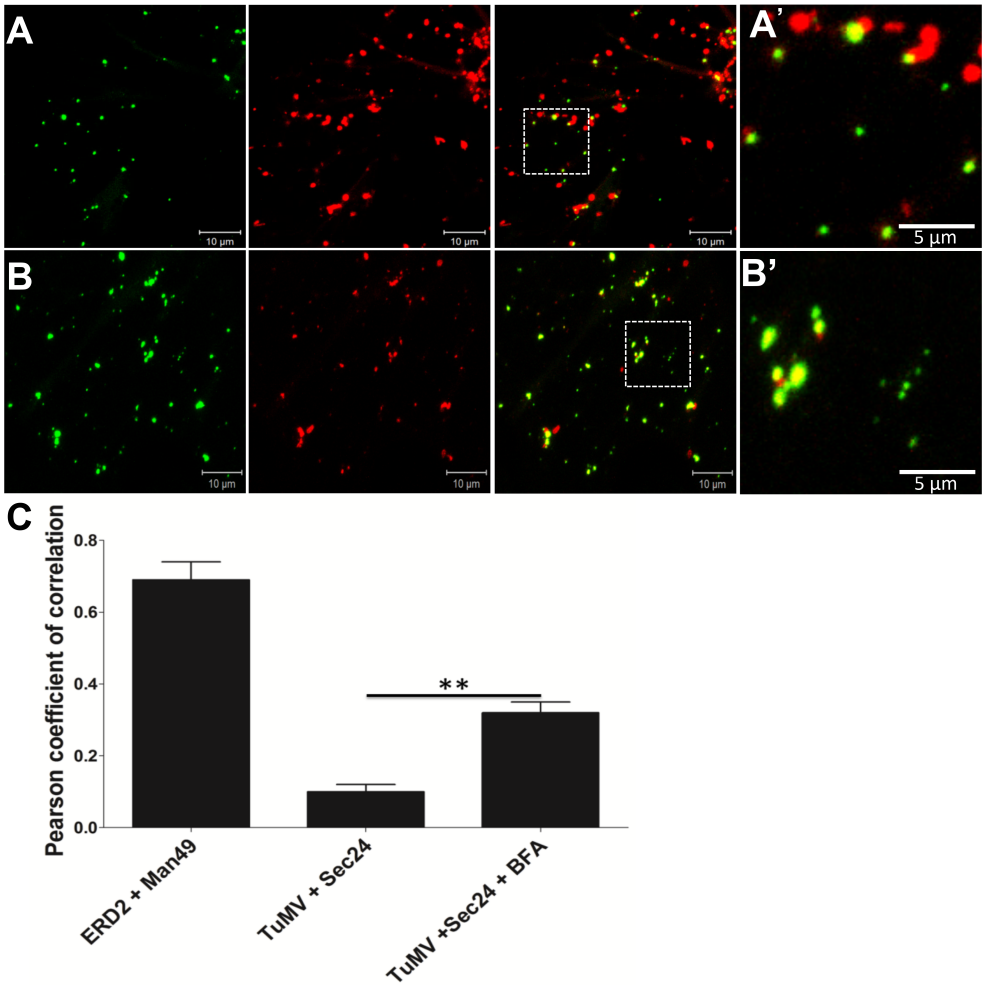

Figure 7. 6K$_2$ co-localizes with COPII coatomer Sec24a.

(A-B) *N. benthamiana* cells co-expressing YFP-Sec24a (left panel) with TuMV/6K$_2$:mCherry (middle panel) in the absence (A) and presence (B) of BFA, with merged panels shown on the right. The dashed box highlighted area of (A) and (B) is shown on the right as (A') and (B'), respectively. (C) Co-localization statistical analysis between YFP-Sec24a and the 6K$_2$-mCherry-tagged vesicles by calculation of the Pearson's correlation coefficient Rr values. Rr values for two co-localizing proteins, ERD2:GFP and Man49:mCherry are given. For TuMV/6K$_2$:mCherry + Sec24a and TuMV/6K$_2$:mCherry + Sec24a + BFA co-localization statistical analysis, sample number (N) is 26 for each tested combination. Significant difference (Student's t tests; 0.001 <

P < 0.01) is indicated by asterisk. Mean values +/- S.D. of three independent experiments are shown.

We next carried out a yeast-two-hybrid (YTH) assay to test whether $6K_2$ is able to interact with Sec24a. As $6K_2$ is a membrane protein, we used the split-ubiquitin membrane-based YTH system that is optimized for membrane protein interaction assay. Co-transformation of LV-Cub-$6K_2$ with the empty vector NubG indicated that $6K_2$ did not autoactivate the system (see Fig. 8A). We used LV-Cub-$6K_2$ and NubG-$6K_2$ as a positive interaction control, since $6K_2$-$6K_2$ interaction was demonstrated by BiFC and CO-IP experiments (data not shown). We next tested the interaction of LV-Cub-$6K_2$ with NubG-Sar1 or NubG-Sec24a. Our results showed that $6K_2$ interacted with Sec24a, but not with Sar1 (Fig. 8A). Although it cannot be excluded, reporter gene activation by Sec24a alone is not likely since interaction between Sec24a and $6K_2$ was subsequently confirmed by CO-IP experiments (see below).

To further confirm this YTH interaction, $6K_2$:mCherry and YFP-Sec24a fusion proteins were transiently expressed in *N. benthamiana* leaves, and interaction was assayed by co-immunopurification of YFP-Sec24a. As shown in Fig. 8B, $6K_2$:mCherry was co-purified along with YFP-Sec24a. Samples co-expressing control mCherry with YFP, mCherry with YFP-Sec24a, or $6K_2$:mCherry with YFP did not show any co-purification. These results indicate that $6K_2$ interacts with Sec24a. To confirm that the N-terminal cytoplasmic tail of $6K_2$ was responsible for Sec24a binding, we tested if N_2-TMD_1-C_1 could bind Sec24a. The Co-IP experiment indicated that indeed N_2-TMD_1-C_1:mCherry was purified along with YFP-Sec24a, but not $6K_1$:mCherry (Fig. 8C). In conclusion, these results showed that $6K_2$ interacts with Sec24a, and that the N-terminal predicted cytoplasmic tail is involved in the binding.

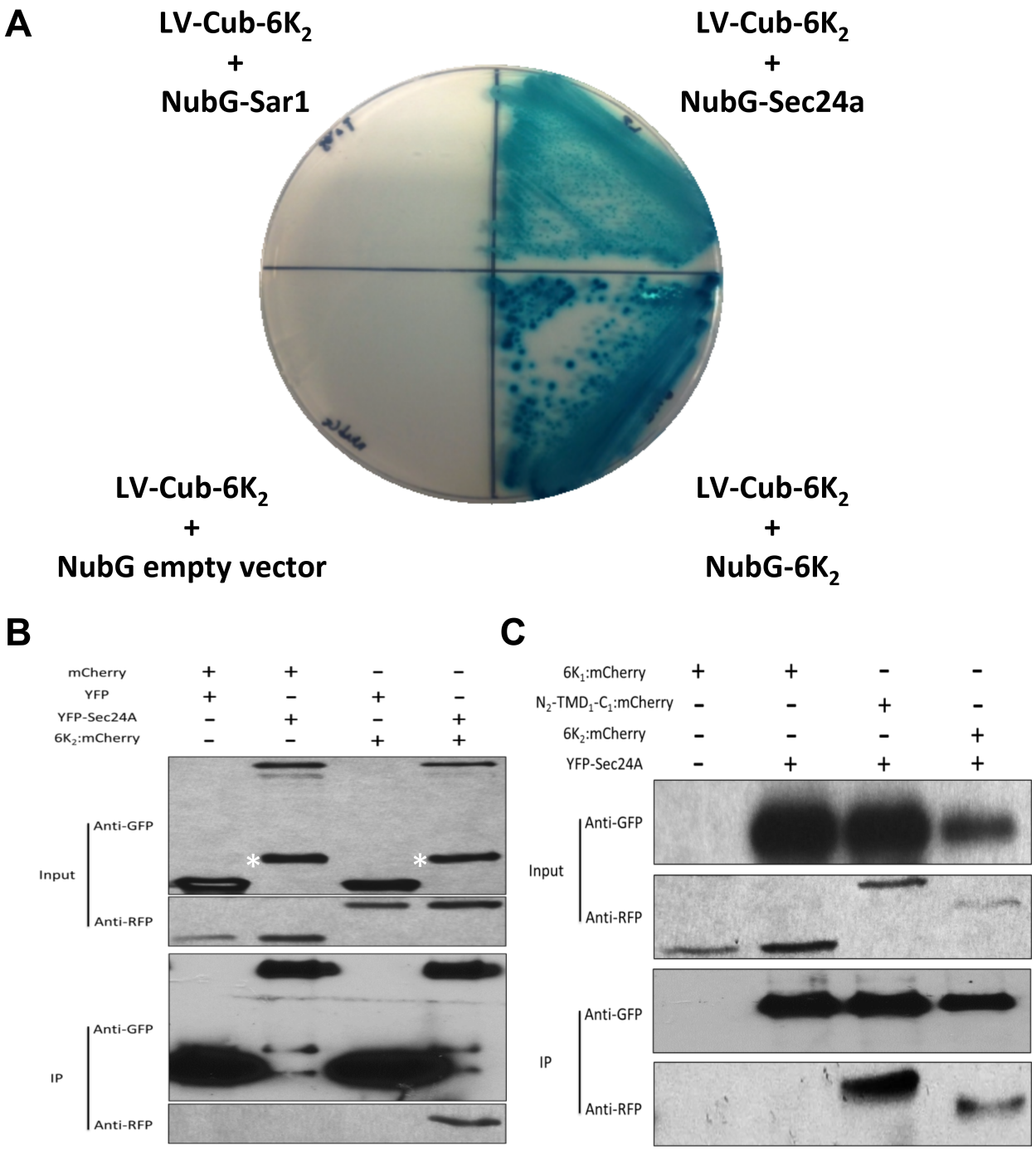

Figure 8. $6K_2$ interacts with COPII coatomer Sec24a.

(A) Yeast two-hybrid assay for protein-protein interactions of TuMV $6K_2$ with Sar1 and Sec24a. The transformants were plated on an SD/-Leu/-Trp/-His + X-Gal+ 3-AT medium. Upper left: $6K_2$ + Sar1 (LV-Cub-6K2 + NubG-Sar1); Upper right: $6K_2$ + Sec24a

(LV-Cub-6K2 + NubG-Sec24a); Lower left: negative control (LV-Cub-6K2 + NubG empty vector); Lower right: positive control (LV-Cub-6K2 + NubG-6K2). (B) *N. benthamiana* leaves expressing combinations of mCherry and YFP, mCherry and YFP-Sec24a, YFP and $6K_2$:mCherry, or YFP-Sec24a and $6K_2$:mCherry were harvested 3 days after agroinfiltration. The cleared lysates (input) were subjected to immunopurification on a GFP-Trap resin, followed by Western blot analysis of input and immunopurified (IP) fractions using antibodies against GFP and RFP. The asterisk indicates a nonspecific or a degradation protein species recognized by the anti-GFP serum. (C) *N. benthamiana* leaves expressing $6K_1$:mCherry alone, $6K_1$:mCherry and YFP-Sec24a, N_2-TMD_1-C_1:mCherry and YFP-Sec24a, $6K_2$:mCherry and YFP-Sec24a were analyzed as in B.

Defective Sec24a slows down TuMV systemic movement

We then verified the impact of a modified Sec24a for TuMV infection. Since homozygous *A. thaliana* knockout mutant for Sec24a cannot be generated, the importance of Sec24a in TuMV systemic movement was evaluated by infecting the *A. thaliana g92* mutant line (Faso, Chen et al. 2009) with TuMV/6K_2:GFP. The *g92* mutant line has a missense mutation in the gene coding for Sec24a that causes conversion of an Arg residue at position 693 to a Lys residue (Sec24a^{R693K}) in a region considered to be important for cargo binding. This partial loss of function of Sec24a induces the accumulation of Golgi bodies in globular structures composed of a mass of convoluted ER, similar to what is observed during TuMV infection. We first tested if Sec24a^{R693K} could interact with 6K_2 by YTH assay, and no growth on selective medium was observed (Fig. 9A). We then infected *A. thaliana* with TuMV/6K_2:GFP and noticed that wild type *A. thaliana* was systemically infected at 11 dpi, while *g92* was not (Fig. 9B). Western blot analysis using a rabbit serum against CP confirmed virus accumulation in the upper non-inoculated leaves of wild type *A. thaliana*, but not *g92* (Fig. 9C). We repeated this experiment three times by infecting 16 plants and scored for systemic infection by uv light evaluation at 11 dpi and 13 dpi. On average, we found that 80% of wt Arabidopsis Columbia-0 plants showed systemic infection, while less than 10% of *g92* plants were systemically infected at 11 dpi (Table 2). At 13 dpi, ~40% of *g92* plants were systemically infected. To assess virus replication at the cellular level, we isolated protoplasts from wt and *g92 A. thaliana* plants, and each protoplast preparation was split into three aliquots and were transfected with mock, p35STuMV^{VNN} and p35STuMV, respectively. After an incubation period of 40h, CP production was assessed by immunoblot analysis. Since protein loading may differ between the wt and *g92* protoplast preparations, CP level for the p35STuMV^{VNN} samples was given a score of 1X. CP quantification for the p35STuMV of wt and *g92* protoplast samples was normalized accordingly. We found that TuMV replication level was similar in both plants (Fig. 9D). We also agroinfiltrated wt and *g92 A. thaliana* leaves with TuMV/6K_2:mCherry//GFP-HDEL to assess intercellular movement of TuMV. At 8 dpi, red-only fluorescence zones, indicative of virus intercellular movement, were clearly

observed in wt *A. thaliana*, while this was not the case for *g92* plants (Fig. 9E vs 9F). Intercellular movement was, however, detected for both plants at 12 dpi. This indicates that the *g92* mutant line does not compromise TuMV cellular production but the presence of a defective Sec24a slows down the systemic movement of TuMV.

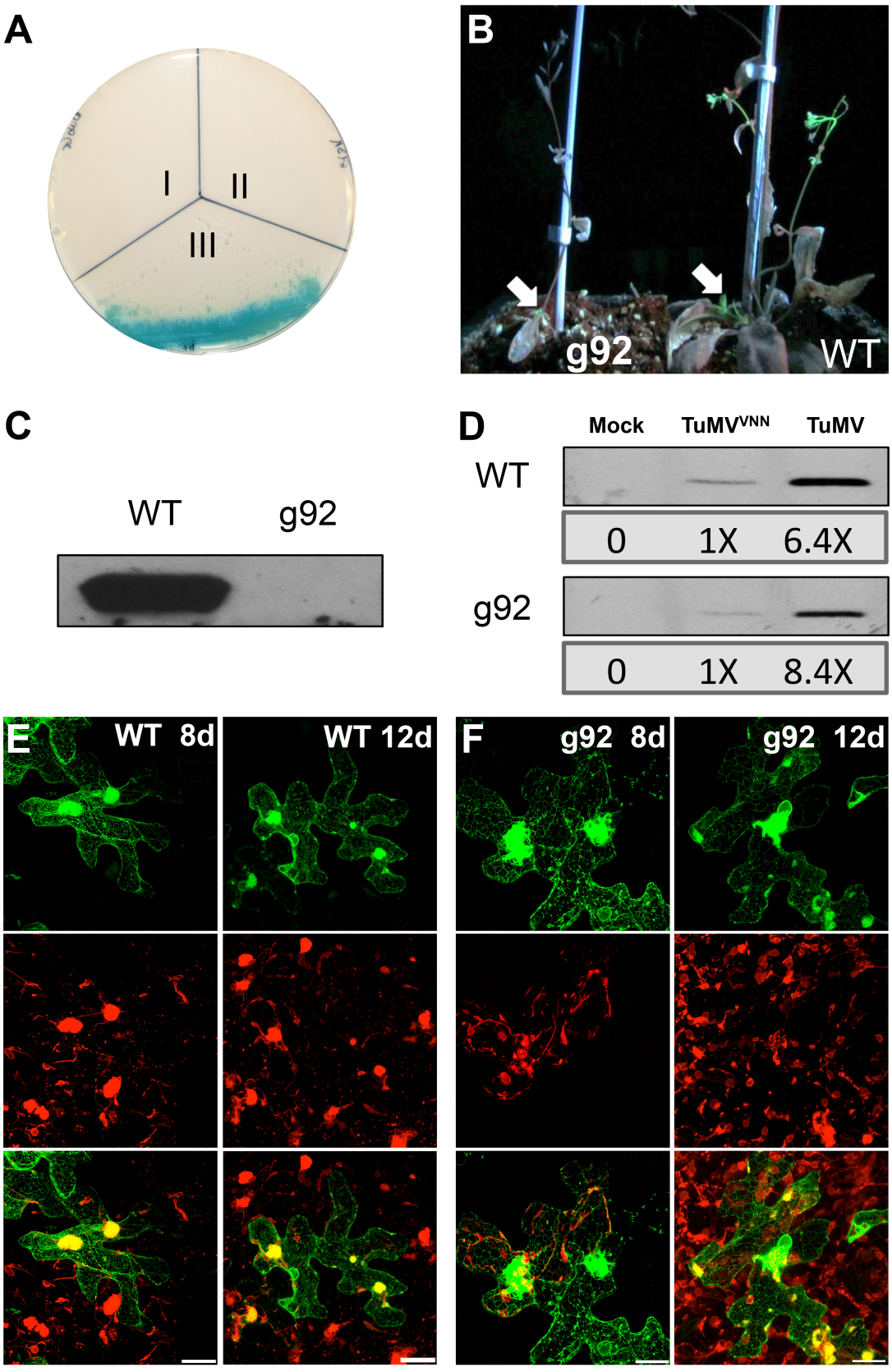
A
I
II
III
B
g92
WT
C
WT
g92
D
Mock
TuMV^VNN
TuMV
WT
0
1X
6.4X
g92
0
1X
8.4X
E
WT 8d
WT 12d
F
g92 8d
g92 12d

Figure 9. Infection of *g92* Arabidopsis thaliana.

(A) Yeast two-hybrid assay for protein-protein interactions of TuMV $6K_2$ with Sec24a^{R693K}. The transformants were plated on an SD/-Leu/-Trp/-His + X-Gal+ 3-AT medium. I: negative control (LV-Cub-6K2 + NubG empty vector); II: $6K_2$ + Sec24a^{R693K} (LV-Cub-6K2 + NubG-Sec24a^{R693K}); III: $6K_2$ + Sec24a (LV-Cub-6K2 + NubG-Sec24a). (B) wt and *g92* A. thaliana plants were inoculated with TuMV/$6K_2$:GFP and observed under UV light 11 days later. White arrows indicate the viral inoculation site. (C) The upper non-agroinfiltrated leaves of wt and *g92 A. thaliana plants* infected with TuMV/$6K_2$:GFP were collected at 11 dpi and analyzed for virus production by immunoblot analysis using a rabbit anti-CP serum. (D) Protoplasts were isolated from wt and *g92* A. thaliana plants and were transfected with mock, p35STuMV^{VNN} and p35STuMV. Production of CP was analyzed 40h after transfection using an anti-TuMV CP rabbit serum. Confocal images of TuMV/$6K_2$:mCherry//GFP-HDEL infiltrated wt (E) and *g92* (F) *A. thaliana* epidermal cells are shown at 8 and 12 dpi. These images are three-dimensional rendering of 60 1-µm-thick slices that overlap by 0.5 µm. Scale bar = 20 µm.

TABLE 2 Systemic viral infection of WT versus *g92* mutant *A. thaliana*

Exp. No.		Plants systemic infected	
		11 dpi	13 dpi
1	Wt	12/16	14/16
	G92	0/16	7/16
2	Wt	14/16	14/16
	G92	2/16	8/16
3	Wt	11/16	13/16
	G92	1/16	6/16

Discussion

TuMV $6K_2$-induced vesicles have been shown to traffic through the secretory pathway for successful viral infection (Cotton, Grangeon et al. 2009, Grangeon, Agbeci et al. 2012, Agbeci, Grangeon et al. 2013, Grangeon, Jiang et al. 2013). Additionally, $6K_2$-induced vesicles of TEV were found at ERES and their formation was shown to be dependent on COPI and COPII factors (Wei and Wang 2008, Lerich, Langhans et al. 2011). These studies, however, did not provide a mechanistic explanation on how $6K_2$ is involved with the COPII machinery and what COPII component is directly interacting with $6K_2$. It is also not known if involvement of COPII components is required for vRNA replication per se, or for cellular movement of the vRNA.

Secondary structure predictions indicated that $6K_2$ is an integral membrane protein (Table 1). According to these predictions, the C-terminal end would be located in the lumen of the $6K_2$ vesicles. This is supported by prior studies demonstrating that the VPg-Pro domain of the precursor form $6K_2$-VPg-Pro is located in the lumen of $6K_2$-induced vesicles (Beauchemin, Boutet et al. 2007), and that PABP, which interacts with VPg, is internalized in these same vesicles (Beauchemin and Laliberté 2007). The observation, however, that some $6K_2$ was released from the P30 fraction upon treatment with urea (Fig. 1) suggests that the viral protein may not be an integral membrane protein, but is rather tightly associated with cellular membranes. Treatment with urea was also shown to release the Tobacco mosaic virus 30K movement protein from membranes and was concluded to be peripherally associated with cellular membranes (Peiró, Martínez-Gil et al. 2014). Consequently, we cannot definitely conclude that $6K_2$ is an integral membrane protein. Experiments involving proteolytic protection and bimolecular fluorescence complementation assays will be needed to solve this issue.

$6K_2$ normally induces the formation of motile vesicles that contain replication complexes (Cotton, Grangeon et al. 2009). In the present study, we found that $6K_2$ was retained in the ER, with fewer vesicles being formed, when the N-terminal 18 amino acids were

deleted (Fig. 3). This indicated that this region contained motif(s) for the ER export of the viral protein. We further defined the motif(s) by showing that changing the tryptophan residue at position 15 or both lysine residues at position 14 and 17 into alanine residues resulted in partial ER retention of the protein (Fig. 4). This indicated that these amino acid residues are non-redundant in ER export, suggesting the presence of a combinatorial ER export motif, which might be required to ensure a tight interaction with COPII vesicles (Franke, Braulke et al. 2013). ER export motifs for many proteins that undergo ER-Golgi transport have been identified. Those ER export motifs can be divided into four types: di-acidic [DXE, EXXD, and YXΦESDG (X is any amino acid and Φ is a bulky, hydrophobic residue)], di-basic [(RK)X(RK)], di-hydrophobic (LL, LxL, VV) and di-aromatic (FF, YY or FY) motifs (Barlowe 2003). In the case of the Norwalk virus, the nonstructural protein p22, which inhibits COPII vesicle trafficking, contains the YXΦESDG motif (Sharp, Guix et al. 2010). The DSSP domain in the N- and the lysine residue in the C-terminal tail of MNSV p7B are required for ER export (Serra-Soriano, Pallás et al. 2014). On the other hand, no clearly defined ER export motifs were identified for the TGBp3 of BaMV (Wu, Lee et al. 2011).

These N-terminal 18 residues were predicted to be exposed in the cytosol (Fig. 1), and were found to possibly interact with membrane-associated host factors (i.e. proteins or lipids) (Fig. 2). One host factor turned out to be Sec24a (Fig. 8), which is consistent with the current model where Sec24a binds the cytoplasmic tail of the cargo membrane proteins for their ER export (Brandizzi and Barlowe 2013). Sec24 is the main COPII coat protein that recognizes specific sorting sequences in cargo proteins and has multiple independent cargo-binding sites, which provides the required plasticity for selecting cargo molecules with distinct sorting signals (Miller, Beilharz et al. 2003). Sec24a binding to cargo membrane proteins is dynamic as this complex disassembles as soon as the vesicle buds off from the ER. Once this takes place, Sec24a is recycled back to the ERES (Brandizzi and Barlowe 2013). This dynamic interaction explains the partial co-localization of Sec24a with $6K_2$-induced vesicles (Fig. 7). Only when ER-to-Golgi trafficking is stalled by the addition of BFA that near complete co-localization can be observed. Hanton et al. (Hanton, Matheson et al. 2009) showed that treatment with

100 μg/ml BFA caused the redistribution of ERES markers to the cytosol. A lower BFA concentration (10 μg/ml) in our case may explain the discrepancy between the two outcomes.

The biological significance of the interaction between Sec24a and $6K_2$ was supported by the delayed systemic infection of the *A. thaliana g92* mutant line (Fig. 9). Sec24a being essential for plant viability, it cannot be excluded that the partial loss of function of this protein may have pleomorphic rather than specific effects on virus infection. We think, however, that the defective Sec24a would have direct impact on virus infection. The partial loss of function of Sec24a in *g92* plants caused unique ER morphology defects and inhibition of protein secretion (Faso, Chen et al. 2009, Nakano, Matsushima et al. 2009). The same membrane rearrangement and inhibition of protein secretion were observed in TuMV-infected cells (Grangeon, Agbeci et al. 2012). Possibly, the same effect points to the same cause – Sec24a function has been modified. The difference is that the R693K mutation alters Sec24a activity in *g92* plants, while $6K_2$ co-opts Sec24a function and thus affects its ability to function normally in ER-to-Golgi vesicular trafficking in TuMV-infected cell.

Replacing the tryptophan residue of $6K_2$ with an alanine within the polyprotein (i.e. $TuMV^{W15A}$) affected TuMV infection. The end result was a reduced level of cellular virus production, with no indication of plant systemic viral infection (Fig. 5). The reduced virus production at the cellular level could be the reason why no virus movement was observed. However, we would have expected a delayed systemic infection since $TuMV^{W15A}$ cellular production was still significant, being half the level of what was obtained for wt TuMV. There was, however, no systemic infection, even after two weeks when normally it is observed at 5 dpi with wt TuMV. Furthermore, the way we analyze cell-to-cell movement is very sensitive and we can easily distinguish movement at a single-cell layer, but we did not observe any cell-to-cell movement for $TuMV^{W15A}/6K_2$:mCherry (Fig. 6). Consequently, it does not appear that reduced virus production is the reason for lack of virus movement. The recent observation that plant virus replication and movement are coupled events (Tilsner, Linnik et al. 2013) suggests

that they should be considered as a unit, where replication and movement cannot be separated from each other. This also appears to be the case for TuMV (Grangeon, Jiang et al. 2013). Thus, we think that the W15A mutation has a primary effect on virus movement, with an overflow effect on virus production.

$6K_2$ is found in the form of $6K_2$-VPg-Pro in infected cells (Beauchemin, Boutet et al. 2007), and VPg has been proposed to act as a hub protein for the assembly of the replication complex (Jiang and Laliberte 2011). This suggests that a much larger protein complex exits as a result of $6K_2$ being recognized as a cargo membrane protein. We thus propose that by interacting with Sec24a, $6K_2$ is able to engage the host cell ER export machinery to initiate viral vesicular formation for transport of vRNA and viral as well as host proteins that are necessary for virus systemic movement.

Acknowledgments

This work was supported by grants from the Natural Science and Engineering Research Council (NSERC) of Canada and from Le Fonds québécois de recherche sur la nature et les technologies (FQRNT) to HZ and JFL.

We thank Jessy Tremblay for helping with confocal microscopy, and Federica Brandizzi for *A. thaliana g92* seeds. We thank Peter Moffett for critically reading the manuscript.

References

1. **den Boon JA, Ahlquist P.** 2010. Organelle-Like Membrane Compartmentalization of Positive-Strand RNA Virus Replication Factories. Annual Review of Microbiology **64:**241-256.

2. **Laliberté J-F, Sanfaçon H.** 2010. Cellular Remodeling During Plant Virus Infection. Annual Review of Phytopathology **48:**69-91.

3. **Belov GA, Nair V, Hansen BT, Hoyt FH, Fischer ER, Ehrenfeld E.** 2012. Complex Dynamic Development of Poliovirus Membranous Replication Complexes. Journal of Virology **86:**302-312.

4. **Knoops K, Kikkert M, Worm SHEvd, Zevenhoven-Dobbe JC, van der Meer Y, Koster AJ, Mommaas AM, Snijder EJ.** 2008. SARS-Coronavirus Replication Is Supported by a Reticulovesicular Network of Modified Endoplasmic Reticulum. PLoS Biol **6:**e226.

5. **Knoops K, Bárcena M, Limpens RWAL, Koster AJ, Mommaas AM, Snijder EJ.** 2012. Ultrastructural Characterization of Arterivirus Replication Structures: Reshaping the Endoplasmic Reticulum To Accommodate Viral RNA Synthesis. Journal of Virology **86:**2474-2487.

6. **Carette JE, Stuiver M, Van Lent J, Wellink J, Van Kammen A.** 2000. Cowpea Mosaic Virus Infection Induces a Massive Proliferation of Endoplasmic Reticulum but Not Golgi Membranes and Is Dependent on De Novo Membrane Synthesis. Journal of Virology **74:**6556-6563.

7. **Hwang Y, McCartney A, Gidda S, Mullen R.** 2008. Localization of the Carnation Italian ringspot virus replication protein p36 to the mitochondrial outer membrane is mediated by an internal targeting signal and the TOM complex. BMC Cell Biology **9:**54.

8. **Prod'homme D, Jakubiec A, Tournier V, Drugeon G, Jupin I.** 2003. Targeting of the Turnip Yellow Mosaic Virus 66K Replication Protein to the Chloroplast Envelope Is Mediated by the 140K Protein. Journal of Virology **77:**9124-9135.

9. **McCartney AW, Greenwood JS, Fabian MR, White KA, Mullen RT.** 2005. Localization of the Tomato Bushy Stunt Virus Replication Protein p33 Reveals a Peroxisome-to-Endoplasmic Reticulum Sorting Pathway. The Plant Cell Online **17:**3513-3531.

10. **Nagy PD, Pogany J.** 2012. The dependence of viral RNA replication on co-opted host factors. Nat Rev Micro **10:**137-149.

11. **Diaz A, Ahlquist P.** 2012. Role of host reticulon proteins in rearranging membranes for positive-strand RNA virus replication. Current Opinion in Microbiology **15:**519-524.

12. **Verchot J.** 2012. Cellular chaperones and folding enzymes are vital contributors to membrane bound replication and movement complexes during plant RNA virus infection. Frontiers in Plant Science **3**.

13. **Schwartz M, Chen J, Janda M, Sullivan M, den Boon J, Ahlquist P.** 2002. A Positive-Strand RNA Virus Replication Complex Parallels Form and Function of Retrovirus Capsids. Molecular Cell **9:**505-514.

14. **Tilsner J, Linnik O, Louveaux M, Roberts IM, Chapman SN, Oparka KJ.** 2013. Replication and trafficking of a plant virus are coupled at the entrances of plasmodesmata. The Journal of Cell Biology **201:**981-995.

15. **Kusumanegara K, Mine A, Hyodo K, Kaido M, Mise K, Okuno T.** 2012. Identification of domains in p27 auxiliary replicase protein essential for its association with the endoplasmic reticulum membranes in Red clover necrotic mosaic virus. Virology **433:**131-141.

16. **Genovés A, Pallás V, Navarro JA.** 2011. Contribution of Topology Determinants of a Viral Movement Protein to Its Membrane Association, Intracellular Traffic, and Viral Cell-to-Cell Movement. Journal of Virology **85:**7797-7809.

17. **Wu C-H, Lee S-C, Wang C-W.** 2011. Viral protein targeting to the cortical endoplasmic reticulum is required for cell–cell spreading in plants. The Journal of Cell Biology **193:**521-535.

18. **Wei T, Zhang C, Hou X, Sanfacon H, Wang A.** 2013. The SNARE protein Syp71 is essential for turnip mosaic virus infection by mediating fusion of virus-induced vesicles with chloroplasts. PLoS Pathog **9:**e1003378.

19. **Hyodo K, Mine A, Taniguchi T, Kaido M, Mise K, Taniguchi H, Okuno T.** 2013. ADP ribosylation factor 1 plays an essential role in the replication of a plant RNA virus. J Virol **87:**163-176.

20. **Brandizzi F, Barlowe C.** 2013. Organization of the ER-Golgi interface for membrane traffic control. Nat Rev Mol Cell Biol **14:**382-392.

21. **Barajas D, Jiang Y, Nagy PD.** 2009. A unique role for the host ESCRT proteins in replication of Tomato bushy stunt virus. PLoS Pathog **5:**e1000705.

22. **Barajas D, Nagy PD.** 2010. Ubiquitination of tombusvirus p33 replication protein plays a role in virus replication and binding to the host Vps23p ESCRT protein. Virology **397:**358-368.

23. **Diaz A, Wang X, Ahlquist P.** 2010. Membrane-shaping host reticulon proteins play crucial roles in viral RNA replication compartment formation and function. Proc Natl Acad Sci U S A **107:**16291-16296.

24. **Mayo MA.** 1995. The Potyviridae. By D. D. SHUKLA, C. W. WARD and A. A. BRUNT. 25 × 17 cm. Pp. 516 with 110 text-figures and 30 tables, Wallingford: CAB International, 1994. Price: £60.00. New Phytologist **131:**289-290.

25. **Grangeon R, Agbeci M, Chen J, Grondin G, Zheng H, Laliberté J-F.** 2012. Impact on the Endoplasmic Reticulum and Golgi Apparatus of Turnip Mosaic Virus Infection. Journal of Virology **86:**9255-9265.

26. **Cotton S, Grangeon R, Thivierge K, Mathieu I, Ide C, Wei T, Wang A, Laliberté J-F.** 2009. Turnip Mosaic Virus RNA Replication Complex Vesicles Are Mobile, Align with Microfilaments, and Are Each Derived from a Single Viral Genome. Journal of Virology **83:**10460-10471.

27. **Grangeon R, Jiang J, Wan J, Agbeci M, Zheng H, Laliberté J-F.** 2013. 6K2-induced vesicles can move cell to cell during turnip mosaic virus infection. Frontiers in Microbiology **4**.

28. **Beauchemin C, Boutet N, Laliberté J-F.** 2007. Visualization of the Interaction between the Precursors of VPg, the Viral Protein Linked to the Genome of Turnip Mosaic Virus, and the Translation Eukaryotic Initiation Factor iso 4E In Planta. Journal of Virology **81:**775-782.

29. **Wei T, Wang A.** 2008. Biogenesis of Cytoplasmic Membranous Vesicles for Plant Potyvirus Replication Occurs at Endoplasmic Reticulum Exit Sites in a COPI- and COPII-Dependent Manner. Journal of Virology **82:**12252-12264.

30. **Krogh A, Larsson B, von Heijne G, Sonnhammer EL.** 2001. Predicting transmembrane protein topology with a hidden Markov model: application to complete genomes. J Mol Biol **305:**567-580.

31. **Hirokawa T, Boon-Chieng S, Mitaku S.** 1998. SOSUI: classification and secondary structure prediction system for membrane proteins. Bioinformatics **14:**378-379.

32. **Claros MG, von Heijne G.** 1994. TopPred II: an improved software for membrane protein structure predictions. Comput Appl Biosci **10:**685-686.

33. **Hessa T, Kim H, Bihlmaier K, Lundin C, Boekel J, Andersson H, Nilsson I, White SH, von Heijne G.** 2005. Recognition of transmembrane helices by the endoplasmic reticulum translocon. Nature **433:**377-381.

34. **Jones DT, Taylor WR, Thornton JM.** 1994. A model recognition approach to the prediction of all-helical membrane protein structure and topology. Biochemistry **33:**3038-3049.

35. **Cserzo M, Wallin E, Simon I, von Heijne G, Elofsson A.** 1997. Prediction of transmembrane alpha-helices in prokaryotic membrane proteins: the dense alignment surface method. Protein Eng **10:**673-676.

36. **Rost B, Yachdav G, Liu J.** 2004. The PredictProtein server. Nucleic Acids Res **32:**W321-326.

37. **Juretic D, Zoranic L, Zucic D.** 2002. Basic charge clusters and predictions of membrane protein topology. J Chem Inf Comput Sci **42:**620-632.

38. **Jayasinghe S, Hristova K, White SH.** 2001. MPtopo: A database of membrane protein topology. Protein Science **10:**455-458.

39. **Thivierge K, Cotton S, Dufresne PJ, Mathieu I, Beauchemin C, Ide C, Fortin MG, Laliberté J-F.** 2008. Eukaryotic elongation factor 1A interacts with Turnip mosaic virus RNA-dependent RNA polymerase and VPg-Pro in virus-induced vesicles. Virology **377:**216-225.

40. **Beauchemin C, Bougie V, Laliberté J-F.** 2005. Simultaneous production of two foreign proteins from a potyvirus-based vector. Virus Research **112:**1-8.

41. **Sparkes IA, Runions J, Kearns A, Hawes C.** 2006. Rapid, transient expression of fluorescent fusion proteins in tobacco plants and generation of stably transformed plants. Nat Protocols **1:**2019-2025.

42. **Chen J, Stefano G, Brandizzi F, Zheng H.** 2011. Arabidopsis RHD3 mediates the generation of the tubular ER network and is required for Golgi distribution and motility in plant cells. Journal of Cell Science **124:**2241-2252.

43. **Yoo SD, Cho YH, Sheen J.** 2007. Arabidopsis mesophyll protoplasts: a versatile cell system for transient gene expression analysis. Nat Protoc **2:**1565-1572.

44. **Grefen C, Lalonde S, Obrdlik P.** 2001. Split-Ubiquitin System for Identifying Protein-Protein Interactions in Membrane and Full-Length Proteins, Current Protocols in Neuroscience doi:10.1002/0471142301.ns0527s41. John Wiley & Sons, Inc.

45. **Beauchemin C, Laliberté J-F.** 2007. The Poly(A) Binding Protein Is Internalized in Virus-Induced Vesicles or Redistributed to the Nucleolus during Turnip Mosaic Virus Infection. Journal of Virology **81:**10905-10913.

46. **von Heijne G.** 1992. Membrane protein structure prediction: Hydrophobicity analysis and the positive-inside rule. Journal of Molecular Biology **225:**487-494.

47. **Krogh A, Larsson B, von Heijne G, Sonnhammer ELL.** 2001. Predicting transmembrane protein topology with a hidden markov model: application to complete genomes. Journal of Molecular Biology **305:**567-580.

48. **von Heijne G, Gavel Y.** 1988. Topogenic signals in integral membrane proteins. European Journal of Biochemistry **174:**671-678.

49. **Brandizzi F, Snapp EL, Roberts AG, Lippincott-Schwartz J, Hawes C.** 2002. Membrane protein transport between the endoplasmic reticulum and the golgi in tobacco leaves is energy dependent but cytoskeleton independent: Evidence from selective photobleaching. Plant Cell **14:**1293-1309.

50. **Barlowe C.** 2003. Signals for COPII-dependent export from the ER: what's the ticket out? Trends in Cell Biology **13:**295-300.

51. **Dunn KW, Kamocka MM, McDonald JH.** 2011. A practical guide to evaluating colocalization in biological microscopy. Am J Physiol Cell Physiol **300:**C723-742.

52. **Giraudo CG, Maccioni HJF.** 2003. Endoplasmic Reticulum Export of Glycosyltransferases Depends on Interaction of a Cytoplasmic Dibasic Motif with Sar1. Molecular Biology of the Cell **14:**3753-3766.

53. **Schoberer J, Vavra U, Stadlmann J, Hawes C, Mach L, Steinkellner H, Strasser R.** 2009. Arginine/Lysine Residues in the Cytoplasmic Tail Promote ER Export of Plant Glycosylation Enzymes. Traffic **10:**101-115.

54. **Li XH, Carrington JC.** 1995. Complementation of tobacco etch potyvirus mutants by active RNA polymerase expressed in transgenic cells. Proceedings of the National Academy of Sciences **92:**457-461.

55. **Agbeci M, Grangeon R, Nelson RS, Zheng H, Laliberté J-F.** 2013. Contribution of Host Intracellular Transport Machineries to Intercellular Movement of Turnip Mosaic Virus. PLoS Pathog **9:**e1003683.

56. **Tanaka Y, Nishimura K, Kawamukai M, Oshima A, Nakagawa T.** 2013. Redundant function of two Arabidopsis COPII components, AtSec24B and AtSec24C, is essential for male and female gametogenesis. Planta **238:**561-575.

57. **Nebenfuhr A, Ritzenthaler C, Robinson DG.** 2002. Brefeldin A: Deciphering an enigmatic inhibitor of secretion. Plant Physiology **130:**1102-1108.

58. **Faso C, Chen YN, Tamura K, Held M, Zemelis S, Marti L, Saravanan R, Hummel E, Kung L, Miller E, Hawes C, Brandizzi F.** 2009. A missense mutation in the Arabidopsis COPII coat protein Sec24A induces the formation of clusters of the endoplasmic reticulum and Golgi apparatus. Plant Cell **21:**3655-3671.

59. **Lerich A, Langhans M, Sturm S, Robinson DG.** 2011. Is the 6 kDa tobacco etch viral protein a bona fide ERES marker? Journal of Experimental Botany **62:**5013-5023.

60. **Peiró A, Martínez-Gil L, Tamborero S, Pallás V, Sánchez-Navarro JA, Mingarro I.** 2014. The Tobacco mosaic virus Movement Protein Associates with but Does Not Integrate into Biological Membranes. Journal of Virology **88:**3016-3026.

61. **Franke M, Braulke T, Storch S.** 2013. Transport of the GlcNAc-1-phosphotransferase α/β-Subunit Precursor Protein to the Golgi Apparatus Requires a Combinatorial Sorting Motif. Journal of Biological Chemistry **288:**1238-1249.

62. **Sharp TM, Guix S, Katayama K, Crawford SE, Estes MK.** 2010. Inhibition of cellular protein secretion by Norwalk virus nonstructural protein p22 requires a mimic of an endoplasmic reticulum export signal. PLoS One **5:**e13130.

63. **Serra-Soriano M, Pallás V, Navarro JA.** 2014. A model for transport of a viral membrane protein through the early secretory pathway: minimal sequence and endoplasmic reticulum lateral mobility requirements. The Plant Journal **77:**863-879.

64. **Miller EA, Beilharz TH, Malkus PN, Lee MCS, Hamamoto S, Orci L, Schekman R.** 2003. Multiple Cargo Binding Sites on the COPII Subunit Sec24p Ensure Capture of Diverse Membrane Proteins into Transport Vesicles. Cell **114:**497-509.

65. **Hanton SL, Matheson LA, Chatre L, Brandizzi F.** 2009. Dynamic organization of COPII coat proteins at endoplasmic reticulum export sites in plant cells. Plant J **57:**963-974.

66. **Nakano RT, Matsushima R, Ueda H, Tamura K, Shimada T, Li L, Hayashi Y, Kondo M, Nishimura M, Hara-Nishimura I.** 2009. GNOM-LIKE1/ERMO1 and SEC24a/ERMO2 Are Required for Maintenance of Endoplasmic Reticulum Morphology in Arabidopsis thaliana. The Plant Cell Online **21:**3672-3685.

67. **Jiang J, Laliberte JF.** 2011. The genome-linked protein VPg of plant viruses-a protein with many partners. Curr Opin Virol **1:**347-354.

CHAPTER 3: $6K_2$ trans-membrane domain GxxxG motif and its Golgi exit (Publication No. 2)

$6K_2$ requires the GXXXG motif for Golgi exit during Turnip mosaic virus infection

Manuscript in preparation for submission to *Virology*

Jun Jiang[1], Fernanda Prieto Bruckner, Juan Wan[1], Huanquan Zheng[2] and Jean-François Laliberté[1#]

1. INRS-Institut Armand-Frappier, 531 Boulevard des Prairies, Laval, Québec, H7V 1B7, Canada
2. Department of Biology, McGill University, 1205 Dr. Penfield Avenue, Montréal, Québec, H3A 1B1, Canada

Author for correspondence : Prof. Jean-François Laliberté

INRS-Institut Armand-Frappier

531, boulevard des Prairies

Laval, Québec, Canada H7V 1B7

Telephone number: 1-450-687-5010, ext. 4445

email address: jean-francois.laliberte@iaf.inrs.ca

Contribution of student

This manuscript is in preparation and will be submitted to *Virology*. I designed and performed most of the experimental work (Fig. 1-4, 6 and Fig. S1) and analysed data with advice from my supervisor Professor Jean-François Laliberté. Juan Wan contributed to Figure 5. I prepared the first draft of this manuscript, and Jean-Francois Laliberté and Huanquan Zheng helped me improve the writing. Fernanda Prieto Bruckner contributed partially to the Western blot assay.

Résumé

La réplication des virus à ARN positif induit la formation de structures membranaires. Dans le cas du virus de la mosaïque du navet (TuMV), la protéine virale $6K_2$ associée aux membranes induit la formation de vésicules de réplication qui proviennent du réticulum endoplasmique (RE). Nous avons précédemment rapporté que l'extrémité N-terminale de la protéine virale est nécessaire pour l'exportation de $6K_2$ du RE en interagissant avec le coatomer COPII Sec24a. Ici, nous avons identifié un motif GXXXG dans le domaine transmembranaire (TMD) présomptif de $6K_2$ qui est important pour la formation de vésicules. La mutation de ce motif s'est traduite par une rétention des vésicules dans le Golgi, et une réduction importante dans la production de virus. La mutation a également aboli l'association entre $6K_2$ et les chloroplastes. Nous avons en outre constaté que l'ARN double brin (ARNdb), qui est la forme réplicative de l'ARN viral, n'était pas associé aux chloroplastes, indiquant ainsi que les chloroplastes ne sont pas le support de la synthèse de l'ARNv, mais ont plutôt un rôle accessoire lors de l'infection du TuMV. Nos résultats démontrent que $6K_2$ transite par l'appareil de Golgi pour la formation de vésicules et pour son association avec les chloroplastes.

Abstract

The replication of positive sense RNA viruses induces membranous structure formation. In the case of *Turnip mosaic virus* (TuMV), the membrane-associated viral protein $6K_2$ induces the formation of replication vesicles that are derived from the endoplasmic reticulum (ER). We have previously reported that the N-terminal tail of this viral protein is required for $6K_2$ ER export by interacting with the COPII coatomer Sec24a. Here, we identified a GXXXG motif within the predicted trans-membrane domain (TMD) of $6K_2$ that is important for vesicle formation. Mutation of this motif resulted in retention of the vesicles in the Golgi, and dramatically impaired virus production. The mutation also abolished $6K_2$-chloroplast association. We further found that double-stranded RNA (dsRNA), the replicative form of the viral RNA (vRNA), was not found associated with chloroplasts, indicating that chloroplasts do not support vRNA synthesis but instead have an accessory role during TuMV infection. Our results thus demonstrate that $6K_2$ transits through the Golgi apparatus for vesicle formation and chloroplast association.

Introduction

As obligate intracellular parasites, viruses co-opt various components of the host cells during infection (Nagy and Pogany 2012). For instance, membranes, which are a fundamental building blocks of the host cell, are required by positive sense RNA [(+) RNA] viruses for their replication (Laliberté and Zheng 2014). Viral replication induces extensive cellular membrane remodeling that leads to the formation of membranous structures termed 'viral factories' (Laliberte and Sanfacon 2010). These viral factories are enriched in viral and host replication factors, thus supporting efficient viral RNA (vRNA) synthesis. Additionally, the confinement of viral components within these viral factories minimizes the potential of being recognized by the host cell immune system (Ishibashi and Ishikawa 2013).

(+) RNA viral genomes invariably encode at least one viral protein that associates with membranes. For example, the p33 protein of *Tomato bushy stunt virus* (TBSV), the 1a protein of *Brome mosaic virus* (BMV) and the triple gene block protein 2 (TGBp2) of *Potato virus X* (PVX) are membrane bound (Ju, Samuels et al. 2005, McCartney, Greenwood et al. 2005, Liu, Westler et al. 2009). Generally, these viral proteins preferentially target only one type of cellular membranes, thus determining which organelle is going to be modified during vRNA replication.

Exceptionally, the membrane-associated viral proteins may switch from one membrane to the other under certain situations. In the absence of the peroxisome, the TBSV p33 protein redirects to the ER (Jonczyk, Pathak et al. 2007). Additionally, several membrane-associated viral proteins may sequentially target two or more different types of cellular membranes. In the case of *Potato mop-top virus* (PMTV), the viral membrane-associated protein TGBp2 initially associates with the ER, and then chloroplasts (Cowan, Roberts et al. 2012).

These membrane-associated viral proteins are multifunctional, due to the presence of different functional domains for protein-protein, protein-RNA and protein-lipid

interactions. Notably, these viral proteins contain either trans-membrane domains (TMDs) and/or amphipathic helices for membrane insertion or association. The viral membrane-associated proteins, such as the p27 protein of *Red clover necrotic mosaic virus* (RCNMV) and the TGBp2 of PVX, are characterized by their membrane association through their TMDs (Mitra, Krishnamurthy et al. 2003, Kusumanegara, Mine et al. 2012). The membrane association of the other viral proteins, such as the BMV 1a protein, is mediated by an amphipathic helix (Liu, Westler et al. 2009). Further characterizations revealed that TMDs and amphipathic helices have also other functions. For instance, the membrane-association domain of the RCNMV p27 protein affects the formation of virus replication complexes (VRCs) and the synthesis of negative strand vRNA (Kusumanegara, Mine et al. 2012). The amphipathic helix of the BMV 1a protein regulates the recruitment of the vRNA templates to the replication sites (Liu, Westler et al. 2009).

Turnip mosaic virus (TuMV) is a (+) RNA virus in the family of *potyviridae* (Mayo 1995). The 9.8 kb genome encodes at least 11 viral proteins, and among them are the membrane-associated P3 and $6K_2$ protein (Restrepo-Hartwig and Carrington 1994, Eiamtanasate, Juricek et al. 2007). $6K_2$ is the only membrane-associated protein that is required to reorganize the ER membrane and for the production of replication vesicles (Schaad, Jensen et al. 1997). These vesicles contain vRNA and viral proteins such as the viral RNA-dependent RNA polymerase (vRdRp) and the helicase, and host components like the eukaryotic translation initiation factor (iso) 4E [eIF(iso)4E], the translation elongation factor 1A (eEF1A) and the poly(A)-binding protein (PABP), for the virus replication (Cotton, Grangeon et al. 2009). These vesicles also support the intracellular, intercellular as well as systemic movement of the virus, leading to the infection of the whole plant (Cotton, Grangeon et al. 2009, Grangeon, Jiang et al. 2013, Wan, Cabanillas et al. 2015). The biogenesis of these vesicles depend on the early secretory pathway, requiring coat protein complex I (COPI) and COPII factors (Wei and Wang 2008). $6K_2$ also associates with chloroplasts (Wei, Huang et al. 2010, Grangeon, Agbeci et al. 2012).

We have begun characterizing the molecular determinants of $6K_2$ for vesicle production. We previously found that its N-terminal cytoplasmic tail is required for the protein ER export during vesicle formation, and that it interacts with the COPII coatomer Sec24a (Jiang, Patarroyo et al. 2015). Not much is known, however, about the pathway that the $6K_2$-induced vesicles take once they have left the ER. In this work, we identified a GXXXG motif within the TMD of the $6K_2$ protein that is necessary for the vesicles to exit from the Golgi apparatus. Mutations in this motif dramatically impaired TuMV replication and prevented $6K_2$ from associating with chloroplasts. We thus conclude that the Golgi apparatus plays an important role during TuMV infection. The $6K_2$ protein needs to exit the Golgi prior to vesicles formation and chloroplast association.

Materials and Methods

Molecular cloning

The coding sequence of GFP flanked by *Xba*I and *Bam*HI was amplified by PCR using the template pGreen/PABP:GFP (Beauchemin and Laliberté 2007). The GFP fragment was digested with *Xba*I/*Bam*HI, and used to replace the mCherry fragment of pCambia/$6K_2$:mCherry (Jiang, Patarroyo et al. 2015) for the construction of plasmid pCambia/$6K_2$:GFP. Mutagenesis was performed using the QuikChange II XL site-directed mutagenesis kit (Agilent), according to the manufacturer's instructions. pCambia/$6K_2$:GFP was used as template to obtain the following $6K_2$ mutant derivatives: pCambia/$6K_2^{G30V}$:GFP, pCambia/$6K_2^{G33V}$:GFP, pCambia/$6K_2^{G34V}$:GFP, pCambia/$6K_2^{G35V}$:GFP and pCambia/$6K_2^{G30V\text{-}G33V\text{-}G34V\text{-}G35V}$:GFP. To get mutants pCambia/$6K_2^{G30V\text{-}G33V\text{-}G34V\text{-}G35V}$:mCherry, the GFP fragment of pCambia/$6K_2^{G30V\text{-}G33V\text{-}G34V\text{-}G35V}$:GFP was replaced with mCherry. To obtain mutants p35S-TuMV^{G30V}, p35S-TuMV^{G34V} and p35S-TuMV$^{G30V\text{-}G33V\text{-}G34V\text{-}G35V}$, the plasmid p35S-TuMV (Beauchemin, Bougie et al. 2005) was used as the template. The mutated *Apa*I/*Sma*I fragments encompassing the full length mutant TuMV genome were used to replace the corresponding fragment of wild type pTuMV (Jiang, Patarroyo et al. 2015) in order to generate the following mutant constructs pTuMV^{G30V}, pTuMV^{G34V} and pTuMV$^{G30V\text{-}G33V\text{-}G34V\text{-}G35V}$. The markers GFP:HDEL, ERD2:GFP and ST-YFP were described in (Saint-Jore, Evins et al. 2002, Zheng, Camacho et al. 2005, Grangeon, Agbeci et al. 2012).

Protein transient expression

Agrobacterium-mediated protein transient expression was performed essentially as described by Cotton et al. (Cotton, Grangeon et al. 2009). Four-week old *N. benthamiana* plants were used for agroinfiltration, and were kept in the green house until analysis. For the expression of $6K_2$:GFP, or the virus and the related mutants, the agrobacterium suspension was adjusted to OD_{600} = 0.3. For co-expression, the equal

volume of agrobacterium suspensions was mixed thoroughly. The OD_{600} was adjusted to 0.03 for GFP:HDEL, to 0.1 for ERD2:GFP and ST:YFP.

Protoplast transfection was performed as described by Yoo et al. (Yoo, Cho et al. 2007). Briefly, the same protoplast preparation was divided into several aliquots. Five micrograms of each plasmid was used to transfect the protoplasts using a PEG4000 solution. The transfected protoplasts were kept at room temperature in the dark for 40 h. The protoplasts were collected, and were suspended in 100 μl of 1 X sample loading buffer and boiled for 5 min for Western blotting.

Confocal laser scanning microscopy

The agroinfiltrated leaf tissues or the chloroplast preparations were loaded on cover slides. These samples were imaged using a 20 X or 63 X objective. The GFP and YFP fusion proteins were excited at 488 nm, and the emitted signal was captured at 500 nm to 535 nm. mCherry was excited at 561 nm, and the emitted light was captured at 580 nm to 640 nm. The chlorophyll autofluorescence was triggered at 561 nm, and the emission light was collected at 650 nm to 680 nm. For co-localization assays, different fluorescent signals were collected simultaneously. The images were processed with the software ZEN2011.

Chloroplast isolation

Chloroplast isolation was performed as described by Cowan et al. (Cowan, Roberts et al. 2012). Leaf tissues (approximately 1 g) were triturated in 5 volumes of grinding buffer (0.35 M sorbitol, 0.05 M HEPES-KOH pH 7.5, 2 mM EDTA, 0.5 mM $MgCl_2$, 1 mM DTT, 10 mg/mL BSA) and filtered through muslin. The extract was centrifuged at 1, 000 X g, and the resulting pellet was resuspended in 1 ml sorbitol medium (0.35 M sorbitol, 0.035 M HEPES-KOH pH 8.3, 10 mM K_2HPO4, 0.5 mM $MgCl_2$, 1 mM DTT). The crude preparation was layered onto a gradient comprising 2 ml of 40 % and 2 ml 85 % percoll

solution (prepared in 0.35 M sorbitol, 0.04 M HEPES-KOH pH 7.5, 0.5 mM $MgCl_2$, 1 mM DTT). After centrifugation at 13, 000 X g for 7 min, the chloroplast fraction located at the interface of the 40 % and 85 % percoll was collected, and washed with 5 volumes of sorbitol medium twice. The purified chloroplast preparation was then used for the following assay.

Cellular fractionation

Cellular fractionation experiment was performed as described by Thivierge et al. (Thivierge, Cotton et al. 2008). The *N. benthamiana* leaf tissues (approximately 1 g) expressing $6K_2$:GFP or $6K_2^{GV}$:GFP were grounded in 4-fold volume of homogenization buffer [50 mM Tris–HCl, pH 7.6, 15 mM $MgCl_2$, 10 mM KCl, 20 % glycerol, 0.1 % β-mercaptoethanol, 1 X cOmplete Protease Inhibitor cocktail (Roche)]. The extract was centrifuged at 3, 000 X g for 10 min, and the resulting supernatant (S3) stands for the total protein fraction. This fraction was further centrifuged at 30, 000 X g, and the supernatant (S30) stands for the soluble protein fraction. The resulting pellet (P30, stands for the membrane fraction) was suspended with the same volume of homogenization buffer. These fractions were diluted with 5 X sample loading buffer and boiled for 5 min for Western blotting.

Immunohistochemistry

Immunohistochemistry was done as described by Wan et al. (Wan, Cabanillas et al. 2015). Briefly, the TuMV systemic infected leaf tissues were fixed at 6 d post infection, and followed with sucrose gradient treatment and cryosectioning. The sucrose gradient treatment utilizes sucrose solutions with increased concentration to treated the fixed leaf tissues, by replacing the remaining water and avoiding the crystal formation. The sections were placed on microscope slides pretreated with 0.01 % poly-L-lysine. After incubation with blocking solution (prepared in PBS, 5 % BSA and 0.3 % Triton X-100) for 1 h, the sections were washed, and then incubated with the primary antibody and the

secondary antibody. SlowFade Gold was mounted on the sections and cover slips were sealed for confocal laser scanning microscopy observation.

Results

$6K_2$ GXXXG motif is required for the production of normal-sized $6K_2$ vesicles

The membrane-associated $6K_2$ protein of TuMV is responsible for the formation of viral replication vesicles (Schaad, Jensen et al. 1997). According to secondary structure predictions, this protein is characterized by the presence of a 23 amino acid α-helix TMD, flanked on either side by a 19 and an 11 amino acid N- and C-terminal tail, respectively (Jiang, Patarroyo et al. 2015). In order to identify the role of the $6K_2$ TMD in replication vesicles biogenesis, we compared the amino acid sequence of the predicted TMDs from different potyviruses. The comparison was performed with the ClustalW2 server online (Larkin, Blackshields et al. 2007). Several glycine residues, at positions 30, 33, 34 and 35 of the TuMV $6K_2$ protein, are conserved among potyviruses (Fig. 1A). In particular, G34 is present in all the aligned sequences, and G35 is present in all, except for the $6K_2$ of *Potato virus A* (PVA). G30 is present in four out of the seven aligned sequences, and for two of these potyviruses, the G is replaced by a small amino acid residue (e.g. A or S). Helical wheel projection of the predicted $6K_2$ TMD of TuMV indicates that G30 and G34 are located on the same side of the predicted α-helix (Fig. 1B). This amino acid organization is characteristic of the GXXXG motif, which has been shown to mediate protein interactions among membrane proteins (Cymer, Veerappan et al. 2012).

To test the importance of the glycine residues in the formation of $6K_2$-induced vesicles, we carried out site-directed mutagenesis to substitute each of them with a valine residue. This branched-chain amino acid was preferred since substitution with alanine was shown to have little to no effect on the function of the GXXXG motif (Kleiger, Grothe et al. 2002, Schneider and Engelman 2004). The generated mutants were $6K_2^{G30V}$, $6K_2^{G33V}$, $6K_2^{G34V}$ and $6K_2^{G35V}$ and $6K_2^{G30V\text{-}G33V\text{-}G34V\text{-}G35V}$ (this mutant will be designated as $6K_2^{GV}$ unless otherwise indicated). These mutated $6K_2$ were fused to the N-terminus of the green fluorescent protein (GFP) and were expressed by agrobacterium-mediated transient protein expression. Expression of $6K_2$:GFP induced

the formation of vesicles of various sizes, ranging from 0.5 to 4.0 μm in diameter (Fig. 1C). The expression patterns of $6K_2^{G33V}$ and $6K_2^{G35V}$ were similar to that of the wild type (wt) $6K_2$ protein (Fig. 1D-E). Expression of $6K_2^{G30V}$, $6K_2^{G34V}$ and $6K_2^{GV}$, however, generated smaller vesicles that were homogenous in size (2.0 μm in diameter) (Fig. 1F-H). In all cases, some retention in the ER of the $6K_2$ protein was observed. Cellular fractionation experiments confirmed that the mutated $6K_2^{GV}$ protein was still membrane-associated (Fig. 1I).

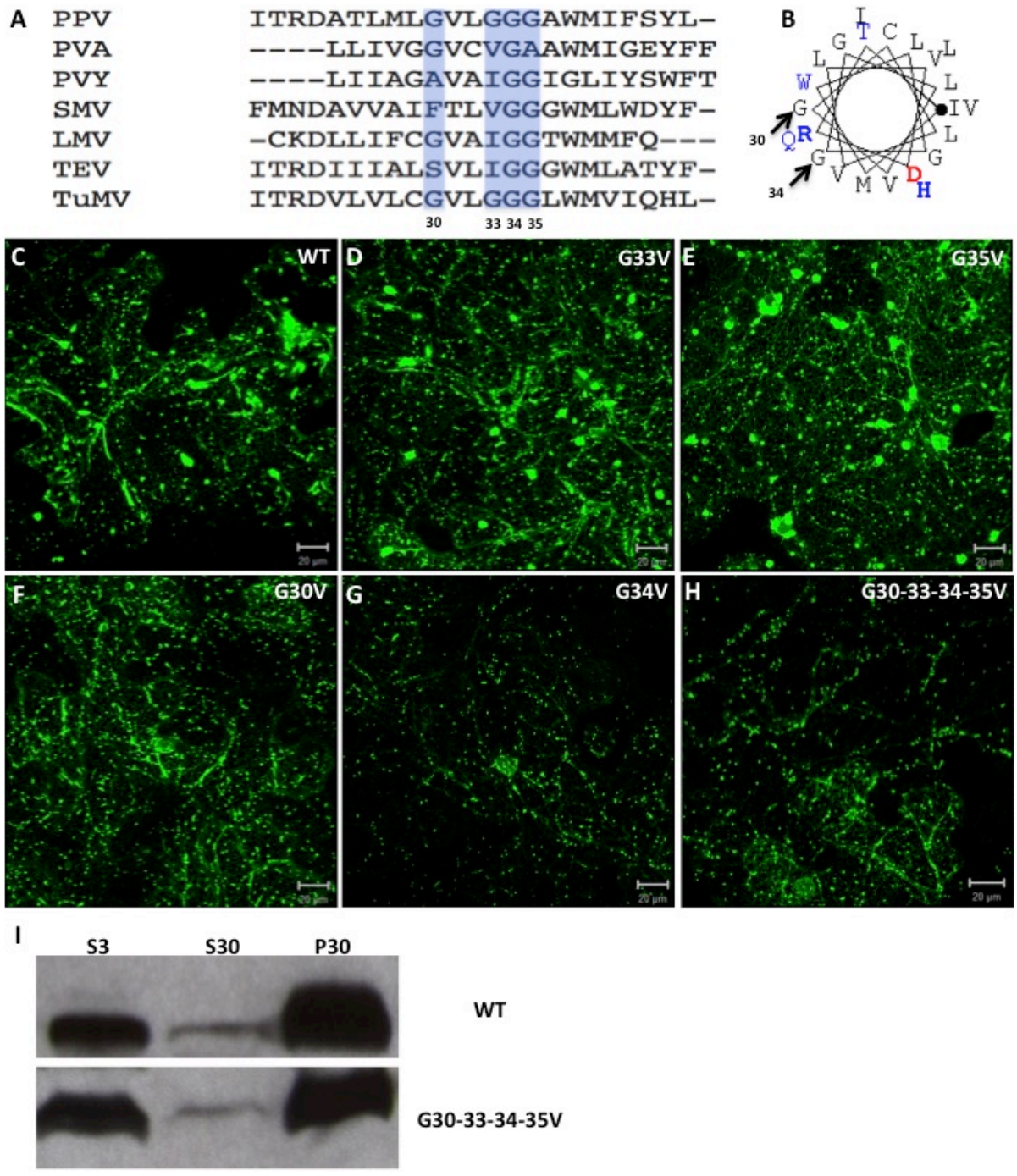

Figure 1. Characterization of the $6K_2$ trans-membrane domain (TMD) GXXXG motif.

(A) Sequence alignment of the predicted TMD of different potyvirus $6K_2$ proteins. The highly conserved glycine residues are shadowed in light blue, with the corresponding

amino acid position indicated below. PPV, *Plum pox virus*; PVA, *Potato virus A*; PVY, *Potato virus Y*; SMV, *Soybean mosaic virus*; LMV, *Lettuce mosaic virus*; TEV, *Tobacco etch virus*; TuMV, *Turnip mosaic virus*. (B) Helical wheel projection of the predicted $6K_2$ TMD of TuMV. The glycine residues located at positions 30 and 34 are indicated by arrows. (C-H) Fluorescent imaging of *N. benthamiana* cells expressing $6K_2$:GFP (C), $6K_2^{G33V}$:GFP (D), $6K_2^{G35V}$:GFP (E), $6K_2^{G30V}$:GFP (F), $6K_2^{G34V}$:GFP (G) and $6K_2^{G30V\text{-}G33V\text{-}G34V\text{-}G35V}$:GFP (H) at 3 d.p.a. (I) Cellular fractionation assay of wild type $6K_2$:GFP and $6K_2^{GV}$:GFP protein. S3, total protein fraction; S30, soluble protein fraction; P30, membrane protein fraction. Western blot was performed with anti-GFP antibodies.

Mutations in the GXXXG motif stall $6K_2$ in Golgi apparatus

The smaller and homogenous size of the vesicles induced by $6K_2^{GV}$ is reminiscent of the Golgi apparatus. We consequently investigated the cellular distribution of this mutant form of $6K_2$. First, $6K_2^{GV}$:mCherry labeled the ER more intensely than wt $6K_2$:mCherry when co-expressed with the ER marker GFP:HDEL (Fig. 2A *vs* 2B), but the mutations did not abolish the capacity of $6K_2^{GV}$ to exit the ER. We next co-expressed $6K_2^{GV}$:mCherry with the cis-Golgi marker ERD2:GFP (Saint-Jore, Evins et al. 2002) or the trans-Golgi marker ST:YFP (Zheng, Camacho et al. 2005). By counting how many $6K_2$-induced vesicles were labeled by these markers, we found that approximately 40% of wt $6K_2$-induced vesicles showed co-localization with both Golgi markers (Fig. 2C-D). On the other hand, almost all $6K_2^{GV}$-induced puncta co-localized with ERD2:GFP and ST:YFP (Fig. 2E-F). Therefore, the $6K_2$-induced vesicles were arrested in the Golgi apparatus and were prevented to exit this organelle when the GXXXG motif was disrupted.

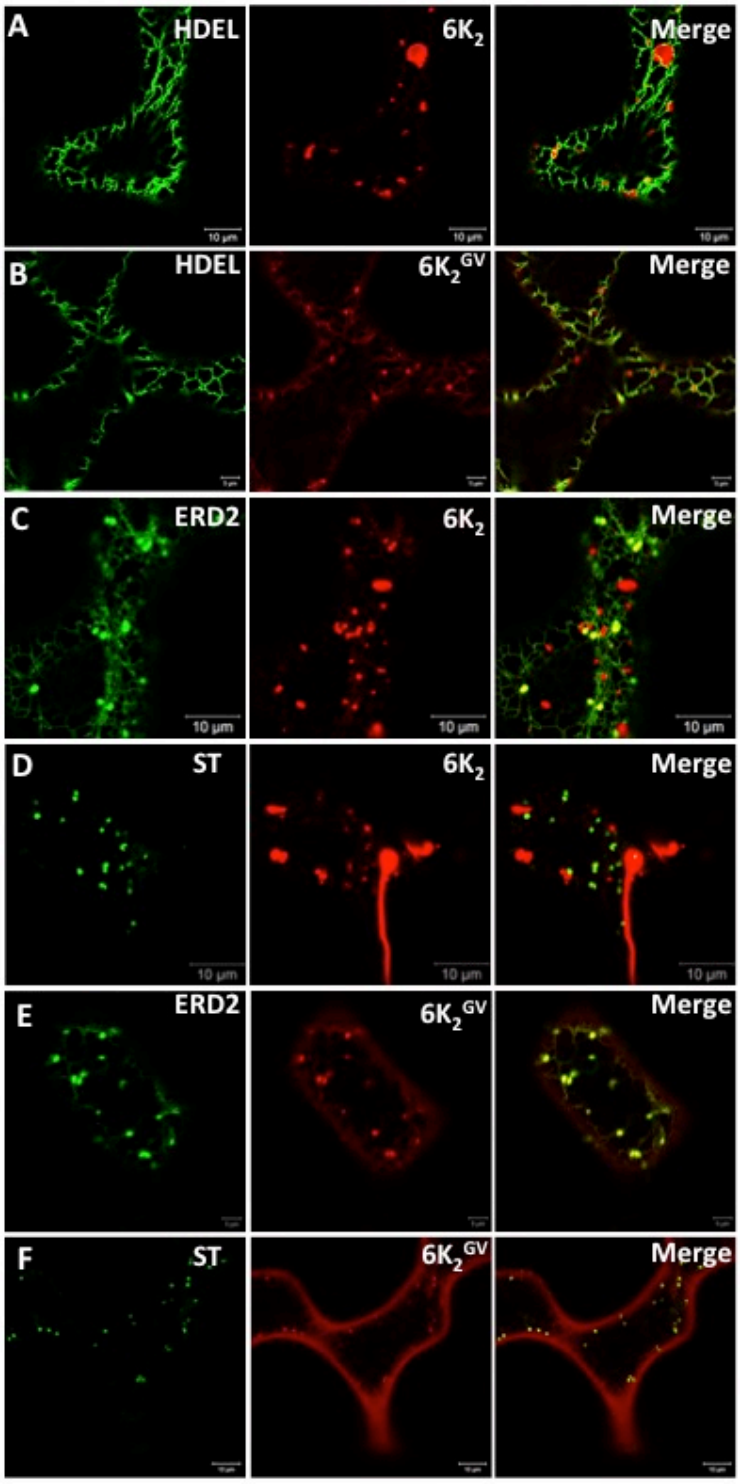

Figure 2. Characterization of the cellular distribution of protein $6K_2$ and $6K_2^{GV}$.

The ER maker GFP:HDEL was co-expressed with $6K_2$:mCherry (A) or with $6K_2^{GV}$:mCherry (B), cis-Golgi marker ERD2:GFP with $6K_2$:mCherry (C) or with $6K_2^{GV}$:mCherry (E), and trans-Golgi marker ST:YFP with $6K_2$:mCherry (D) or with $6K_2^{GV}$:mCherry (F).

$6K_2$-chloroplast association depends on the GXXXG motif

It was previously reported that $6K_2$ associates with chloroplasts during TuMV infection (Wei, Huang et al. 2010). Since $6K_2^{GV}$ was retained in the Golgi, we checked if its association with chloroplasts was affected by the introduced mutations. Fig. 3A shows the association of wt $6K_2$ with chloroplasts in *N. benthamiana* live cells. This association was characterized by the formation of $6K_2$ ring-like structures surrounding the chloroplasts, as previously reported (Wei, Huang et al. 2010, Wei, Zhang et al. 2013). $6K_2^{GV}$ did not, however, associate with chloroplasts (Fig. 3B). To confirm this result, chloroplasts were purified from leaf tissues expressing GFP:HDEL, $6K_2$:GFP or $6K_2^{GV}$:GFP. The isolated chloroplasts were observed by confocal laser scanning microscopy. No GFP signal was detected in the chloroplast preparation isolated from leaf tissues expressing GFP:HDEL (data not shown). The wt $6K_2$ was found to associate with and to surround the chloroplasts, while $6K_2^{GV}$ did not (Fig. 3C *vs* 3D). Western blotting was further conducted to detect the presence of GFP fusion proteins in these purified chloroplasts (Fig. 3E). No GFP protein signal was observed from GFP:HDEL-expressing cells, indicating that our purified chloroplasts were not contaminated with ER components. As expected, wt $6K_2$:GFP was detected in the chloroplast preparation, but not $6K_2^{GV}$:GFP. These results suggest that $6K_2$-chloroplast association requires that the viral protein traffics through the Golgi apparatus in order to reach the chloroplast.

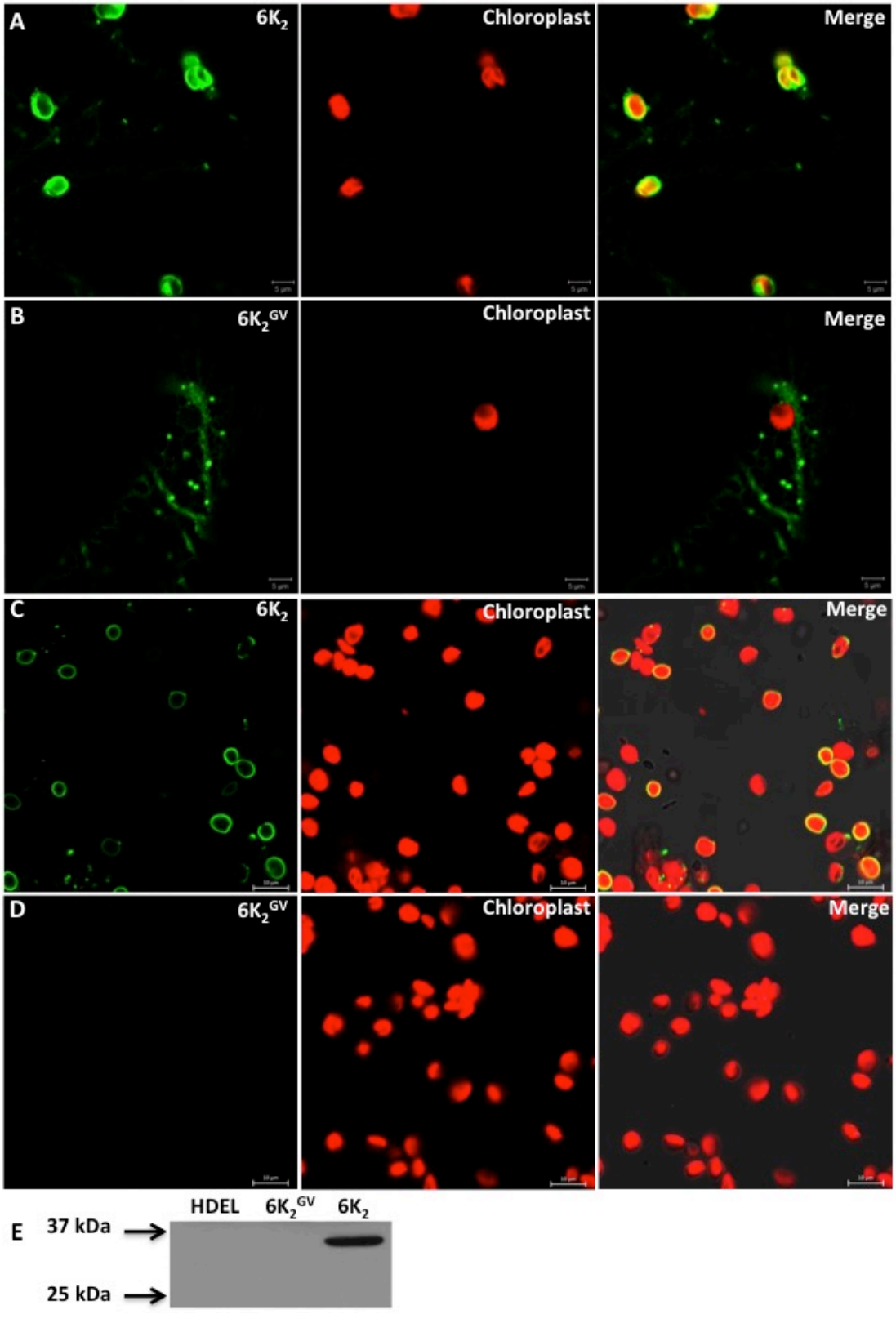
A
6K2
Chloroplast
Merge
B
6K2GV
Chloroplast
Merge
C
6K2
Chloroplast
Merge
D
6K2GV
Chloroplast
Merge
E
HDEL
6K2GV
6K2
37 kDa
25 kDa

Figure 3. $6K_2$- and $6K_2^{GV}$-chloroplast association.

Leaf tissues expressing $6K_2$:GFP (A) or $6K_2^{GV}$:GFP (B) were imaged, with the autofluorescence of chloroplast shown in red. The chloroplast preparations isolated from the leaf tissues expressing $6K_2$:GFP (C) or $6K_2^{GV}$:GFP (D) were analyzed by confocal laser scanning microscopy. Western blot analysis was further conducted to detect the presence of $6K_2$ or $6K_2^{GV}$ in the purified chloroplast preparations (E). Western blot was performed with anti-GFP antibodies.

TuMV efficient infection requires the GXXXG motif

We then evaluated the impact of mutating the GXXXG motif of $6K_2$ on TuMV infection. Mutations coding for $6K_2^{G30V}$, $6K_2^{G34V}$ and $6K_2^{GV}$ were introduced in the infectious clone p35S-TuMV (Sánchez, Martínez-Herrera et al. 1998), and the resulting constructs were identified as p35S-TuMV^{G30V}, p35S-TuMV^{G34V} and p35S-TuMV^{GV}, respectively. p35S-TuMV^{VNN}, in which the vRdRp core motif GDD was changed to VNN, was used a non-replicating virus control (Li and Carrington 1995). The above infectious constructs were then subcloned into the binary vector pCambia 0390 for agrobacterium-mediated virus inoculation in order to analyze the infection process, in both the agro-inoculated and the non agro-inoculated leaf tissues. The resulting infectious clones were pTuMV^{G30V}, pTuMV^{G34V}, pTuMV^{GV}, and pTuMV^{VNN}. Fig. 4A shows that CP levels from the agro-inoculated leaves of pTuMV^{G30V}-, pTuMV^{G34V}-, pTuMV^{GV} are significantly lower than the CP level from wt pTuMV-infected plant. The CP levels are, however, higher than that of pTuMV^{VNN}-infected leaf tissues. The upper non-agroinfiltrated leaf tissues of Mock-, pTuMV^{VNN}-, pTuMV^{G30V}-, pTuMV^{G34V}-, pTuMV^{GV}- and pTuMV-infected *N. benthamiana* plants were assayed for CP production five days later. Fig. 4B shows that CP accumulation in upper non-agroinfiltrated leaves was observed only for pTuMV. These results indicate that the GXXXG motif is required for efficient TuMV infection.

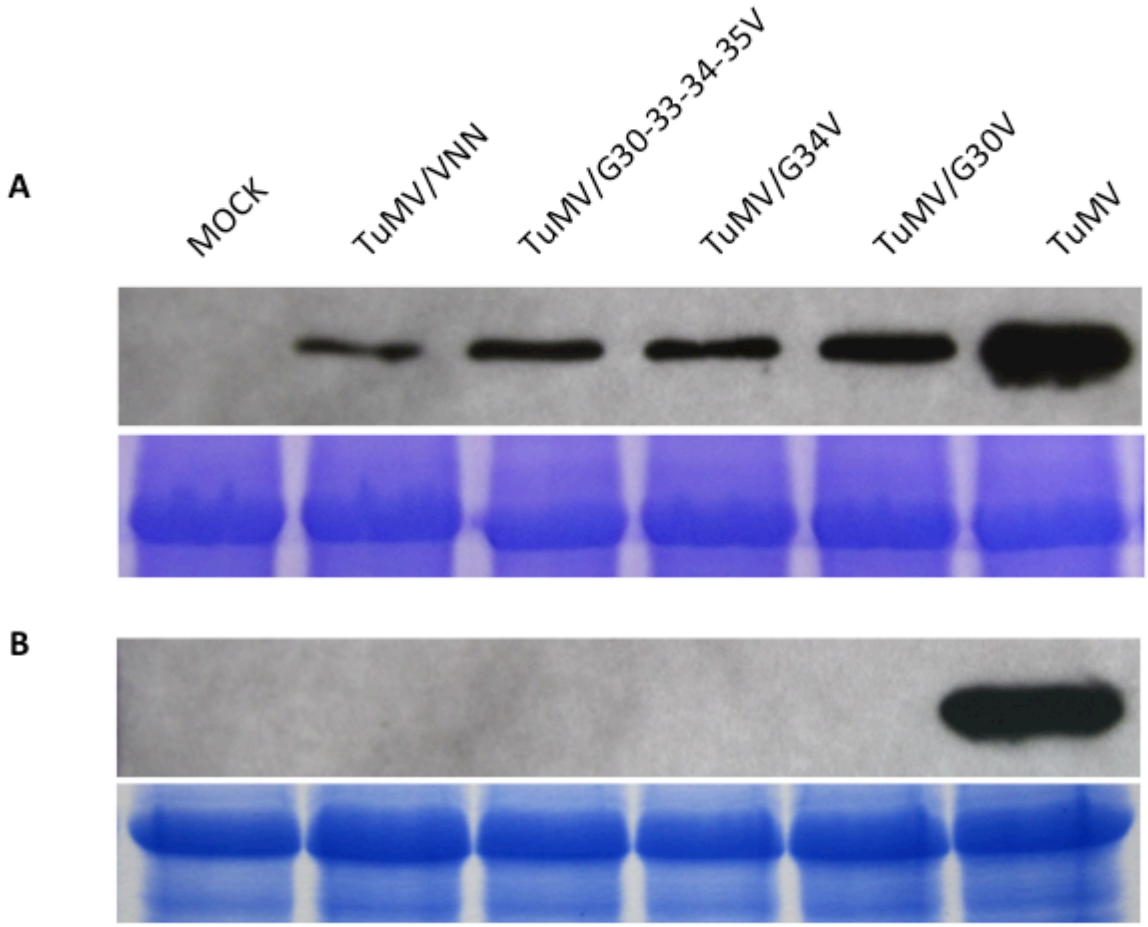

Figure 4. Western blot assay of TuMV infection.

The Mock-, TuMV^{VNN}-, TuMV^{GV}-, TuMV^{G34V}-, TuMV^{G30V}- and TuMV- agroinfiltrated (A) and non-agroinfiltrated (B) leaf tissues were analyzed at 5 d.p.a. Western blot was performed with anti-TuMV CP antibodies. Coomassie blue staining (bottom panel) shows equal protein loading.

TuMV replication is associated with ER amalgamates rather than with chloroplasts

As mentioned above, $6K_2$-chloroplast association is taking place during TuMV infection (Wei, Huang et al. 2010). TuMV replication is also characterized by the formation of numerous $6K_2$ vesicles that amalgamates with the ER into a globular structure near the nucleus (Grangeon, Agbeci et al. 2012). The observation that TuMV replication was still taking place, albeit at low levels, in the $6K_2$ mutants despite the lack of an association between the viral mutant proteins and chloroplasts, prompted us to examine if vRNA replication was associated with chloroplasts. The systemically infected leaf tissues of TuMV/$6K_2$:GFP agroinfiltrated *N. benthamiana* plants were cryosectioned into 30-µm-thick cross-section samples at 6 d.p.a, and were immunostained with an anti-dsRNA antibody and processed for confocal laser scanning microscopy observation. The dsRNA, which is the intermediate of (+) RNA replication, was found as puncta in the ER amalgamates, but not in the chloroplasts (Fig. 5A). As expected, only the ER amalgamates contain the TuMV RdRp (Fig. 5B). These results suggest that the ER amalgamates are the sites of vRNA replication, but not the chloroplasts.

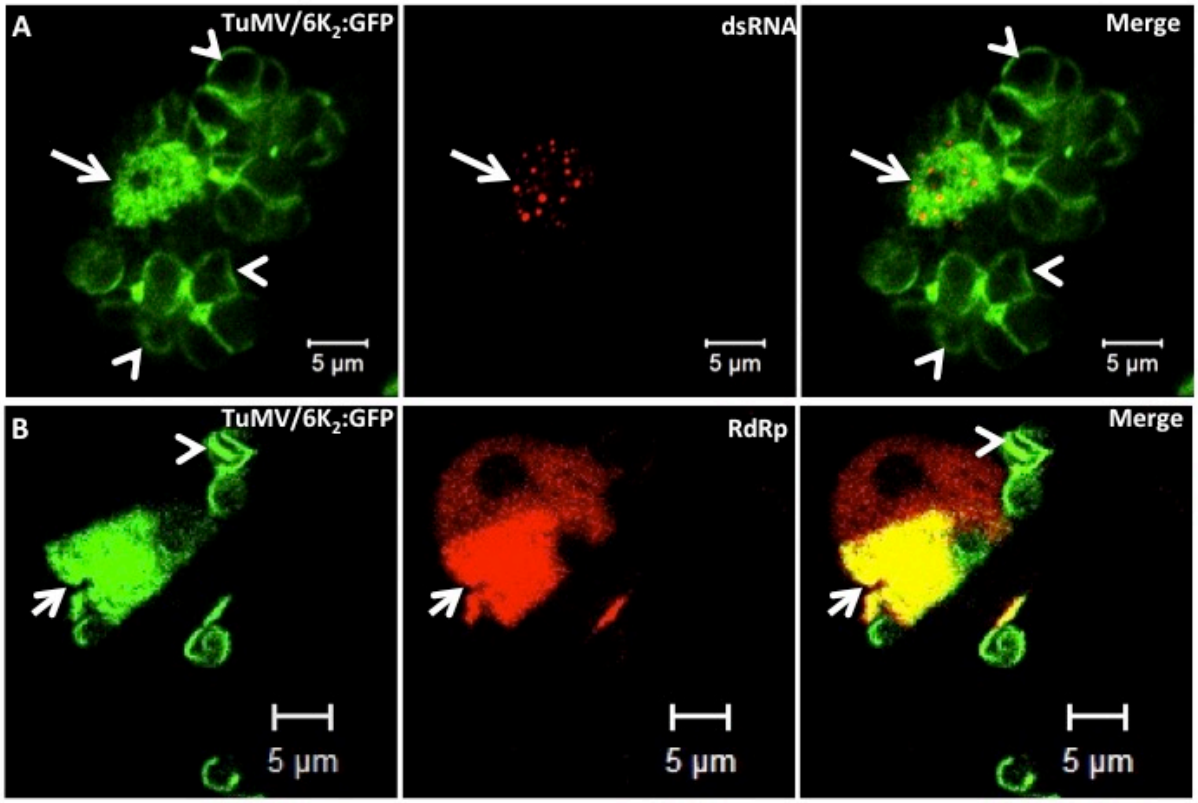

Figure 5. Immunostaining assay of the distribution of dsRNA and vRdRp.

Leaf tissues infected with TuMV/$6K_2$:GFP were processed for immunostaining assay. The viral double-stranded RNA (A) and the viral RNA-dependent RNA polymerase (B) in the ER amalgamates (indicated by arrows) and the chloroplast (indicated by arrowheads) were analyzed.

Chloroplasts may nevertheless have an accessory role in TuMV replication. To further confirm this result, we investigated whether TuMV^{GV} could induce ER amalgamates. The mutated infectious clone pTuMV^{GV} or the wt pTuMV were co-expressed with the ER marker GFP:HDEL. As expected, ER amalgamation near the nucleus was not observed when leaves were co-agroinfiltrated with GFP:HDEL and the non-replicating virus pTuMV^{VNN} (Fig. 6A), but was clearly visible in the presence of wt pTuMV (Fig. 6B). A low level of ER amalgamation was however visible in cells agroinfiltrated with pTuMV^{GV} (Fig. 6C). This result highlights the importance of the GXXXG motif for TuMV infection.

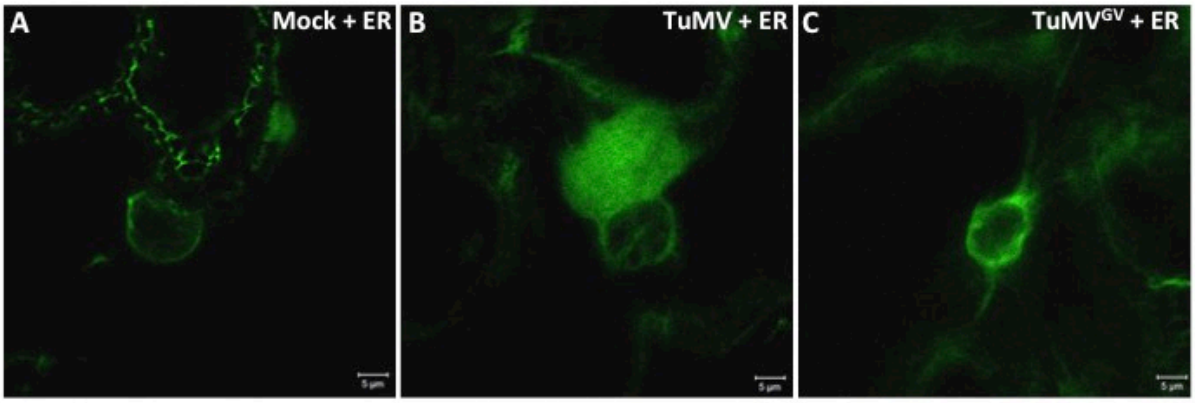

Figure 6. Detection of the ER amalgamates induced by the wt or mutated TuMV.

Confocal fluorescence images of leaves co-expressing the ER marker GFP:HDEL with the non-replicating TuMV^{VNN} (A), or wt TuMV (B), or mutated TuMV^{GV} (C).

Discussion

The $6K_2$ protein has been demonstrated to induce replication vesicles formation in a COPI and COPII dependent manner (Wei and Wang 2008, Grangeon, Agbeci et al. 2012). We have found recently that the N-terminal tail of this protein is required for its exit from the ER by interacting with the COPII coatomer Sec24a (Jiang, Patarroyo et al. 2015). In this work, we further identified a GXXXG motif in the $6K_2$ TMD that is required for normal-sized vesicles formation (Fig. 1). Using several fluorescent cellular markers, we showed that the mutated $6K_2^{GV}$-induced replication vesicles were arrested in the Golgi apparatus (Fig. 2). These results indicate that a combinatorial signal, which includes the N-terminal tail and the TMD GXXXG motif, sequentially directs the ER and Golgi exit of $6K_2$ for the formation of replication vesicles. Deletion of the N-terminal tail and mutation of the GXXXG motif simultaneously may result in the complete ER retention of the $6K_2$ protein (supplemental Fig. 1). Furthermore, the mutant $6K_2^{GV}$ still can interact with the Sec24a due to the presence of the N-terminal tail (data not shown). This confirms the importance of this combinatorial motif for the biogenesis of TuMV replication vesicles. This is consistent with the previous observation that the majority of Golgi-resident glycosyltransferases are retained within this compartment via their respective cytoplasmic tail and TMD (Banfield 2011). In particular, these enzymes contain basic amino acids (e.g. K or R) within their cytoplasmic tail that mediate interaction with the COPII vesicle for ER export, as well as aromatic amino acids (e.g. F, Y or W) within their TMDs that promote Golgi retention (Tu and Banfield 2010).

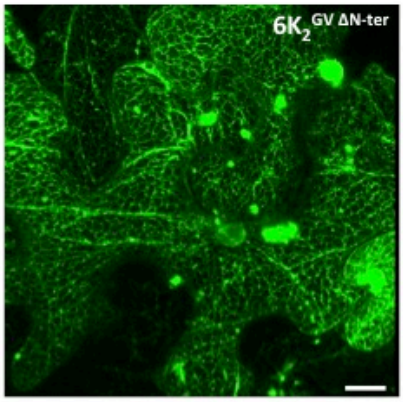

Figure S1. The cellular distribution of mutated $6K_2^{GV_{\Delta}1\text{-}18}$:GFP.

Scale bar = 20 μm.

The GXXXG sequence is one of the most-represented motifs that mediate protein-protein interactions (Kleiger, Grothe et al. 2002, Fink, Sal-Man et al. 2012). Many important cellular membrane-associated protein factors, such as the epidermal growth factor and glycophorin, contain a GXXXG motif (Fink, Sal-Man et al. 2012). Mutation of this motif is associated with many diseases. In addition to those membrane-associated proteins, many soluble proteins also contain this motif (Kleiger, Grothe et al. 2002). This motif is known to be important for many animal viruses, such as *Human papillomavirus type 16* (HPV16), *Human immunodeficiency virus* (HIV) and the *Hepatitis C virus* (HCV), but the underling mechanism is unknown (Han, Aligo et al. 2011, Faingold, Cohen et al. 2012, Bronnimann, Chapman et al. 2013).

The reason why the mutated GXXXG motif resulted in $6K_2$-induced replication vesicle retention in the Golgi apparatus is not known. Several properties, such as oligomerization, length of the TMD, and protein-protein interaction, regulate protein Golgi retention (Banfield 2011). We have previously demonstrated that $6K_2$ can interact with itself (Jiang, Patarroyo et al. 2015), but this self-association was not significantly disrupted by mutating the GXXXG motif (data not shown). Although the strength of protein interaction may have been affected, protein oligomerization does not appear to be regulated by the GXXXG motif. Furthermore, protein secondary structure predictions indicated that the length of the TMD did not change when the GXXXG motif was mutated (data not shown). Thus, it is possible that mutation of the GXXXG motif abolished the interaction of $6K_2$ with one or more host factors. Candidates include tethering factors, the Rab GTPases, the SNAREs (soluble N-ethylmaleimide-sensitive factor attachment protein receptor), factors that are involved in vesicle fusion (Bassham, Brandizzi et al. 2008).

Arrest of the $6K_2$-induced vesicles in the Golgi apparatus significantly impaired virus replication, abolished viral systemic infection (Fig 4), and affected the formation of ER amalgamates (Fig. 6). These results further confirm the virus replication and movement is coupled, with the weaker virus replication results in the abolition of virus movement. It is possibe that the virus replication vesicle is prevented from reaching the PD for the

following virus movement when the GXXXG motif is mutated. Furthermore, mutating the GXXXG motif completely disrupted $6K_2$-chloroplast association (Fig. 3). It is still not clear if chloroplasts support TuMV RNA synthesis. The observations that vRNA synthesis can still take place in the absence of $6K_2$-chloroplast association and that dsRNA, the replicative form of vRNA, is not found in the vicinity of this organelle (Fig. 5), suggest instead that chloroplasts play an accessory role during the infection. Chloroplasts might be needed to provide lipids for TuMV replication. It is known that large quantities of lipids are synthesized during plant viral infection (Lee and Ahlquist 2003, Barajas, Xu et al. 2014), and that significant lipid accumulation is observed in TuMV-infected cells (Wan, Cabanillas et al. 2015). The chloroplast is one of the major organelle for lipid biosynthesis, and the synthesized lipids are transferred between the chloroplast and the ER through membrane contact sites (Wang and Benning 2012, Block and Jouhet 2015). Thus, it is possible that lipids originating from chloroplasts are transferred to $6K_2$ vesicles involving a transit through the Golgi apparatus. In the case of TBSV, the co-opted host VAP proteins (vesicle-associated membrane protein-associated proteins) facilitate the formation of membrane contact sites between the sterol biosynthetic ER membrane and viral factories (Barajas, Xu et al. 2014). TBSV further recruits the oxysterol-binding protein-related proteins that are host lipid transfer proteins, likely channeling the sterols to the viral factories. Similarly, the VAP proteins are also redirected to sites where TuMV $6K_2$-induced vesicles and chloroplasts associate (Wei, Zhang et al. 2013).

Acknowledgments

This work was supported by grants from the Natural Science and Engineering Research Council (NSERC) of Canada and from Le Fonds québécois de recherche sur la nature et les technologies (FQRNT) to HZ and JFL.

References

Banfield, D. K. (2011). "Mechanisms of protein retention in the Golgi." Cold Spring Harb Perspect Biol **3**(8): a005264.

Barajas, D., K. Xu, I. F. de Castro Martín, Z. Sasvari, F. Brandizzi, C. Risco and P. D. Nagy (2014). "Co-opted Oxysterol-Binding ORP and VAP Proteins Channel Sterols to RNA Virus Replication Sites via Membrane Contact Sites." PLoS Pathog **10**(10): e1004388.

Barajas, D., K. Xu, M. Sharma, C. Y. Wu and P. D. Nagy (2014). "Tombusviruses upregulate phospholipid biosynthesis via interaction between p33 replication protein and yeast lipid sensor proteins during virus replication in yeast." Virology **471-473**: 72-80.

Bassham, D. C., F. Brandizzi, M. S. Otegui and A. A. Sanderfoot (2008). "The secretory system of Arabidopsis." Arabidopsis Book **6**: e0116.

Beauchemin, C., V. Bougie and J.-F. Laliberté (2005). "Simultaneous production of two foreign proteins from a potyvirus-based vector." Virus Research **112**(1–2): 1-8.

Beauchemin, C. and J.-F. Laliberté (2007). "The Poly(A) Binding Protein Is Internalized in Virus-Induced Vesicles or Redistributed to the Nucleolus during Turnip Mosaic Virus Infection." Journal of Virology **81**(20): 10905-10913.

Block, M. A. and J. Jouhet (2015). "Lipid trafficking at endoplasmic reticulum–chloroplast membrane contact sites." Current Opinion in Cell Biology **35**(0): 21-29.

Bronnimann, M. P., J. A. Chapman, C. K. Park and S. K. Campos (2013). "A Transmembrane Domain and GxxxG Motifs within L2 Are Essential for Papillomavirus Infection." Journal of Virology **87**(1): 464-473.

Cotton, S., R. Grangeon, K. Thivierge, I. Mathieu, C. Ide, T. Wei, A. Wang and J.-F. Laliberté (2009). "Turnip Mosaic Virus RNA Replication Complex Vesicles Are Mobile, Align with Microfilaments, and Are Each Derived from a Single Viral Genome." Journal of Virology **83**(20): 10460-10471.

Cowan, G. H., A. G. Roberts, S. N. Chapman, A. Ziegler, E. I. Savenkov and L. Torrance (2012). "The potato mop-top virus TGB2 protein and viral RNA associate with chloroplasts and viral infection induces inclusions in the plastids." Frontiers in Plant Science **3**.

Cymer, F., A. Veerappan and D. Schneider (2012). "Transmembrane helix–helix interactions are modulated by the sequence context and by lipid bilayer properties." Biochimica et Biophysica Acta (BBA) - Biomembranes **1818**(4): 963-973.

Eiamtanasate, S., M. Juricek and Y.-K. Yap (2007). "C-terminal hydrophobic region leads PRSV P3 protein to endoplasmic reticulum." Virus Genes **35**(3): 611-617.

Faingold, O., T. Cohen and Y. Shai (2012). "A GxxxG-like Motif within HIV-1 Fusion Peptide Is Critical to Its Immunosuppressant Activity, Structure, and Interaction with the Transmembrane Domain of the T-cell Receptor." Journal of Biological Chemistry **287**(40): 33503-33511.

Fink, A., N. Sal-Man, D. Gerber and Y. Shai (2012). "Transmembrane domains interactions within the membrane milieu: Principles, advances and challenges." Biochimica et Biophysica Acta (BBA) - Biomembranes **1818**(4): 974-983.

Grangeon, R., M. Agbeci, J. Chen, G. Grondin, H. Zheng and J. F. Laliberte (2012). "Impact on the endoplasmic reticulum and Golgi apparatus of turnip mosaic virus infection." J Virol **86**(17): 9255-9265.

Grangeon, R., J. Jiang, J. Wan, M. Agbeci, H. Zheng and J. F. Laliberte (2013). "6K2-induced vesicles can move cell to cell during turnip mosaic virus infection." Front Microbiol **4**: 351.

Han, Q., J. Aligo, D. Manna, K. Belton, S. V. Chintapalli, Y. Hong, R. L. Patterson, D. B. van Rossum and K. V. Konan (2011). "Conserved GXXXG- and S/T-Like Motifs in the Transmembrane Domains of NS4B Protein Are Required for Hepatitis C Virus Replication." Journal of Virology **85**(13): 6464-6479.

Ishibashi, K. and M. Ishikawa (2013). "The resistance protein Tm-1 inhibits formation of a Tomato mosaic virus replication protein-host membrane protein complex." J Virol **87**(14): 7933-7939.

Jiang, J., C. Patarroyo, D. Garcia Cabanillas, H. Zheng and J. F. Laliberte (2015). "The Vesicle-Forming 6K2 Protein of Turnip Mosaic Virus Interacts with the COPII Coatomer Sec24a for Viral Systemic Infection." J Virol **89**(13): 6695-6710.

Jonczyk, M., K. B. Pathak, M. Sharma and P. D. Nagy (2007). "Exploiting alternative subcellular location for replication: Tombusvirus replication switches to the endoplasmic reticulum in the absence of peroxisomes." Virology **362**(2): 320-330.

Ju, H. J., T. D. Samuels, Y. S. Wang, E. Blancaflor, M. Payton, R. Mitra, K. Krishnamurthy, R. S. Nelson and J. Verchot-Lubicz (2005). "The potato virus X TGBp2 movement protein associates with endoplasmic reticulum-derived vesicles during virus infection." Plant Physiol **138**(4): 1877-1895.

Kleiger, G., R. Grothe, P. Mallick and D. Eisenberg (2002). "GXXXG and AXXXA: common alpha-helical interaction motifs in proteins, particularly in extremophiles." Biochemistry **41**(19): 5990-5997.

Kusumanegara, K., A. Mine, K. Hyodo, M. Kaido, K. Mise and T. Okuno (2012). "Identification of domains in p27 auxiliary replicase protein essential for its association with the endoplasmic reticulum membranes in Red clover necrotic mosaic virus." Virology **433**(1): 131-141.

Laliberté, J.-F. and H. Zheng (2014). "Viral Manipulation of Plant Host Membranes." Annual Review of Virology **1**(1): 237-259.

Laliberte, J. F. and H. Sanfacon (2010). "Cellular remodeling during plant virus infection." Annu Rev Phytopathol **48**: 69-91.

Larkin, M. A., G. Blackshields, N. P. Brown, R. Chenna, P. A. McGettigan, H. McWilliam, F. Valentin, I. M. Wallace, A. Wilm, R. Lopez, J. D. Thompson, T. J. Gibson and D. G. Higgins (2007). "Clustal W and Clustal X version 2.0." Bioinformatics (Oxford, England) **23**(21): 2947-2948.

Lee, W. M. and P. Ahlquist (2003). "Membrane synthesis, specific lipid requirements, and localized lipid composition changes associated with a positive-strand RNA virus RNA replication protein." J Virol **77**(23): 12819-12828.

Li, X. H. and J. C. Carrington (1995). "Complementation of tobacco etch potyvirus mutants by active RNA polymerase expressed in transgenic cells." Proc Natl Acad Sci U S A **92**(2): 457-461.

Liu, L., W. M. Westler, J. A. den Boon, X. Wang, A. Diaz, H. A. Steinberg and P. Ahlquist (2009). "An amphipathic alpha-helix controls multiple roles of brome mosaic virus protein 1a in RNA replication complex assembly and function." PLoS Pathog **5**(3): e1000351.

Mayo, M. A. (1995). "The Potyviridae. By D. D. SHUKLA, C. W. WARD and A. A. BRUNT. 25 × 17 cm. Pp. 516 with 110 text-figures and 30 tables, Wallingford: CAB International, 1994. Price: £60.00." New Phytologist **131**(2): 289-290.

McCartney, A. W., J. S. Greenwood, M. R. Fabian, K. A. White and R. T. Mullen (2005). "Localization of the tomato bushy stunt virus replication protein p33 reveals a peroxisome-to-endoplasmic reticulum sorting pathway." Plant Cell **17**(12): 3513-3531.

Mitra, R., K. Krishnamurthy, E. Blancaflor, M. Payton, R. S. Nelson and J. Verchot-Lubicz (2003). "The potato virus x TGBp2 protein association with the endoplasmic reticulum plays a role in but is not sufficient for viral cell-to-cell movement." Virology **312**(1): 35-48.

Nagy, P. D. and J. Pogany (2012). "The dependence of viral RNA replication on co-opted host factors." Nat Rev Micro **10**(2): 137-149.

Restrepo-Hartwig, M. A. and J. C. Carrington (1994). "The tobacco etch potyvirus 6-kilodalton protein is membrane associated and involved in viral replication." Journal of Virology **68**(4): 2388-2397.

Saint-Jore, C. M., J. Evins, H. Batoko, F. Brandizzi, I. Moore and C. Hawes (2002). "Redistribution of membrane proteins between the Golgi apparatus and endoplasmic reticulum in plants is reversible and not dependent on cytoskeletal networks." The Plant Journal **29**(5): 661-678.

Sánchez, F., D. Martínez-Herrera, I. Aguilar and F. Ponz (1998). "Infectivity of turnip mosaic potyvirus cDNA clones and transcripts on the systemic host Arabidopsis thaliana and local lesion hosts." Virus Research **55**(2): 207-219.

Schaad, M. C., P. E. Jensen and J. C. Carrington (1997). Formation of plant RNA virus replication complexes on membranes: role of an endoplasmic reticulum-targeted viral protein.

Schneider, D. and D. M. Engelman (2004). "Motifs of two small residues can assist but are not sufficient to mediate transmembrane helix interactions." J Mol Biol **343**(4): 799-804.

Thivierge, K., S. Cotton, P. J. Dufresne, I. Mathieu, C. Beauchemin, C. Ide, M. G. Fortin and J.-F. Laliberté (2008). "Eukaryotic elongation factor 1A interacts with Turnip mosaic virus RNA-dependent RNA polymerase and VPg-Pro in virus-induced vesicles." Virology **377**(1): 216-225.

Tu, L. and D. Banfield (2010). "Localization of Golgi-resident glycosyltransferases." Cellular and Molecular Life Sciences **67**(1): 29-41.

Wan, J., D. G. Cabanillas, H. Zheng and J. F. Laliberte (2015). "Turnip mosaic virus Moves Systemically through Both Phloem and Xylem as Membrane-Associated Complexes." Plant Physiol **167**(4): 1374-1388.

Wang, Z. and C. Benning (2012). "Chloroplast lipid synthesis and lipid trafficking through ER-plastid membrane contact sites." Biochem Soc Trans **40**(2): 457-463.

Wei, T., T. S. Huang, J. McNeil, J. F. Laliberte, J. Hong, R. S. Nelson and A. Wang (2010). "Sequential recruitment of the endoplasmic reticulum and chloroplasts for plant potyvirus replication." J Virol **84**(2): 799-809.

Wei, T. and A. Wang (2008). "Biogenesis of cytoplasmic membranous vesicles for plant potyvirus replication occurs at endoplasmic reticulum exit sites in a COPI- and COPII-dependent manner." J Virol **82**(24): 12252-12264.

Wei, T., C. Zhang, X. Hou, H. Sanfacon and A. Wang (2013). "The SNARE protein Syp71 is essential for turnip mosaic virus infection by mediating fusion of virus-induced vesicles with chloroplasts." PLoS Pathog **9**(5): e1003378.

Yoo, S.-D., Y.-H. Cho and J. Sheen (2007). "Arabidopsis mesophyll protoplasts: a versatile cell system for transient gene expression analysis." Nat. Protocols **2**(7): 1565-1572.

Zheng, H., L. Camacho, E. Wee, H. Batoko, J. Legen, C. J. Leaver, R. Malhó, P. J. Hussey and I. Moore (2005). "A Rab-E GTPase Mutant Acts Downstream of the Rab-D Subclass in Biosynthetic Membrane Traffic to the Plasma Membrane in Tobacco Leaf Epidermis." The Plant Cell **17**(7): 2020-2036.

CHAPTER 4: Golgi SNAREs function as Turnip mosaic virus restriction factors (Publication No. 3)

Golgi SNAREs function as Turnip mosaic virus restriction factors

Manuscript in preparation for submission to *Journal of virology*

Jun Jiang[1], Huanquan Zheng[2] and Jean-François Laliberté[1#]

1. INRS-Institut Armand-Frappier, 531 Boulevard des Prairies, Laval, Québec, H7V 1B7, Canada
2. Department of Biology, McGill University, 1205 Dr. Penfield Avenue, Montréal, Québec, H3A 1B1, Canada

Author for correspondence : Prof Jean-François Laliberté

INRS-Institut Armand-Frappier

531, boulevard des Prairies

Laval, Québec, Canada H7V 1B7

Telephone number: 1-450-687-5010, ext. 4445

email address: jean-francois.laliberte@iaf.inrs.ca

Contribution of student

This manuscript is in preparation and will be submitted to *Journal of virology*. I designed and performed all the experimental work (Fig. 1-5, Table. 1 and Fig. S1-2) and analysed the data with advice from my supervisor Professor Jean-François Laliberté. I prepared the first draft of this manuscript, and Jean-Francois Laliberté helped me improve the writing.

Résumé

Les virus à ARN positif [ARN (+)] modifient le système endomembranaire de la cellule hôte lors de l'infections virale, ce qui conduit à la formation de compartiments qui abritent tous les composants nécessaires pour soutenir la réplication virale. Le virus de la mosaïque du navet (TuMV) est un virus à ARN (+) avec un génome d'environ 10kb qui peut infecter de nombreuses cultures en champs à haute valeur économique. La protéine virale $6K_2$ est une protéine associée aux membranes et est responsable de la formation des vésicules de réplication virale. Nous avons montré que $6K_2$ se déplace dans la voie de sécrétion précoce, et que la mutation du motif GXXXG dans le domaine trans-membranaire de la protéine résulte en une rétention des vésicules de réplication dans l'appareil de Golgi. Ici, nous avons étudié le rôle de certaines Golgi SNAREs dans l'infection du TuMV. Nous avons constaté que $6K_2$ peut interagir avec les Golgi SNAREs BET11, GOS11 et VAMP714. Dans des plantes d'Arabidopsis thaliana KO pour BET11, une sensibilité accrue aux TuMV a été observée. Grâce à l'utilisation d'un clone infectieux doublement étiqueté avec des protéines fluorescentes, nous avons suivi le mouvement du virus lors de l'infection virale par microscopie confocale. Nous avons constaté que le mouvement du TuMV a été plus rapide quand ce dernier était co-exprimé avec des mutants dominants négatifs de Golgi SNARE. Sur la base de ces résultats, nous proposons que certaines Golgi SNAREs peuvent fonctionner comme facteurs de restriction du TuMV.

Abstract

Positive sense RNA [(+) RNA] virus infections modify host cell endomembranes, which leads to the formation of viral compartments that harbor all the required components to support virus replication. *Turnip mosaic virus* (TuMV) is a (+) RNA virus with a ~10kb genome that can infect many economical important crops. The viral protein $6K_2$ is a membrane-associated protein and is responsible for viral replication vesicle formation. We have shown that $6K_2$ traffics through the early secretory pathway, and that mutation of its trans-membrane domain GXXXG motif results in Golgi retention of the replication vesicles. Here, we have investigated the role of Golgi SNAREs in TuMV infection. We have found that $6K_2$ can interact with Golgi SNARE BET11, GOS11 and VAMP714. In BET11 knockout *Arabidopsis thaliana* plant, an increased susceptibility to TuMV was observed. Using a dual fluorescent-tagged virus infectious clone, we monitored virus infection and movement by confocal microscopy. We found that TuMV movement was faster when co-expressed with Golgi SNARE dominant negative mutant proteins. Based on these results, we propose that Golgi SNAREs may function as TuMV viral restriction factors.

Introduction

Positive-sense RNA [(+) RNA] virus infection induces extensive host cell endomembrane remodeling, which results in the formation of viral membranous compartments termed 'viral factories' (Laliberte and Sanfacon 2010). These viral factories are associated with viral replication complexes (VRCs), which are made up of the viral RNA dependent RNA polymerase (vRdRp), replication-associated viral and host proteins, viral RNA (vRNA) and its associated double-stranded RNA (dsRNA) replicative form. Engulfing viral replication components within membranous structures can also help avoiding the host cell antiviral defense by impeding the recognition of these foreign components (Ishibashi and Ishikawa 2013). Furthermore, in the case of plant viruses, some of these viral factories are motile and are involved in vRNA intracellular and intercellular movement (Kawakami, Watanabe et al. 2004, Grangeon, Jiang et al. 2013).

Biogenesis of viral factories requires the host secretory pathway [reviewed by (Patarroyo, Laliberte et al. 2012)]. Several factors involved in vesicular transport are hijacked by viruses for their infection. For instance, the vesicle coatomer ε-COPI subunit is important for virus entry and gene expression of *Vesicular stomatitis virus* (VSV) (Cureton, Burdeinick-Kerr et al. 2012). The COPI coatomers also interact with the *Enterovirus 71* (EV71) spike protein, and this interaction may be required for the spike protein to be incorporated into the assembling virion (McBride, Li et al. 2007). The GTPase Arf1 interacts with the p27 protein and is incorporated in the viral factories of the *Red clover necrotic mosaic virus* (RCNMV) (Hyodo, Mine et al. 2013).

Intracellular communication among various eukaryotic membrane-bound compartments is largely membranous vesicle-based (Bassham, Brandizzi et al. 2008). Several steps ensure the proper vesicular transport, which includes vesicle formation initiation and scission at the specific site of the donor membrane followed by the targeting and fusion of the vesicle with the target membrane (Hwang and Robinson 2009). A variety of cellular factors are involved in this process. In particular, coat protein complexes I, II

and clathrin as well as GTPases selectively incorporate cargo proteins that are going to be transported in coated vesicles. Additional factors then tether these coated vesicles during the initial phase of membrane fusion, which is subsequently accomplished by the soluble N-ethylmaleimide attachment protein receptor (SNARE) proteins (Bonifacino and Glick 2004).

The SNARE proteins are trans-membrane proteins with a cytoplasmic N-terminal tail, which contains a functional SNARE motif (a heptad repeat of 60 - 70 amino acids), and a trans-membrane domain (TMD) C-terminal tail. According to their cellular locations, SNARE proteins are classified as endoplasmic reticulum (ER) SNAREs, Golgi SNAREs, and so on. Furthermore, SNARE proteins are classified as vesicle associated-SNARE (v-SNARE) and target membrane associated-SNARE (t-SNARE). In general, one v-SNARE and three t-SNAREs form a helix-bundle to bring the opposing membranes in close proximity to favor membrane fusion. In the model plant *Arabidopsis thaliana*, there are as many as 65 SNAREs, and 9 of them are located in the Golgi (Uemura, Ueda et al. 2004, Kim and Brandizzi 2012). SNARE proteins are multifunctional, and are involved in regulating cell wall organization, modulating plasma membrane permeability and mediating extracellular disease resistance (Besserer, Burnotte et al. 2012, Uemura, Kim et al. 2012, Hachez, Laloux et al. 2014, Larson, Domozych et al. 2014).

Turnip mosaic virus (TuMV) is a (+) RNA virus in the family of *Potyviridae* (Mayo 1995). The membrane-associated viral protein $6K_2$, which has a molecular weight of 6 kDa, is the only protein required for the formation of replication vesicles (Schaad, Jensen et al. 1997). The ER-Golgi vesicular transport, which is conducted in a COPII/I dependent manner, is required for $6K_2$-induced vesicle biogenesis (Wei and Wang 2008). The cytoplasmic N-terminal tail of $6K_2$ binds the COPII coat protein Sec24a for ER export (Jiang, Patarroyo et al. 2015). The viral protein also has a GXXXG motif within its TMD that is required for $6K_2$ Golgi exit (Chaper 3). The role of ER SNAREs during TuMV infection has been investigated, demonstrating that the ER SNARE Syp71 is important for vesicle-chloroplast fusion (Wei, Zhang et al. 2013). In this paper, we analyzed the impact of Golgi SNAREs on TuMV infection. We found that the Golgi SNARE Bet11,

Gos11 and Vamp714 interact with the $6K_2$ protein. We observed enhanced susceptibility to TuMV in Bet11 knockout *A. thaliana* plants and increased cell-to-cell movement in leaf tissues expressing SNARE dominant negative mutant proteins. These data thus suggest that the tested Golgi SNAREs function as TuMV restriction factors.

Materials and Methods

Molecular cloning

The coding sequences of Golgi SNARE AtBET11 (AT3G58170), AtGOS11 (AT1G15880), AtMEMB11 (AT2G36900) and AtVAMP714 (AT5G22360) were amplified from the cDNA derived from the mRNA isolated from *Arabidopsis thaliana* (Col-0) leaf tissues. The total polyadenylated mRNA was isolated using the RNeasy Plant Mini Kit (QIAGEN), and the cDNA was synthesized using the iScript cDNA Synthesis Kit (Bio-Rad). The amplified DNA fragments were digested with the corresponding endonuclease restriction enzymes and inserted into the expression vector pCambia/GFP, and the resulting constructs were termed pCambia/Bet11:GFP, pCambia/Gos11:GFP, pCambia/Memb11:GFP and pCambia/Vamp714:GFP. For the construction of the dominant negative mutant proteins, the SNARE cytosolic tails were predicted using the SOSUI server online (http://harrier.nagahama-i-bio.ac.jp/sosui/sosui_submit.html). The DNA fragments encoding the cytosolic tails were amplified by PCR using the corresponding full length coding fragments as the template. The digested fragments were ligated into the vector pCambia 1380, and the generated constructs were pCambia/Bet11 DN, pCambia/Gos11 DN, pCambia/Memb11 DN and pCambia/Vamp714 DN respectively. The primers used for gene amplification are: BET11F: 5'-GCTCTAGAATGAATCCTAGAAGGG-3'; BET11R:5'-CGGGATCCCCGAGTAAGATAGT-3'; GOS11F: 5'-GCTCTAGAATGGATGTGCCTAGCT-3'; GOS11R: 5'-CGGGATCCCTTGGTTATCCAGT-3'; VAMP714F: 5'-GCTCTAGAATGGCGATTGTCTATGC-3'; VAMP714R: 5'-GCTCTAGAAGATCTGCATGATGGT-3'; MEMB11F: 5'-GCTCTAGAATGGCGTCTGGTATC-3'; MEMB11R: 5'-GCTCTAGAGCGTGTCCATCTTAT-3'. pCambia/6K$_2$:mCherry, pCambiaTuMV/6K$_2$:GFP, p35S-TuMV, pCambiaTuMV/6K$_2$:mCherry//HDEL:GFP and the marker GFP-OsSCAMP1 were described in (Cai, Jia et al. 2011, Grangeon, Agbeci et al. 2012, Agbeci, Grangeon et al. 2013, Jiang, Patarroyo et al. 2015). All constructs were verified by sequencing.

Protein expression

Protein transient expression in leaf tissue was done by agroinfiltration as described by Cotton et al. (Cotton, Grangeon et al. 2009). The OD_{600} was adjusted to 0.05 for the SNARE dominant negative mutants (Bet11 DN, Gos11 DN, Memb11 DN and Vamp714 DN), to 0.1 for the SNARE GFP fusions (Bet11:GFP, Gos11:GFP, Memb11:GFP and Vamp714:GFP), and to 0.3 for $6K_2$:mCherry and TuMV/$6K_2$:mCherry//HDEL:GFP. For co-expression, equal volume of agrobacterium suspension was mixed thoroughly. After agroinfiltration, the plants were kept in the green house for 3-5 days until analysis.

Protoplast transfection was performed as described in (Jiang, Patarroyo et al. 2015). Briefly, the leaf tissue strips (around 1 mm wide) were incubated in a solution comprising cellulase R10 and macerozyme R10, and the protoplasts were collected by centrifugation. The protoplasts were either transfected with 5 μg of GFP-OsSCAMP1 plasmid with 15 μg of SNARE dominant negative mutant plasmids, or 3 μg TuMV infectious plasmids by PEG4000 mediated gene transfection. The transfected protoplasts were incubated at room temperature in the dark until analysis.

Confocal laser scanning microscopy

Leaf tissues or protoplasts expressing protein of interest were observed using a 10×, 20× or 63× oil immersion objective on a LSM780 confocal microscope (Zeiss). Argon and HeNe lasers were used to excite fluorescent proteins and signals from both green and red channels were collected simultaneously. GFP was excited at 488 nm, and the emission light was captured at 500 nm to 535 nm; mCherry was excited at 561 nm, and the emission light was captured at 580 nm to 640 nm. To quantify virus movement, large areas (1.13cm × 1.13cm) of the leaf tissues were imaged using the ‘tile’ scan mode of LSM780. Image processing was performed with the ZEN 2011 software and Image J.

Co-immunoprecipitation

N. benthamiana leaf tissues (approximately 0.3 g) expressing proteins of interest were grounded in liquid nitrogen and then mixed with 3.0 ml of IP buffer [50 mM Tris (pH 7.5), 150 mM NaCl, 10% glycerol, 0.1% Nonidet P-40, 5 mM dithiothreitol, and 1 × Complete Protease Inhibitor Cocktail (Roche)]. After centrifugation (20,000×g, 15 min, 4°C), 1.0 ml of the cleared supernatant was incubated with GFP-Trap resin (Chromotek). Elution of the bound proteins was done according to the manufacturer's instructions.

Results

$6K_2$ interacts with Golgi SNAREs

Previously, we found that the TuMV membrane-associated viral protein $6K_2$ exits from the ER and Golgi sequentially for the biogenesis of replication vesicles (Jiang, Patarroyo et al. 2015). SNARE proteins mediate vesicle fusion, which is a process involved in protein vesicular trafficking (Lipka, Kwon et al. 2007). The ER SNARE Syp71 has been reported to be involved in the fusion process that takes place between $6K_2$-induced replication vesicles and chloroplasts during TuMV infection (Wei, Zhang et al. 2013). Thus, we investigated the roles of Golgi SNAREs in TuMV infection. In the model plant *Arabidopsis thaliana*, at least nine out of sixty-five encoded SNARE proteins are located at the Golgi apparatus (Uemura, Ueda et al. 2004, Kim and Brandizzi 2012). In this project, we select one SNARE from each group. Therefore we focused our analysis on four Golgi SNAREs, AtBET11 (AT3G58170), AtGOS11 (AT1G15880), AtMEMB11 (AT2G36900) and AtVAMP714 (AT5G22360).

Structurally, the majority of SNARE proteins are characterized by a long N-terminal cytoplasmic tail that contains the functional SNARE motif mediating SNARE protein recognition, and a short C-terminal tail that is composed of a trans-membrane domain (TMD) for membrane association (Lipka, Kwon et al. 2007). Consequently, the Golgi SNAREs were fused to the N-terminal portion of the green fluorescent protein (GFP) in order to mitigate any deleterious effect on their proper cellular locations and functions. Four-week old *N. benthamiana* plants were agroinfiltrated to express these Golgi SNARE:GFP fusion proteins, and were observed by confocal laser scanning microscopy three days later. As expected, all these Golgi SNAREs were distributed as punctate bodies, with VAMP714 equally labeling the ER network (Fig. 1A-D, green panels). These SNARE fusions were then co-expressed with $6K_2$:mCherry. We found that the vesicles induced by $6K_2$ co-localized with all of these Golgi SNAREs (Fig. 1A-D), suggesting that these SNAREs may interact with $6K_2$.

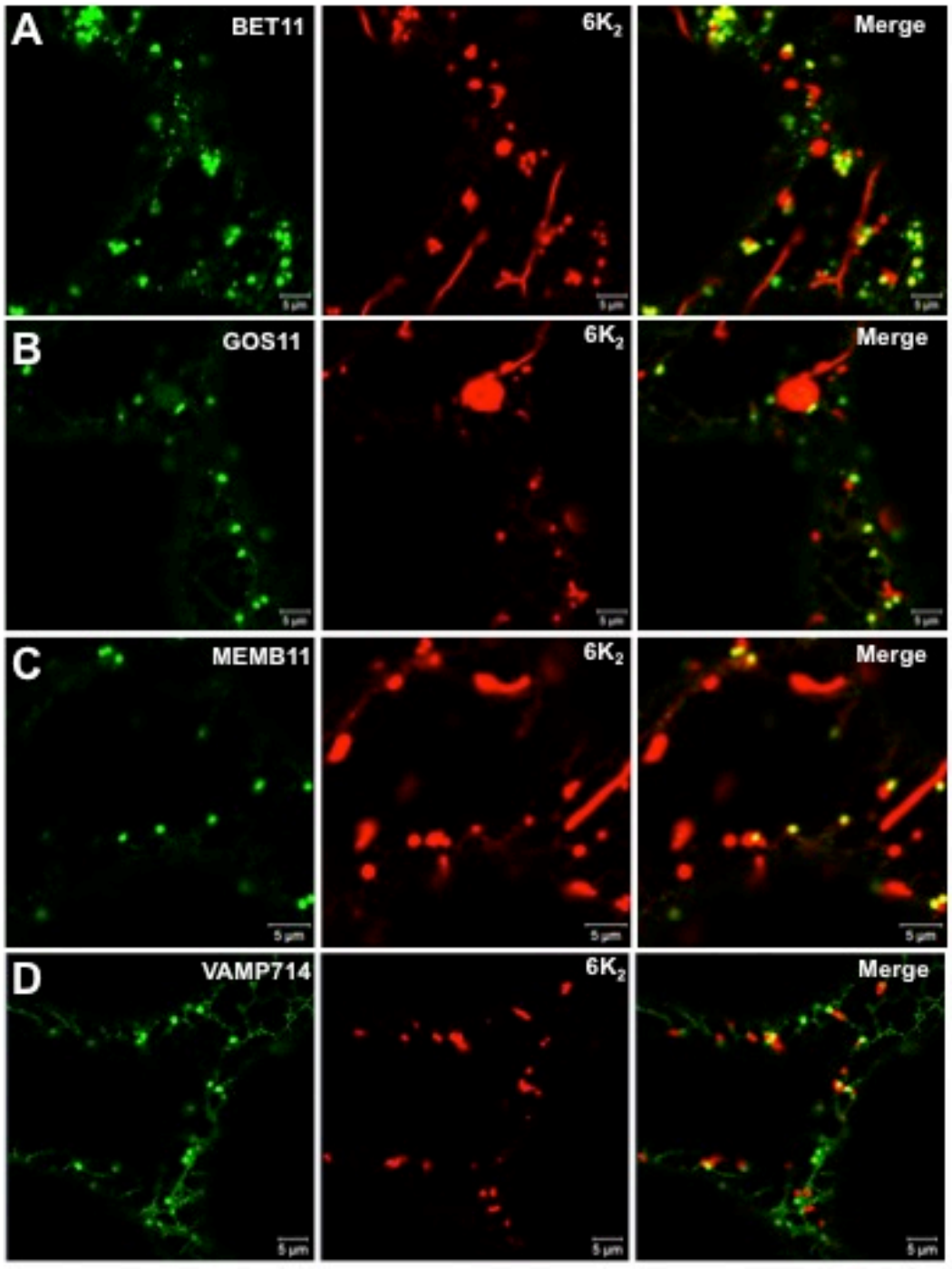

Figure 1. Co-localization analysis of $6K_2$ vesicles with Golgi SNAREs.

N. benthamiana leaf tissues were agroinfiltrated with $6K_2$:mCherry and BET11:GFP (A), GOS11:GFP (B), MEMB11:GFP (C) and VAMP714:GFP (D), and were observed 3 days

later. Images of the emitted green and red fluorescence and of the merged signals are shown in the left, middle and right panels, respectively. The green panels are shown on the left, red panels in the middle and with merged panels on the right.

We consequently tested for protein interaction by co-immunoprecipitation (CO-IP) experiment. Leaf tissues co-expressing $6K_2$:mCherry with BET11:GFP, GOS11:GFP, MEMB11:GFP or VAMP714:GFP were processed for CO-IP. Three of the Golgi SNAREs, BET11, GOS11 and the VAMP714 were co-purified along with $6K_2$, but not MEMB11 (Fig. 2). Negative controls co-expressing mCherry with GFP, $6K_2$:mCherry with GFP, mCherry with BET11:GFP, mCherry with GOS11:GFP, and mCherry with VAMP714:GFP did not show any co-purification (see supplemental Fig. 1). These results show that $6K_2$ interacts with at least three Golgi SNAREs.

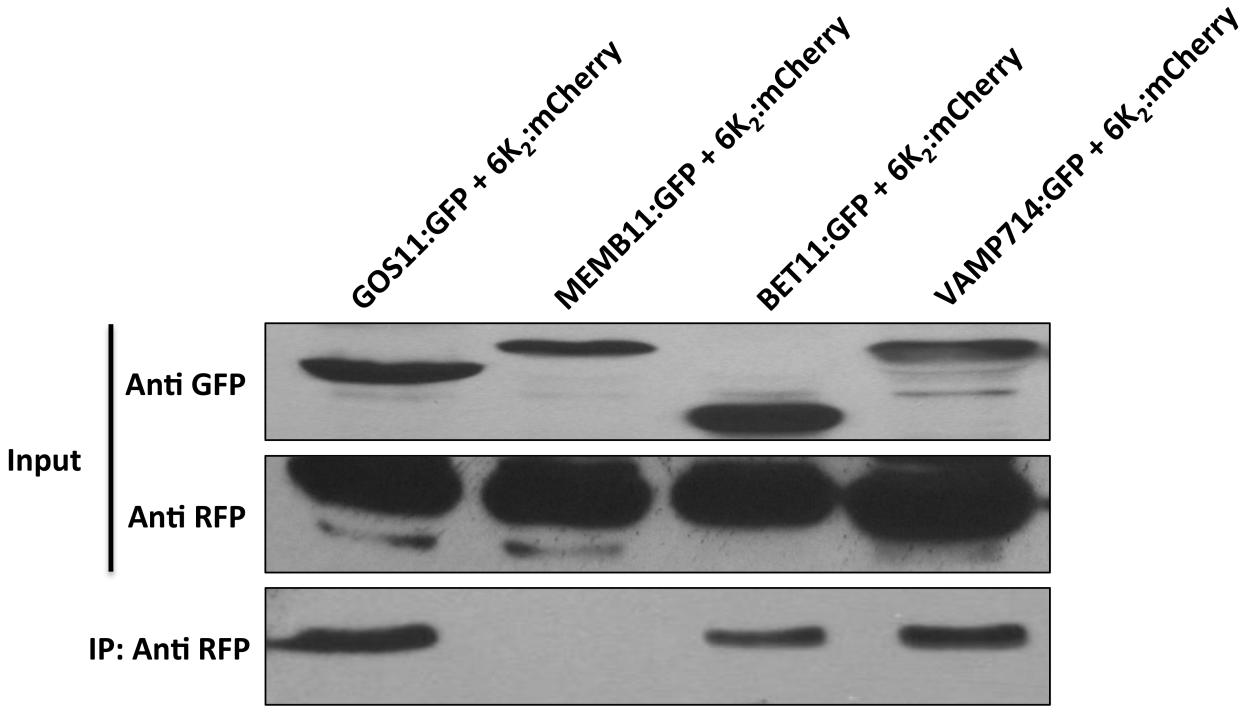

Figure 2. Protein interaction assay between $6K_2$ and Golgi SNAREs.

N. benthamiana leaf tissues co-expressing Golgi SNAREs GOS11:GFP, or MEMB11:GFP, or BET11:GFP, or VAMP714:GFP with $6K_2$:mCherry were processed for co-immunoprecipitation. Western blots were performed with anti-GFP and anti-RFP antibodies.

Increased susceptibility of *bet11 Arabidopsis thaliana* knockout plants to TuMV infection

We next verified the susceptibility to TuMV infection of *A. thaliana* knockout plants lacking *gos11* and *bet11* (*A. thaliana* knockout plants for *vamp714* is not available). Homozygous *A. thaliana* SALK T-DNA lines of *gos11* (SALK_053828C) and *bet11* (SALK_150636C) were obtained from The Arabidopsis Information Resource (TAIR). These T-DNA insertion mutants were verified by PCR using primer pairs LP + RP and LB + RP, and following the protocol available at http://signal.salk.edu/tdnaprimers.2.html (data not shown). Five-week old *A. thaliana* SALK T-DNA lines and wt *A. thaliana* Columbia-0 were agro-infected with TuMV/6K_2:GFP, and virus systemic infection was assessed every day by monitoring the appearance and spread of fluorescence using a hand-held UV lamp. The first indication of TuMV infection of wt *A. thaliana* was noted at 9 d.p.i, and 80 % of the plants were systemically infected at 11 d.p.i (Fig. 3). TuMV susceptibility in *gos11* KO plants was similar to that in wt *A. thaliana*. TuMV systemic infection, however, was faster in *bet11* knockout plants. Eight out of 23 inoculated plants showed GFP fluorescence at 8 d.p.i, and there were always more infected KO plants than wt plants thereafter. This experiment was repeated two more times and the combined data are presented in Table 1. Although the number of plants showing GFP fluorescence varied from one experiment to another, the average percentage of infected *A. thaliana* at 9 dpi was lower for wt plants than for their BET11 KO derivatives *bet11* KO plants (i.e. 10% vs 31%). Equally, on average, 81% of *bet11* KO plants were systemically infected at 11 dpi, compared to 65% for the wt plants. On the other hand, there was no indication in these two additional experiments that *gos11* KO plants were more susceptible to TuMV than wt plants, hence confirming the initial result.

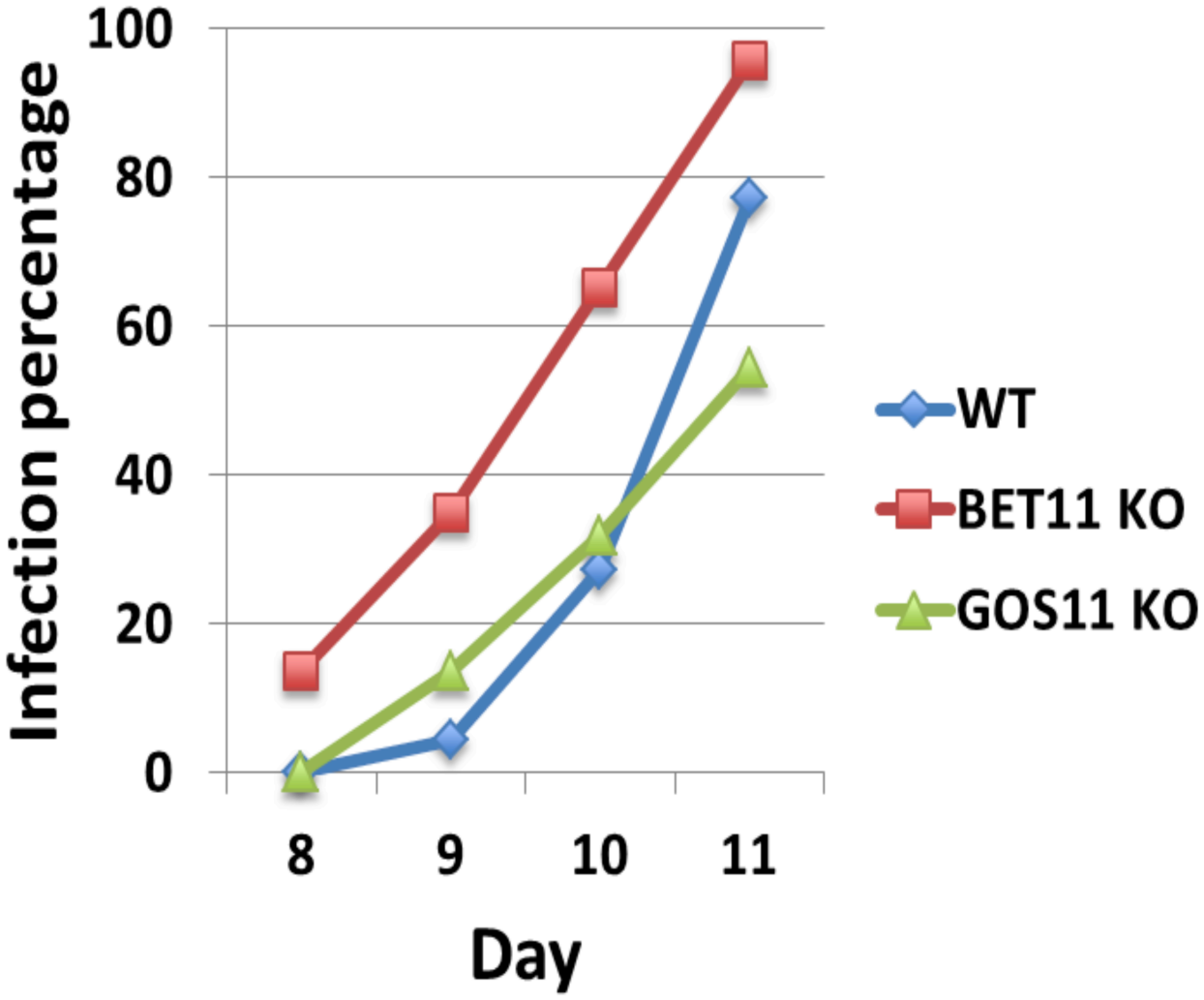

Figure 3. TuMV systemic infection assay.

Wild type as well as *bet11*, and *gos11* knockout *Arabidopsis thaliana* plants were agroinnoculated with TuMV/6K_2:GFP. The value infection percentage (infected versus total plants) was plotted against the time points.

Exp. No.		No. of systemically infected plants	
		9 d.p.i	11 d.p.i
1	WT	1/22	17/22
	GOS11	3/22	12/22
	BET11	8/23	22/23
2	WT	4/20	12/20
	GOS11	5/20	9/20
	BET11	8/21	16/21
3	WT	1/22	13/22
	GOS11	5/22	12/22
	BET11	4/21	15/21

Table 1: TuMV systemic infection assay. The virus systemic infection was checked at 9 d.p.i and 11 d.p.i. Experiments were performed three times, with the number of systemically infected plant/number of total of inoculated plants shown.

Golgi SNAREs dominant negative mutants

In order to confirm the role of these Golgi SNAREs in TuMV infection, dominant negative mutant version of these proteins were produced. This was achieved by expressing solely the cytoplasmic tail of each Golgi SNARE in order to interfere with the normal cellular function of the endogenous protein (Tyrrell, Campanoni et al. 2007). A GFP fusion of the rice Secretory Carrier Membrane Protein 1 (GFP-SCAMP1), which reaches the plasma membrane (PM) via the ER-Golgi-TGN-PM pathway (Cai, Jia et al. 2011), was used as a marker for assessing the dominant negative effect of the SNARE mutants. Protoplasts were isolated from *N. benthamiana* leaves, and were transfected either with the GFP-SCAMP1 alone or together with the corresponding Golgi SNARE dominant negative mutants. After 20h, the GFP signal was detected only at the PM for most protoplasts transfected with the GFP:SCAMP1 alone (Fig. 4A). Occasionally, the GFP signal could be detected in the cytoplasm, which may be due to protein over production. However, the GFP signal, in addition to being found at the PM, was detected more frequently in the cytoplasm when the GFP:SCAMP1 was co-transfected with the dominant negative versions of BET11, GOS11 or VAMP714 (Fig. 4B-D). Statistically, while around 20 % of the GFP:SCAMP1 transfected protoplasts showed cytoplasmic retention, this value rose to 70-80 % in the presence of the dominant negative proteins (Fig. 4E). This experiment thus demonstrated that the Golgi SNARE dominant negative proteins were functional in weakening the action of the endogenous Golgi SNAREs.

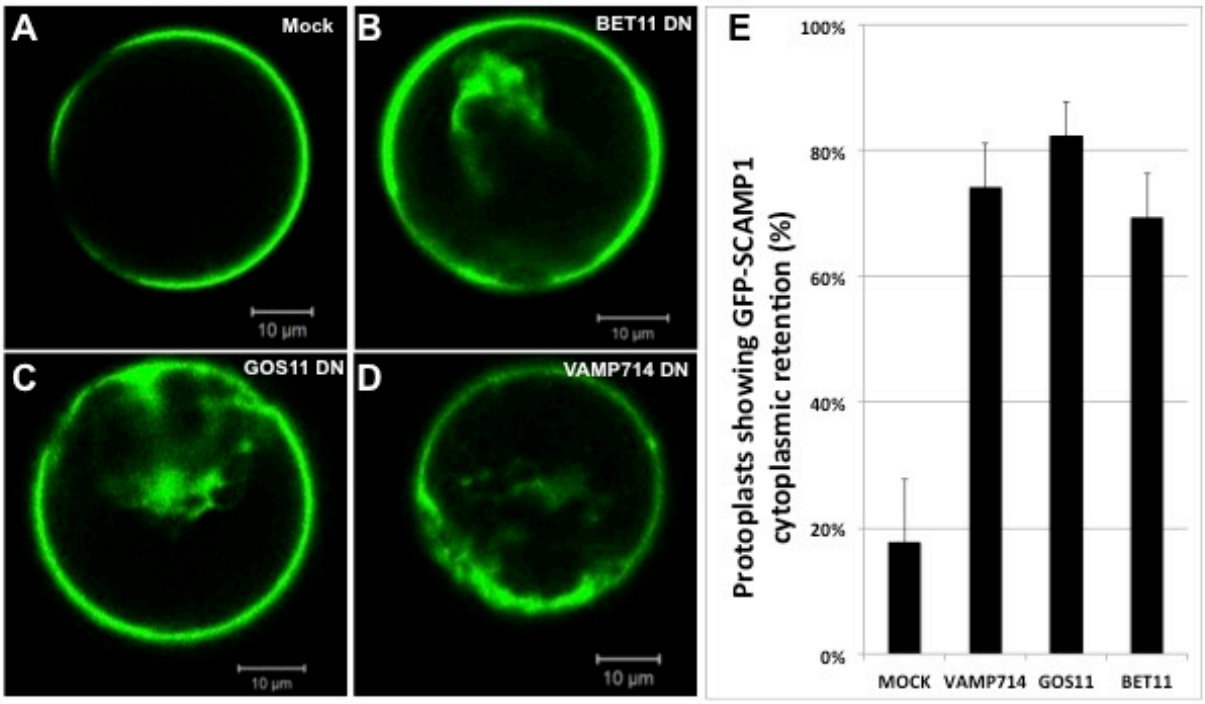

Figure 4. Characterization of Golgi SNARE dominant negative (DN) activities.

PM marker GFP-SCAMP1 was transiently expressed with Mock (A), or BET11 DN (B), or GOS11 DN (C), or VAMP714 DN (D). (E) Statistical analysis of the transfected protoplasts showing cytoplasmic retention of GFP-SCAMP1.

Golgi SNAREs impair TuMV cell-to-cell movement

The dominant negative SNARE proteins were then expressed with the infectious clone TuMV/6K_2:mCherry//HDEL:GFP. The dual tagged fluorescent TuMV infectious clone can be used to distinguish the virus spreading at the cellular level, as the primary infected cells express both mCherry and GFP while the secondary infected cells express the mCherry only (Agbeci, Grangeon et al. 2013). Entire *N. benthamiana* leaves were agroinfiltrated with vectors encoding the dominant negative SNARE proteins and inoculated, one day later, with the TuMV infectious clone in small regions of approximately 0.5 cm in diameter. The plants were analyzed 4 days later. Representative foci of TuMV infection in mock, and in dominant negative mutant of BET11, GOS11 or VAMP714-agroinfiltrated leaves are shown in Fig. 5A-D. The surface areas of red and green fluorescence were calculated for 21 samples and the ratio of red over green area is presented in Fig. 5E. A ratio greater than 1.0 is indicative of the extent of virus cell-to-cell movement (Agbeci, Grangeon et al. 2013). Statistical analysis showed that the virus moves significantly faster in the presence of the Golgi SNARE dominant negative proteins (Fig. 5E). The results of two additional experiments are shown in Fig. S2, and increased cell-to-cell movement was always observed in Golgi SNARE dominant negative mutant samples.

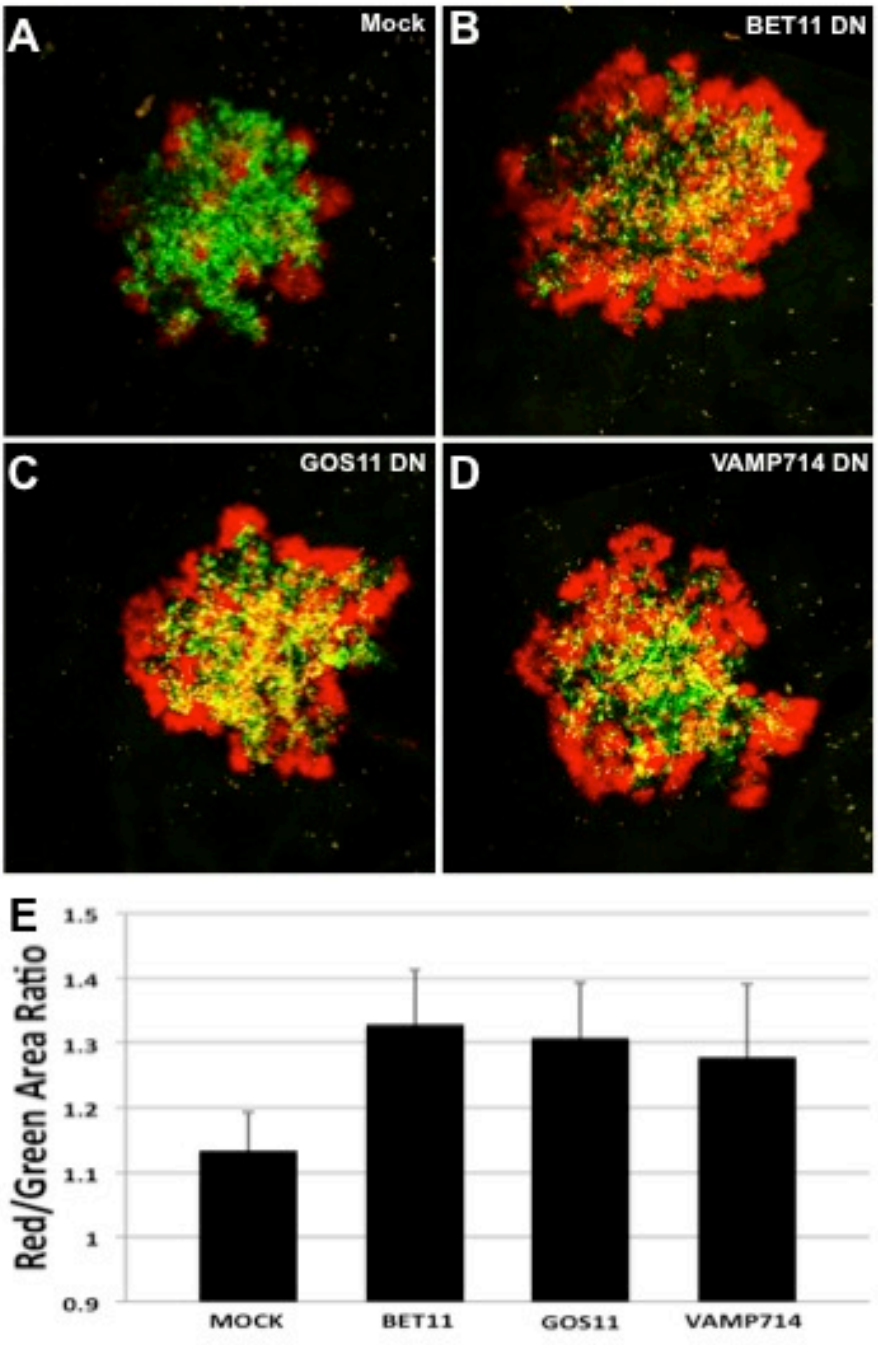

Figure 5. Impact of Golgi SNARE DN on TuMV cell-to-cell movement.

Confocal microscopy images of leaf tissues expressing TuMV/6K_2:mCherry//HDEL:GFP with Mock (A), or BET11 DN (B), or GOS11 DN (C), or VAMP714 DN (D). (E) Quantification of virus cell-to-cell movement as determined by the red/green area ratio.

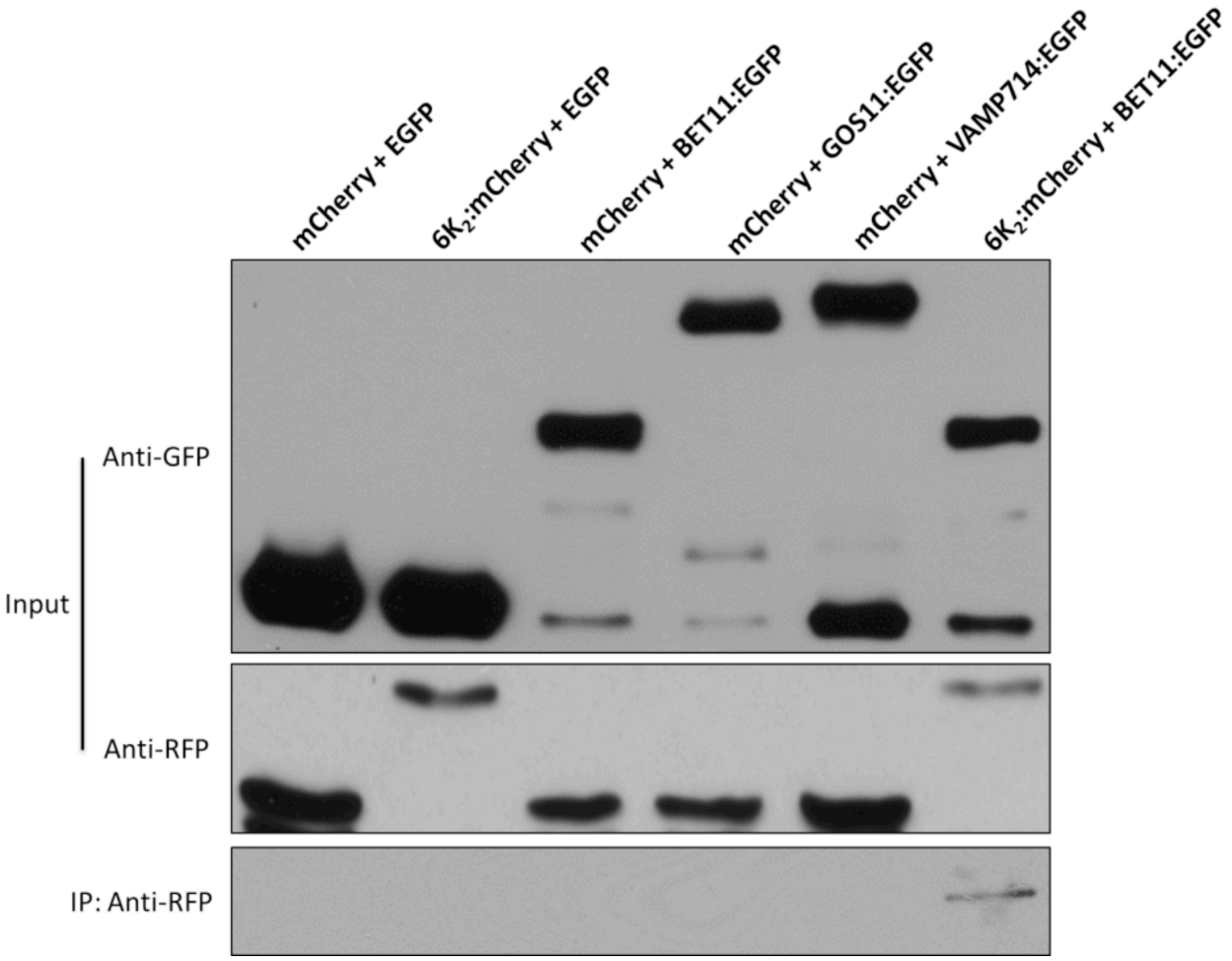

Figure S1. CO-IP controls.

N. benthamiana leaf tissues co-expressing mCherry and GFP, $6K_2$:mCherry and GFP, mCherry and BET11:GFP, mCherry and GOS11:GFP, mCherry and VAMP714:GFP, $6K_2$:mCherry and BET11:GFP were processed for co-immunoprecipitation. Western blots were performed with anti-GFP and anti-RFP antibodies.

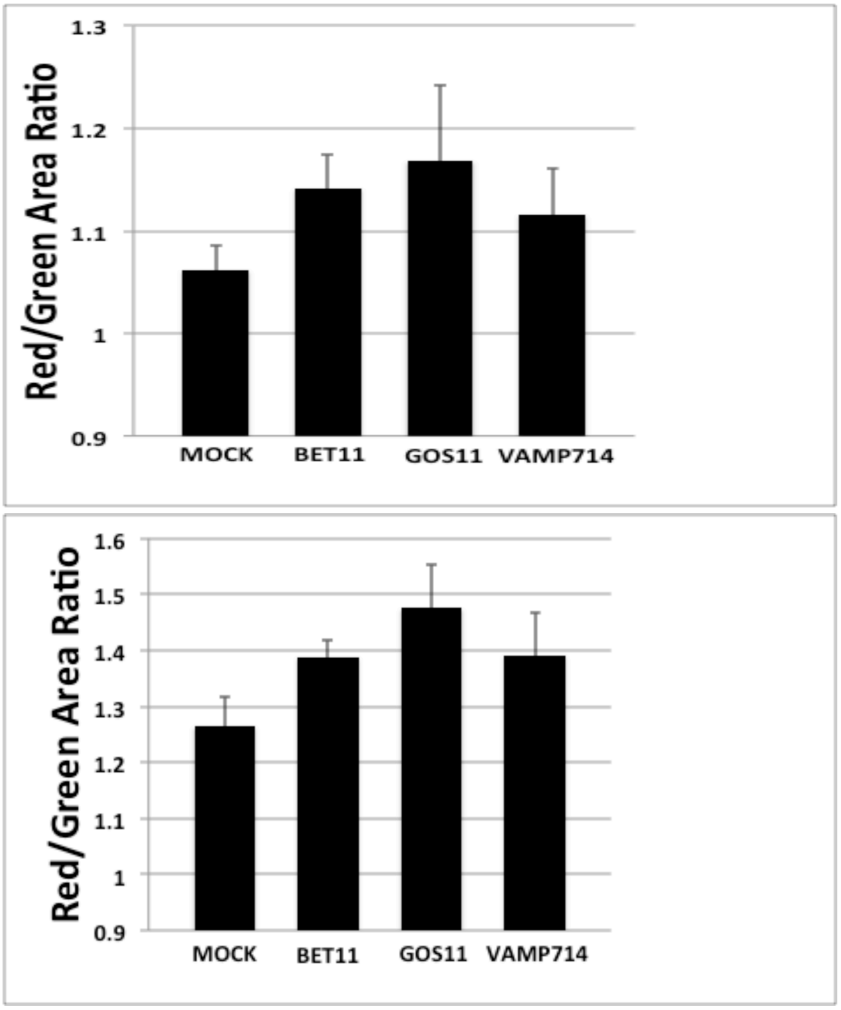

Figure S2. Quantification of virus cell-to-cell movement using the red/green area ratio.

Discussion

Very little is known about the Golgi SNAREs, if not that the SNARE Bet11 functions as a v-SNARE for ER-Golgi vesicular trafficking (Chatre, Brandizzi et al. 2005). We have investigated the impact of Golgi SNAREs on TuMV infection and found that Bet11, Gos11 and Vamp714 can interact with the viral protein $6K_2$ (Fig. 1 and 2). The importance of these interactions was revealed by using an *Arabidopsis thaliana* knockout plant for Bet11 that showed enhanced susceptibility to TuMV infection (Fig. 3 and Table 1). Golgi SNARE dominant negative versions of Bet11, Gos11 and Vamp714 were generated (Fig. 4), and their expression in *N. benthamiana* cells facilitated virus cell-to-cell movement (Fig. 5). These results thus suggest that these Golgi SNAREs function as TuMV viral restriction factors. Consistent with this conclusion is the observation that the expression levels of endogenous Bet11 are down regulated during TuMV infection (Li, Zhang et al. 2014). Although the other Golgi SNARE GOS11 and VAMP714 also interact with $6K_2$ as BET11, they did not inhibit the spread of TuMV significantly. It suggests that they may contribute differently during the virus infection.

Host factors play important roles in almost every steps of the virus infectious cycle, including viral genome translation, formation of viral factories, virus dissemination (Wang 2015). Most factors that have been characterized show positive regulatory roles during virus infection. For instance, translation factors, such as the eukaryotic initiation factor (eIF) 4E and its isoform iso4E, or the eukaryotic elongation factors (eEF) 1A and 1B, are essential for successful infection by TuMV, *Tobacco mosaic virus* (TMV) and *Potato virus X* (PVX) (Leonard, Plante et al. 2000, Thivierge, Cotton et al. 2008, Hwang, Oh et al. 2013, Hwang, Lee et al. 2015). Other protein families, such as heat shock proteins (HSPs) and myosins, are required for the infection by many viruses (Mine, Hyodo et al. 2012, Agbeci, Grangeon et al. 2013, Gorovits, Moshe et al. 2013, Amari, Di Donato et al. 2014, Jiang, Lu et al. 2014).

Alternatively, host cells have developed defensive pathways that restrict viral replication. Many restriction factors have been identified in the case of animal virus

infections, especially for retroviruses. Factors, such as TRIM5α, Mx2/MxB, TRIM22/Staf50, SAMHD1, p21/CDKN1, tetherin/BST2/CD137, APOBEC3G and APOBEC3F all have been proposed as *Human immunodeficiency virus type 1* (HIV-1) restriction factors [reviewed by (Merindol and Berthoux 2015)]. For instance, the restriction factor TRIM5α recognizes and interacts with the coat protein of the incoming HIV-1 and disrupts the uncoating of the virus particle, while tetherin/BST2/CD137 inhibits the release of the virus particle from the plasma membrane (Stremlau, Owens et al. 2004, Neil, Zang et al. 2008). Interestingly, the viral protein Vpu functions as a Tetherin antagonist, thereby counteracting the inhibition of viral release by tetherin (Rollason, Dunstan et al. 2013). Other restriction factors are the intracellular innate immune sensor IFI16 that inhibits *Human cytomegalovirus* (HCMV) DNA replication and transcription, and the cholesterol 25-hydroxylase (CH25H) that inhibits *Hepatitis C virus* (HCV) infection by regulating host lipid metabolism (Gariano, Dell'Oste et al. 2012, Xiang, Tang et al. 2015). In the case of plant viruses, restriction factors have mainly been identified for the *Tomato bushy stunt virus* (TBSV). Those restriction factors include the RNA-binding protein nucleolin, ribonucleases, WW-domain [(AP)-P-P-(AP)-Y] proteins, single- and multi-domain cyclophilins, TPR (tetratricopeptide repeats) -domain co-chaperones and cellular ion pumps [reviewed by (Sasvari, Alatriste Gonzalez et al. 2014)]. These restriction factors were identified by high-throughput genome-wide screening in yeast, and their impact on virus infection analyzed in cell-free systems, yeast cells and model plants (Sasvari, Alatriste Gonzalez et al. 2014). Their function was further confirmed by using VIGS, knockdown, knockout and dominant negative mutant.

How these Golgi SNAREs function as TuMV restriction factors is not known. Previously, we identified the mutant $6K_2^{GV}$ was arrested in the Golgi. However, this mutated $6K_2$ still can interact with Golgi SNAREs (data not shown), suggesting the Golgi SNAREs are not the key factors that regulate the Golgi exit of the $6K_2$-induced vesicles. One possibility is that these Golgi SNAREs regulate the plant antiviral response. SNARE proteins have been demonstrated to play a role against pathogen infections. For instance, members of the SYP4 group of trans-Golgi network resident SNAREs are

required for the host extracellular resistance responses to fungal pathogens (Uemura, Kim et al. 2012). Additionally, the Golgi SNARE Memb12 is involved in plant antibacterial response (Zhang, Zhao et al. 2011). Finally, the expression level of SNAREs is correlated with host resistance against pathogens (Wang, Wang et al. 2014). Furthermore, pathogens can encode proteins that contain SNARE-like motifs in order to manipulate host cell membrane fusion events for their benefit (Delevoye, Nilges et al. 2008, Paumet, Wesolowski et al. 2009). Consequently, it is possible that the host cell Golgi SNARE proteins also function to combat virus infection.

Acknowledgments

This work was supported by grants from the Natural Science and Engineering Research Council (NSERC) of Canada and from Le Fonds québécois de recherche sur la nature et les technologies (FQRNT) to HZ and JFL.

We thank Dr. Liwen Jiang (The Chinese University of Hong Kong) for the plasmid GFP-SCAMP1.

References

1. **Laliberte JF, Sanfacon H.** 2010. Cellular remodeling during plant virus infection. Annu Rev Phytopathol **48:**69-91.

2. **Ishibashi K, Ishikawa M.** 2013. The resistance protein Tm-1 inhibits formation of a Tomato mosaic virus replication protein-host membrane protein complex. J Virol **87:**7933-7939.

3. **Grangeon R, Jiang J, Wan J, Agbeci M, Zheng H, Laliberte JF.** 2013. 6K2-induced vesicles can move cell to cell during turnip mosaic virus infection. Front Microbiol **4:**351.

4. **Kawakami S, Watanabe Y, Beachy RN.** 2004. Tobacco mosaic virus infection spreads cell to cell as intact replication complexes. Proceedings of the National Academy of Sciences of the United States of America **101:**6291-6296.

5. **Patarroyo C, Laliberte JF, Zheng H.** 2012. Hijack it, change it: how do plant viruses utilize the host secretory pathway for efficient viral replication and spread? Front Plant Sci **3:**308.

6. **Cureton DK, Burdeinick-Kerr R, Whelan SPJ.** 2012. Genetic Inactivation of COPI Coatomer Separately Inhibits Vesicular Stomatitis Virus Entry and Gene Expression. Journal of Virology **86:**655-666.

7. **McBride CE, Li J, Machamer CE.** 2007. The Cytoplasmic Tail of the Severe Acute Respiratory Syndrome Coronavirus Spike Protein Contains a Novel Endoplasmic Reticulum Retrieval Signal That Binds COPI and Promotes Interaction with Membrane Protein. Journal of Virology **81:**2418-2428.

8. **Hyodo K, Mine A, Taniguchi T, Kaido M, Mise K, Taniguchi H, Okuno T.** 2013. ADP ribosylation factor 1 plays an essential role in the replication of a plant RNA virus. J Virol **87:**163-176.

9. **Bassham DC, Brandizzi F, Otegui MS, Sanderfoot AA.** 2008. The Secretory System of Arabidopsis. The Arabidopsis Book doi:10.1199/tab.0116**:**e0116.

10. **Hwang I, Robinson DG.** 2009. Transport vesicle formation in plant cells. Current Opinion in Plant Biology **12:**660-669.

11. **Bonifacino JS, Glick BS.** 2004. The mechanisms of vesicle budding and fusion. Cell **116:**153-166.

12. **Uemura T, Ueda T, Ohniwa RL, Nakano A, Takeyasu K, Sato MH.** 2004. Systematic Analysis of SNARE Molecules in Arabidopsis: Dissection of the post-Golgi Network in Plant Cells. Cell Structure and Function **29:**49-65.

13. **Kim S-J, Brandizzi F.** 2012. News and Views into the SNARE Complexity in Arabidopsis. Frontiers in Plant Science **3**.

14. **Hachez C, Laloux T, Reinhardt H, Cavez D, Degand H, Grefen C, De Rycke R, Inze D, Blatt MR, Russinova E, Chaumont F.** 2014. Arabidopsis SNAREs SYP61 and SYP121 coordinate the trafficking of plasma membrane aquaporin PIP2;7 to modulate the cell membrane water permeability. Plant Cell **26:**3132-3147.

15. **Besserer A, Burnotte E, Bienert GP, Chevalier AS, Errachid A, Grefen C, Blatt MR, Chaumont F.** 2012. Selective regulation of maize plasma membrane aquaporin trafficking and activity by the SNARE SYP121. Plant Cell **24:**3463-3481.

16. **Uemura T, Kim H, Saito C, Ebine K, Ueda T, Schulze-Lefert P, Nakano A.** 2012. Qa-SNAREs localized to the trans-Golgi network regulate multiple transport pathways and extracellular disease resistance in plants. Proc Natl Acad Sci U S A **109:**1784-1789.

17. **Larson ER, Domozych DS, Tierney ML.** 2014. SNARE VTI13 plays a unique role in endosomal trafficking pathways associated with the vacuole and is essential for cell wall organization and root hair growth in arabidopsis. Ann Bot **114:**1147-1159.

18. **Mayo MA.** 1995. The Potyviridae. By D. D. SHUKLA, C. W. WARD and A. A. BRUNT. 25 × 17 cm. Pp. 516 with 110 text-figures and 30 tables, Wallingford: CAB International, 1994. Price: £60.00. New Phytologist **131:**289-290.

19. **Schaad MC, Jensen PE, Carrington JC.** 1997. Formation of plant RNA virus replication complexes on membranes: role of an endoplasmic reticulum‐targeted viral protein, vol 16.

20. **Wei T, Wang A.** 2008. Biogenesis of cytoplasmic membranous vesicles for plant potyvirus replication occurs at endoplasmic reticulum exit sites in a COPI- and COPII-dependent manner. J Virol **82:**12252-12264.

21. **Jiang J, Patarroyo C, Garcia Cabanillas D, Zheng H, Laliberte JF.** 2015. The Vesicle-Forming 6K2 Protein of Turnip Mosaic Virus Interacts with the COPII Coatomer Sec24a for Viral Systemic Infection. J Virol **89:**6695-6710.

22. **Wei T, Zhang C, Hou X, Sanfacon H, Wang A.** 2013. The SNARE protein Syp71 is essential for turnip mosaic virus infection by mediating fusion of virus-induced vesicles with chloroplasts. PLoS Pathog **9:**e1003378.

23. **Agbeci M, Grangeon R, Nelson RS, Zheng H, Laliberte JF.** 2013. Contribution of host intracellular transport machineries to intercellular movement of turnip mosaic virus. PLoS Pathog **9:**e1003683.

24. **Cai Y, Jia T, Lam SK, Ding Y, Gao C, San MWY, Pimpl P, Jiang L.** 2011. Multiple cytosolic and transmembrane determinants are required for the trafficking of SCAMP1 via an ER–Golgi–TGN–PM pathway. The Plant Journal **65:**882-896.

25. **Grangeon R, Agbeci M, Chen J, Grondin G, Zheng H, Laliberte JF.** 2012. Impact on the endoplasmic reticulum and Golgi apparatus of turnip mosaic virus infection. J Virol **86:**9255-9265.

26. **Cotton S, Grangeon R, Thivierge K, Mathieu I, Ide C, Wei T, Wang A, Laliberté J-F.** 2009. Turnip Mosaic Virus RNA Replication Complex Vesicles Are Mobile, Align with Microfilaments, and Are Each Derived from a Single Viral Genome. Journal of Virology **83:**10460-10471.

27. **Lipka V, Kwon C, Panstruga R.** 2007. SNARE-ware: the role of SNARE-domain proteins in plant biology. Annu Rev Cell Dev Biol **23:**147-174.

28. **Tyrrell M, Campanoni P, Sutter J-U, Pratelli R, Paneque M, Sokolovski S, Blatt MR.** 2007. Selective targeting of plasma membrane and tonoplast traffic by inhibitory (dominant-negative) SNARE fragments. The Plant Journal **51:**1099-1115.

29. **Chatre L, Brandizzi F, Hocquellet A, Hawes C, Moreau P.** 2005. Sec22 and Memb11 Are v-SNAREs of the Anterograde Endoplasmic Reticulum-Golgi Pathway in Tobacco Leaf Epidermal Cells. Plant Physiology **139:**1244-1254.

30. **Li Y, Zhang C, Song X, Lv S, Hou X.** 2014. Using an Arabidopsis oligonucleotide microarray to analyze the secretory pathway genes' Response to TuMV infection in Brassica rapa. Physiological and Molecular Plant Pathology **88:**85-93.

31. **Wang A.** 2015. Dissecting the Molecular Network of Virus-Plant Interactions: The Complex Roles of Host Factors. Annu Rev Phytopathol doi:10.1146/annurev-phyto-080614-120001.

32. **Hwang J, Oh CS, Kang BC.** 2013. Translation elongation factor 1B (eEF1B) is an essential host factor for Tobacco mosaic virus infection in plants. Virology **439:**105-114.

33. **Hwang J, Lee S, Lee JH, Kang WH, Kang JH, Kang MY, Oh CS, Kang BC.** 2015. Plant Translation Elongation Factor 1Bbeta Facilitates Potato Virus X (PVX) Infection and Interacts with PVX Triple Gene Block Protein 1. PLoS One **10:**e0128014.

34. **Thivierge K, Cotton S, Dufresne PJ, Mathieu I, Beauchemin C, Ide C, Fortin MG, Laliberté J-F.** 2008. Eukaryotic elongation factor 1A interacts with Turnip mosaic virus RNA-dependent RNA polymerase and VPg-Pro in virus-induced vesicles. Virology **377:**216-225.

35. **Leonard S, Plante D, Wittmann S, Daigneault N, Fortin MG, Laliberte JF.** 2000. Complex formation between potyvirus VPg and translation eukaryotic initiation factor 4E correlates with virus infectivity. J Virol **74:**7730-7737.

36. **Jiang S, Lu Y, Li K, Lin L, Zheng H, Yan F, Chen J.** 2014. Heat shock protein 70 is necessary for Rice stripe virus infection in plants. Mol Plant Pathol **15:**907-917.

37. **Gorovits R, Moshe A, Ghanim M, Czosnek H.** 2013. Recruitment of the host plant heat shock protein 70 by Tomato yellow leaf curl virus coat protein is required for virus infection. PLoS One **8:**e70280.

38. **Mine A, Hyodo K, Tajima Y, Kusumanegara K, Taniguchi T, Kaido M, Mise K, Taniguchi H, Okuno T.** 2012. Differential roles of Hsp70 and Hsp90 in the assembly of the replicase complex of a positive-strand RNA plant virus. J Virol **86:**12091-12104.

39. **Amari K, Di Donato M, Dolja VV, Heinlein M.** 2014. Myosins VIII and XI Play Distinct Roles in Reproduction and Transport of <italic>Tobacco Mosaic Virus</italic>. PLoS Pathog **10:**e1004448.

40. **Merindol N, Berthoux L.** 2015. Restriction Factors in HIV-1 Disease Progression. Curr HIV Res.

41. **Neil SJ, Zang T, Bieniasz PD.** 2008. Tetherin inhibits retrovirus release and is antagonized by HIV-1 Vpu. Nature **451:**425-430.

42. **Stremlau M, Owens CM, Perron MJ, Kiessling M, Autissier P, Sodroski J.** 2004. The cytoplasmic body component TRIM5[alpha] restricts HIV-1 infection in Old World monkeys. Nature **427:**848-853.

43. **Rollason R, Dunstan K, Billcliff PG, Bishop P, Gleeson P, Wise H, Digard P, Banting G.** 2013. Expression of HIV-1 Vpu leads to loss of the viral restriction factor CD317/Tetherin from lipid rafts and its enhanced lysosomal degradation. PLoS One **8:**e75680.

44. **Gariano GR, Dell'Oste V, Bronzini M, Gatti D, Luganini A, De Andrea M, Gribaudo G, Gariglio M, Landolfo S.** 2012. The intracellular DNA sensor IFI16 gene

acts as restriction factor for human cytomegalovirus replication. PLoS Pathog **8:**e1002498.

45. **Xiang Y, Tang JJ, Tao W, Cao X, Song BL, Zhong J.** 2015. Identification of Cholesterol 25-Hydroxylase as a Novel Host Restriction Factor and a Part of the Primary Innate Immune Responses against Hepatitis C Virus Infection. J Virol **89:**6805-6816.

46. **Sasvari Z, Alatriste Gonzalez P, Nagy P.** 2014. Tombusvirus-yeast interactions identify conserved cell-intrinsic viral restriction factors. Frontiers in Plant Science **5**.

47. **Uemura T, Kim H, Saito C, Ebine K, Ueda T, Schulze-Lefert P, Nakano A.** 2012. Qa-SNAREs localized to the trans-Golgi network regulate multiple transport pathways and extracellular disease resistance in plants. Proceedings of the National Academy of Sciences **109:**1784-1789.

48. **Zhang X, Zhao H, Gao S, Wang WC, Katiyar-Agarwal S, Huang HD, Raikhel N, Jin H.** 2011. Arabidopsis Argonaute 2 regulates innate immunity via miRNA393(*)-mediated silencing of a Golgi-localized SNARE gene, MEMB12. Mol Cell **42:**356-366.

49. **Wang X, Wang X, Deng L, Chang H, Dubcovsky J, Feng H, Han Q, Huang L, Kang Z.** 2014. Wheat TaNPSN SNARE homologues are involved in vesicle-mediated resistance to stripe rust (Puccinia striiformis f. sp. tritici). J Exp Bot **65:**4807-4820.

50. **Paumet F, Wesolowski J, Garcia-Diaz A, Delevoye C, Aulner N, Shuman HA, Subtil A, Rothman JE.** 2009. Intracellular Bacteria Encode Inhibitory SNARE-Like Proteins. PLoS ONE **4:**e7375.

51. **Delevoye C, Nilges M, Dehoux P, Paumet F, Perrinet S, Dautry-Varsat A, Subtil A.** 2008. SNARE protein mimicry by an intracellular bacterium. PLoS Pathog **4:**e1000022.

CHAPTER 5: DISCUSSION

1. Overview

It has been shown some time ago that the potyviral membrane-associated protein $6K_2$ is able to induce the formation of virus replication vesicles (Schaad, Jensen et al. 1997), but the underlying mechanism for their formation is still not known. My Ph.D. project was thus to understand the cellular biogenesis of $6K_2$-induced replication vesicle using TuMV as the model potyvirus. Two aspects, in particular, needed to be answered: What are the molecular determinants of $6K_2$ for vesicle formation, and which host factors are involved in the $6K_2$-induced vesicle production?

Using site-directed mutagenesis coupled to confocal laser scanning microscopy, I identified a combinatorial motif that is required for the $6K_2$ protein to exit the early secretory pathway and for the formation of replication vesicles. Specifically, the N-terminal cytoplasmic tail contains a tryptophan-based motif that is required for $6K_2$ ER exit, while the trans-membrane domain (TMD) GXXXG motif is indispensable for $6K_2$ Golgi exit. Consequently, this combinatorial motif directs $6K_2$ ER and Golgi exit sequentially. These results are consistent with the previous finding showing that $6K_2$ induces replication vesicle formation in a COPII- and COPI-dependent manner (Wei and Wang 2008).

The biological importance of these $6K_2$ motifs in TuMV infection has been addressed. Mutating the N-terminal tryptophan-based ER export motif impairs virus replication, but not entirely. However, it abolishes the virus cell-to-cell movement completely. This suggests that the tryptophan-based motif is not only involved in the replication vesicle biogenesis, but is also vital for the virus movement. Mutating the TMD GXXXG Golgi exit motif also blocks $6K_2$ from reaching chloroplasts. This indicates that the $6K_2$-induced vesicles need to traverse the Golgi apparatus once it leaves the ER in order to associate with the chloroplasts. The function of this $6K_2$-chloroplast association is not known.

Using yeast two-hybrid and co-immunoprecipitation experiments, I identified several host factors that interact with the viral protein $6K_2$. One of these host factors is the COPII coatomer Sec24a. Sec24a is known as a key factor for protein ER export, and mediates the cargo protein recognition in most cases (Brandizzi and Barlowe 2013). The specificity of the $6K_2$-Sec24a interaction is supported by the following two observations: $6K_2$ interacts with Sec24a, but not with the mutant Sec24a^{R693K} that has a defective B binding site (Faso, Chen et al. 2009) and the $6K_2$ N-terminal cytoplasmic tail is enough to mediate this interaction. The other host factors that interact with the viral protein $6K_2$ are the Golgi SNARE proteins Bet11, Gos11 and Vamp714.

The role of these host factors in TuMV infection has been assessed by using knockout *Arabidopsis thaliana* plants for these proteins, and their corresponding dominant negative mutants. Using the Sec24a mutated *Arabidopsis thaliana* G92 plant, a delayed TuMV cell-to-cell and systemic movement was observed. On the contrary, an enhanced TuMV movement was found in the Golgi SNARE knockout plants, as well as when Golgi SNARE dominant negative proteins were co-expressed with TuMV. These results suggest that the host factor Sec24a is required for virus infection, while the Golgi SNAREs function as viral restriction factors.

2. Combinatorial motif for protein trafficking

In eukaryotic cells, the trafficking of many membrane-associated proteins and of soluble proteins that follow the secretory pathway to reach their proper cellular locations are directed by protein export signals (Marti, Fornaciari et al. 2010). In addition to the export signal, the length of the TMD and the tertiary structure of certain regions of the protein can also influence the protein cellular location (Watson and Pessin 2001, Ma, Taneja et al. 2011). By comparison to ER export signals, which are generally well-defined, Golgi export signals have not been extensively characterized. Those identified as ER export signals have been classified as: diacidic (DXE, EXXD), dibasic [(RK)X(RK)], dihydrophobic (LL, LXL, VV) and diaromatic (FF, YY or FY) motif (Barlowe 2003, Marti, Fornaciari et al. 2010). Golgi/TGN export identified to date include the tyrosine-based

motif YS and YXX∅ (∅ representing a bulky hydrophobic residue, and X representing any amino acid residue) and the dileucine-based motif [(D/E)XXXL(L/I)]. These Golgi export motifs have however been characterized for few proteins only (Ohno, Stewart et al. 1995, Bonifacino and Traub 2003, Dong and Wu 2006).

In the case of $6K_2$, the combinatorial motif includes the N-terminal tail tryptophan-based motif and the TMD GXXXG motif. The N-terminal tryptophan-based motif was defined as a 12-amino acid stretch (KFLKLKGKWNKT) originally (Jiang, Patarroyo et al. 2015). N-terminal deleteion mapping experiments on the $6K_2^{GV}$ mutant protein (Fig. 1) allowed this motif to be shortened to a 6-amino acid stretch (GKWNKT). To the best of my knowledge, this is the first report that a plant virus uses a combinatorial motif to follow the secretory pathway for replication vesicle biogenesis. The other viral protein that is known to use a combinatorial motif to reach its proper cellular location is the spike (S) protein of coronaviruses. A dilysine motif retains the S protein in the ER-Golgi intermediate compartment, and a tyrosine-based endocytosis signal retrieves any escaped S protein back to this location (Lontok, Corse et al. 2004).

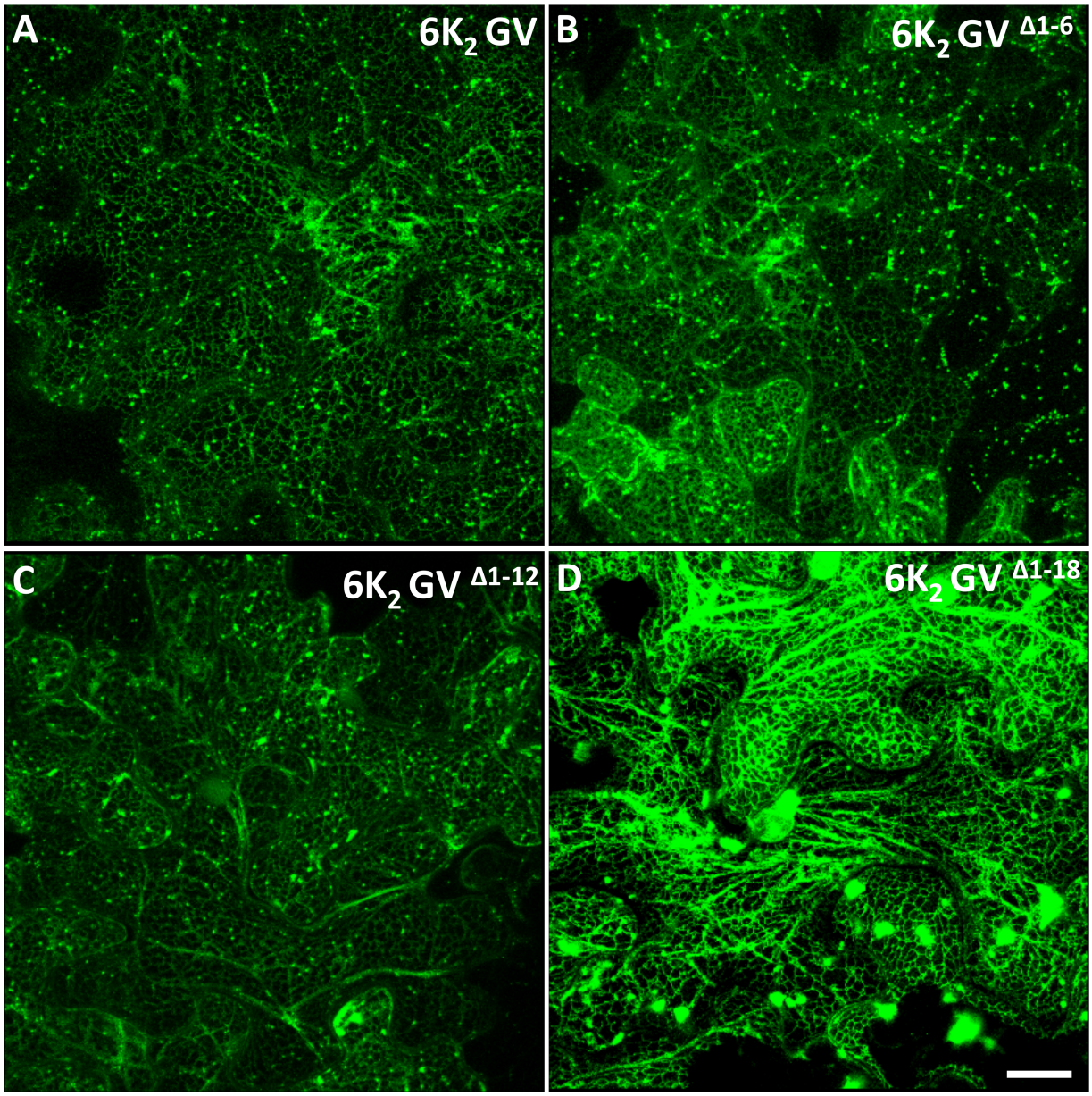

Figure 1. Confocal microscopy images of *Nicotiana benthamiana* leaf epidermal cells expressing wild type $6K_2^{GV}$:GFP and mutant derivatives.

Wild type $6K_2^{GV}$:GFP (A), the deleted $6K_2^{GV_\Delta 1\text{-}6}$:GFP (B), $6K_2^{GV_\Delta 1\text{-}12}$:GFP (C) were able to induce vesicles formation, while $6K_2^{GV_\Delta 1\text{-}18}$:GFP (D) was completely retained in the ER. Scale bar = 20 μm.

In plant cells, a similar paradigm for protein trafficking is exemplified by the protein family aquaporin. Aquaporins are a family of trans-membrane proteins that facilitates the diffusion of water and small neutral molecules across biological membranes. Topologically, the aquaporins have six TMDs and their N- and C-terminal tails are both located in the cytoplasm. In particular, research focusing on the aquaporins of the plasma membrane (PM) intrinsic protein (PIP) subfamily has revealed two distinct sorting motifs that are required to direct PIPs to the PM, one is cytosolic and the other buried in the membrane (reviewed by (Chevalier and Chaumont 2015)). For instance, the diacidic DXE motif and the TMD LXXXA motif directs PM targeting of the maize (*Zea mays*) ZmPIP2;5 protein (Zelazny, Miecielica et al. 2009, Chevalier, Bienert et al. 2014).

3. ER-Golgi-chloroplast trafficking pathway

Although many of the trafficking routes between organelles have been well-defined in plants, the existence of an ER-Golgi-chloroplast trafficking pathway is in debate. For some time, it was believed that proteins located in chloroplasts were first synthesized in the cytoplasm and subsequently targeted to these organelles via signal peptides recognized by translocons of the outer and inner envelope membrane of chloroplasts (Toc and Tic, respectively) (Soll and Schleiff 2004).

An increasing amount of data has been gathered in recent years, supporting the existence of an ER-Golgi-chloroplast trafficking pathway. Firstly, many chloroplast-located proteins lack a chloroplast targeting signal peptide, but do contain ER export signals (Kleffmann, Russenberger et al. 2004). As the import of these proteins in chloroplasts is unlikely to involve the Toc/Tic-dependent system, these observations raise the possibility that other mechanisms might be involved. Secondly, homologues of the COPII coated vesicle transporting system were found in the chloroplast proteome (Andersson and Sandelius 2004). Thirdly, there is direct evidence for an ER-Golgi-chloroplast protein transport pathway. For instance, brefeldin A (BFA) blocks the chloroplast-located protein CAH1 to reach this organelle, resulting in its ER and Golgi

retention (Villarejo, Buren et al. 2005). A similar phenomenon is observed with the rice plastidial N-glycosylated nucleotide pyrophosphatase/phosphodiesterase 1 (NPP1) (Nanjo, Oka et al. 2006). Based on these evidences, a speculative model of vesicle-mediated ER-Golgi-chloroplast protein transport has been proposed (Fig. 2) (Radhamony and Theg 2006).

The data obtained in this project supports the presence of a bona fide ER-Golgi-chloroplast protein transport pathway. Previously, it has been shown that the viral protein $6K_2$ follows the early secretory pathway and associates with chloroplast (Wei, Huang et al. 2010). However, whether $6K_2$ reaches the chloroplasts by traversing the Golgi apparatus or independent of this organelle was not known prior to this thesis. By mutating the TMD GXXXG motif, the $6K_2$ protein was prevented from reaching the chloroplasts and was arrested in the Golgi apparatus, demonstrating that the Golgi apparatus is indeed involved in $6K_2$-chloroplast association.

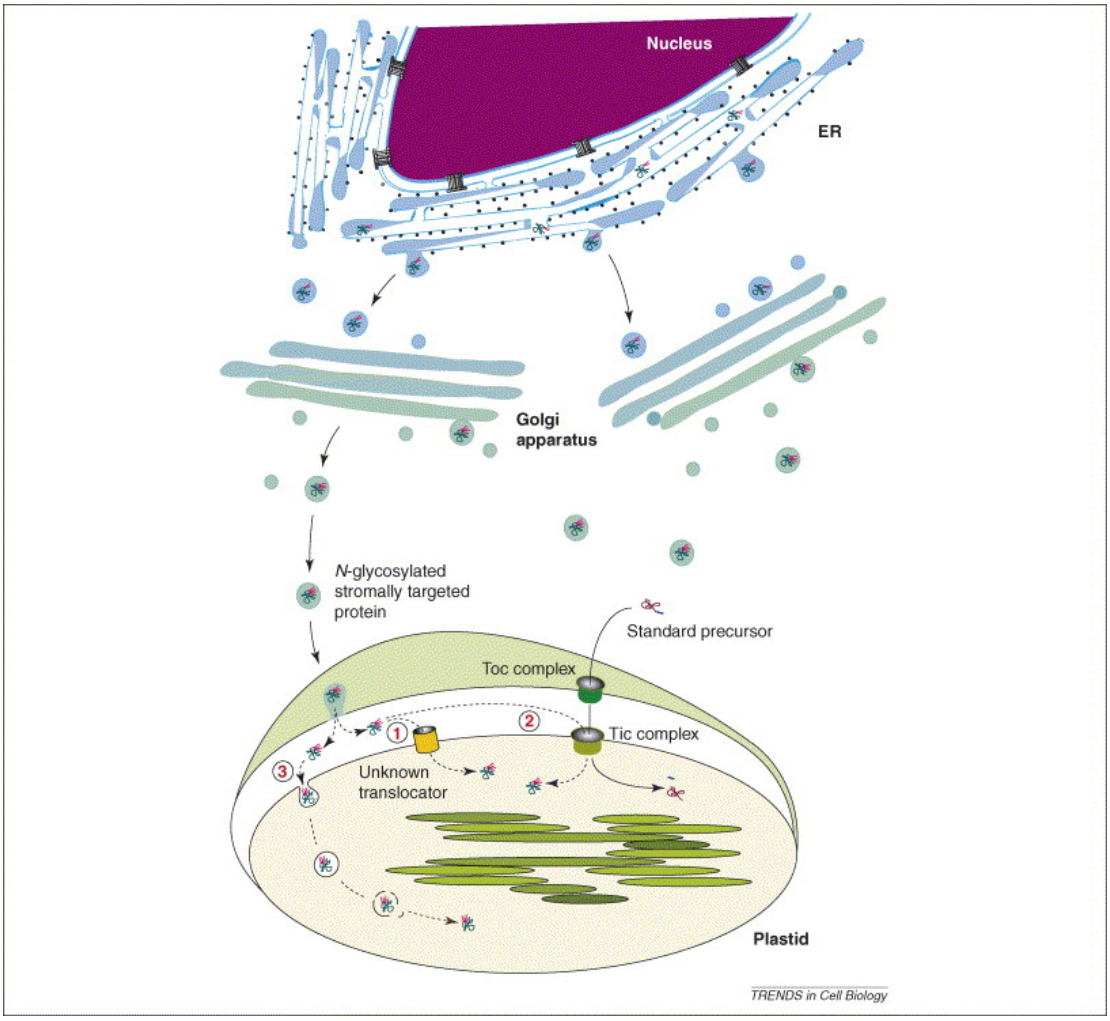

Figure 2. A speculative model of vesicle-mediated ER-Golgi-chloroplast trafficking.

The targeted protein that is synthesized by ER-associated ribosomes, passes through the Golgi on its way to the chloroplast. The protein is transported to the stromal space by (1) an as yet-unknown translocator, or by (2) the Tic complex, or through (3) the vesiculation of the chloroplast membrane. Image taken from (Radhamony and Theg 2006).

4. Factors involved in replication vesicle biogenesis

4.1 Viral factors

Plant viruses encode at least one membrane-associated viral protein to trigger host cell membrane modifications for the production of replication vesicles. These proteins assemble into higher order protein complexes through protein homo-oligomerization and hetero-oligomerization.

Homo-oligomerization has been shown to be a property of many replication vesicle inducing viral proteins, such as the viral protein 1a of *Brome mosaic virus* (BMV) and the p33 protein of *Tomato bushy stunt virus* (TBSV) (Panavas, Hawkins et al. 2005, Diaz, Gallei et al. 2012). Although it has not been investigated deeply, the data suggests that homo-oligomerization of this viral protein can cause asymmetry between the two leaflets of the membrane, thus inducing membrane curvature. In the case of BMV and TBSV, homo-oligomerization of the 1a and p33 proteins is required for efficient virus replication (Panavas, Hawkins et al. 2005, Diaz, Gallei et al. 2012). The protein homo-oligomerization may determine the cellular membranes that are going to be modified by viruses, as this process can be regulated by specific lipid or membrane (Qiu, Wang et al. 2014). In the case of the viral protein $6K_2$, its homo-oligomerization has been demonstrated by both Bi-FC and CO-IP (Fig. 3). However, the importance of this interaction still needs to be investigated.

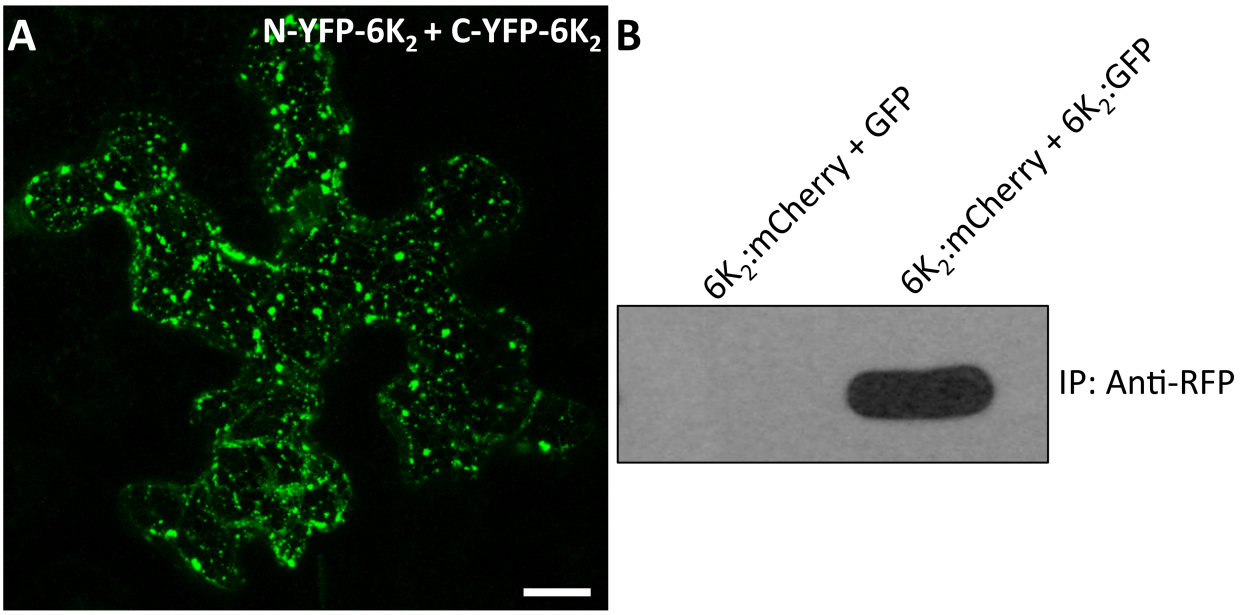

Figure 3. $6K_2$ protein self-interaction assay.

(A) Bi-FC assay of *Nicotiana benthamiana* cell co-expressing N-YFP-$6K_2$ and C-YFP-$6K_2$. Scale bar = 10 μm. (B) Co-IP assay performed with samples co-expressing $6K_2$:mCherry and GFP, or $6K_2$:mCherry and $6K_2$:GFP. Western blot was carried out with anti-RFP antibodies.

Hetero-oligomerization of the viral vesicle inducing protein with other viral proteins plays an important role in the assembly of the replication complex. Several viral proteins, including at the very least the viral RNA-dependent RNA polymerase (vRdRp) and the helicase, are recruited to the vesicle in support of vRNA synthesis. In several cases, the viral movement protein is also recruited, thus enabling the vesicle to move intracellularly and intercellularly. For TuMV, the hetero-oligomerization of $6K_2$-VPg-Pro with other viral protein has been described (see Chapter 1, Fig. 10). Through these interactions, variety of host factors are hijacked to support viral infection (see below).

4.2 Host factors

During the past two decades, more and more host factors have been demonstrated to play important roles in replication vesicle biogenesis. For example, the reticulons and the endosomal sorting complexes required for transport (ESCRT) factors regulate the formation of BMV induced ER-derived spherules (Diaz, Zhang et al. 2015). The heat shock protein 70 (HSP70) is required for the assembly of the TBSV replication complex (Pogany, Stork et al. 2008). Those identified host factors are classified as groups of membrane shaping factors, lipid metabolism factors, HSPs and so on.

Although the COPI and COPII dependent ER-Golgi vesicular transport system was shown to be important for the formation of $6K_2$-induced vesicle previously (Wei and Wang 2008), the host factors that are involved remain elusive. By yeast two-hybrid and CO-IP, my colleague and I showed that the host factor Sec24a interacts with the N-terminal tail of $6K_2$. This finding further highlights the importance of the host secretory pathway in viral replication vesicle biogenesis. Upto now, this factor has been demonstrated to be important for the formation of potyvirus-induced replication vesicles only. However, the involvement of other related factors, such as Arf1 and the COPI coatomer, still needs to be assessed. An important role in replication vesicle biogenesis has also been reported for the interaction between the p27 protein of *Red clover necrotic mosaic virus* (RCNMV) with Arf1 (Hyodo, Kaido et al. 2014).

The other host factors that we identified as interacting with the viral protein $6K_2$ are the Golgi SNARE proteins Bet11, Gos11 and Vamp714. These factors are not required for viral replication vesicle formation, but play a negative regulatory role during virus infection. Whether these factors affect the morphology or the dynamics of $6K_2$-induced vesicles still needs to be tested.

Additional host factors, besides those already identified, may also participate in TuMV replication vesicle formation, such as the autophagy related ATG proteins, the lipid biosynthesis related kinase, and the cellular organelle fusion and division factors. The

ATG proteins are particularly intriguing as they are involved in the formation of autophagosome (He and Klionsky 2009) that are morphologically similar to TuMV-induced replication vesicles. Coupled to the fact that plant viruses such as TMV are known to induce autophagy during virus replication (Li, Wang et al. 2012), these observations suggest a possible involvement of autophagy factors in the formation of TuMV replication vesicles.

5. TuMV replication site: ER versus chloroplast

Plant viruses modify various cellular membranes for their replication, such as those of ER, the chloroplasts, and the peroxisomes. Usually, the virus reorganizes only a certain type of membrane for replication. However, virus replication can switch to use other types of membrane under certain situations (Jonczyk, Pathak et al. 2007). This indicates a certain degree of flexibility in the source of membrane used for plant virus replication.

Different membranes may be targeted sequentially by viruses, thus raising the question of where is vRNA replication actually taking place? In the case of TuMV, the viral protein $6K_2$ targets the ER initially and then the chloroplasts. It is still not clear if vesicular virus replication is ER-derived or chloroplast-associated. In this project, I have shown that mutation of the $6K_2$ TMD GXXXG motif abolishes the $6K_2$-chloroplast association completely, but that it can still support a low level of virus replication. This would seem to indicate that the chloroplast is not indispensable for TuMV replication. I found that the mutant virus was still able to modify the ER membrane, although to a much lesser extent than the wt virus. This suggests that the ER is required for virus replication. Furthermore, the immunofluorescence microscopy observations showed the presence of double-stranded (dsRNA) in the ER amalgamate, but not in the chloroplasts (Wan, Basu et al. 2015). Collectively, these results prove that the ER-derived vesicle is the TuMV replication site, while the chloroplasts has likely an accessory role in vRNA replication.

6. Virus replication and movement are coupled events

For a long time, virus replication and movement were considered as separate events. However, it is becoming clear that these two processes are coupled, at least in the case of *Tobacco mosaic virus* (TMV), *Potato virus X* (PVX), and TuMV. The ability of the virus-induced replication vesicle to support both the vRNA synthesis and virus movement, allows the virus infection to be established in the entire plant rapidly.

In the case of TMV, it takes 20 h to infect the primary inoculated cell but only 4 h to infect adjacent non-infected cells (Kawakami, Watanabe et al. 2004). In the primary inoculated cell, the introduced exogenous vRNA needs to be translated into viral proteins and replicated in motile viral replication vesicles, as well as moved intracellularly and intercellularly. In contrast, the infection only needs to be amplified and be transmitted to the adjacent cell in the secondary infected cells. This suggests that the cellular movement of TMV is carried out in the form of vesicular replication complexes. In the case of PVX, the coreplicational insertion model has been proposed. The membrane-associated viral protein TGBp2 induces the formation ER-derived granules, to which TGBp3 is recruited. These granules are the site of vRNA synthesis, and either associate with the ER network or become anchored at the plasmodesmata (PD) with the assistance of the viral protein TGBp1. The PD-anchored granules develop into PD-associated caps, and remodel the ER network adjacent to the PD entrance. The newly synthesized vRNA leaves the granules and is partially encapsidated, and inserted into the modified PD for virus movement (Tilsner, Linnik et al. 2013).

In the case of TuMV, the replication vesicle follows the cellular secretory pathway and moves along the cytoskeleton microfilaments for virus movement (Cotton, Grangeon et al. 2009, Agbeci, Grangeon et al. 2013). Using a photoactivatable GFP fusion protein ($6K_2$:PAGFP), the TuMV replication vesicle was visualized to move intercellularly (Grangeon, Jiang et al. 2013). Recently, the replication vesicle has been shown to be the entity for the long distance movement of TuMV (Wan, Cabanillas et al. 2015). The results showing that the mutation $6K_2^{W15A}$ affects virus replication and abolishes virus

movement completely and that the defective version of Sec24a not only affects virus replication but also its movement (Chapter II) provide further support to the notion that virus replication and movement are intertwined.

7. Perspectives and future direction

7.1 Topological characterization of $6K_2$

The results presented in Chapter II show that $6K_2$ is tightly membrane-associated. The secondary structure prediction suggests that $6K_2$ is a trans-membrane protein with a type II topology; the N- and C-terminal tails being located in the cytoplasm and the lumen, respectively (Fig. 4). I have begun to characterize the topology of this viral protein. My preliminary result showed that the $6K_2$ N-terminal and C-terminal tail can be both located in the cytoplasm (Fig. 4). It is possible that during the biogenesis of virus replication vesicle, the topology of the $6K_2$ may convert from type II to type I (the N- and C-terminal tail being located in the lumen and the cytoplasm, respectively). This conversion may occur as a result of an altered interaction between the net positive charge of the $6K_2$ N-terminal cytoplasmic surface and the negative charge density of the membrane bilayer (Bogdanov, Xie et al. 2008). Obiviously, the topology of the $6K_2$ protein still needs further characterization. This could be done using Bi-FC by co-expressing a fragment of the yellow fluorescent protein (YFP) fused to the N- or C-terminal region of $6K_2$ and the counterpart fragment targeted to the cytoplasm or to the ER luminal space (Zamyatnin, Solovyev et al. 2006).

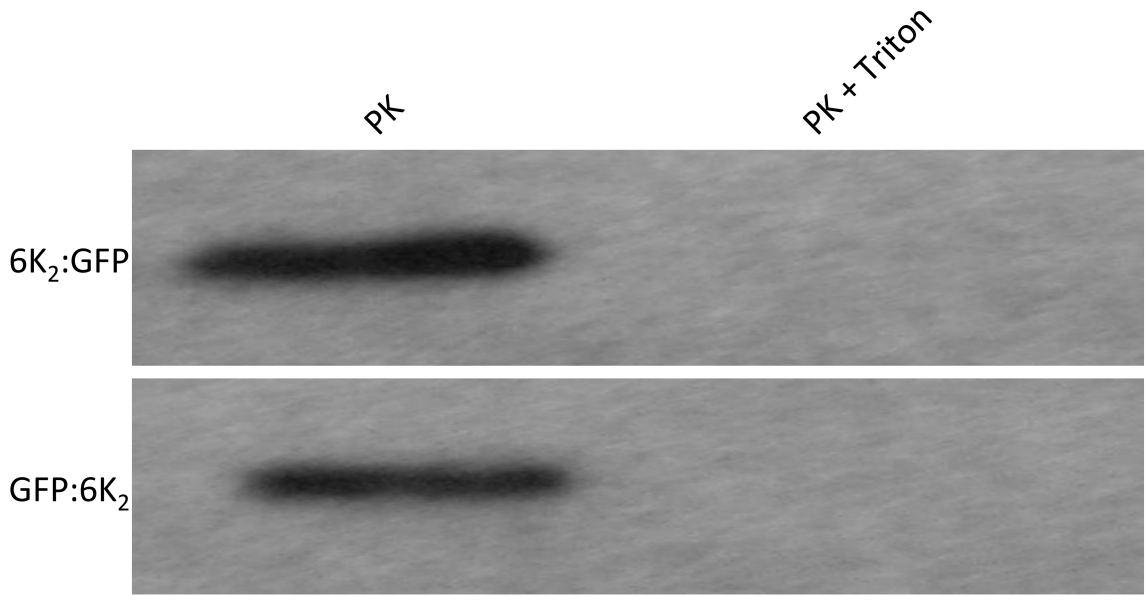

Figure 4. Topological analysis of the viral protein $6K_2$.

Protease protection assay. The membrane fraction containing $6K_2$:GFP and GFP:$6K_2$ were analyzed by immunoblotting with anti-GFP antibodies after treatment with proteinase K in the presence or absence of Triton X-100.

7.2 The TuMV replication vesicle components

Up to now, several components of the TuMV replication vesicle have been revealed. The identified viral proteins include $6K_2$, VPg-Pro, vRdRp and helicase, and the identified host proteins include PABP2, eIF(iso)4E, eEF1A, Sec24a and SNARE Vap27, Bet11, Gos11 and Vamp714. Additional components could be obtained by purification of replication vesicles through a combination of ultracentrifugation and immunopurification, followed by the identification of the purified protein complexes by mass spectrometry. The presence of these novel components in the replication vesicle would need to be validated by co-localization experiments in live cells or by immunofluorescence experiments in fixed leaf tissues. The biological importance of these components could then be tested using various knockout plants, dominant negative proteins or virus-induced gene silencing.

7.3 The protein interactor(s) of the $6K_2$ GXXXG motif

Although the importance of the $6K_2$ GXXXG motif for TuMV infection has been demonstrated in this project, the protein target of this motif remains to be identified. The GXXXG motif is widely distributed in host protein TMDs, and known to mediate protein-protein interactions. The protein target of this motif could be sought using the following approaches. One approach would involve comparing the protein content of purified replication vesicles induced by wt $6K_2$ and $6K_2^{GV}$ using the same method described above. Proteins present in wt 6K2 replication vesicles but absent in 6K2GV-containing vesicle preparations would be prime GXXXG motif-interacting canadidates. The second approach would involve yeast two-hybrid screening of an *Arabidopsis thaliana* cDNA library using wt $6K_2$ as the bait and testing of the potential interactions for those that are affected by the $6K_2^{GV}$ mutation. These candidates can be further screened in plants by CO-IP or Bi-FC experiments, It is anticipated that the identified host protein interactor should also possess the characteristic GXXXG motif. By mutating this GXXXG motif, the role of the identified protein interactor in TuMV infection could be validated.

7.4 The mechanism by which Golgi SNARE proteins act as restriction factors

Golgi SNARE proteins were found to function as TuMV restriction factors (Chapter IV), but the underlying mechanism is not known. Two possibilities would be tested in the following project. One possibility is related to the dynamics of the replication vesicle. This could be tested in the Golgi SNARE knockout plants or by co-expressing the virus with Golgi SNARE dominant negative proteins. The dynamics of the replication vesicle could be evaluated by live cell imaging. The dynamics include the fusion of the replication vesicle (reflected by the size of the vesicle), its speed during intracellular trafficking and its ability to target PD (assayed by co-expression with PD markers). The other possibility is related to the plant anti-viral response. This could be verified by measuring the transcriptional induction of anti-viral response genes, such as WRKY, APETALA2/ethylene responsive factor (AP2/ERF), basic-domain leucine-zipper (bZIP), basic helix-loop-helix (bHLH) and NAM/ATAF/CUC (NAC) in Golgi SNARE knockout plants in the presence of TuMV infection (Seo, Choi et al. 2015).

7.5 Other cellular pathways for TuMV replication vesicle biogenesis

7.5.1 The lipid biosynthetic pathway

It is known that a large amount of lipids is required during TuMV infection (Wan, Cabanillas et al. 2015). However, a deeper characterization is needed for better understanding of the importance of lipids in TuMV infection. The virus replication level could be compared by treating TuMV transfected protoplasts with or without cerulenin, which is an antifungal antibiotic that inhibits fatty acid and steroid biosynthesis. The affinity of $6K_2$ protein for lipids can be assayed by using membrane lipid strips. The lipid composition of the $6K_2$-induced replication vesicle could be analyzed by thin layer chromatography. The key enzymes that are involved in the biosynthesis of lipids and which show a high affinity for $6K_2$ could then be knockdown, and the resulting impact on the morphology of the replication vesicle and the virus infection can be investigated.

7.5.2 The ER stress and autophagy pathway

As mentioned above, the contribution of the autophagy pathway in viral replication vesicle formation needs to be further explored. The key factor ATG8 that is required for autophagosome formation could be co-expressed with TuMV, and its co-localization and interaction with $6K_2$ can be analyzed. In parallel, the fluorescent dye monodansylcadaverine that is used to monitor autophagy can be used to stain TuMV replication vesicles. Using VIGS, the importance of these factors in TuMV infection could be tested.

On the other hand, the $6K_2$ protein is known to induce significant ER stress by activating the unfolded protein response (UPR) branch IRE1-bZIP60 (Zhang, Chen et al. 2015). The IRE1 factor links the ER UPR and the autophagy pathway (Pu and Bassham 2013). Consequently, the role of ER stress in TuMV viral factories biogenesis should be addressed accordingly.

8. Conclusion

In this project, I characterized the molecular determinants of the $6K_2$ protein needed for the replication vesicle biogenesis. The identified motifs include a 6-amino acid stretch in the N-terminal tail that is required for vesicle formation and exit from the ER, and the TMD GXXXG motif for Golgi exit of the replication vesicle. Ultimately, the secretory pathway component COPII coatomer Sec24a was shown to interact with the $6K_2$ N-terminal tail. The $6K_2$-Sec24a interaction is not only required for efficient virus replication, but also essential for the virus movement. The Golgi SNARE proteins Bet11, Gos11 and Vamp714 were shown to interact with $6K_2$. Interestingly, they function as TuMV restriction factor.

These results uncover the mechanism underlying the cellular biogenesis of TuMV replication vesicles (Fig. 5). They also highlight how a viral protein can actively take advantage of the host cell secretory pathway for its infection.

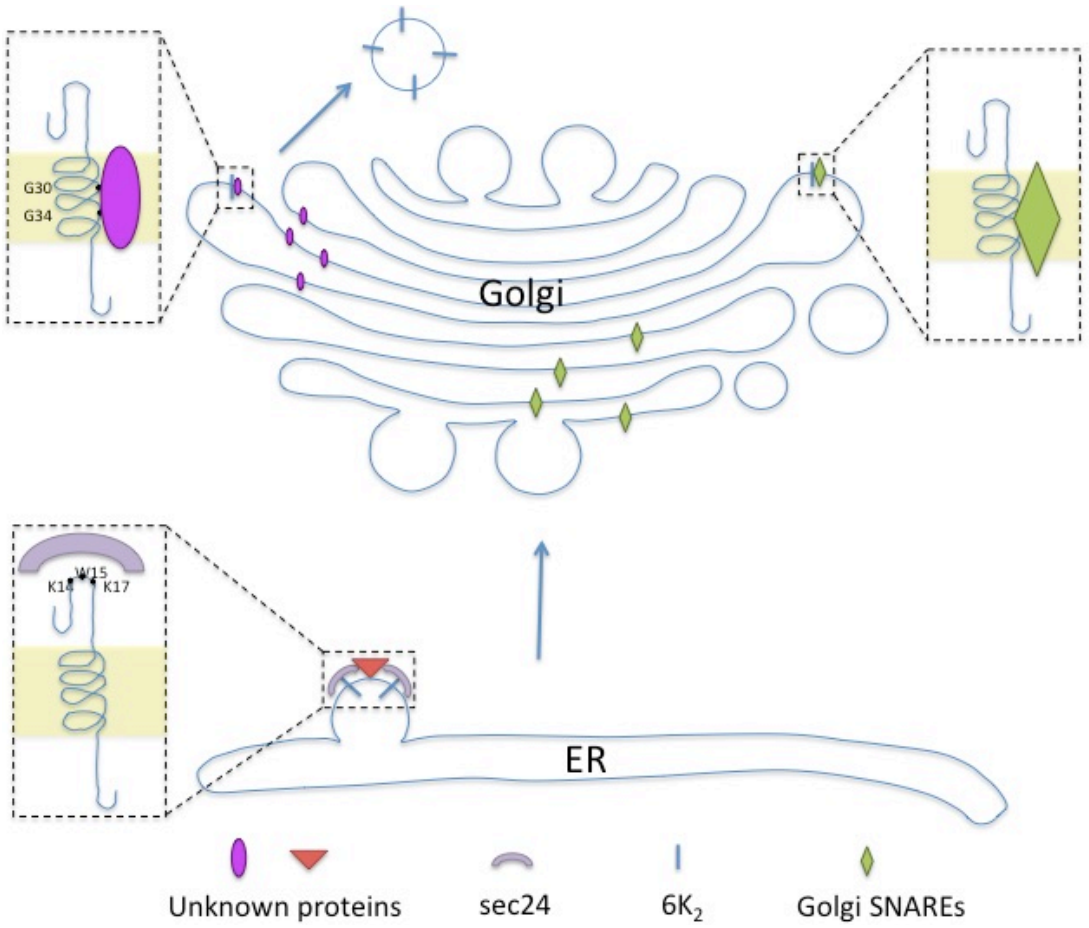

Figure 5. Model of TuMV $6K_2$ protein ER and Golgi sequential exit for the production of virus replication vesicle.

The $6K_2$ N-terminal tail, in particular, the K14, W15 and K17, mediates the $6K_2$-Sec24a interaction for its ER export, as well as the TMD GXXXG motif interacts with unknown protein factors for its Golgi exit. The $6K_2$ protein also interacts with certain Golgi SNAREs and plays a role in virus infection.

REFERENCES

Agbeci, M., R. Grangeon, R. S. Nelson, H. Zheng and J.-F. Laliberté (2013). "Contribution of Host Intracellular Transport Machineries to Intercellular Movement of Turnip Mosaic Virus." PLoS Pathog **9**(10): e1003683.

Agbeci, M., R. Grangeon, R. S. Nelson, H. Zheng and J. F. Laliberte (2013). "Contribution of host intracellular transport machineries to intercellular movement of turnip mosaic virus." PLoS Pathog **9**(10): e1003683.

Amari, K., M. Di Donato, V. V. Dolja and M. Heinlein (2014). "Myosins VIII and XI Play Distinct Roles in Reproduction and Transport of <italic>Tobacco Mosaic Virus</italic>." PLoS Pathog **10**(10): e1004448.

Amari, K., A. Lerich, C. Schmitt-Keichinger, V. V. Dolja and C. Ritzenthaler (2011). "Tubule-guided cell-to-cell movement of a plant virus requires class XI myosin motors." PLoS Pathog **7**(10): e1002327.

Andersson, M. and A. Sandelius (2004). "A chloroplast-localized vesicular transport system: a bio-informatics approach." BMC Genomics **5**(1): 40.

Anindya, R. and H. S. Savithri (2003). "Surface-exposed amino- and carboxy-terminal residues are crucial for the initiation of assembly in Pepper vein banding virus: a flexuous rod-shaped virus." Virology **316**(2): 325-336.

Arbatova, J., K. Lehto, E. Pehu and T. Pehu (1998). "Localization of the P1 protein of potato Y potyvirus in association with cytoplasmic inclusion bodies and in the cytoplasm of infected cells." J Gen Virol **79 (Pt 10)**: 2319-2323.

Banfield, D. K. (2011). "Mechanisms of protein retention in the Golgi." Cold Spring Harb Perspect Biol **3**(8): a005264.

Barajas, D., Y. Jiang and P. D. Nagy (2009). "A unique role for the host ESCRT proteins in replication of Tomato bushy stunt virus." PLoS Pathog **5**(12): e1000705.

Barajas, D., I. F. Martin, J. Pogany, C. Risco and P. D. Nagy (2014). "Noncanonical role for the host Vps4 AAA+ ATPase ESCRT protein in the formation of Tomato bushy stunt virus replicase." PLoS Pathog **10**(4): e1004087.

Barajas, D. and P. D. Nagy (2010). "Ubiquitination of tombusvirus p33 replication protein plays a role in virus replication and binding to the host Vps23p ESCRT protein." Virology **397**(2): 358-368.

Barajas, D. and P. D. Nagy (2010). "Ubiquitination of tombusvirus p33 replication protein plays a role in virus replication and binding to the host Vps23p ESCRT protein." Virology **397**(2): 358-368.

Barajas, D., K. Xu, I. F. de Castro Martín, Z. Sasvari, F. Brandizzi, C. Risco and P. D. Nagy (2014). "Co-opted Oxysterol-Binding ORP and VAP Proteins Channel Sterols to RNA Virus Replication Sites via Membrane Contact Sites." PLoS Pathog **10**(10): e1004388.

Barajas, D., K. Xu, M. Sharma, C. Y. Wu and P. D. Nagy (2014). "Tombusviruses upregulate phospholipid biosynthesis via interaction between p33 replication protein and yeast lipid sensor proteins during virus replication in yeast." Virology **471-473**: 72-80.

Barlowe, C. (2003). "Signals for COPII-dependent export from the ER: what's the ticket out?" Trends in Cell Biology **13**(6): 295-300.

Bassham, D. C., F. Brandizzi, M. S. Otegui and A. A. Sanderfoot (2008). "The secretory system of Arabidopsis." Arabidopsis Book **6**: e0116.

Bassham, D. C., F. Brandizzi, M. S. Otegui and A. A. Sanderfoot (2008). "The Secretory System of Arabidopsis." The Arabidopsis Book: e0116.
Beauchemin, C., V. Bougie and J.-F. Laliberté (2005). "Simultaneous production of two foreign proteins from a potyvirus-based vector." Virus Research **112**(1–2): 1-8.
Beauchemin, C., N. Boutet and J.-F. Laliberté (2007). "Visualization of the Interaction between the Precursors of VPg, the Viral Protein Linked to the Genome of Turnip Mosaic Virus, and the Translation Eukaryotic Initiation Factor iso 4E In Planta." Journal of Virology **81**(2): 775-782.
Beauchemin, C. and J.-F. Laliberté (2007). "The Poly(A) Binding Protein Is Internalized in Virus-Induced Vesicles or Redistributed to the Nucleolus during Turnip Mosaic Virus Infection." Journal of Virology **81**(20): 10905-10913.
Beck, R., M. Ravet, F. T. Wieland and D. Cassel (2009). "The COPI system: Molecular mechanisms and function." FEBS Letters **583**(17): 2701-2709.
Belov, G. A., V. Nair, B. T. Hansen, F. H. Hoyt, E. R. Fischer and E. Ehrenfeld (2012). "Complex Dynamic Development of Poliovirus Membranous Replication Complexes." Journal of Virology **86**(1): 302-312.
Besserer, A., E. Burnotte, G. P. Bienert, A. S. Chevalier, A. Errachid, C. Grefen, M. R. Blatt and F. Chaumont (2012). "Selective regulation of maize plasma membrane aquaporin trafficking and activity by the SNARE SYP121." Plant Cell **24**(8): 3463-3481.
Bhat, S., S. Y. Folimonova, A. B. Cole, K. D. Ballard, Z. Lei, B. S. Watson, L. W. Sumner and R. S. Nelson (2013). "Influence of Host Chloroplast Proteins on Tobacco mosaic virus Accumulation and Intercellular Movement." Plant Physiology **161**(1): 134-147.
Block, M. A. and J. Jouhet (2015). "Lipid trafficking at endoplasmic reticulum–chloroplast membrane contact sites." Current Opinion in Cell Biology **35**(0): 21-29.
Bogdanov, M., J. Xie, P. Heacock and W. Dowhan (2008). "To flip or not to flip: lipid-protein charge interactions are a determinant of final membrane protein topology." J Cell Biol **182**(5): 925-935.
Bonifacino, J. S. and B. S. Glick (2004). "The mechanisms of vesicle budding and fusion." Cell **116**(2): 153-166.
Bonifacino, J. S. and L. M. Traub (2003). "Signals for sorting of transmembrane proteins to endosomes and lysosomes." Annu Rev Biochem **72**: 395-447.
Brandizzi, F. and C. Barlowe (2013). "Organization of the ER-Golgi interface for membrane traffic control." Nat Rev Mol Cell Biol **14**(6): 382-392.
Brandizzi, F. and C. Barlowe (2013). "Organization of the ER-Golgi interface for membrane traffic control." Nat Rev Mol Cell Biol **14**(6): 382-392.
Brandizzi, F., E. L. Snapp, A. G. Roberts, J. Lippincott-Schwartz and C. Hawes (2002). "Membrane protein transport between the endoplasmic reticulum and the golgi in tobacco leaves is energy dependent but cytoskeleton independent: Evidence from selective photobleaching." Plant Cell **14**(6): 1293-1309.
Bronnimann, M. P., J. A. Chapman, C. K. Park and S. K. Campos (2013). "A Transmembrane Domain and GxxxG Motifs within L2 Are Essential for Papillomavirus Infection." Journal of Virology **87**(1): 464-473.
Bruce Alberts, A. J., Julian Lewis, Martin Raff, Keith Roberts, Peter Walter (2007). Molecular Biology of the Cell.
Cai, Y., T. Jia, S. K. Lam, Y. Ding, C. Gao, M. W. Y. San, P. Pimpl and L. Jiang (2011). "Multiple cytosolic and transmembrane determinants are required for the trafficking of SCAMP1 via an ER–Golgi–TGN–PM pathway." The Plant Journal **65**(6): 882-896.

Cao, X., X. Jin, X. Zhang, Y. Li, C. Wang, X. Wang, J. Hong, X. Wang, D. Li and Y. Zhang (2015). "Morphogenesis of Endoplasmic Reticulum Membrane-Invaginated Vesicles during Beet Black Scorch Virus Infection: Role of Auxiliary Replication Protein and New Implications of Three-Dimensional Architecture." Journal of Virology **89**(12): 6184-6195.
Carette, J. E., M. Stuiver, J. Van Lent, J. Wellink and A. Van Kammen (2000). "Cowpea Mosaic Virus Infection Induces a Massive Proliferation of Endoplasmic Reticulum but Not Golgi Membranes and Is Dependent on De Novo Membrane Synthesis." Journal of Virology **74**(14): 6556-6563.
Carette, J. E., J. Verver, J. Martens, T. van Kampen, J. Wellink and A. van Kammen (2002). "Characterization of plant proteins that interact with cowpea mosaic virus '60K' protein in the yeast two-hybrid system." Journal of General Virology **83**(4): 885-893.
Chatre, L., F. Brandizzi, A. Hocquellet, C. Hawes and P. Moreau (2005). "Sec22 and Memb11 Are v-SNAREs of the Anterograde Endoplasmic Reticulum-Golgi Pathway in Tobacco Leaf Epidermal Cells." Plant Physiology **139**(3): 1244-1254.
Chaturvedi, S. and A. L. Rao (2014). "Live cell imaging of interactions between replicase and capsid protein of Brome mosaic virus using Bimolecular Fluorescence Complementation: implications for replication and genome packaging." Virology **464-465**: 67-75.
Chen, J., C. Doyle, X. Qi and H. Zheng (2012). "The Endoplasmic Reticulum: A Social Network in Plant CellsF." Journal of Integrative Plant Biology **54**(11): 840-850.
Chen, J., G. Stefano, F. Brandizzi and H. Zheng (2011). "Arabidopsis RHD3 mediates the generation of the tubular ER network and is required for Golgi distribution and motility in plant cells." Journal of Cell Science **124**(13): 2241-2252.
Cheng, Y. Q., Z. M. Liu, J. Xu, T. Zhou, M. Wang, Y. T. Chen, H. F. Li and Z. F. Fan (2008). "HC-Pro protein of sugar cane mosaic virus interacts specifically with maize ferredoxin-5 in vitro and in planta." J Gen Virol **89**(Pt 8): 2046-2054.
Chevalier, A. S., G. P. Bienert and F. Chaumont (2014). "A new LxxxA motif in the transmembrane Helix3 of maize aquaporins belonging to the plasma membrane intrinsic protein PIP2 group is required for their trafficking to the plasma membrane." Plant Physiol **166**(1): 125-138.
Chevalier, A. S. and F. Chaumont (2015). "Trafficking of Plant Plasma Membrane Aquaporins: Multiple Regulation Levels and Complex Sorting Signals." Plant and Cell Physiology **56**(5): 819-829.
Choi, S. H., Y. Hagiwara-Komoda, K. S. Nakahara, G. Atsumi, R. Shimada, Y. Hisa, S. Naito and I. Uyeda (2013). "Quantitative and qualitative involvement of P3N-PIPO in overcoming recessive resistance against Clover yellow vein virus in pea carrying the cyv1 gene." J Virol **87**(13): 7326-7337.
Chou, Y. L., Y. J. Hung, Y. H. Tseng, H. T. Hsu, J. Y. Yang, C. H. Wung, N. S. Lin, M. Meng, Y. H. Hsu and B. Y. Chang (2013). "The stable association of virion with the triple-gene-block protein 3-based complex of Bamboo mosaic virus." PLoS Pathog **9**(6): e1003405.
Chung, B. Y.-W., W. A. Miller, J. F. Atkins and A. E. Firth (2008). "An overlapping essential gene in the Potyviridae." Proceedings of the National Academy of Sciences **105**(15): 5897-5902.
Claros, M. G. and G. von Heijne (1994). "TopPred II: an improved software for membrane protein structure predictions." Comput Appl Biosci **10**(6): 685-686.
Cotton, S., R. Grangeon, K. Thivierge, I. Mathieu, C. Ide, T. Wei, A. Wang and J.-F. Laliberté (2009). "Turnip Mosaic Virus RNA Replication Complex Vesicles Are Mobile, Align with

Microfilaments, and Are Each Derived from a Single Viral Genome." Journal of Virology **83**(20): 10460-10471.
Cowan, G. H., A. G. Roberts, S. N. Chapman, A. Ziegler, E. I. Savenkov and L. Torrance (2012). "The potato mop-top virus TGB2 protein and viral RNA associate with chloroplasts and viral infection induces inclusions in the plastids." Frontiers in Plant Science **3**.
Cruz, S. S., A. G. Roberts, D. A. M. Prior, S. Chapman and K. J. Oparka (1998). "Cell-to-Cell and Phloem-Mediated Transport of Potato Virus X: The Role of Virions." The Plant Cell **10**(4): 495-510.
Cserzo, M., E. Wallin, I. Simon, G. von Heijne and A. Elofsson (1997). "Prediction of transmembrane alpha-helices in prokaryotic membrane proteins: the dense alignment surface method." Protein Eng **10**(6): 673-676.
Cui, X., T. Wei, R. V. Chowda-Reddy, G. Sun and A. Wang (2010). "The Tobacco etch virus P3 protein forms mobile inclusions via the early secretory pathway and traffics along actin microfilaments." Virology **397**(1): 56-63.
Cureton, D. K., R. Burdeinick-Kerr and S. P. J. Whelan (2012). "Genetic Inactivation of COPI Coatomer Separately Inhibits Vesicular Stomatitis Virus Entry and Gene Expression." Journal of Virology **86**(2): 655-666.
Cymer, F., A. Veerappan and D. Schneider (2012). "Transmembrane helix–helix interactions are modulated by the sequence context and by lipid bilayer properties." Biochimica et Biophysica Acta (BBA) - Biomembranes **1818**(4): 963-973.
del Toro, F., F. T. Fernandez, J. Tilsner, K. M. Wright, F. Tenllado, B. N. Chung, S. Praveen and T. Canto (2014). "Potato virus Y HCPro localization at distinct, dynamically related and environment-influenced structures in the cell cytoplasm." Mol Plant Microbe Interact **27**(12): 1331-1343.
Delevoye, C., M. Nilges, P. Dehoux, F. Paumet, S. Perrinet, A. Dautry-Varsat and A. Subtil (2008). "SNARE protein mimicry by an intracellular bacterium." PLoS Pathog **4**(3): e1000022.
den Boon, J. A. and P. Ahlquist (2010). "Organelle-Like Membrane Compartmentalization of Positive-Strand RNA Virus Replication Factories." Annual Review of Microbiology **64**(1): 241-256.
Diaz, A. and P. Ahlquist (2012). "Role of host reticulon proteins in rearranging membranes for positive-strand RNA virus replication." Current Opinion in Microbiology **15**(4): 519-524.
Diaz, A., A. Gallei and P. Ahlquist (2012). "Bromovirus RNA replication compartment formation requires concerted action of 1a's self-interacting RNA capping and helicase domains." J Virol **86**(2): 821-834.
Diaz, A., X. Wang and P. Ahlquist (2010). "Membrane-shaping host reticulon proteins play crucial roles in viral RNA replication compartment formation and function." Proc Natl Acad Sci U S A **107**(37): 16291-16296.
Diaz, A., X. Wang and P. Ahlquist (2010). "Membrane-shaping host reticulon proteins play crucial roles in viral RNA replication compartment formation and function." Proceedings of the National Academy of Sciences **107**(37): 16291-16296.
Diaz, A., J. Zhang, A. Ollwerther, X. Wang and P. Ahlquist (2015). "Host ESCRT Proteins Are Required for Bromovirus RNA Replication Compartment Assembly and Function." PLoS Pathog **11**(3): e1004742.
Dohner, K. and B. Sodeik (2005). "The role of the cytoskeleton during viral infection." Curr Top Microbiol Immunol **285**: 67-108.

Dong, C. and G. Wu (2006). "Regulation of anterograde transport of alpha2-adrenergic receptors by the N termini at multiple intracellular compartments." J Biol Chem **281**(50): 38543-38554.
Dunn, K. W., M. M. Kamocka and J. H. McDonald (2011). "A practical guide to evaluating colocalization in biological microscopy." Am J Physiol Cell Physiol **300**(4): C723-742.
Eiamtanasate, S., M. Juricek and Y.-K. Yap (2007). "C-terminal hydrophobic region leads PRSV P3 protein to endoplasmic reticulum." Virus Genes **35**(3): 611-617.
Faingold, O., T. Cohen and Y. Shai (2012). "A GxxxG-like Motif within HIV-1 Fusion Peptide Is Critical to Its Immunosuppressant Activity, Structure, and Interaction with the Transmembrane Domain of the T-cell Receptor." Journal of Biological Chemistry **287**(40): 33503-33511.
Faso, C., Y.-N. Chen, K. Tamura, M. Held, S. Zemelis, L. Marti, R. Saravanan, E. Hummel, L. Kung, E. Miller, C. Hawes and F. Brandizzi (2009). "A Missense Mutation in the Arabidopsis COPII Coat Protein Sec24A Induces the Formation of Clusters of the Endoplasmic Reticulum and Golgi Apparatus." The Plant Cell **21**(11): 3655-3671.
Faso, C., Y. N. Chen, K. Tamura, M. Held, S. Zemelis, L. Marti, R. Saravanan, E. Hummel, L. Kung, E. Miller, C. Hawes and F. Brandizzi (2009). "A missense mutation in the Arabidopsis COPII coat protein Sec24A induces the formation of clusters of the endoplasmic reticulum and Golgi apparatus." Plant Cell **21**(11): 3655-3671.
Fellers, J., J. Wan, Y. Hong, G. B. Collins and A. G. Hunt (1998). "In vitro interactions between a potyvirus-encoded, genome-linked protein and RNA-dependent RNA polymerase." J Gen Virol **79 (Pt 8)**: 2043-2049.
Fernandez, A. and J. A. Garcia (1996). "The RNA helicase CI from plum pox potyvirus has two regions involved in binding to RNA." FEBS Lett **388**(2-3): 206-210.
Fernández-Calvino, L., S. Osorio, M. L. Hernández, I. B. Hamada, F. J. del Toro, L. Donaire, A. Yu, R. Bustos, A. R. Fernie, J. M. Martínez-Rivas and C. Llave (2014). "Virus-Induced Alterations in Primary Metabolism Modulate Susceptibility to Tobacco rattle virus in Arabidopsis." Plant Physiology **166**(4): 1821-1838.
Fink, A., N. Sal-Man, D. Gerber and Y. Shai (2012). "Transmembrane domains interactions within the membrane milieu: Principles, advances and challenges." Biochimica et Biophysica Acta (BBA) - Biomembranes **1818**(4): 974-983.
Franke, M., T. Braulke and S. Storch (2013). "Transport of the GlcNAc-1-phosphotransferase α/β-Subunit Precursor Protein to the Golgi Apparatus Requires a Combinatorial Sorting Motif." Journal of Biological Chemistry **288**(2): 1238-1249.
Gariano, G. R., V. Dell'Oste, M. Bronzini, D. Gatti, A. Luganini, M. De Andrea, G. Gribaudo, M. Gariglio and S. Landolfo (2012). "The intracellular DNA sensor IFI16 gene acts as restriction factor for human cytomegalovirus replication." PLoS Pathog **8**(1): e1002498.
Genoves, A., J. A. Navarro and V. Pallas (2009). "A self-interacting carmovirus movement protein plays a role in binding of viral RNA during the cell-to-cell movement and shows an actin cytoskeleton dependent location in cell periphery." Virology **395**(1): 133-142.
Genovés, A., V. Pallás and J. A. Navarro (2011). "Contribution of Topology Determinants of a Viral Movement Protein to Its Membrane Association, Intracellular Traffic, and Viral Cell-to-Cell Movement." Journal of Virology **85**(15): 7797-7809.
Giraudo, C. G. and H. J. F. Maccioni (2003). "Endoplasmic Reticulum Export of Glycosyltransferases Depends on Interaction of a Cytoplasmic Dibasic Motif with Sar1." Molecular Biology of the Cell **14**(9): 3753-3766.

Gomez-Aix, C., M. Garcia-Garcia, M. A. Aranda and M. A. Sanchez-Pina (2015). "Melon necrotic spot virus Replication Occurs in Association with Altered Mitochondria." Mol Plant Microbe Interact **28**(4): 387-397.
Gorovits, R., A. Moshe, M. Ghanim and H. Czosnek (2013). "Recruitment of the host plant heat shock protein 70 by Tomato yellow leaf curl virus coat protein is required for virus infection." PLoS One **8**(7): e70280.
Grangeon, R., M. Agbeci, J. Chen, G. Grondin, H. Zheng and J.-F. Laliberté (2012). "Impact on the Endoplasmic Reticulum and Golgi Apparatus of Turnip Mosaic Virus Infection." Journal of Virology **86**(17): 9255-9265.
Grangeon, R., M. Agbeci, J. Chen, G. Grondin, H. Zheng and J. F. Laliberte (2012). "Impact on the endoplasmic reticulum and Golgi apparatus of turnip mosaic virus infection." J Virol **86**(17): 9255-9265.
Grangeon, R., J. Jiang, J. Wan, M. Agbeci, H. Zheng and J.-F. Laliberté (2013). "6K2-induced vesicles can move cell to cell during turnip mosaic virus infection." Frontiers in Microbiology **4**.
Grangeon, R., J. Jiang, J. Wan, M. Agbeci, H. Zheng and J. F. Laliberte (2013). "6K2-induced vesicles can move cell to cell during turnip mosaic virus infection." Front Microbiol **4**: 351.
Grefen, C., S. Lalonde and P. Obrdlik (2001). Split-Ubiquitin System for Identifying Protein-Protein Interactions in Membrane and Full-Length Proteins. Current Protocols in Neuroscience, John Wiley & Sons, Inc.
Gupton, S. L., D. A. Collings and N. S. Allen (2006). "Endoplasmic reticulum targeted GFP reveals ER organization in tobacco NT-1 cells during cell division." Plant Physiology and Biochemistry **44**(2–3): 95-105.
Gutiérrez, S., Y. Michalakis and S. Blanc (2012). "Virus population bottlenecks during within-host progression and host-to-host transmission." Current Opinion in Virology **2**(5): 546-555.
Hachez, C., A. Besserer, A. S. Chevalier and F. Chaumont (2013). "Insights into plant plasma membrane aquaporin trafficking." Trends Plant Sci **18**(6): 344-352.
Hachez, C., T. Laloux, H. Reinhardt, D. Cavez, H. Degand, C. Grefen, R. De Rycke, D. Inze, M. R. Blatt, E. Russinova and F. Chaumont (2014). "Arabidopsis SNAREs SYP61 and SYP121 coordinate the trafficking of plasma membrane aquaporin PIP2;7 to modulate the cell membrane water permeability." Plant Cell **26**(7): 3132-3147.
Haikonen, T., M. L. Rajamaki and J. P. Valkonen (2013). "Interaction of the microtubule-associated host protein HIP2 with viral helper component proteinase is important in infection with potato virus A." Mol Plant Microbe Interact **26**(7): 734-744.
Halk, E. and J. McGuire (1973). "Translocation of tobacco ringspot virus in soybean." Phytopathology **63**: 10.
Han, Q., J. Aligo, D. Manna, K. Belton, S. V. Chintapalli, Y. Hong, R. L. Patterson, D. B. van Rossum and K. V. Konan (2011). "Conserved GXXXG- and S/T-Like Motifs in the Transmembrane Domains of NS4B Protein Are Required for Hepatitis C Virus Replication." Journal of Virology **85**(13): 6464-6479.
Hanton, S. L., L. A. Matheson, L. Chatre and F. Brandizzi (2009). "Dynamic organization of COPII coat proteins at endoplasmic reticulum export sites in plant cells." Plant J **57**(6): 963-974.
He, C. and D. J. Klionsky (2009). "Regulation mechanisms and signaling pathways of autophagy." Annu Rev Genet **43**: 67-93.
Heinlein, M., H. S. Padgett, J. S. Gens, B. G. Pickard, S. J. Casper, B. L. Epel and R. N. Beachy (1998). "Changing patterns of localization of the tobacco mosaic virus movement protein and

replicase to the endoplasmic reticulum and microtubules during infection." The Plant Cell **10**(7): 1107-1120.
Hessa, T., H. Kim, K. Bihlmaier, C. Lundin, J. Boekel, H. Andersson, I. Nilsson, S. H. White and G. von Heijne (2005). "Recognition of transmembrane helices by the endoplasmic reticulum translocon." Nature **433**(7024): 377-381.
Hirokawa, T., S. Boon-Chieng and S. Mitaku (1998). "SOSUI: classification and secondary structure prediction system for membrane proteins." Bioinformatics **14**(4): 378-379.
Howard, A. R., M. L. Heppler, H. J. Ju, K. Krishnamurthy, M. E. Payton and J. Verchot-Lubicz (2004). "Potato virus X TGBp1 induces plasmodesmata gating and moves between cells in several host species whereas CP moves only in N. benthamiana leaves." Virology **328**(2): 185-197.
Hsu, N. Y., O. Ilnytska, G. Belov, M. Santiana, Y. H. Chen, P. M. Takvorian, C. Pau, H. van der Schaar, N. Kaushik-Basu, T. Balla, C. E. Cameron, E. Ehrenfeld, F. J. van Kuppeveld and N. Altan-Bonnet (2010). "Viral reorganization of the secretory pathway generates distinct organelles for RNA replication." Cell **141**(5): 799-811.
Huang, T. S. and P. D. Nagy (2011). "Direct inhibition of tombusvirus plus-strand RNA synthesis by a dominant negative mutant of a host metabolic enzyme, glyceraldehyde-3-phosphate dehydrogenase, in yeast and plants." J Virol **85**(17): 9090-9102.
Hwang, I. and D. G. Robinson (2009). "Transport vesicle formation in plant cells." Current Opinion in Plant Biology **12**(6): 660-669.
Hwang, J., S. Lee, J. H. Lee, W. H. Kang, J. H. Kang, M. Y. Kang, C. S. Oh and B. C. Kang (2015). "Plant Translation Elongation Factor 1Bbeta Facilitates Potato Virus X (PVX) Infection and Interacts with PVX Triple Gene Block Protein 1." PLoS One **10**(5): e0128014.
Hwang, J., C. S. Oh and B. C. Kang (2013). "Translation elongation factor 1B (eEF1B) is an essential host factor for Tobacco mosaic virus infection in plants." Virology **439**(2): 105-114.
Hwang, Y., A. McCartney, S. Gidda and R. Mullen (2008). "Localization of the Carnation Italian ringspot virus replication protein p36 to the mitochondrial outer membrane is mediated by an internal targeting signal and the TOM complex." BMC Cell Biology **9**(1): 54.
Hyodo, K., M. Kaido and T. Okuno (2014). "Traffic jam on the cellular secretory pathway generated by a replication protein from a plant RNA virus." Plant Signal Behav **9**(3): e28644.
Hyodo, K., A. Mine, T. Taniguchi, M. Kaido, K. Mise, H. Taniguchi and T. Okuno (2013). "ADP ribosylation factor 1 plays an essential role in the replication of a plant RNA virus." J Virol **87**(1): 163-176.
Ishibashi, K. and M. Ishikawa (2013). "The resistance protein Tm-1 inhibits formation of a Tomato mosaic virus replication protein-host membrane protein complex." J Virol **87**(14): 7933-7939.
Ivanov, K. I., P. Puustinen, R. Gabrenaite, H. Vihinen, L. Ronnstrand, L. Valmu, N. Kalkkinen and K. Makinen (2003). "Phosphorylation of the potyvirus capsid protein by protein kinase CK2 and its relevance for virus infection." Plant Cell **15**(9): 2124-2139.
Jayasinghe, S., K. Hristova and S. H. White (2001). "MPtopo: A database of membrane protein topology." Protein Science **10**(2): 455-458.
Jenner, C. E., F. Sanchez, S. B. Nettleship, G. D. Foster, F. Ponz and J. A. Walsh (2000). "The cylindrical inclusion gene of Turnip mosaic virus encodes a pathogenic determinant to the Brassica resistance gene TuRB01." Mol Plant Microbe Interact **13**(10): 1102-1108.

Jenner, C. E., X. Wang, K. Tomimura, K. Ohshima, F. Ponz and J. A. Walsh (2003). "The dual role of the potyvirus P3 protein of Turnip mosaic virus as a symptom and avirulence determinant in brassicas." Mol Plant Microbe Interact **16**(9): 777-784.
Jenner, C. E., X. Wang, K. Tomimura, K. Ohshima, F. Ponz and J. A. Walsh (2003). "The Dual Role of the Potyvirus P3 Protein of Turnip mosaic virus as a Symptom and Avirulence Determinant in Brassicas." Molecular Plant-Microbe Interactions **16**(9): 777-784.
Jiang, J. and J. F. Laliberte (2011). "The genome-linked protein VPg of plant viruses-a protein with many partners." Curr Opin Virol **1**(5): 347-354.
Jiang, J., C. Patarroyo, D. Garcia Cabanillas, H. Zheng and J. F. Laliberte (2015). "The Vesicle-Forming 6K2 Protein of Turnip Mosaic Virus Interacts with the COPII Coatomer Sec24a for Viral Systemic Infection." J Virol **89**(13): 6695-6710.
Jiang, S., Y. Lu, K. Li, L. Lin, H. Zheng, F. Yan and J. Chen (2014). "Heat shock protein 70 is necessary for Rice stripe virus infection in plants." Mol Plant Pathol **15**(9): 907-917.
Jiménez, I., L. López, J. M. Alamillo, A. Valli and J. A. García (2006). "Identification of a Plum pox virus CI-Interacting Protein from Chloroplast That Has a Negative Effect in Virus Infection." Molecular Plant-Microbe Interactions **19**(3): 350-358.
Jonczyk, M., K. B. Pathak, M. Sharma and P. D. Nagy (2007). "Exploiting alternative subcellular location for replication: Tombusvirus replication switches to the endoplasmic reticulum in the absence of peroxisomes." Virology **362**(2): 320-330.
Jones, D. T., W. R. Taylor and J. M. Thornton (1994). "A model recognition approach to the prediction of all-helical membrane protein structure and topology." Biochemistry **33**(10): 3038-3049.
Ju, H.-J., J. E. Brown, C.-M. Ye and J. Verchot-Lubicz (2007). "Mutations in the Central Domain of Potato Virus X TGBp2 Eliminate Granular Vesicles and Virus Cell-to-Cell Trafficking." Journal of Virology **81**(4): 1899-1911.
Ju, H. J., T. D. Samuels, Y. S. Wang, E. Blancaflor, M. Payton, R. Mitra, K. Krishnamurthy, R. S. Nelson and J. Verchot-Lubicz (2005). "The potato virus X TGBp2 movement protein associates with endoplasmic reticulum-derived vesicles during virus infection." Plant Physiol **138**(4): 1877-1895.
Juretic, D., L. Zoranic and D. Zucic (2002). "Basic charge clusters and predictions of membrane protein topology." J Chem Inf Comput Sci **42**(3): 620-632.
Kawakami, S., Y. Watanabe and R. N. Beachy (2004). "Tobacco mosaic virus infection spreads cell to cell as intact replication complexes." Proc Natl Acad Sci U S A **101**(16): 6291-6296.
Kawakami, S., Y. Watanabe and R. N. Beachy (2004). "Tobacco mosaic virus infection spreads cell to cell as intact replication complexes." Proceedings of the National Academy of Sciences of the United States of America **101**(16): 6291-6296.
Kim, S.-J. and F. Brandizzi (2012). "News and Views into the SNARE Complexity in Arabidopsis." Frontiers in Plant Science **3**.
Kleffmann, T., D. Russenberger, A. von Zychlinski, W. Christopher, K. Sjölander, W. Gruissem and S. Baginsky (2004). "The Arabidopsis thaliana Chloroplast Proteome Reveals Pathway Abundance and Novel Protein Functions." Current Biology **14**(5): 354-362.
Kleiger, G., R. Grothe, P. Mallick and D. Eisenberg (2002). "GXXXG and AXXXA: common alpha-helical interaction motifs in proteins, particularly in extremophiles." Biochemistry **41**(19): 5990-5997.
Kneller, E. L., A. M. Rakotondrafara and W. A. Miller (2006). "Cap-independent translation of plant viral RNAs." Virus Res **119**(1): 63-75.

Knoops, K., M. Bárcena, R. W. A. L. Limpens, A. J. Koster, A. M. Mommaas and E. J. Snijder (2012). "Ultrastructural Characterization of Arterivirus Replication Structures: Reshaping the Endoplasmic Reticulum To Accommodate Viral RNA Synthesis." Journal of Virology **86**(5): 2474-2487.
Knoops, K., M. Kikkert, S. H. E. v. d. Worm, J. C. Zevenhoven-Dobbe, Y. van der Meer, A. J. Koster, A. M. Mommaas and E. J. Snijder (2008). "SARS-Coronavirus Replication Is Supported by a Reticulovesicular Network of Modified Endoplasmic Reticulum." PLoS Biol **6**(9): e226.
Krogh, A., B. Larsson, G. von Heijne and E. L. Sonnhammer (2001). "Predicting transmembrane protein topology with a hidden Markov model: application to complete genomes." J Mol Biol **305**(3): 567-580.
Krogh, A., B. Larsson, G. von Heijne and E. L. L. Sonnhammer (2001). "Predicting transmembrane protein topology with a hidden markov model: application to complete genomes." Journal of Molecular Biology **305**(3): 567-580.
Kusumanegara, K., A. Mine, K. Hyodo, M. Kaido, K. Mise and T. Okuno (2012). "Identification of domains in p27 auxiliary replicase protein essential for its association with the endoplasmic reticulum membranes in Red clover necrotic mosaic virus." Virology **433**(1): 131-141.
Laliberté, J.-F. and H. Sanfaçon (2010). "Cellular Remodeling During Plant Virus Infection." Annual Review of Phytopathology **48**(1): 69-91.
Laliberté, J.-F. and H. Zheng (2014). "Viral Manipulation of Plant Host Membranes." Annual Review of Virology **1**(1): 237-259.
Laliberte, J. F. and H. Sanfacon (2010). "Cellular remodeling during plant virus infection." Annu Rev Phytopathol **48**: 69-91.
Larkin, M. A., G. Blackshields, N. P. Brown, R. Chenna, P. A. McGettigan, H. McWilliam, F. Valentin, I. M. Wallace, A. Wilm, R. Lopez, J. D. Thompson, T. J. Gibson and D. G. Higgins (2007). "Clustal W and Clustal X version 2.0." Bioinformatics (Oxford, England) **23**(21): 2947-2948.
Larson, E. R., D. S. Domozych and M. L. Tierney (2014). "SNARE VTI13 plays a unique role in endosomal trafficking pathways associated with the vacuole and is essential for cell wall organization and root hair growth in arabidopsis." Ann Bot **114**(6): 1147-1159.
Lee, M. C. S. and E. A. Miller (2007). "Molecular mechanisms of COPII vesicle formation." Seminars in Cell & Developmental Biology **18**(4): 424-434.
Lee, W. M. and P. Ahlquist (2003). "Membrane synthesis, specific lipid requirements, and localized lipid composition changes associated with a positive-strand RNA virus RNA replication protein." J Virol **77**(23): 12819-12828.
Lee, W. M., M. Ishikawa and P. Ahlquist (2001). "Mutation of host delta9 fatty acid desaturase inhibits brome mosaic virus RNA replication between template recognition and RNA synthesis." J Virol **75**(5): 2097-2106.
Leonard, S., D. Plante, S. Wittmann, N. Daigneault, M. G. Fortin and J. F. Laliberte (2000). "Complex formation between potyvirus VPg and translation eukaryotic initiation factor 4E correlates with virus infectivity." J Virol **74**(17): 7730-7737.
Lerich, A., M. Langhans, S. Sturm and D. G. Robinson (2011). "Is the 6 kDa tobacco etch viral protein a bona fide ERES marker?" Journal of Experimental Botany **62**(14): 5013-5023.
Li, L., L. Wang, R. Xiao, G. Zhu, Y. Li, C. Liu, R. Yang, Z. Tang, J. Li, W. Huang, L. Chen, X. Zheng, Y. He and J. Tan (2012). "The invasion of tobacco mosaic virus RNA induces endoplasmic reticulum stress-related autophagy in HeLa cells." Biosci Rep **32**(2): 171-186.

Li, X. H. and J. C. Carrington (1995). "Complementation of tobacco etch potyvirus mutants by active RNA polymerase expressed in transgenic cells." Proc Natl Acad Sci U S A **92**(2): 457-461.
Li, X. H. and J. C. Carrington (1995). "Complementation of tobacco etch potyvirus mutants by active RNA polymerase expressed in transgenic cells." Proceedings of the National Academy of Sciences **92**(2): 457-461.
Li, X. H., P. Valdez, R. E. Olvera and J. C. Carrington (1997). "Functions of the tobacco etch virus RNA polymerase (NIb): subcellular transport and protein-protein interaction with VPg/proteinase (NIa)." J Virol **71**(2): 1598-1607.
Li, Y., C. Zhang, X. Song, S. Lv and X. Hou (2014). "Using an Arabidopsis oligonucleotide microarray to analyze the secretory pathway genes' Response to TuMV infection in Brassica rapa." Physiological and Molecular Plant Pathology **88**(0): 85-93.
Li, Z., J. Pogany, T. Panavas, K. Xu, A. M. Esposito, T. G. Kinzy and P. D. Nagy (2009). "Translation elongation factor 1A is a component of the tombusvirus replicase complex and affects the stability of the p33 replication co-factor." Virology **385**(1): 245-260.
Lin, L., Z. Luo, F. Yan, Y. Lu, H. Zheng and J. Chen (2011). "Interaction between potyvirus P3 and ribulose-1,5-bisphosphate carboxylase/oxygenase (RubisCO) of host plants." Virus Genes **43**(1): 90-92.
Lipka, V., C. Kwon and R. Panstruga (2007). "SNARE-ware: the role of SNARE-domain proteins in plant biology." Annu Rev Cell Dev Biol **23**: 147-174.
Liu, L., W. M. Westler, J. A. den Boon, X. Wang, A. Diaz, H. A. Steinberg and P. Ahlquist (2009). "An amphipathic alpha-helix controls multiple roles of brome mosaic virus protein 1a in RNA replication complex assembly and function." PLoS Pathog **5**(3): e1000351.
Lontok, E., E. Corse and C. E. Machamer (2004). "Intracellular Targeting Signals Contribute to Localization of Coronavirus Spike Proteins near the Virus Assembly Site." Journal of Virology **78**(11): 5913-5922.
Lu, L., G. Wu, X. Xu, H. Luan, H. Zhi, J. Cui, X. Cui and X. Chen (2015). "Soybean actin-depolymerizing factor 2 interacts with Soybean mosaic virus-encoded P3 protein." Virus Genes **50**(2): 333-339.
Ma, D., Tarvinder K. Taneja, Brian M. Hagen, B.-Y. Kim, B. Ortega, W. J. Lederer and Paul A. Welling (2011). "Golgi Export of the Kir2.1 Channel Is Driven by a Trafficking Signal Located within Its Tertiary Structure." Cell **145**(7): 1102-1115.
Marti, L., S. Fornaciari, L. Renna, G. Stefano and F. Brandizzi (2010). "COPII-mediated traffic in plants." Trends in Plant Science **15**(9): 522-528.
Martinez, F. and J. A. Daros (2014). "Tobacco etch virus protein P1 traffics to the nucleolus and associates with the host 60S ribosomal subunits during infection." J Virol **88**(18): 10725-10737.
Mayo, M. A. (1995). "The Potyviridae. By D. D. SHUKLA, C. W. WARD and A. A. BRUNT. 25 × 17 cm. Pp. 516 with 110 text-figures and 30 tables, Wallingford: CAB International, 1994. Price: £60.00." New Phytologist **131**(2): 289-290.
McBride, C. E., J. Li and C. E. Machamer (2007). "The Cytoplasmic Tail of the Severe Acute Respiratory Syndrome Coronavirus Spike Protein Contains a Novel Endoplasmic Reticulum Retrieval Signal That Binds COPI and Promotes Interaction with Membrane Protein." Journal of Virology **81**(5): 2418-2428.
McCartney, A. W., J. S. Greenwood, M. R. Fabian, K. A. White and R. T. Mullen (2005). "Localization of the Tomato Bushy Stunt Virus Replication Protein p33 Reveals a Peroxisome-to-Endoplasmic Reticulum Sorting Pathway." The Plant Cell Online **17**(12): 3513-3531.

McCartney, A. W., J. S. Greenwood, M. R. Fabian, K. A. White and R. T. Mullen (2005). "Localization of the tomato bushy stunt virus replication protein p33 reveals a peroxisome-to-endoplasmic reticulum sorting pathway." Plant Cell **17**(12): 3513-3531.
McMahon, H. T. and J. L. Gallop (2005). "Membrane curvature and mechanisms of dynamic cell membrane remodelling." Nature **438**(7068): 590-596.
Merindol, N. and L. Berthoux (2015). "Restriction Factors in HIV-1 Disease Progression." Curr HIV Res.
Miller, E., B. Antonny, S. Hamamoto and R. Schekman (2002). "Cargo selection into COPII vesicles is driven by the Sec24p subunit." EMBO J **21**(22): 6105-6113.
Miller, E. A., T. H. Beilharz, P. N. Malkus, M. C. S. Lee, S. Hamamoto, L. Orci and R. Schekman (2003). "Multiple Cargo Binding Sites on the COPII Subunit Sec24p Ensure Capture of Diverse Membrane Proteins into Transport Vesicles." Cell **114**(4): 497-509.
Miller, S. and J. Krijnse-Locker (2008). "Modification of intracellular membrane structures for virus replication." Nat Rev Microbiol **6**(5): 363-374.
Mine, A., K. Hyodo, Y. Tajima, K. Kusumanegara, T. Taniguchi, M. Kaido, K. Mise, H. Taniguchi and T. Okuno (2012). "Differential roles of Hsp70 and Hsp90 in the assembly of the replicase complex of a positive-strand RNA plant virus." J Virol **86**(22): 12091-12104.
Mitra, R., K. Krishnamurthy, E. Blancaflor, M. Payton, R. S. Nelson and J. Verchot-Lubicz (2003). "The potato virus x TGBp2 protein association with the endoplasmic reticulum plays a role in but is not sufficient for viral cell-to-cell movement." Virology **312**(1): 35-48.
Moreno, I. M., J. R. Thompson and F. García-Arenal (2004). "Analysis of the systemic colonization of cucumber plants by Cucumber green mottle mosaic virus." Journal of General Virology **85**(3): 749-759.
Mossessova, E., L. C. Bickford and J. Goldberg (2003). "SNARE selectivity of the COPII coat." Cell **114**(4): 483-495.
Nagy, P. D. and J. Pogany (2012). "The dependence of viral RNA replication on co-opted host factors." Nat Rev Micro **10**(2): 137-149.
Nakano, R. T., R. Matsushima, H. Ueda, K. Tamura, T. Shimada, L. Li, Y. Hayashi, M. Kondo, M. Nishimura and I. Hara-Nishimura (2009). "GNOM-LIKE1/ERMO1 and SEC24a/ERMO2 Are Required for Maintenance of Endoplasmic Reticulum Morphology in Arabidopsis thaliana." The Plant Cell Online **21**(11): 3672-3685.
Nanjo, Y., H. Oka, N. Ikarashi, K. Kaneko, A. Kitajima, T. Mitsui, F. J. Muñoz, M. Rodríguez-López, E. Baroja-Fernández and J. Pozueta-Romero (2006). "Rice Plastidial N-Glycosylated Nucleotide Pyrophosphatase/Phosphodiesterase Is Transported from the ER-Golgi to the Chloroplast through the Secretory Pathway." The Plant Cell **18**(10): 2582-2592.
Nebenfuhr, A., C. Ritzenthaler and D. G. Robinson (2002). "Brefeldin A: Deciphering an enigmatic inhibitor of secretion." Plant Physiology **130**(3): 1102-1108.
Neil, S. J., T. Zang and P. D. Bieniasz (2008). "Tetherin inhibits retrovirus release and is antagonized by HIV-1 Vpu." Nature **451**(7177): 425-430.
Nishikiori, M., K. Dohi, M. Mori, T. Meshi, S. Naito and M. Ishikawa (2006). "Membrane-bound tomato mosaic virus replication proteins participate in RNA synthesis and are associated with host proteins in a pattern distinct from those that are not membrane bound." J Virol **80**(17): 8459-8468.
Nishikiori, M., M. Mori, K. Dohi, H. Okamura, E. Katoh, S. Naito, T. Meshi and M. Ishikawa (2011). "A Host Small GTP-binding Protein ARL8 Plays Crucial Roles in Tobamovirus RNA Replication." PLoS Pathog **7**(12): e1002409.

Ohno, H., J. Stewart, M. C. Fournier, H. Bosshart, I. Rhee, S. Miyatake, T. Saito, A. Gallusser, T. Kirchhausen and J. S. Bonifacino (1995). "Interaction of tyrosine-based sorting signals with clathrin-associated proteins." Science **269**(5232): 1872-1875.
Olspert, A., B. Y. W. Chung, J. F. Atkins, J. P. Carr and A. E. Firth (2015). Transcriptional slippage in the positive-sense RNA virus family Potyviridae.
Opalka, N., C. Brugidou, C. Bonneau, M. Nicole, R. N. Beachy, M. Yeager and C. Fauquet (1998). "Movement of rice yellow mottle virus between xylem cells through pit membranes." Proc Natl Acad Sci U S A **95**(6): 3323-3328.
Panavas, T., C. M. Hawkins, Z. Panaviene and P. D. Nagy (2005). "The role of the p33:p33/p92 interaction domain in RNA replication and intracellular localization of p33 and p92 proteins of Cucumber necrosis tombusvirus." Virology **338**(1): 81-95.
Patarroyo, C., J. F. Laliberte and H. Zheng (2012). "Hijack it, change it: how do plant viruses utilize the host secretory pathway for efficient viral replication and spread?" Front Plant Sci **3**: 308.
Paumet, F., J. Wesolowski, A. Garcia-Diaz, C. Delevoye, N. Aulner, H. A. Shuman, A. Subtil and J. E. Rothman (2009). "Intracellular Bacteria Encode Inhibitory SNARE-Like Proteins." PLoS ONE **4**(10): e7375.
Peiró, A., L. Martínez-Gil, S. Tamborero, V. Pallás, J. A. Sánchez-Navarro and I. Mingarro (2014). "The Tobacco mosaic virus Movement Protein Associates with but Does Not Integrate into Biological Membranes." Journal of Virology **88**(5): 3016-3026.
Peremyslov, V. V., A. L. Klocko, J. E. Fowler and V. V. Dolja (2012). "Arabidopsis Myosin XI-K Localizes to the Motile Endomembrane Vesicles Associated with F-actin." Front Plant Sci **3**: 184.
Pérez, J. d. J., N. D. Udeshi, J. Shabanowitz, S. Ciordia, S. Juárez, C. L. Scott, N. E. Olszewski, D. F. Hunt and J. A. García (2013). "O-GlcNAc modification of the coat protein of the potyvirus Plum pox virus enhances viral infection." Virology **442**(2): 122-131.
Plisson, C., M. Drucker, S. Blanc, S. German-Retana, O. Le Gall, D. Thomas and P. Bron (2003). "Structural Characterization of HC-Pro, a Plant Virus Multifunctional Protein." Journal of Biological Chemistry **278**(26): 23753-23761.
Pogany, J. and P. D. Nagy (2015). "Activation of Tomato bushy stunt virus RdRp by cellular Hsp70 is enhanced by phospholipids in vitro." J Virol.
Pogany, J., J. Stork, Z. Li and P. D. Nagy (2008). "In vitro assembly of the Tomato bushy stunt virus replicase requires the host Heat shock protein 70." Proceedings of the National Academy of Sciences **105**(50): 19956-19961.
Pogany, J., K. A. White and P. D. Nagy (2005). "Specific binding of tombusvirus replication protein p33 to an internal replication element in the viral RNA is essential for replication." J Virol **79**(8): 4859-4869.
Prod'homme, D., A. Jakubiec, V. Tournier, G. Drugeon and I. Jupin (2003). "Targeting of the Turnip Yellow Mosaic Virus 66K Replication Protein to the Chloroplast Envelope Is Mediated by the 140K Protein." Journal of Virology **77**(17): 9124-9135.
Pu, Y. and D. C. Bassham (2013). "Links between ER stress and autophagy in plants." Plant Signaling & Behavior **8**(6): e24297.
Qiu, Y., Z. Wang, Y. Liu, Y. Han, M. Miao, N. Qi, J. Yang, H. Xia, X. Li, C.-F. Qin, Y. Hu and X. Zhou (2014). "The Self-Interaction of a Nodavirus Replicase Is Enhanced by Mitochondrial Membrane Lipids." PLoS ONE **9**(2): e89628.

Radhamony, R. N. and S. M. Theg (2006). "Evidence for an ER to Golgi to chloroplast protein transport pathway." Trends in Cell Biology **16**(8): 385-387.
Rajendran, K. S. and P. D. Nagy (2004). "Interaction between the replicase proteins of Tomato Bushy Stunt virus in vitro and in vivo." Virology **326**(2): 250-261.
Rajendran, K. S. and P. D. Nagy (2004). "Interaction between the replicase proteins of Tomato bushy stunt virus in vitro and in vivo." Virology **326**(2): 250-261.
Restrepo-Hartwig, M. A. and J. C. Carrington (1994). "The tobacco etch potyvirus 6-kilodalton protein is membrane associated and involved in viral replication." Journal of Virology **68**(4): 2388-2397.
Ribeiro, D., O. Foresti, J. Denecke, J. Wellink, R. Goldbach and R. J. M. Kormelink (2008). "Tomato spotted wilt virus glycoproteins induce the formation of endoplasmic reticulum- and Golgi-derived pleomorphic membrane structures in plant cells." Journal of General Virology **89**(8): 1811-1818.
Richardson, L. G., E. A. Clendening, H. Sheen, S. K. Gidda, K. A. White and R. T. Mullen (2014). "A unique N-terminal sequence in the Carnation Italian ringspot virus p36 replicase-associated protein interacts with the host cell ESCRT-I component Vps23." J Virol **88**(11): 6329-6344.
Riechmann, J. L., M. T. Cervera and J. A. Garcia (1995). "Processing of the plum pox virus polyprotein at the P3-6K1 junction is not required for virus viability." J Gen Virol **76 (Pt 4)**: 951-956.
Ritzenthaler, C., C. Laporte, F. Gaire, P. Dunoyer, C. Schmitt, S. Duval, A. Piéquet, A. M. Loudes, O. Rohfritsch, C. Stussi-Garaud and P. Pfeiffer (2002). "Grapevine Fanleaf Virus Replication Occurs on Endoplasmic Reticulum-Derived Membranes." Journal of Virology **76**(17): 8808-8819.
Ritzenthaler, C., A.-C. Schmit, P. Michler, C. Stussi-Garaud and L. Pinck (1995). "Grapevine Fanleaf Nepovirus P38 Putative Movement Protein Is Located on Tubules In Vivo." MPMI **8**(3): 9.
Rochon, D. A., B. Singh, R. Reade, J. Theilmann, K. Ghoshal, S. B. Alam and A. Maghodia (2014). "The p33 auxiliary replicase protein of Cucumber necrosis virus targets peroxisomes and infection induces de novo peroxisome formation from the endoplasmic reticulum." Virology **452–453**(0): 133-142.
Rodriguez-Cerezo, E., E. D. Ammar, T. P. Pirone and J. G. Shaw (1993). "Association of the non-structural P3 viral protein with cylindrical inclusions in potyvirus-infected cells." J Gen Virol **74 (Pt 9)**: 1945-1949.
Rodriguez-Cerezo, E., K. Findlay, J. G. Shaw, G. P. Lomonossoff, S. G. Qiu, P. Linstead, M. Shanks and C. Risco (1997). "The coat and cylindrical inclusion proteins of a potyvirus are associated with connections between plant cells." Virology **236**(2): 296-306.
Rojas, M. R., F. M. Zerbini, R. F. Allison, R. L. Gilbertson and W. J. Lucas (1997). "Capsid Protein and Helper Component-Proteinase Function as Potyvirus Cell-to-Cell Movement Proteins." Virology **237**(2): 283-295.
Rollason, R., K. Dunstan, P. G. Billcliff, P. Bishop, P. Gleeson, H. Wise, P. Digard and G. Banting (2013). "Expression of HIV-1 Vpu leads to loss of the viral restriction factor CD317/Tetherin from lipid rafts and its enhanced lysosomal degradation." PLoS One **8**(9): e75680.
Rost, B., G. Yachdav and J. Liu (2004). "The PredictProtein server." Nucleic Acids Res **32**(Web Server issue): W321-326.

Russo, M., A. Di Franco and G. P. Martelli (1983). "The fine structure of Cymbidium ringspot virus infections in host tissues. III. Role of peroxisomes in the genesis of multivesicular bodies." J Ultrastruct Res **82**(1): 52-63.
Russo, M. and G. P. Martelli (1972). "Ultrastructural observations on tomato bushy stunt virus in plant cells." Virology **49**(1): 122-129.
Saint-Jore, C. M., J. Evins, H. Batoko, F. Brandizzi, I. Moore and C. Hawes (2002). "Redistribution of membrane proteins between the Golgi apparatus and endoplasmic reticulum in plants is reversible and not dependent on cytoskeletal networks." The Plant Journal **29**(5): 661-678.
Samuels, T. D., H. J. Ju, C. M. Ye, C. M. Motes, E. B. Blancaflor and J. Verchot-Lubicz (2007). "Subcellular targeting and interactions among the Potato virus X TGB proteins." Virology **367**(2): 375-389.
Sánchez, F., D. Martínez-Herrera, I. Aguilar and F. Ponz (1998). "Infectivity of turnip mosaic potyvirus cDNA clones and transcripts on the systemic host Arabidopsis thaliana and local lesion hosts." Virus Research **55**(2): 207-219.
Sasvari, Z., P. Alatriste Gonzalez and P. Nagy (2014). "Tombusvirus-yeast interactions identify conserved cell-intrinsic viral restriction factors." Frontiers in Plant Science **5**.
Schaad, M. C., P. E. Jensen and J. C. Carrington (1997). Formation of plant RNA virus replication complexes on membranes: role of an endoplasmic reticulum-targeted viral protein.
Schepetilnikov, M. V., U. Manske, A. G. Solovyev, A. A. Zamyatnin, Jr., J. Schiemann and S. Y. Morozov (2005). "The hydrophobic segment of Potato virus X TGBp3 is a major determinant of the protein intracellular trafficking." J Gen Virol **86**(Pt 8): 2379-2391.
Schmidt, O. and D. Teis (2012). "The ESCRT machinery." Current Biology **22**(4): R116-R120.
Schneider, D. and D. M. Engelman (2004). "Motifs of two small residues can assist but are not sufficient to mediate transmembrane helix interactions." J Mol Biol **343**(4): 799-804.
Schoberer, J., U. Vavra, J. Stadlmann, C. Hawes, L. Mach, H. Steinkellner and R. Strasser (2009). "Arginine/Lysine Residues in the Cytoplasmic Tail Promote ER Export of Plant Glycosylation Enzymes." Traffic **10**(1): 101-115.
Schwartz, M., J. Chen, M. Janda, M. Sullivan, J. den Boon and P. Ahlquist "A Positive-Strand RNA Virus Replication Complex Parallels Form and Function of Retrovirus Capsids." Molecular Cell **9**(3): 505-514.
Schwartz, M., J. Chen, M. Janda, M. Sullivan, J. den Boon and P. Ahlquist (2002). "A Positive-Strand RNA Virus Replication Complex Parallels Form and Function of Retrovirus Capsids." Molecular Cell **9**(3): 505-514.
Schwartz, M., J. Chen, M. Janda, M. Sullivan, J. den Boon and P. Ahlquist (2002). "A positive-strand RNA virus replication complex parallels form and function of retrovirus capsids." Mol Cell **9**(3): 505-514.
Schwartz, M., J. Chen, W.-M. Lee, M. Janda and P. Ahlquist (2004). "Alternate, virus-induced membrane rearrangements support positive-strand RNA virus genome replication." Proceedings of the National Academy of Sciences of the United States of America **101**(31): 11263-11268.
Seo, E., D. Choi and Choi (2015). "Functional studies of transcription factors involved in plant defenses in the genomics era." Briefings in Functional Genomics.
Serra-Soriano, M., V. Pallás and J. A. Navarro (2014). "A model for transport of a viral membrane protein through the early secretory pathway: minimal sequence and endoplasmic reticulum lateral mobility requirements." The Plant Journal **77**(6): 863-879.

Sharma, M., Z. Sasvari and P. D. Nagy (2011). "Inhibition of phospholipid biosynthesis decreases the activity of the tombusvirus replicase and alters the subcellular localization of replication proteins." Virology **415**(2): 141-152.
Sharp, T. M., S. Guix, K. Katayama, S. E. Crawford and M. K. Estes (2010). "Inhibition of cellular protein secretion by Norwalk virus nonstructural protein p22 requires a mimic of an endoplasmic reticulum export signal." PLoS One **5**(10): e13130.
Silva, M. S., J. Wellink, R. W. Goldbach and J. W. M. van Lent (2002). "Phloem loading and unloading of Cowpea mosaic virus in Vigna unguiculata." Journal of General Virology **83**(6): 1493-1504.
Soll, J. and E. Schleiff (2004). "Protein import into chloroplasts." Nat Rev Mol Cell Biol **5**(3): 198-208.
Soumounou, Y. and J. F. Laliberte (1994). "Nucleic acid-binding properties of the P1 protein of turnip mosaic potyvirus produced in Escherichia coli." J Gen Virol **75 (Pt 10)**: 2567-2573.
Sparkes, I. A., J. Runions, A. Kearns and C. Hawes (2006). "Rapid, transient expression of fluorescent fusion proteins in tobacco plants and generation of stably transformed plants." Nat. Protocols **1**(4): 2019-2025.
Staehelin, L. A. and B.-H. Kang (2008). "Nanoscale Architecture of Endoplasmic Reticulum Export Sites and of Golgi Membranes as Determined by Electron Tomography." Plant Physiology **147**(4): 1454-1468.
Stremlau, M., C. M. Owens, M. J. Perron, M. Kiessling, P. Autissier and J. Sodroski (2004). "The cytoplasmic body component TRIM5[alpha] restricts HIV-1 infection in Old World monkeys." Nature **427**(6977): 848-853.
Suehiro, N., T. Natsuaki, T. Watanabe and S. Okuda (2004). "An important determinant of the ability of Turnip mosaic virus to infect Brassica spp. and/or Raphanus sativus is in its P3 protein." J Gen Virol **85**(Pt 7): 2087-2098.
Sun, L., I. B. Andika, J. Shen, D. Yang and J. Chen (2014). "The P2 of Wheat yellow mosaic virus rearranges the endoplasmic reticulum and recruits other viral proteins into replication-associated inclusion bodies." Mol Plant Pathol **15**(5): 466-478.
Tanaka, Y., K. Nishimura, M. Kawamukai, A. Oshima and T. Nakagawa (2013). "Redundant function of two Arabidopsis COPII components, AtSec24B and AtSec24C, is essential for male and female gametogenesis." Planta **238**(3): 561-575.
Tang, W. F., S. Y. Yang, B. W. Wu, J. R. Jheng, Y. L. Chen, C. H. Shih, K. H. Lin, H. C. Lai, P. Tang and J. T. Horng (2007). "Reticulon 3 binds the 2C protein of enterovirus 71 and is required for viral replication." J Biol Chem **282**(8): 5888-5898.
Thivierge, K., S. Cotton, P. J. Dufresne, I. Mathieu, C. Beauchemin, C. Ide, M. G. Fortin and J.-F. Laliberté (2008). "Eukaryotic elongation factor 1A interacts with Turnip mosaic virus RNA-dependent RNA polymerase and VPg-Pro in virus-induced vesicles." Virology **377**(1): 216-225.
Tilsner, J., O. Linnik, M. Louveaux, I. M. Roberts, S. N. Chapman and K. J. Oparka (2013). "Replication and trafficking of a plant virus are coupled at the entrances of plasmodesmata." The Journal of Cell Biology **201**(7): 981-995.
Tilsner, J., O. Linnik, M. Louveaux, I. M. Roberts, S. N. Chapman and K. J. Oparka (2013). "Replication and trafficking of a plant virus are coupled at the entrances of plasmodesmata." J Cell Biol **201**(7): 981-995.
Tilsner, J., O. Linnik, K. M. Wright, K. Bell, A. G. Roberts, C. Lacomme, S. Santa Cruz and K. J. Oparka (2012). "The TGB1 movement protein of Potato virus X reorganizes actin and endomembranes into the X-body, a viral replication factory." Plant Physiol **158**(3): 1359-1370.

Tu, L. and D. Banfield (2010). "Localization of Golgi-resident glycosyltransferases." Cellular and Molecular Life Sciences **67**(1): 29-41.
Tyrrell, M., P. Campanoni, J.-U. Sutter, R. Pratelli, M. Paneque, S. Sokolovski and M. R. Blatt (2007). "Selective targeting of plasma membrane and tonoplast traffic by inhibitory (dominant-negative) SNARE fragments." The Plant Journal **51**(6): 1099-1115.
Uchiyama, A., H. Shimada-Beltran, A. Levy, J. Y. Zheng, P. A. Javia and S. G. Lazarowitz (2014). "The Arabidopsis synaptotagmin SYTA regulates the cell-to-cell movement of diverse plant viruses." Front Plant Sci **5**: 584.
Uemura, T., H. Kim, C. Saito, K. Ebine, T. Ueda, P. Schulze-Lefert and A. Nakano (2012). "Qa-SNAREs localized to the trans-Golgi network regulate multiple transport pathways and extracellular disease resistance in plants." Proceedings of the National Academy of Sciences **109**(5): 1784-1789.
Uemura, T., H. Kim, C. Saito, K. Ebine, T. Ueda, P. Schulze-Lefert and A. Nakano (2012). "Qa-SNAREs localized to the trans-Golgi network regulate multiple transport pathways and extracellular disease resistance in plants." Proc Natl Acad Sci U S A **109**(5): 1784-1789.
Uemura, T., T. Ueda, R. L. Ohniwa, A. Nakano, K. Takeyasu and M. H. Sato (2004). "Systematic Analysis of SNARE Molecules in Arabidopsis: Dissection of the post-Golgi Network in Plant Cells." Cell Structure and Function **29**(2): 49-65.
Valli, A., A. Gallo, M. Calvo, J. de Jesus Perez and J. A. Garcia (2014). "A novel role of the potyviral helper component proteinase contributes to enhance the yield of viral particles." J Virol **88**(17): 9808-9818.
Verchot, J. (2012). "Cellular chaperones and folding enzymes are vital contributors to membrane bound replication and movement complexes during plant RNA virus infection." Frontiers in Plant Science **3**.
Verchot, J. and J. C. Carrington (1995). "Debilitation of plant potyvirus infectivity by P1 proteinase-inactivating mutations and restoration by second-site modifications." J Virol **69**(3): 1582-1590.
Verchot, J. and J. C. Carrington (1995). "Evidence that the potyvirus P1 proteinase functions in trans as an accessory factor for genome amplification." J Virol **69**(6): 3668-3674.
Verchot, J., B. A. Driskel, Y. Zhu, R. M. Hunger and L. J. Littlefield (2001). "Evidence that soilborne wheat mosaic virus moves long distance through the xylem in wheat." Protoplasma **218**(1-2): 57-66.
Verchot, J., E. V. Koonin and J. C. Carrington (1991). "The 35-kDa protein from the N-terminus of the potyviral polyprotein functions as a third virus-encoded proteinase." Virology **185**(2): 527-535.
Vijayapalani, P., M. Maeshima, N. Nagasaki-Takekuchi and W. A. Miller (2012). "Interaction of the trans-frame potyvirus protein P3N-PIPO with host protein PCaP1 facilitates potyvirus movement." PLoS Pathog **8**(4): e1002639.
Villarejo, A., S. Buren, S. Larsson, A. Dejardin, M. Monne, C. Rudhe, J. Karlsson, S. Jansson, P. Lerouge, N. Rolland, G. von Heijne, M. Grebe, L. Bako and G. Samuelsson (2005). "Evidence for a protein transported through the secretory pathway en route to the higher plant chloroplast." Nat Cell Biol **7**(12): 1224-1231.
Voeltz, G. K., W. A. Prinz, Y. Shibata, J. M. Rist and T. A. Rapoport (2006). "A Class of Membrane Proteins Shaping the Tubular Endoplasmic Reticulum." Cell **124**(3): 573-586.
von Heijne, G. (1992). "Membrane protein structure prediction: Hydrophobicity analysis and the positive-inside rule." Journal of Molecular Biology **225**(2): 487-494.

von Heijne, G. and Y. Gavel (1988). "Topogenic signals in integral membrane proteins." European Journal of Biochemistry **174**(4): 671-678.
Waltermann, A. and E. Maiss (2006). "Detection of 6K1 as a mature protein of 6 kDa in plum pox virus-infected Nicotiana benthamiana." J Gen Virol **87**(Pt 8): 2381-2386.
Wan, J., K. Basu, J. Mui, H. Vali, H. Zheng and J. F. Laliberte (2015). "Ultrastructural characterization of Turnip mosaic virus induced cellular rearrangements reveal membrane-bound viral particles accumulating in vacuoles." J Virol.
Wan, J., D. G. Cabanillas, H. Zheng and J. F. Laliberte (2015). "Turnip mosaic virus Moves Systemically through Both Phloem and Xylem as Membrane-Associated Complexes." Plant Physiol **167**(4): 1374-1388.
Wang, A. (2015). "Dissecting the Molecular Network of Virus-Plant Interactions: The Complex Roles of Host Factors." Annu Rev Phytopathol.
Wang, X., W. M. Lee, T. Watanabe, M. Schwartz, M. Janda and P. Ahlquist (2005). "Brome mosaic virus 1a nucleoside triphosphatase/helicase domain plays crucial roles in recruiting RNA replication templates." J Virol **79**(21): 13747-13758.
Wang, X., Z. Ullah and R. Grumet (2000). "Interaction between Zucchini Yellow Mosaic Potyvirus RNA-Dependent RNA Polymerase and Host Poly-(A) Binding Protein." Virology **275**(2): 433-443.
Wang, X., X. Wang, L. Deng, H. Chang, J. Dubcovsky, H. Feng, Q. Han, L. Huang and Z. Kang (2014). "Wheat TaNPSN SNARE homologues are involved in vesicle-mediated resistance to stripe rust (Puccinia striiformis f. sp. tritici)." J Exp Bot **65**(17): 4807-4820.
Wang, Z. and C. Benning (2012). "Chloroplast lipid synthesis and lipid trafficking through ER-plastid membrane contact sites." Biochem Soc Trans **40**(2): 457-463.
Watson, R. T. and J. E. Pessin (2001). "Transmembrane domain length determines intracellular membrane compartment localization of syntaxins 3, 4, and 5." Am J Physiol Cell Physiol **281**(1): C215-223.
Wei, T., T. S. Huang, J. McNeil, J. F. Laliberte, J. Hong, R. S. Nelson and A. Wang (2010). "Sequential recruitment of the endoplasmic reticulum and chloroplasts for plant potyvirus replication." J Virol **84**(2): 799-809.
Wei, T. and A. Wang (2008). "Biogenesis of Cytoplasmic Membranous Vesicles for Plant Potyvirus Replication Occurs at Endoplasmic Reticulum Exit Sites in a COPI- and COPII-Dependent Manner." Journal of Virology **82**(24): 12252-12264.
Wei, T. and A. Wang (2008). "Biogenesis of cytoplasmic membranous vesicles for plant potyvirus replication occurs at endoplasmic reticulum exit sites in a COPI- and COPII-dependent manner." J Virol **82**(24): 12252-12264.
Wei, T., C. Zhang, J. Hong, R. Xiong, K. D. Kasschau, X. Zhou, J. C. Carrington and A. Wang (2010). "Formation of complexes at plasmodesmata for potyvirus intercellular movement is mediated by the viral protein P3N-PIPO." PLoS Pathog **6**(6): e1000962.
Wei, T., C. Zhang, X. Hou, H. Sanfacon and A. Wang (2013). "The SNARE protein Syp71 is essential for turnip mosaic virus infection by mediating fusion of virus-induced vesicles with chloroplasts." PLoS Pathog **9**(5): e1003378.
Wu, C.-H., S.-C. Lee and C.-W. Wang (2011). "Viral protein targeting to the cortical endoplasmic reticulum is required for cell–cell spreading in plants." The Journal of Cell Biology **193**(3): 521-535.

Wung, C. H., Y. H. Hsu, D. Y. Liou, W. C. Huang, N. S. Lin and B. Y. Chang (1999). "Identification of the RNA-binding sites of the triple gene block protein 1 of bamboo mosaic potexvirus." J Gen Virol **80 (Pt 5)**: 1119-1126.
Xiang, Y., J. J. Tang, W. Tao, X. Cao, B. L. Song and J. Zhong (2015). "Identification of Cholesterol 25-Hydroxylase as a Novel Host Restriction Factor and a Part of the Primary Innate Immune Responses against Hepatitis C Virus Infection." J Virol **89**(13): 6805-6816.
Xiong, R. and A. Wang (2013). "SCE1, the SUMO-Conjugating Enzyme in Plants That Interacts with NIb, the RNA-Dependent RNA Polymerase of Turnip Mosaic Virus, Is Required for Viral Infection." Journal of Virology **87**(8): 4704-4715.
Xu, K. and P. D. Nagy (2015). "RNA virus replication depends on enrichment of phosphatidylethanolamine at replication sites in subcellular membranes." Proc Natl Acad Sci U S A **112**(14): E1782-1791.
Yang, Y. S. and S. M. Strittmatter (2007). "The reticulons: a family of proteins with diverse functions." Genome Biology **8**(12): 234-234.
Yoo, S.-D., Y.-H. Cho and J. Sheen (2007). "Arabidopsis mesophyll protoplasts: a versatile cell system for transient gene expression analysis." Nat. Protocols **2**(7): 1565-1572.
Yoo, S. D., Y. H. Cho and J. Sheen (2007). "Arabidopsis mesophyll protoplasts: a versatile cell system for transient gene expression analysis." Nat Protoc **2**(7): 1565-1572.
Zamyatnin, A. A., A. G. Solovyev, P. V. Bozhkov, J. P. T. Valkonen, S. Y. Morozov and E. I. Savenkov (2006). "Assessment of the integral membrane protein topology in living cells." The Plant Journal **46**(1): 145-154.
Zelazny, E., U. Miecielica, J. W. Borst, M. A. Hemminga and F. Chaumont (2009). "An N-terminal diacidic motif is required for the trafficking of maize aquaporins ZmPIP2;4 and ZmPIP2;5 to the plasma membrane." Plant J **57**(2): 346-355.
Zhang, L., H. Chen, F. Brandizzi, J. Verchot and A. Wang (2015). "The UPR branch IRE1-bZIP60 in plants plays an essential role in viral infection and is complementary to the only UPR pathway in yeast." PLoS Genet **11**(4): e1005164.
Zhang, S. C., G. Zhang, L. Yang, J. Chisholm and H. Sanfacon (2005). "Evidence that insertion of Tomato ringspot nepovirus NTB-VPg protein in endoplasmic reticulum membranes is directed by two domains: a C-terminal transmembrane helix and an N-terminal amphipathic helix." J Virol **79**(18): 11752-11765.
Zhang, X., H. Zhao, S. Gao, W. C. Wang, S. Katiyar-Agarwal, H. D. Huang, N. Raikhel and H. Jin (2011). "Arabidopsis Argonaute 2 regulates innate immunity via miRNA393(*)-mediated silencing of a Golgi-localized SNARE gene, MEMB12." Mol Cell **42**(3): 356-366.
Zheng, H., L. Camacho, E. Wee, H. Batoko, J. Legen, C. J. Leaver, R. Malhó, P. J. Hussey and I. Moore (2005). "A Rab-E GTPase Mutant Acts Downstream of the Rab-D Subclass in Biosynthetic Membrane Traffic to the Plasma Membrane in Tobacco Leaf Epidermis." The Plant Cell **17**(7): 2020-2036.
Zilian, E. and E. Maiss (2011). "Detection of plum pox potyviral protein-protein interactions in planta using an optimized mRFP-based bimolecular fluorescence complementation system." J Gen Virol **92**(Pt 12): 2711-2723.

CHAPTER 6: OTHER CONTRIBUTIONS

PUBLICATION NO. 4

$6K_2$-induced vesicles can move cell to cell during turnip mosaic virus infection

Frontiers in Microbiology

December 2013, Volume 4, Article 351.

Romain Grangeon[1], Jun Jiang[1], Juan Wan[1], Maxime Agbeci[1], Huanquan Zheng[2] and Jean-François Laliberté[1*]

1. Institut national de la recherche scientifique, INRS-Institut Armand-Frappier, Laval, QC, Canada
2. Department of Biology, McGill University, Montréal, QC, Canada

*** Author for correspondence**: Prof. Jean-François Laliberté

Email: jean-francois.laliberte@iaf.inrs.ca

Contribution

This manuscript has been published in *Frontiers in Microbiology*. I did the live cell imaging experiments to detect the vRdRp in $6K_2$-tagged small vesicles, and wrote the relative text in this manuscript.

REVIEW NO. 1

Host endomembrane recruitment for plant RNA virus replication

Current Opinion in Virology

Volume 2, Issue 6, December 2012, Pages 683–690

Romain Grangeon, Jun Jiang and Jean-François Laliberté

INRS-Institut Armand-Frappier; Laval, QC Canada

* Corresponding author : Jean-François Laliberté

Email: jeanfrancois.laliberte@iaf.inrs.ca

Contribution

This review has been published in *Current Opinion in Virology*. I wrote 40 % of the text and Romain Grangeon wrote another 60 %.

REVIEW NO. 2

The genome-linked protein VPg of plant viruses — a protein with many partners

Current Opinion in Virology

Volume 1, Issue 5, November 2011, Pages 347–354

Jun Jiang and Jean-François Laliberté

INRS-Institut Armand-Frappier; Laval, QC Canada

* Corresponding author : Jean-François Laliberté

Email: jeanfrancois.laliberte@iaf.inrs.ca

Contribution

This review has been published in *Current Opinion in Virology*. I draw the Figure 2 for this review paper.

APPENDIX: LIST OF PUBLICATIONS AND COMMUNICATIONS

Publications

1. **Jiang J**, Patarroyo C, Garcia Cabanillas D, Zheng H, Laliberté JF. The Vesicle-Forming $6K_2$ Protein of Turnip Mosaic Virus Interacts with the COPII Coatomer Sec24a for Viral Systemic Infection. *J Virol*. 2015 Jul;89(13):6695-710.
2. Grangeon R, **Jiang J**, Wan J, Agbeci M, Zheng H, Laliberté JF. $6K_2$-induced vesicles can move cell to cell during turnip mosaic virus infection. *Front Microbiol*. 2013 Dec 4;4:351.
3. Grangeon R, **Jiang J**, Laliberté JF. Host endomembrane recruitment for plant RNA virus replication. *Curr Opin Virol*. 2012 Dec;2(6):683-90.
4. **Jiang J**, Laliberté JF. The genome-linked protein VPg of plant viruses-a protein with many partners. *Curr Opin Virol*. 2011 Nov;1(5):347-54.

Chapters

1. **Jiang, J**. and Laliberté, JF. *Current Topics in Plant Virology*: Membrane association for plant virus replication and movement, Springer. (expected October 2015)

Communications

Oral

1. **Jiang J**, Patarroyo C, Wan J, Agbeci M, Garcia Cabanillas D, Grangeon R, Zheng H, Laliberté JF. Molecular determinants of turnip mosaic virus $6K_2$ protein in viral replication complex cellular biogenesis. IUMS-XVIth International Congress of Virology 2014, Montréal, Québec.
2. **Jiang J**, Zheng H, Laliberté JF. SNARE proteins function as Turnip mosaic virus restriction factors. Montréal plant meeting 2014, Montréal, Québec.
3. **Jiang J**, Wan J, Agbeci M, Grangeon R, Zheng H, Laliberté JF. Molecular determinants of Turnip mosaic virus $6K_2$ protein in viral replication complex

cellular biogenesis. American Society for Virology, 32nd Annual Meeting 2013, Penn State University, USA.

4. **Jiang J**, Patarroyo C, Garcia Cabanillas D, Agbeci M, Wan J, Grangeon R, Zheng H, Laliberté JF. Caractérisation des déterminants moléculaires de la protéine 6K2 du TuMV dans la biogenèse des complexes viraux cellulaires de réplication du TuMV. Congrès Armand-Frappier 2013, Orford, Québec.

Poster

1. **Jiang J**, Grangeon R, Agbeci M, Wan J, Zheng H and Laliberté JF. Molecular determinants of Turnip mosaic virus $6K_2$ protein in replication vesicle biogenesis. American Society for Virology, 31st Annual Meeting, University of Wisconsin-Madison, USA.
2. **Jiang J**, Grangeon R, Agbeci M, Laliberté JF. Les déterminants moléculaires de la protéine $6K_2$ du virus de la mosaïque du navet dans la formation des usines virales. Congrès Armand-Frappier 2011, Canada.